The WELDING JOURNAL

OCTOBER 1952

IN THIS ISSUE

Technical Aspects of Soldering Practices 881
Welding Low-Alloy Ferritic Pipe 898
Corrosion of Structural Spot Welds 903
Hard-Facing Alloys of Chromium Carbide 917
Expression of Spot-Weld Properties 931
Vacuum Brazing of Clad Steels 441-s
Weld Cracking of Aluminum Alloys 448-s
Contact Resistance 457-s
Spot Welding Titanium Alloy Sheet 469-s
Effect of Strain-Rate on Brittle Fracture 475-s
Nature of Cleavage Fracture in Steel 493-s
Table of Contents 879
Index to Advertisers 981

OFFICIAL PUBLICATION OF THE AMERICAN WELDING SOCIETY

The man on the job wants a *RUGGED CUTTING TORCH*

VICTOR Models CTS400 and 1400 with stainless steel head and tube assemblies meet the challenge. They cut longer and stand up better with a minimum of maintenance costs. Mixer and mixer tubes of special heat resistant copper alloys prevent overheating. VICTOR's famous Spiral Mixer thoroughly mixes the preheat gases for safe, efficient and economical operations.

The stainless steel head and tube assembly is a single unit available with either 90° or 75° head. Uses standard VICTOR cutting tips.

Try it on heavy scrap cutting as shown here. Ask your VICTOR dealer for a demonstration NOW.

VICTOR

LOOK FOR THE VICTOR DEALER SIGN!

Ask him to show you why it costs less to own and operate VICTOR.

Dealer inquiries invited.

293

VICTOR EQUIPMENT COMPANY

3821 Santa Fe Ave.
LOS ANGELES 58

844 Folsom Street
SAN FRANCISCO 7

1312 W. Lake St.
CHICAGO 7

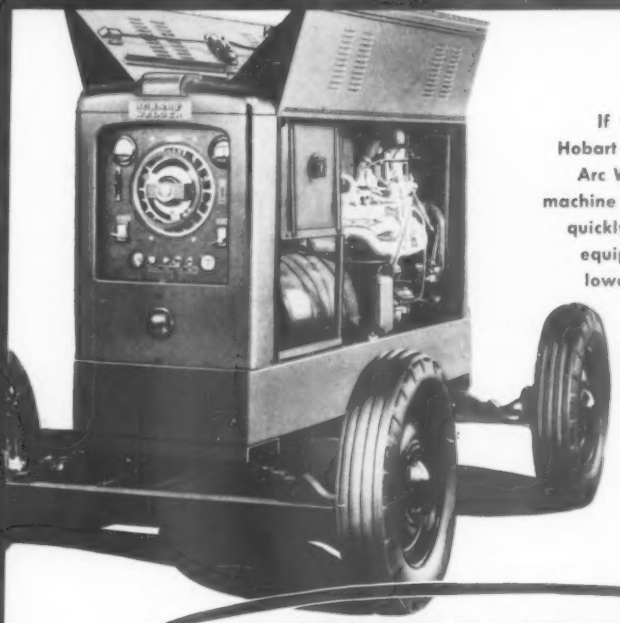

If you'll just compare a Hobart Gas Engine Drive DC Arc Welder with any other machine on the market—you'll quickly see why it is better equipped to give you the lower costs and constant performance so essential to profitable production welding. Mail coupon today for full details.

HOBART

WELDERS

HOBART BROTHERS COMPANY, Box WJ-102,, TROY, OHIO

"One of the world's largest builders of arc welders"

Rugged construction . . . trouble-free service . . . long life . . . extra capacity . . . simplicity of operation . . . all of these are yours with the Hobart Electric Drive DC Arc Welder. Prove its value . . . TRY IT YOURSELF. The coupon will bring you full details.

While attending the
METAL SHOW
make
your headquarters
for Arc
Welding Equipment
Hobart Welder Sales Co.
3908 Lancaster Ave.
Phone EV. 2-4988

HOBART BROTHERS COMPANY, BOX WJ-102, TROY, OHIO

Without obligation, send me information on items checked below
☐ Gas Drive Welder ☐ Electric Drive Welder ☐ Pipeliner Welder

NAME _____ POSITION _____

FIRM _____

ADDRESS _____

Send me
☐ Welder Catalog
☐ Electrode Catalog
☐ Accessory Catalog

FREE ☐ Check here for vest pocket guide "How to get better Welds"

BUTTERING WAS THE ANSWER!

Saved costly casting . . .

allowed use of low cost rods

Need for complete re-making of a large, costly composite machine frame threatened a prominent Western mining equipment builder. Weld metal was picking up harmful impurities from the cast part—it was impossible to obtain satisfactory welds using the electrodes specified.

The local M&T salesman joined with company welding engineers . . . experimented . . . and sparked a solution! On his advice surfaces of the casting where welding was required were simply "buttered" with Murex Type HTS before the bulk of the weld metal was deposited.

Results were: complete elimination of pickup so that remaking of the casting to new metallurgical specifications became unnecessary. And, the specified electrodes, on hand for the job, could be used.

Your nearby M&T representative is qualified to give you expert assistance on any welding problem. Call on him when you need help. Make use of his broad background of experience in every phase of welding.

MUREX®

Electrodes

Arc Welders • Accessories

METAL & THERMIT CORPORATION 100 East 42nd Street, New York 17, N. Y.

48,000 Spot Welds

with a single MALLORY "Nu-Wrinkle Cap"* Electrode

Outstanding Design Features of MALLORY "Nu-Wrinkle Cap" Electrodes

1. Smooth, annular corrugations of cap skirt provide positive electrical and thermal contact with shank.
2. Resilience of corrugations effects secure attachment of cap to shank.
3. Wiping action of corrugations cleans adjoining surfaces of shank, assures low electrical contact resistance.
4. Hollow cap skirt has the largest practicable cooling area, results in a maximum rate of heat transfer.
5. Smoothly rounded skirt corrugations minimize damage to shank, insure maximum shank life.
6. Unique design eliminates possibility of cap being forced askew into shank.

A well-known manufacturer of farm equipment put Mallory "Nu-Wrinkle" replaceable cap electrodes to work on his production line . . . got more than 48,000 welds with a single cap. Here are the facts:

Material . . . . . 1025 Steel—Pickled
Gauge . . 18 and 20 gauge (0.050"-0.037" thick)
Welding Speed, About 147 spots per minute
Machine 75KVA
Weld Time . . . . . 8 cycles

AND DRESSING TIME WAS CUT TWO-THIRDS by the use of the Mallory "Nu-Wrinkle Caps". Thus the manufacturer was able to save both time and money . . . got more welds per dollar.

• • •

Used 75 "Nu-Wrinkle Caps" on a Single Shank . . .

Additional proof of the economy offered by Mallory "Nu-Wrinkle Caps" is shown by the experience of a West Coast manufacturer who used 75 caps on a single shank. This is exceptional but other users average between 20 and 25 caps per shank . . . save real money.

• • •

It will pay you to team up Mallory "Nu-Wrinkle Caps", shanks and electrode holders . . . to count on Mallory for all your resistance welding needs—electrodes . . . holders . . . dies . . . castings . . . forgings . . . rod and bar stock . . . Elkonite®. Get details today from your distributor . . . or call or write direct to Mallory.

Trade Mark, Patent Pending

In Canada, made and sold by Johnson Matthey and Mallory, Ltd., 110 Industry St., Toronto 15, Ontario

P. R. MALLORY & CO. Inc.
MALLORY

SERVING INDUSTRY WITH THESE PRODUCTS:
Electromechanical—Resistors • Switches • Television Tuners • Vibrators
Electrochemical—Capacitors • Rectifiers • Mercury Dry Batteries
Metallurgical—Contacts • Special Metals and Ceramics • Welding Materials

P. R. MALLORY & CO., INC., INDIANAPOLIS 6, INDIANA

For information on titanium developments, contact Mallory-Sharon Titanium Corp., Niles, Ohio.

LINDE'S News of Metalworking

Worn Parts Rebuilt Economically by UNIONMELT Welding

Repair of worn tractor parts is most practical and economical with specially developed fixtures on which standard UNIONMELT welding units are mounted. The metal deposited by UNIONMELT welding is so smooth that no grinding or finishing is required. Experience indicates that resurfaced areas will wear as long as new parts.

The Berkeley "Conservall" fixture is designed especially for rebuilding crawler tractor track links or rails without disassembling them. The track is placed in a trough and clamped in position. A LINDE side-beam carriage

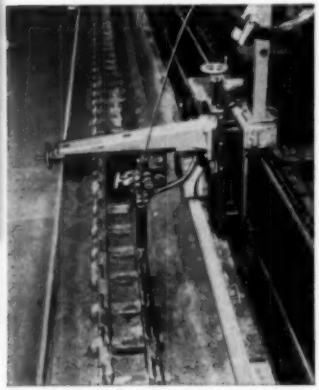

Tractor rail links rebuilt in "Conservall" machine by UNIONMELT welding. Cams automatically control welding action for each link.

moves the UNIONMELT welding equipment over the positioned track and the welding of each link is automatically started, stopped, and accurately controlled. Rollers, idlers, sheaves, and other circular work can also be welded or resurfaced on another section of the machine.

The "Leader" machine is also available for rebuilding both cylindrical and flat parts. Rollers are rebuilt on top of the machine. Larger parts, such as idlers, are mounted in the chuck at the side of the machine as shown. With the flat work attachment, parts such as disassembled track rail links, grousers, bulldozer blades, end bits and fabricated members can be resurfaced easily. This attachment is operated by a gear which is mounted in the chuck.

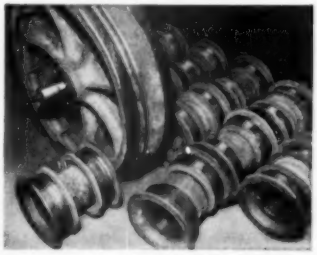

These tractor rollers and an idler were rebuilt at a speed of 30 in. per min. by UNIONMELT welding.

With both machines, the wheels can be tilted for rebuilding the flanges. It takes only 80 to 90 minutes to rebuild a D-8 track roller. Idlers take about three times as long.

OXWELD 1928 rod is normally used in making these repairs. When wear is excessive, OXWELD 296 rod is sometimes used for the initial buildup which is then finished with OXWELD 1928 rod. For such resurfacing, use either Grade 80 or Grade 90 UNIONMELT welding compositions.

For some services, a finishing pass with a higher alloy tube rod is applied to produce a harder surface. While material of almost any hardness can be applied, one combining hardness and toughness lasts longer than one of higher hardness that tends to spall and chip. As deposited, OXWELD 1928 material has a hardness of about Rockwell C-25, but in service the working surfaces actually develop properties which cause them to outwear deposits that are substantially harder.

Advantages of UNIONMELT Build-up

UNIONMELT welded resurfacing is especially attractive with these automatic machines which readily permit deposit rates of 20 lbs. per hour. Savings in time and the advantages of a smooth uniform deposit justify the initial investment in automatic equipment. Important in these times is the conservation of metal realized with the process. The use of approximately *one hundred pounds of weld metal saves replacement of 2,000 to 3,000 pounds of new parts.*

LINDE's engineers and technicians will be glad to give further information about UNIONMELT welding. Telephone or write today.

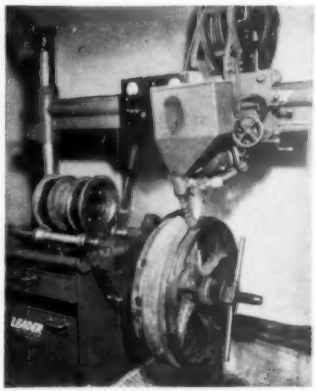

UNIONMELT welding head on "Leader" fixture rebuilds rollers and idlers. Rollers are welded on top of the machine, idlers at the side, and flat parts, depending on their size, can be welded on top of the machine or in the flat work attachment.

LINDE AIR PRODUCTS COMPANY
A Division of Union Carbide and Carbon Corporation
30 East 42nd Street UCC New York 17, N. Y.
Offices in Other Principal Cities
In Canada: Dominion Oxygen Company, Limited, Toronto

The terms "Linde," "Oxweld," and "Unionmelt" are registered trade-marks of Union Carbide and Carbon Corporation.

Published for the advancement of the science and art of welding by the AMERICAN WELDING SOCIETY

Editor
W. SPRARAGEN
Assistant Editor
B. E. ROSSI

The WELDING JOURNAL

Volume 31 **OCTOBER 1952** *Number 10*

TECHNICAL PAPERS, ITEMS AND REPORTS

Technical Aspects of Soldering Practices, by Robert M. MacIntosh 881

New Rules for Welding Low-Alloy Ferritic Pipe Material, by Commander Charles F. Perry, USCG 898

Current Welding Literature 902

Corrosion of Structural Spot Welds, by B. Karnisky, E. Kinelski and E. Gruca 903

Hard-Facing Alloys of the Chromium Carbide Type, by Howard S. Avery and Henry J. Chapin 917

The Expression of Spot-Weld Properties, by Julius Heuschkel 931

PRACTICAL WELDER AND DESIGNER

Improved Welds for Galvanized Metal 944

Flame-Plating 945

Flash Welding of Titanium Alloys, by Dr. I. A. Oehler 950

Powder-Cutting Halves 5 Billets per Minute 951

Welded Build-Up of Worn Spoke Surfaces of Tractor Trailer, by L. J. MacLennan, Jr. 952

Portable Sigma-Welding Equipment 953

Principles of Braze Welding, by H. K. Schmuck 954

SOCIETY AND RELATED EVENTS

Society News 955

News of the Industry 958

Personnel 964

Abstracts of Current Welding Patents 966

New Literature 970

Employment Service Bulletin 978

Index to Advertisers 981

New Products 982

Section News and Events 998

List of New Members 1002

WELDING RESEARCH SUPPLEMENT

High-Strength Vacuum Brazing of Clad Steels, by R. C. Bertossa 441-s

Weld Cracking of Aluminum Alloys, by J. D. Dowd 448-s

Contact Resistance, by W. B. Kouwenhoven and C. W. Little 457-s

Basic Flame Studies and Their Relationship to Welding Equipment, by James A. Browning and Merle L. Thorpe 465-s

Spot Welding of Titanium Alloy Sheet, by M. L. Begeman, E. H. Block, Jr. and Frank W. McBee, Jr. 469-s

The Effect of Strain-Rate on Twinning and Brittle Fracture, by D. Rosenthal and C. C. Woolsey, Jr. 475-s

The Pressure Vessel Research Committee Realizes Its First Objective 492-s

The Nature of Cleavage Fracture in Steel, by H. M. Miekk-oja 493-s

Stress Concentrations in Steel Under Cyclic Load, Discussion by Wendell P. Roop 502-s

OFFICERS OF THE SOCIETY

C. H. JENNINGS	*President*
F. L. PLUMMER	*1st Vice-President*
E. R. SEABLOOM	*2nd Vice-President*
R. S. DONALD	*Treasurer*
J. G. MAGRATH	*Secretary*
F. J. MOONEY	*Asst. Secretary*
S. A. GREENBERG	*Technical Secretary*

DISTRICT VICE-PRESIDENTS

1—New York and New England	E. N. ADAM
2—Mid-Eastern	H. L. INGRAM, JR.
3—Southern	J. U. DURHAM
4—Central	T. J. CRAWFORD
5—Mid-Western	T. B. JEFFERSON
6—Mid-Southern	A. E. WISLER
7—Western	DAVID P. BRISBEE

Published monthly by the American Welding Society. Publication office, 20th and Northampton Streets, Easton, Pa. Editorial and general offices, 33 West 39th St., New York 18, N. Y. Subscriptions $6.00 per year in United States and possessions; foreign countries $7.50. Single copies, nonmembers $1.00; members 75 cents. Entered as second-class matter January 5, 1932, at the Post Office at Easton, Pa., under the act of March 3, 1879. Copyright 1952, by the American Welding Society. The Society is not responsible for any statement made or opinion expressed in its publications. Permission is given to reprint any article after its date of publication provided proper credit is given.

HOW...to weld Ductile Iron

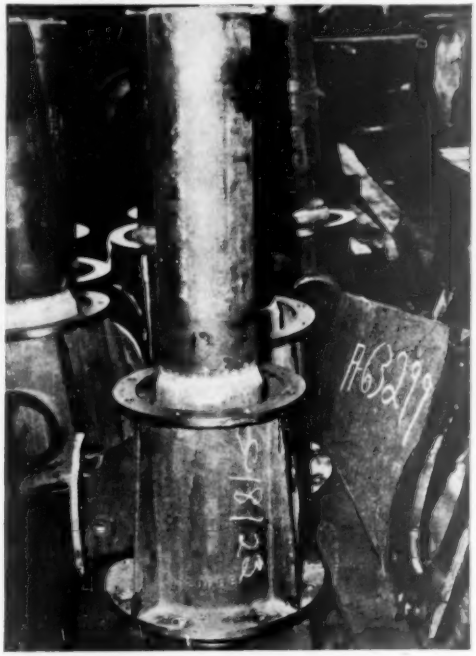

This large diameter Hydrafuge gives all of the advantages of welded construction. A sound weld . . . in less time, with less trouble . . . means more production at less cost. It's done with Ni-Rod "55", the ideal electrode for welding Ductile Iron to steel pipe.

DUCTILE IRON is a new type iron . . . with greater toughness, higher tensile strength and better weldability.

The commercial types (with tensile strengths ranging between 65,000 and 105,000 psi) can be readily welded to each other or to dissimilar metals such as carbon steel or alloy steels.

How? With Ni-Rod "55"® . . . the recommended electrode for any Ductile Iron welding job.

And for the best weld here's the procedure: clean off all oil, grease and dirt. Grind off "skin." Bevel edges. Pre-heat to about 600° F. when pressure-tight joint is required. Weld with lowest possible current that gives smooth operation.

For welding in flat position, 3/32" electrodes take 60-70 amps, 1/8" take 90-100 amps, 5/32" take 120-130 amps, 3/16" take 140-150 amps. Lower currents for out-of-position welding.

Heating should not be concentrated in one area. Use intermittent bead method to heat evenly. Peen gently with a round-nosed tool. Then cool off weld area slowly by covering with asbestos or other insulating material.

A sound weld? Yes . . . just as sound as the Ni-Rod "55" weld on the Hydrafuge Casting shown above. In this case the ability of Ni-Rod "55" to produce a solid joint between Ductile Iron and carbon steel made available all of the advantages of welded construction.

Do Ni-Rod "55"'s weldability and Ductile Iron's engineering properties offer an opportunity to improve production (or repair, or salvage) in your plant? Then consult INCO's Technical Service Section. They will be glad to help with any questions you may have about welding Ductile Cast Iron.

It will also pay you to anticipate your needs for Ni-Rod "55" and the other Nickel and Nickel Alloy products. Today's defense demands mean extended deliveries. So always order well in advance of work schedules.

INCO NI-ROD TRADE MARK

THE INTERNATIONAL NICKEL COMPANY, INC.

67 Wall Street, New York 5, N. Y.

The WELDING JOURNAL

volume 31 October 1952 number 10

Technical Aspects of Soldering Practices

Fundamental properties of solder alloys and methods of applying them efficiently at modern production speeds

by Robert M. MacIntosh

INTRODUCTION

ONE of the most common ways to join metal parts solidly is to solder them. This operation hardly needs definition since practically everyone has seen sections of tinplate or electrical connections or lead pipes soldered together.

The process of soldering is relatively simple, but it requires considerable skill and ingenuity to produce a joint of optimum properties. A thorough knowledge of the fundamental properties of solder alloys and methods of applying them is needed in order to use solder efficiently at modern production speeds.

Soldering is broadly recognized as the process whereby a metallic substance of lower melting point than the metals to be joined is made to flow between metal surfaces which remain unmelted but are solidly united when the joining metal solidifies.

The soft solders, mainly the tin-lead solders, are used at temperatures of 400 to 700° F. A few solders containing cadmium, zinc or silver are classed as soft solders.

Soldering operations are limited to the joining of metals where the major requirement is sealing and solidifying the assembly and the minor requirement is high joint strength.

The essential feature of a good soldered joint is that each of the joined surfaces is wetted by a film of solder and that the two films of solder are continuous with the solder filling the space between them. The films are formed by intermetallic combination and to some extent by adhesive forces. These films can only form on a clean or oxide-free surface.

The practical considerations involved in the development of good soldering techniques are discussed in this paper. Attention is given to the selection of the correct solder composition for a specific application and to a discussion of the heating methods available. Equal attention is given to surface preparation, to design and assembly, and to special techniques for the hard-to-solder metals.

The technical aspects of soldering considered in this paper emphasize the advantages of soldering over other methods of joining. Fabrication at low temperatures is often the most convenient, the most simple and inexpensive method of joining a single article or for quantity production.

BASIC STEPS IN SOLDERING

The selection of the soldering process over other methods of joining metals is usually based on the ease of application to comparatively thin parts. The selection also rules out large joints of great strength and joints to be used near the melting range of solders.

Joining by soldering can be a successful process if all of the factors involved are carefully considered in stepwise order. The factors of most vital interest are:

A. Soldering Processes and Equipment
   A brief description of heating methods and equipment commonly used in soldering.
B. Influence of the Basis Metals
   A discussion and comparison of the base metals with respect to ease of solderability.
C. Properties of Solders and Soldered Joints.
   1. Constitution of Solder Alloys.
   2. Wetability and Intermetallic Growth.
   3. Composition of Solders.

Robert M. MacIntosh, Chemical Development, Tin Research Institute, Inc., Columbus 1, Ohio.

Scheduled for presentation at the Thirty-Third National Fall Meeting, AWS, Philadelphia, Pa., week of Oct. 20, 1952. Closing date for discussion Dec. 15, 1952.

D. Fluxes and Atmospheres
A discussion of corrosive and noncorrosive fluxes.
E. Joint Design
F. Precleaning and Surface Preparation
G. Assembly
H. Soldering Techniques
A complete discussion of heating methods used in soldering processes.
I. Postsoldering Operations
1. Cooling the Joint.
2. Removal of Flux Residue.
J. Inspection
1. Nondestructive Examination.
2. Destructive Testing
K. Soldering the Individual Metals
1. Carbon and Low-Carbon Steels.
2. Stainless and Alloy Steels.
3. Cast Iron.
4. Copper.
5. Copper Alloys.
(*a*) Brass.
(*b*) Bronze and Gunmetal.
(*c*) Aluminum and Silicon Bronze.
(*d*) Beryllium-Copper.
6. Nickel and Nickel Alloys.
7. Lead and Lead Alloys.
8. Aluminum.
9. Electroplated Coatings.
(*a*) Tin.
(*b*) Cadmium.
(*c*) Nickel and Chromium.
(*d*) Silver.
(*e*) Zinc Plating and Galvanized Iron.
(*f*) Tin-Zinc and Tin-Nickel Plating.
L. Appendix
1. Solder Specifications.
2. Manufacturers' Data.
3. Tables.
M. Reference

A. SOLDERING PROCESSES AND EQUIPMENT

General

The practical methods of soldering in common use may be divided into nine processes as follows:

1. Soldering with the Copper Bit.
2. Soldering by Torch or Flame.
3. Hot Plate Soldering.
4. Induction Soldering.
5. Dip Soldering.
6. Electrode Soldering.
7. Resistance Soldering.
8. Spray Soldering.
9. Supersonic Soldering.

Whatever the process used, the solder metal is nonferrous and has a melting point below 700° F.

Soldering with the Copper Bit

This method is the most common means of soldering. The bit may be electrically heated, or be heated by a burner built into the iron, or be heated externally by means of a furnace or torch.

The size and shape of the bit must be chosen with respect to the work which is to be done. The heat source should be easily controlled so that the bit is held at the proper temperature.

The soldering bit, usually hand operated, may be held stationary or it may be part of an automatic soldering machine. Figure 1 shows the construction of a typical soldering copper bit.

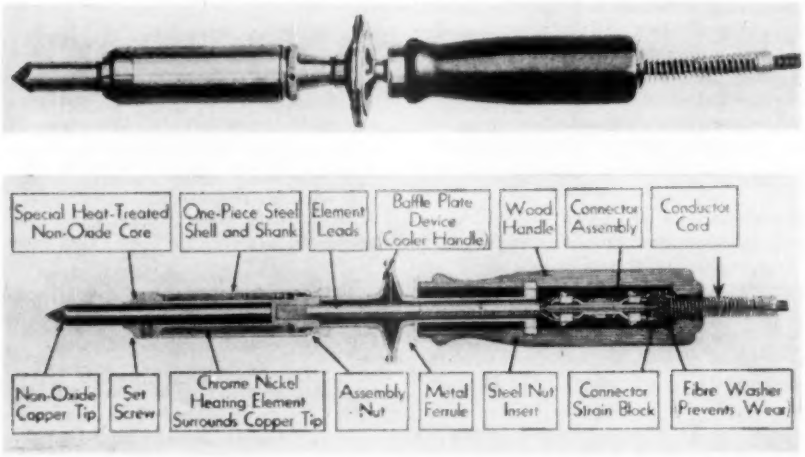

Fig. 1 The electric soldering iron

Soldering by Torch or Flame

The torch method is one of the fastest means of applying heat. The fuel used may be any combination of air, gas, oxygen or acetylene.

For manual torch soldering, the torch may be equipped with single or multiflame tips. Machine operations can be set up with one or more flames and may be designed to move the work or the torches or both.

The torch is useful in heating objects too large for the bit, or to concentrate heat at one particular part of a complicated assembly.

Hot Plate Soldering

Furnace soldering or hot plate soldering is used extensively where the parts to be soldered can be assembled with the solder preplaced near or in the joint. The process is particularly applicable for high-speed production work.

The solder may be in any shape or form to suit the application. Fluxing of the joint is essential and a nonoxidizing atmosphere may be used.

The furnace should have time and temperature controls. The work may be placed in the furnace singly, in batches or on a continuous conveyor.

Induction Soldering

The heat necessary for soldering by induction is induced in the joint by eddy currents when the parts are placed in or near the high-frequency coil. Close control of temperature without risk of local overheating gives this method special merit.

The solder and flux in any suitable form are preplaced. Batch or continuous operation on belts or rotating tables can be done equally well. Careful design of the joint and the coil setup are necessary to avoid shielding the work from the energizing coil.

The three common sources of high-frequency current used for induction soldering are the motor-generator, resonant spark gap and vacuum tube oscillator.

Dip Soldering

Dip soldering comprises the immersion of the article in a bath of molten solder. The method is usually applied to the joining of thin sheet metal where clearances are small and where large fillets are not required, as for example, copper radiators.

The size of the bath is determined by the size of the articles, the depth they are submerged and the amount of heat abstracted by the article. Automatic means of replenishing the solder can be used.

Solder baths are equipped with temperature controls. Operation of the process of fluxing and dipping can be manual or continuous. Special precautions are necessary to maintain the parts in contact until the solder solidifies.

A modification of dip soldering is used in sealing the side seams of cans. The seam is coated with solder on passing over a roller revolving in a solder bath.

Electrode Soldering

In this method, the article is jointed to one terminal of a low voltage supply and the soldering tool to the other. Heat is generated whenever the bit makes contact with the work.

Resistance Soldering

In resistance soldering, the joint forms a part of the electric circuit. Heat is brought about by the resistance at the joint when a large current is passed.

The parts to be soldered are held between two electrodes in the form of tongs or clamps. When the current is applied, the preplaced solder melts by local heating. The pressure is maintained until the solder solidifies.

Spray Soldering

Solder is applied to a prefluxed surface with a metallizing gun which atomizes the metal. It has limited application in autobody repair.

Supersonic Soldering

This method is a new development based on the theory that cavitation erosion of oxide films can be performed by sound waves at ultrasonic frequencies.

The ultrasonic soldering iron generates ultrasonic power in the range of 16–20 kc/sec by means of a magnetostriction unit. The method is adaptable only to small units and is specifically designed for soldering aluminum.

B. INFLUENCE OF THE BASIS METALS

The composition of the base metal has a considerable influence on the choice of soldering process and also in the choice of solder and flux used.

Copper, bronze, iron and unalloyed steels can be joined successfully with any type of tin-lead solder. Because of the incompatibility of tin and zinc in solder, brass is one of the less easy materials to solder. For the same reason antimonial solders are not recommended for brass because of the affinity of the antimony and the zinc contained in the brass. The main difficulty in soldering brass is that the solder becomes contaminated with zinc compounds which render the joint brittle.

The alloyed steels, those containing considerable amounts of chromium, nickel, manganese, molybdenum, tungsten and vanadium, can be soldered, but special cleaning methods and strong fluxes are necessary to remove surface films of oxide which prevent action between the steel and the tin in the solder.

Aluminum and silicon bronzes and beryllium-copper oxidize superficially when exposed to air and the oxides are hard and infusible. Where possible, the acid type fluxes are applied as soon as the refractory oxides are removed by mechanical abrasion.

The soldering of aluminum is difficult because there is no flux capable of removing, at ordinary temperatures, the film of oxide which forms again instantaneously as fast as it is removed from the surface. Certain practices of scratching the surface of the aluminum while in contact with solder aid in tinning the aluminum. Ultrasonic vibration methods are to some extent successful. Special high tin-zinc alloys are of most value in joining aluminum.

Soldering of zinc-base die-castings is subject to danger of contamination of the zinc base since both tin-lead and cadmium-zinc solders tend to diffuse in the zinc. Zinc-base die-castings should be given a heavy electroplate of nickel or tin-nickel before attempting to solder.

Articles plated with tin, tin-zinc and tin-nickel are easy to solder with mild fluxes. Such coatings are advocated to assist in the soldering of difficult metals. Silver and cadmium plated articles are readily soldered although the latter may require a hotter iron. Galvanized iron is one of the most difficult metal surfaces to solder. Treatment of the zinc surface with free hydrochloric acid is the only available method for preparing the joint for soldering.

An important factor in joining metals often not given attention is the possibility of galvanic corrosion. Two metals that are far apart in the galvanic series of metals may be subjected to galvanic corrosion. This factor is important in selecting the best solder for maximum corrosion resistance.

C. PROPERTIES OF SOLDERS AND SOLDERED JOINTS

Constitution of Solder Alloys

While the composition of a soft solder is defined in percentage of tin, lead, antimony, etc., and impurities, the physical structure, as regards melting and solidifying, is most easily indicated by the equilibrium diagram (Fig. 2).

Mixtures of tin and lead have their melting range indicated by the lines AE and EB. E is the point of main interest because it indicates the composition known as the eutectic composition, 63% tin, remainder lead. The eutectic composition is the only composition of pure tin and lead which transforms sharply from liquid to solid state without passing through a pasty state.

The diagram shows that tin-lead alloys containing 20 to 97% tin, with the exception of the eutectic mixture, pass from the solid state to a pasty state when they are heated to a temperature of 361° F. The proportion of eutectic for each solder composition is in the ratio of the distances RC to the distance RE shown on the curve. That is, the eutectic portion of a solder rises to 100% at E and falls away in direct proportion until at C (and D) there is none present.

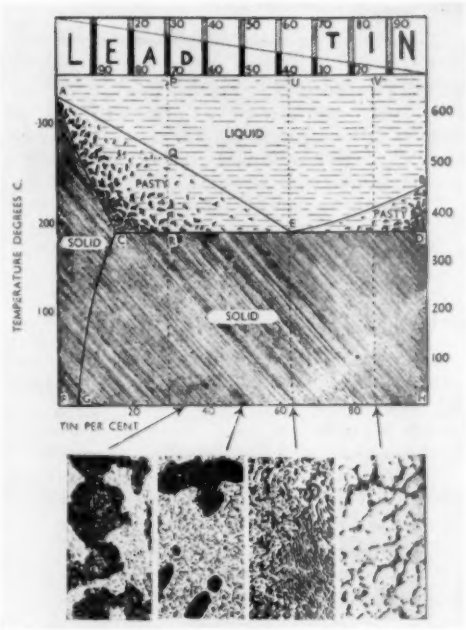

Fig. 2 Equilibrium diagram of the tin-lead alloys

In the pasty range, they are devoid of strength and even at 100° F below the eutectic melting point, solders are only half as strong as at room temperature. For that reason, it is necessary to avoid straining soldered joints before they have had time to cool.

The plastic range of a solder, therefore, has a direct influence on the soldering temperature and on the speed at which the soldering operation can be carried out. For fast soldering, the 60/40 alloy melts most quickly and sets solid most quickly and is the choice over the 40/60 alloy which has a plastic range of almost 100° F.

To get practical speed and a good joint, it is common practice to solder at a temperature of 100–150° F above the actual liquidus of the alloy used.

Wetability and Intermetallic Growth

An indispensable property of soft solders which has given them a wide range of adaptability is their ready adherence to the surface of other metals. This appears to be due largely to the ease with which molten tin wets other metals. This property is usually associated with a slight alloying action. Metals are easily wet by solder if intermetallic compounds are readily formed between some constituent of the solder and the metal parts being joined. Actual penetration of the joint members by molten tin to an extent that is detectable may seldom occur, but the best joints are those where

conditions are favorable for a very slight alloying action. Thus, it is impossible to get sound, strong joints between metals with pure lead because lead does not readily alloy with the base metal. Even a small amount of tin added to lead causes wetting of the joint and a far different effect is obtained.

In the case of steel and copper, the intermetallic compounds consist principally of $FeSn_2$ and of Cu_6Sn_5, respectively. The intermetallic compounds are extremely hard and brittle; they are relatively easy to break by shock or by tearing forces, but they are usually quite strong when tested under steady tension or shear. Thick alloy layers are weaker in tearing tests than thin layers, and for that reason the alloy layers should be as thin as possible. This is accomplished by soldering as quickly as possible and at the lowest possible temperature.

Controlled alloy formation in a joint between copper members improves the creep resistance but it renders the joint more susceptible to fracture by shock or tearing. The rate of alloying at the surface of steel or iron is much slower and the effect on joint strength is of less importance. On brass surfaces, the zinc in the brass as well as the copper reacts with the tin in the solder. Thus, the shear strength of soldered brass joints is rather less than those of copper.

Soft solders are not satisfactory for joints subjected to any appreciable stress, and good design demands interlocking seams, crimping, riveting, etc., to aid in strengthening the joint. Strength also varies with the type of joint, the joint thickness, temperature and duration of soldering. Short-term tensile strengths range from 3700 to 6800 psi; under continuous load the tensile strength is about 300 psi.

Composition of Solders

Typical soft solder compositions are given in Table 3 (Appendix). The three grades most generally used are 40/60, 50/50 and 60/40, the first figure referring to the percentage of tin, the second to lead. Lower compositions of tin-lead are used for specific applications; the 35:65 alloy is widely used in the plumbing industry, the 2:98 alloy is exclusively used for sealing the reinforced side seam of the food can (Fig. 3).

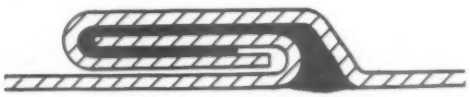

Fig. 3 Cross section of can side seam

The experiences with substitute solders of low tin content have been disappointing because of the frequency of defective joints. The high-tin solders (40–60%) have four outstanding properties:

1. Low liquidus.
2. High wetting power.
3. High capillarity.
4. Shorter freezing and cooling range with greater probability of getting sound joints.

In addition to pure tin-lead solders, small amounts of other metals are added in order to secure increased strength and hardness and for use at temperatures above or below room temperature.

A lead-free alloy of 95 tin : 5 antimony is frequently used in soldering electric commutators, oil coolers, etc., and retains its strength well up to 390° F (200° C). The addition of silver to tin (3.5%) is made to raise the tensile strength, corrosion resistance and conductivity.

Other types of solder include lead-silver, bismuth-lead-tin, indium-lead-tin, cadmium-silver and cadmium-zinc. The bismuth containing solders have shown bad cooling characteristics and are subject to both "hot shortness" and "cold shortness."

Solders which must be exposed to extreme cold should contain more lead than tin and should have an antimony content of not less than 0.5%. The general effects of cold on the mechanical properties of tin-lead solders are an increase in hardness, improved electrical conductivity and a tendency to lower the impact strength.

Impurities other than those metals intentionally added are held to a minimum by reliable solder manufacturers. In particular, zinc and aluminum are detrimental and should not be in excess of 0.001%. The amounts of iron, copper, nickel and arsenic that will be tolerated are covered by specifications given in the appendix.

D. FLUXES AND ATMOSPHERES

The efficiency of the soldering operation is dependent on the chemical cleanliness of the surfaces of the base metal and the molten solder. Metals, whether solid or liquid, become coated with a film or oxide. This prevents proper bonding and must be removed. A soldering flux, solid, liquid or gaseous, is used for this purpose.

The function of a flux is to keep all of the reacting surfaces chemically clean until the base metal and the solder are united. The flux must be able to react with, dissolve or remove oxides; it should be a barrier to the reoxidation of the metal surface; it should be capable of being displaced from the solid metal by the liquid solder. Another important requirement of a flux is that it be fluid below the liquidus of the solder used.

Fluxes, in general, may be classed as inorganic and organic and subdivided into groups of which typical members are listed below:

I. Inorganic Fluxes
   - Acids
     - (*a*) Hydrochloric (muriatic).
     - (*b*) Ortho-phosphoric.
     - (*c*) Hydrofluoric.
   - Salts
     - (*a*) Zinc chloride (zinc and muriatic acid).
     - (*b*) Ammonium chloride (sal ammoniac).

(*c*) Zinc-ammonium chloride (eutectic mixture).
(*d*) Miscellaneous inorganic halogen compounds such as hydrazine hydrochloride, boron trifluoride.

II. Organic Fluxes
Organic acids
(*a*) Lactic acid.
(*b*) Oleic.
(*c*) Stearic.
(*d*) Glutamic.
Organic halogens
(*a*) Aniline hydrochloride.
(*b*) Glutamic acid hydrochloride.
(*c*) Cetyl pyridinium bromide.
(*d*) Ethyl dimethyl cetyl ammonium-bromide.
(*e*) Cetyl trimethyl ammonium-bromide.
Amines and amides
(*a*) Urea.
(*b*) Ethylene diamine.
Rosin fluxes
(*a*) Rosin.
(*b*) Special patented rosin-base fluxes.
(*c*) Activated rosin.

The inorganic acids and salts are corrosive and require postcleaning treatment of the soldered part to remove flux residue and condensed spray. The mixture of nine parts zinc chloride and one part ammonium chloride is both rapid and sure in eliminating oxide films and exposing a clean etched metal surface. The mixture melts far below that of zinc chloride alone and remains fluid at temperatures met with in soft soldering. Proprietary fluxes based on zinc-ammonium chloride are available in an endless number of compositions.

Organic fluxes are, as a class, weaker fluxes than the inorganic acids and salts, and any corrosion products formed are slower in their action. The organic compounds are easily decomposed, yet some are quite active for a limited time. They are useful in quick spot soldering operations where they volatilize completely or leave comparatively harmless residues which are easily removed.

Rosin, the best known and most widely used organic flux, is only mildly active but is unusual in leaving a noncorrosive residue which is nonconductive and whose hard shell is impervious to air and moisture. Recent attempts to combine the speed of an active acid flux with the protection of a rosin residue have resulted in a large class of activated rosin fluxes. Activated rosin fluxes, supplied as a liquid or in a solder core, are more active than rosin and satisfy the need for high production speeds. They are based on the theory that the activating agents are decomposed at the soldering temperature, are either inactive in the flux residue, or are unable to penetrate through the impervious surface of the rosin. Practical tests in their use are advisable especially when closed assemblies are to be joined.

It is sometimes convenient to have fluxes in the form of pastes. Paste fluxes can be applied easily and can be carried as a core in a wire of solder and applied simultaneously with the solder. Paste flux is often mixed with powdered solder to form a soldering paste. This method of applying the flux and the solder is well suited to oven soldering and to resistance and induction heating.

Gaseous fluxes such as hydrogen chloride have up to now rather limited application because of economic factors involved in their use.

A convenient summary of fluxes and their uses is given in Table 1 (Appendix).

E. JOINT DESIGN

Parts should be designed with the requirements of the soldering process in mind so that it is easy to make good joints. Hand soldering is still extensively used but where there is sufficient production of a unit to warrant development and installation of soldering machinery, semiautomatic and automatic soldering means have flourished. In automatic soldering, the joint is usually of relatively simple design so that it requires little individual attention.

Tin, lead and their alloys, the solders, are weak metals in comparison with steel, copper and brass upon which they are used. Under sustained load or stress, solders cannot safely withstand a load of more than about 300 psi. Joint design, therefore, should avoid dependence upon the strength of the solders. Surfaces should be shaped so that they engage or interlock and leave the solder principally the functions of sealing and solidifying the assembly. One good example of joint design is seen in the interlocking joint members of a food can (Fig 3) which can withstand a bursting pressure from inside of three or four atmospheres.

Spot welding or tacking of the surfaces before soldering to relieve stress is part of the design picture. Soldering at corners or edges where the stress is greatest should be avoided. In some cases, lids and ends of containers can be formed by stamping or pressing so that the soldered seam is on the side. Lock seams are stronger than lap seams.

Joints should not be too close to insulation which might be damaged by heat, nor should they be placed close together so that there is risk of melting or weakening the joints made earlier.

Joint clearance is important in designing the part. Parts to be joined should fit closely so that the space between them is narrow enough to become completely filled with molten solder, drawn in by capillary force as the solder wets the metal. On the other hand, when there is not enough clearance between surfaces, the solder can not penetrate and dry joints may result at some points.

In general, a clearance of from three to five thousandths of an inch is satisfactory with surfaces that have not been coated with tin or solder before being assembled. In the case of round or tubular members, this

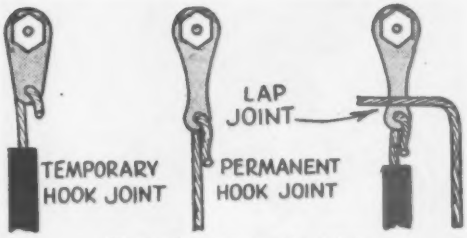

Fig. 4 Three types of lug joints

means a clearance on the radius. When tinned metals, such as tinplate, are to be joined, a clearance of one thousandth of an inch is sufficient.

In designing the clearance, thermal expansion or contraction must be allowed for, particularly if the metals are dissimilar. A good rule is to allow for a rise in temperature of about 500° F. For making long soldered seams it is advisable to specify tacking the surface at the middle and then at each end and at 2 or 3 in. intervals in between; this method maintains more uniform temperature conditions and reduces buckling due to uneven expansion.

The joining of lead pipes requires special designing. The outlet pipe is opened to form a socket of slightly wider angle. The spigot or inner pipe is smoothly tapered to fit closely at the interior end of the socket; this permits solder to penetrate easily but not flow into the pipe. Care is needed when fitting branch joints to prevent the branch projecting into the bore of the main pipe.

Three types of joints most often used in connecting wire to lugs are the temporary hook, permanent hook and lap joint (Fig. 4).

The joining of wires is illustrated in the Western Union splice and the Bell splice (Fig. 5).

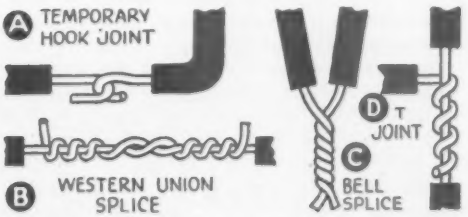

Fig. 5 Western Union splice and Bell splice

F. PRECLEANING AND SURFACE PREPARATION

One of the first and most important considerations in making a perfect joint is that the two surfaces are chemically clean, i.e., free from oxides, grease or rust.

Methods of cleaning the surface preparatory to soldering may be either mechanical or chemical. Mechanical methods make use of abrasive wheels, filing, scratching or shaving. Shot blasting is an effective method as is rubbing with steel wool. Freshly machined parts require no further preparation.

Chemical methods involve the removal of grease with organic solvents or with hot alkaline detergents. Rust on steel or heavy oxide coatings on copper are effectively removed by immersion in inorganic acids. On complicated assemblies, light pickling is the most efficient method of surface preparation.

A convenient and well used method of preparation for soldering involves precoating the surfaces with tin or with tin-lead solder. Precoated parts simplify the soldering process, speeds up the operation, and usually avoids the need for a corrosive flux. Small parts can be precoated in large quantities by immersion in hot tin or in solder of the same composition used to fill the joint space. Excess solder can be removed by rotating in a centrifuge.

Parts can be precoated with tin or solder by electrodeposition. This method is especially recommended for brass. Large parts are plated in conveyorized equipment. Small parts are better done in a wire basket suspended in the bath or in a rotating barrel suspended in the bath. The recommended minimum thickness of electrotinned coatings for soldering are as follows:

Thickness in Inches of Electro-Tinned Coatings for Soldering

Brass	0.0005
Copper	0.0003
Steel	0.0002

Difficult-to-tin metals may be given an electrodeposited coating of copper, iron, silver or tin-zinc if preferred. All of these coatings facilitate soldering.

G. ASSEMBLY

Proper means of securing parts firmly together during the soldering operation and subsequent cooling are essential.

For occasional work, parts can be bound together with wire, with screw clamps, toggle clamps, pliers, pressing together under a weight held in a vise or by spring clips. Spring loaded clamps are most useful because they squeeze parts in closer contact as soon as their tinned surfaces are melted; but spacers may be necessary to provide the proper clearance for penetration of the solder.

For repetition work and in automatic machine soldering, clamps, jigs, skeleton mandrels are used. They usually conform to the following requirements:

1. Be simply and quickly fixed or removed.
2. Hold the parts firmly and accurately.
3. Not obstruct the operator.
4. Withstand repeated heating or cooling.
5. Not hinder the quick heating or cooling of the parts.

6. Not become tinned and stick to the article.

In electrical resistance soldering, the clamps can also act as electrical connections for the heating current; for this purpose they must be massively made from good electrical conducting metal. When high-frequency heating is used, the clamps must be so placed that they do not shield the joint.

Spot welding or tacking at a few points is a common method of assuring that the parts are fixed together. Seams of containers are then readily soldered by simply dipping in solder.

H. SOLDERING TECHNIQUES

This section is devoted to a complete coverage of the heating methods mentioned earlier in Section A.

Soldering with the Copper Bit

The traditional tool is the copper bit. The bit must have a large heat storage capacity which is the product of its weight and specific heat. The weight is limited by the ability of the operator to wield it and by the need to be small enough to reach the joints in confined spaces. Nickel, iron, aluminum and zinc have thermal capacities per unit volume equal to silver or copper but are far inferior in thermal conductivity, that is, the capacity to deliver heat to the job. They make poor substitutes for the copper bit.

The size of the bit is determined by the rate at which it has to supply heat to the work. This depends upon the conductivity of the metals being soldered and the volume of metal within heating range of the bit while it is raising the joint surface to soldering temperature.

Fig. 6 Bit soldering of electrical connections on ignition coil base (Ford Motor Co.)

Fig. 7 Soldering operation on television components (Radio Corporation of America)

If continuously heated, the bit need not be massive in comparison with the work.

Assistance in the selection of the size of the copper bit to fit the work may be found in the Appendix, Table 2.

The copper bit can be electrically heated, or heated by a burner built into the iron, or externally heated by means of a furnace or torch (Fig. 6).

The electric iron consists of a wire-wound resistance unit in the body which generates heat. The heat in turn is delivered through a conductor to the copper tip. In addition to the plain copper bit, special armor clad tips are available. A thin sheath of plated iron eliminates excessive wear, oxidation, pitting and alloying of the copper with the solder.

Temperature-regulating equipment aids greatly in production soldering. A temperature-regulating stand equipped with a variable resistor allows individual control in use and while the iron is idle (Fig. 7).

In production soldering, devices are available which are treadle operated and can be had with automatic adjustable solder feed so that both hands may be used on the work. A trigger-type soldering gun is an adaptation of the soldering iron.

The function of a soldering bit is:

1. To store and carry heat to the work.
2. To store molten solder.
3. To deliver molten solder.
4. To withdraw surplus solder.

To store and carry heat to the work requires proper consideration of the bit size in comparison with the work to be done.

If the bit is to act as a reservoir for the molten solder, the tip or face must be completely wetted or "tinned" with molten solder. To tin the bit, the heated iron is filed or cleaned free from scale, fluxed and placed in contact with solder on a tinned plate until the surface is solder coated. A cloth pad wipe is useful in removing the excess solder. This "tinning" is repeated whenever the working faces become tarnished or drossy.

The solder when applied between the work and the properly tinned bit will become molten. The bit is used to pick up and deliver the solder evenly over the joint. A slow back and forth motion with a firm pressure is all that is needed. After this initial application, a thin fillet is built up, and the excess solder is removed on the iron as it is withdrawn.

Soldering by Torch or Flame

The torch is one of the fastest methods of applying heat. It provides a means of applying a high temperature source of highly localized heat, and for that reason the soldered joints can be made with the minimum of heating of the article as a whole. Various combinations such as gas and air, gas and oxygen, oxygen and acetylene are used.

The torch may be hand operated where much depends on the skill of the operator in directing the flame of the right size for just the correct interval of time (Fig. 8). Torch soldering is especially useful for filling seams on large articles made of sheet metal. It is also used in filling weldmarks and dents in automobile bodies.

Can lids and boxes of special design are soldered by passage or rotation between a double row of Bunsen type jets. The solder is sometimes applied as a preform or as a paste in flame soldering methods.

Hot Plate and Oven Soldering

The principle of hot plate soldering is that cleaned and fluxed parts, painted with solder paste over their adjoining surfaces, may be clamped firmly in contact and placed on a heated plate a sufficient time to allow the solder to run. Foil or wire preforms may be substituted for solder paste.

Fig. 8 Flame soldering Brittania metal

Oven soldering is similar to hot plate soldering. A nonoxidizing atmosphere may be used. The work, properly cleaned, fluxed and with the solder applied to or between the surfaces to be joined, is conveyed through an oven for an interval sufficient to melt the solder. Clips and jigs are essential to maintain proper alignment.

Induction Soldering

The special merit of high-frequency heating is the close control of temperature which is possible without risk of local overheating. Local overheating may soften, work harden or anneal adjoining surfaces and cause damage to the work.

Induction soldering is particularly well adapted to continuous and automatic production. The class of soldering operation especially suitable is where everything is prearranged; the small assemblies, properly fitted, are fluxed, solder applied as paste or preform, and are conveyed between the high-frequency coil to raise the temperature of the assembly in the immediate vicinity of the joint to the soldering temperature.

High-frequency current is passed through one or more copper tubes provided with water cooling. Through the coil there is an intense magnetic flux. When a piece of metal is placed in this magnetic field, there is induced in it an eddy current which flows in the opposite direction. These induced eddy currents flowing in the metal produce the heating effect.

There are several variables which affect and may be used to control the intensity of the heating. The frequency can be varied, and it is possible to vary the voltage, the number of turns in the coil, the shape of the coil, the spacing between the coil and the assembly, or to vary the time of application of the energy.

Innumerable arrangements are possible in achieving the passage of the assembly through the coil. If the job is large, the current may be applied for a predetermined time. The same may be done for a batch of articles. In other cases, the current is continuously applied and the surfaces to be soldered are moved on a belt at a controlled rate. Again, articles may be brought in one at a time on a rotary table and removed at fixed positions (Fig. 9).

Coils are of an infinite variety of shapes. They are fitted as closely as practicable to the assembly. In some cases where heavy material must be joined to light material, external and internal coils having different energy inputs are used.

Some major considerations in the use of induction heating for soldering should be noted. Rate of heating is important. Very rapid heating is possible but not desirable. Surface heating in the small area of contact is rapid, that of the screened surfaces slow. Heating should proceed at a speed comparable with the speed at which heat can flow to the other surface by thermal conduction.

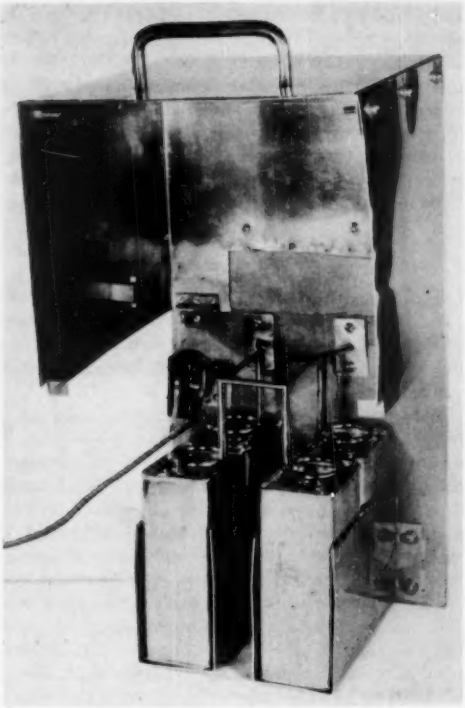

Fig. 9 Induction soldering

Surface oxidation is avoided by protection with a flux. Washers, rings, disks and foil forms of solder can be coated with flux or the flux incorporated in the solder core.

The clips or jigs should be designed so as not to shield the work from the energizing coil. Parts should not be clamped too tightly so that all the solder is forced out. A clearance of 0.003 to 0.005 in. is desirable.

Dip Soldering

Dip soldering comprises a method of immersion of the articles in a bath of molten solder after the usual cleaning and fluxing treatments. The surfaces are wetted and wherever the interstices are sufficiently narrow, the solder is retained between them by capillary attraction until cooled when it exerts its usual adhesive and solidifying actions. The dipping process is confined to joining two surfaces where the clearance between them is small. A typical example is in the manufacture of automobile radiator cores.

The size of the bath is decided by the size of the articles and the depth they are submerged (Fig. 10). As a source or reservoir of heat, the bath should be of sufficient size to minimize great fluctuations in temperature.

It is advisable for fast working to maintain the solder temperature above its liquidus. i.e., 100 to 150° F above

Fig. 10 Dip soldering of armatures (Westinghouse Electric Co.)

the liquidus of the solder used. Excessive operating temperatures increase drossing, may cause distortion of the sample and also increase the chance of forming brittle alloy layers as well as causing discomfort to the operator.

The operating temperature of the bath is governed by the composition of the solder. The eutectic composition, 63 Sn-37 Pb, offers a low operating temperature, speedy wetting and penetration of joint crevices, superior resistance to corrosion and fatigue. Solder of eutectic composition rapidly attacks copper and brass which may lead to contamination of the solder and give rough gritty coatings. The low-tin solders on the other hand have a high operating temperature, less rapid wetting ability, but have reduced action on copper and brass.

Electrode Soldering

In this method, the article is joined to one terminal of a low voltage supply and the soldering tool to the other. The tool consists of a carbon resistance rod which completes the circuit so that heat is generated whenever the bit is in contact with the work.

The working surface of the electrode can be shaped to fit the article to be soldered so that heat is applied simultaneously to a joint of long length. An independent circuit breaker is used to cut off the heat leaving the tool in position and serving to clamp the work until it solidifies. Pliers with electrodes fitted to the jaws are also worked on this principle.

Resistance Soldering

The principle is that the heat for melting the solder is

brought about by the resistance at the joint surfaces when a large current is passed. A piece of solder foil or a smear of solder paste is placed between the joint surfaces which are pressed firmly together by spring clips connected to the terminals of a low voltage supply. When the circuit is completed, there is rapid local heating which melts the solder, enabling it to wet the surfaces; in consequence, the resistance falls and the current rapidly builds up until it actuates a circuit breaker. The heat is rapidly dissipated to the metal close to the joint and the solder sets almost instantly.

Advantages of resistance soldering are the clean and neat appearance of the joint. The soldering operation is a rapid one, and several joints can be made simultaneously. Resistance soldering of fender members is being done in the automobile industry.

Spray Soldering

Spray soldering is a limited application whereby solder is applied with a metallizing gun. This method is used for repair on auto bodies or to conceal hammer and roller marks before painting.

Supersonic Soldering

Supersonic soldering is a relatively new method whereby the solder is made to key or penetrate on the base metal by interatomic attraction. The method depends on the cavitation erosion of surface oxide by sound waves. Ultrasonic frequencies usually in the range of 16–20 kc/sec are used for promoting cavitation. The ultrasonic soldering iron generates ultrasonic power in this range by means of a magnetostriction unit. This method of soldering is especially adaptable to the joining of aluminum. Tinning and joining is effected only in the immediate proximity of the point of contact with the iron. Long seams and large massive sheets are not within the scope of the iron.

I. POSTSOLDERING OPERATIONS

Cooling the Soldered Joint

Several factors are involved in cooling the joint to atmospheric temperature. If the joint is held at the soldering temperature, the growth of intermetallic compound into a thick layer of larger crystals aggrevates the brittleness of the bond. It is advisable to cool quickly down to the solidus. Below the solidus for a considerable range, down to 140° C (285° F) as a rule, solders continue to be structurally weak and liable to fracture from jolting or vibration. This state is called "hot-shortness." It is particularly noticeable with solders between 7 and 20% tin.

The temperature range between the solidus and about 140° C (285° F) should be passed through as quickly as possible without movement to reduce the opportunity for cracking.

Metal articles soldered by hand are usually cooled quickly by conduction from the joint into the adjacent colder metal. Mechanically soldered work on moving belts or mandrels is cooled by an air blast or by applying water. From the production point of view, the aim in soldering is to put in just the amount of heat needed to melt the solder and heat the surfaces sufficiently to allow penetration.

Removal of Flux Residues

Excess flux of the inorganic type will cause severe corrosion later if not removed. The inorganic acids are easily removed with a water rinse. Fused residues of zinc chloride will cause severe corrosion. They are best removed at once by washing in hot water containing a few drops per gallon of muriatic acid. This acidified water removes the white water insoluble crust of zinc oxychloride which retards the removal of the residue beneath. A subsequent treatment in hot water containing some crystals of washing soda assures removal of all acidic compounds.

If the articles are allowed to stand for some hours before rinsing, the zinc chloride absorbs moisture from the air and in this state is more easily removed by washing when nonacidified water has to be used.

Some of the organic flux residues can be removed simply by rinsing the part in hot water. This procedure is advisable unless rosin is the flux.

Rosin residues are noncorrosive and need not be removed. Methyl and ethyl alcohol, trichloroethylene, however, are efficient solvents for rosin if the production job requires a clean joint.

Smoothing the Joint

Solder used as body filler to smooth welded joints in automobile bodies requires mechanical treatment with a grinding wheel before painting. Articles to be plated after soldering may also require filing or smoothing.

J. INSPECTION

Inspection is the last of the basic steps in soldering. Methods of inspection to be employed are generally determined by the application for which the assembled part is to be used. In most cases inspection procedures are specified by the ultimate user.

Inspection methods fall into one of two classifications: Nondestructive and destructive.

Nondestructive Examination

The most widely used method of inspection is visual examination; comparisons are usually made with specimens which show minimum acceptable quality of the soldered joint. Visual inspection is a convenient method in production line soldering; it is often possible to repair slight defects with torch or iron without in-

terrupting production. Visual inspection under ultraviolet light is often used in inspecting the soldered seams on wax or oil filled capacitors.

Pressure testing is necessary where gas or liquid tightness is required of a joint. Automatic air machines are used in can manufacture (Fig. 11); refrigerator parts are gas tested and joints designed for liquid tightness are tested hydrostatically. Test pressures are always greater than service pressure requirements and are usually specified by purchase agreements.

Destructive Testing

It is common practice to select a small percentage of all production for destructive testing.

The peel test is generally employed for shear or lap joints to determine the quality of the bond and the appearance of voids in the joint. Sawing of the part across the joint and sectioning the joint under a binocular microscope is used more widely for development than for production control, although selected samples are often tested in this way. Tension or shear tests, impact tests, fatigue tests, and corrosion tests are seldom used for quality control but they are useful in determining causes of failure.

K. SOLDERING THE INDIVIDUAL METALS

The purpose of this section is to amplify the information of a general nature about each specific metal covered in the article. All of the soldering processes mentioned earlier can be applied to most metals, but the use of special techniques and special solders requires clarification.

Carbon and Low-Carbon Steels

Low-carbon steels can be soldered successfully with any type of tin-lead solder and by any of the recognized processes. Provided the steel is clean and an acid type flux is used, no difficulties should arise. Precoating of steel with tin or solder facilitates soldering with noncorrosive fluxes.

Stainless and Alloy Steels

Stainless steels are soldered with more difficulty because of their low thermal conductivity and because of the tightly adhering oxide film on the surface. Stronger fluxes such as zinc chloride fortified with from 1 to 25% muriatic acid are necessary. Stainless steels containing molybdenum, titanium or columbium may require a flux containing a few per cent hydrofluoric acid in addition to the zinc chloride and muriatic acid. Proprietary fluxes formulated for stainless steel are available from most flux manufacturers. Care should be used in handling and removing such fluxes.

Tin-lead solders can be used successfully on stainless steels by using any of the customary processes. Silver-tin solder is sometimes used. Hand soldering requires the use of a large bit to overcome the poor conduction of the heat.

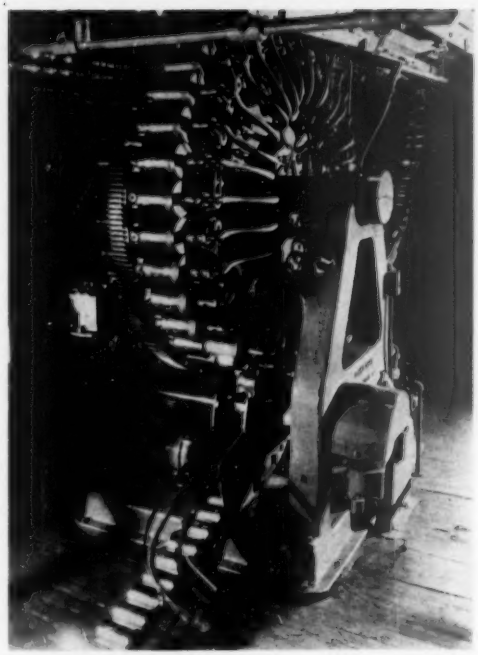

Courtesy National Can Co.

Fig. 11 Can tester. Faulty cans ejected automatically. Rate five cans per second

Overheating of the soldered members should be avoided since embrittlement of the stainless steel may occur if the temperature of the joint exceeds 700° F. Thin gage materials should be clamped together to prevent buckling or movement of the parts.

Precoating of stainless steel parts to improve soldering also applies.

Cast Iron

Cast iron can be difficult to solder because it may have an oxide skin, a smear of graphite or even minute particles of sand on the surface.

Shot blasting followed by degreasing is the most effective cleaning process. Tinning of the surface by intense rubbing with the iron and with solder will aid in preparing the joint. Pretinning of cast iron by hot dipping or by electrolysis is highly recommended if a mild flux must be used. Repair of heavy castings requires the use of torch heating.

Copper

Copper parts are the easiest of the metals to solder. Any type of tin-lead solder is applicable, but 40–50% tin is most used. Cleaning the metal can be effected by

abrasion or by dipping in weak acids. Rosin flux is almost exclusively used. Copper will dissolve in molten solder so that the soldering temperature and time of soldering should be kept to a minimum.

Copper Alloys

(*a*) *Brass.* Enormous amounts of brass components are soldered daily although the incompatibility of the tin in the solder with the zinc in the brass makes soldering difficult sometimes. Brass is easily abraded or lightly pickled to provide a clean surface. If given an electrotinned coating, much of the difficulty is avoided.

Solders should contain 40–50% tin, but the solder should be nonantimonial with a limit of 0.5% for the antimony. Antimony also combines with the zinc in the brass to form coarse crystals that render the joint brittle. Rosin flux is effective if the brass is chemically clean. Acid fluxes, of course, are always effective. Chemically clean brass, bronze or copper can be preserved with a "water-dip" lacquer coating which does not impair subsequent soldering.

(*b*) *Bronze and Gunmetal.* The true bronzes contain only copper and tin but sometimes lead is added for special purposes. The bronzes solder readily with the higher tin solders. Solder composition of 45–60% tin are recommended because bronze articles are normally specified for arduous duties. The gunmetals contain a few per cent zinc, but they are readily soldered like the bronzes.

(*c*) *Aluminum and Silicon Bronze.* Aluminum and silicon bronzes are not readily soldered unless they have been specially cleaned. The superficial oxide forms in air, and it is necessary to dip in flux immediately after cleaning.

Cleaning by the Kolene Process, by sodium hydride, by treatment in hydrofluoric acid, or in a mixture of hydrochloric and nitric acids has each been advocated. The flux recommended consists of equal parts of hydrochloric acid and zinc chloride (25% in water). Post-cleaning of the part is essential.

(*d*) *Beryllium-Copper.* Beryllium-copper also forms hard and infusible oxide in air and requires special cleaning before soldering. Since beryllium-copper is used in the manufacture of balance wheels, springs aneroid diaphragms, hearing aids and Bourdon gages, it is important that a noncorrosive flux be used. Beryllium-copper will not solder if plain rosin is used; rosin flux activated with glutamic acid hydrochloride or with cetyl pyridinium bromide has been successfully used.

Nickel and Nickel Alloys

Nickel alloys such as Monel, Inconel, nichrome and nickel-plated parts cannot be soldered with plain rosin flux. Nickel plate and Monel solder reasonably well with activated rosin fluxes. The usual choice of flux is zinc-ammonium chloride with free muriatic acid as in stainless steel. The ordinary types of tin-lead solder are satisfactory, but a hotter iron than is used on mild steel is necessary.

Lead and Lead Alloys

The joining of lead to lead and lead to other metals such as copper and brass requires a special technique of wiping and also requires a solder with a long pasty range. A solder containing about 35% tin and 65% lead is employed.

The joints are prepared so that the two ends form a bell and spigot which are then placed in close contact. The pipe away from the joint is covered with plumber's black to keep the solder from adhering. The pipe in proximity to the joint is shaved clean and immediately covered with tallow.

Two methods of tinning the joint can be used:

(1) Blow-lamp method: The flame is played over the prepared area and when the surface is hot enough, a solder stick is applied to tin the surface around the pipe. Additional solder is built up and is caught on a wiping cloth which has been soaked in tallow and then worked around and around to insure an even consistency in the plastic mass. The plastic mass is melted off onto the cloth and then wiped around the pipe. The molten pasty solder is kept moving and the shaping completed before any setting is apparent.

(2) Pot-wipe method: The pipes are assembled and fluxed with tallow. Molten solder is ladled or splashed onto the joint. The solder solidifies at first but gradually the mass gathers heat and becomes pasty. The pipe becomes tinned and some fully molten solder is drawn into the joint by capillary attraction.

The pasty solder is wiped around the pipe and gently molded into a smooth curve, the greatest thickness being over the junction of the pipe ends. Excessive thickness of the joint, however, should be avoided. At the proper wiping temperature (640–680° F), the solder has a bright metallic gleam and a creamy consistency. Porosity is guarded against by applying a layer of pasty solder after the wipe is made. When the surface is wiped, liquid solder, rich in tin, is drawn into the surface and fills up any pores.

Joints in Lead-Sheathed Cables. The jointing and splicing of lead-sheathed cables involves a combination of two methods of soldering. The copper conductors are joined by sweating and the lead sheathing by wiping. Improvements in cable wiping techniques have indicated that small fillet wipe joints are easier to make and less likely to be porous. The fillet wipe uses much less solder and there is much less tendency to draw eutectic from the space between sheath and sleeve because thermal conduction causes rapid solidification of the solder at the joint. The addition of 0.1% arsenic to wiping solder adds to the strength of the joint.

Pipes made of the ternary alloy of lead, 98.25% lead; 1.5% tin; 0.25% cadmium and pipes of tellurium-lead or calcium-lead are soldered or joined in the same way as ordinary lead pipe.

In recent years, there has been a movement to replace wiped joints by plain chamfered joints having the mating surfaces shaped to fit with precision.

Aluminum

With proper materials and methods, it is entirely practical to join many aluminum assemblies by soldering. The size of the parts being joined is the critical factor. Small parts can be soldered; large parts await development of a practical method.

The high thermal conductivity of aluminum (three times that of sheet iron) poses the problem. Small parts can be brought up to soldering temperature, roughly 550–700° F, and held there. On large parts, the sections adjoining the area to be soldered will conduct heat away so fast that it is not possible to hold the working area at the correct temperature long enough to complete the joint. Also distortion enters the picture because of aluminum's greater coefficient of expansion. The practical limits appear to be near a maximum of 20 sq in.

One method that appears to offer the most possibilities is the vibrating of the work at supersonic frequencies while making the joint. This breaks up and helps remove the oxide film. The power output of ultrasonic equipment appears to be sufficient only for small parts. The development of more powerful supersonic equipment may eventually overcome present size limitations.

Special fluxes usually containing fluorides are manufactured and are commercially available.

In the friction method no flux is used. The coating of oxide is broken up by mechanically abrading the surface of the aluminum through a layer of molten solder. Best abrading action is obtained with a multiple-toothed tool such as a wire brush or hacksaw blade. Properly tinned aluminum surfaces can then be joined by sweating and pressing the surfaces together until the solder cools and solidifies.

Most alloys sold commercially for soldering aluminum contain 70–90% tin with the balance zinc. For many years, a 70 tin–30 zinc has been recommended, but the 90 tin–10 zinc alloy has superior corrosion resistance when the joints are exposed to a humid atmosphere.

For most parts, and especially massive parts, a torch is preferred using a neutral or reducing flame. Avoid overheating the flux. Temperatures above 750° F cause the flux to form a crust, and the entire operation may be spoiled. It is advisable also to use a solder and flux designed by the manufacturer to work together.

Flux removal is vital. A recommended procedure is to apply a 2% solution of sulfuric acid followed by a 1% nitric acid solution and rinsing in warm water.

Commercial and high purity aluminum are the easiest to solder. Next come the wrought aluminum alloys containing not more than 1% manganese or magnesium. The heat-treatable aluminum alloys are more difficult. Soldering cast and forged aluminum parts can be done but is not generally recommended.

In soldering aluminum to other metals, the parts may be coated with tin or cadmium. An important factor to consider is electrogalvanic action if the parts are to be exposed to moisture.

Electroplated Coatings

(*a*) *Tin.* Tin and tin-lead plated parts are extremely easy to solder with noncorrosive fluxes. The thickness of 0.0003–0.0005 in. of tin assures good storage properties. The slight oxidized film which forms on long storage may be removed by tumbling. Water dip lacquers applied immediately after plating enhance storage properties.

(*b*) *Cadmium.* The soldering characteristics of cadmium on copper or brass are about two-thirds that of tin using a resin-type flux. On steel, a coating thickness of not less than 0.0003 in. is usually specified. Preplating the steel with copper assists in soldering with mild fluxes. If it is permissible to use zinc chloride solution, cadmium can be soldered readily but usually a hotter iron than is needed on tin is required.

(*c*) *Nickel and Chromium.* The flux that gives the best results is the ordinary zinc chloride solution containing muriatic acid. The solder should contain 50–60% tin.

(*d*) *Silver.* Silver plating can be soldered readily with the usual qualities of tin-lead solders using noncorrosive rosin fluxes. Thin silver coatings dissolve in the solder. The silver coating should be not less than 0.0003 in., preferably 0.0005 in. thick.

(*e*) *Zinc Plating and Galvanized Iron.* The soldering of zinc coatings is practically impossible with rosin fluxes. Some activated rosin fluxes have come on the market and have met with slight success.

A zinc chloride flux containing free hydrochloric acid is the most effective.

(*f*) *Tin-Zinc and Tin-Nickel Plating.* The new tin-alloy electroplates recently developed as corrosion resistant coatings for iron and steel are readily solderable with rosin or other mildly reactive fluxes.

L. APPENDIX

Manufacturers' Data

Soft solders are manufactured in an endless variety of forms to meet special needs and circumstances, among them being:

Pig, Slabs and Ingots. Pig solder is supplied in 50- and 100-lb lots and in slabs weighing 15 or 35 lb. Ingots weighing 5 and 10 lb can be produced in any desired analysis of lead and tin.

Bar Solders. Regular bars—hand cast, weighing 1 1/2, 1 or 1/2 lb each. Capping bars—1/4 x 1/4 x 12 in. long, weighing 1/2 lb. Also available in half-pound cross section. Meter bars—3/8 x 1/4 x 14 in. for seam soldering gas meters. Triangular bars—14 in. long with 1/4-, 5/16- and 3/8-in. sides. Tinner's bars—12 in. long, 1/2 to 3/4 in. wide, 1/2 in. thick.

Table 1—Soldering Fluxes

Flux	*Characteristics*	*Use*
Rosin Activated rosin	Noncorrosive, nonconducting, nonhygroscopic	Electrical
Tallow	Very mildly corrosive	Lead, brass, clean copper
Stearic acid	Mildly corrosive, almost nonconductive	Electrical, lead
Aniline phosphate or aniline chloride	Mildly corrosive, almost nonconductive	Electrical
Lactic acid Phthalic acid Phosphoric acid mixed with tallow, resin, etc.	Mildly corrosive, slightly conductive	Electrical
Zinc chloride	Corrosive	Iron, steel, zinc, copper, brass, bronze, terne and lead plate
Zinc chloride and HCl	Corrosive	Stainless steel, nickel and Monel
Zinc chloride + HF	Corrosive	Brasses and bronzes containing aluminum, silicon and manganese
Orthophosphoric acid	Corrosive	High-tensile manganese bronze
Numerous proprietary pastes usually containing zinc chloride	Corrosive	.....
Zinc chloride and ammonium chloride	Corrosive	Iron, zinc, copper, brass, bronze
Dilute hydrochloric acid	Corrosive	Dirty zinc
Fused salts of zinc chloride and ammonium chloride	Corrosive	On dip pots

Wiping Solder. For plumbing, cable work and other joints. Wiping solder is supplied in cakes or oval-shaped bars weighing 1, $2^1/_2$ or 5 lb each.

Auto Body Solder. Furnished in convenient lengths, $^3/_8$ in. square, weighing 4 to 8 oz.

Ribbon Solder. An extruded product for laying in seams. Supplied in thicknesses of $^1/_{16}$ to $^3/_{16}$-in., in widths $^1/_8$ to 1 in. Available in 12-in. lengths or on spools.

Drop or Segment Solder. Triangular bar or wire solder cut in lengths or slices to make 500 pieces to the pound. Convenient for preplacing in accessible places.

Powdered Solder. For use in tinning, making solder pastes or other special applications. Available in any tin-lead composition and in screen size down to 200 mesh.

Solder Foil. Foil available in thicknesses 0.00125 in. upward. Sheets 24 x 36 in. in thicknesses from 0.01 to 0.10 in.

High-Temperature Solder. Available in 1-, 5- and 50-lb wire spool of composition 95% tin, 5% antimony. Melting range 450 to 464° F.

Wire Solder. Extruded wire starting from 0.010 in. diam to 0.25 in. in 1-, 5-, 20-, 25- and 50-lb spools, available in a wide variety of compositions.

Flux Cored Solders. A variety of wire and flux combinations are on the market. One type has the flux grooves on the outside of the wire, others have more than one flux core. All are designed to get the flux on the work first and to avoid dry sections in the core. All cored solders are available in diameters from 0.01 in. and in spools of 1 to 50 lb.

The acid core solders are used for general-purpose soldering. The flux is corrosive and generally is a combination of zinc and ammonium chlorides. These fast-acting flux solders remove oxides quickly to produce a quick and lasting bond.

The organic type core solders have corrosion characteristics intermediate between the acid type and the noncorrosive rosin type. The residues are easily removed with water after soldering.

The rosin cored solders are an integral part of solder-

Table 2—Selection of Bit Size

Work to be done	*Choice of tip diam, in.*	*Approximate watts of electric iron*	*Weight size of nonelectric iron, lb*
Very light radio, telephone, electric appliance, fuses, fine instruments, and for home use	$^1/_8$– $^7/_{16}$	44–52	$^1/_2$ (1 lb per pr.)
Medium soldering on switchboards, telephones, radios, electric appliances and light manufacturing	$^3/_8$– $^1/_2$	60– 70	1 (2 lb per pr.)
Fast soldering on radios, telephones, electrical appliances, jewelry, etc. For light medium jobs in home, factory and schools	$^3/_8$–$^9/_{16}$	85–100	$1^1/_2$ (3 lb per pr.)
High-speed soldering on radios, telephones. Medium light soldering on tinware, toy motors, type bars, fuses, etc., tinsmithing, plumbing and wiring	$^5/_8$– $^7/_8$	130–150	2 (4 lb per pr.)
High-speed soldering on light tinware, art glass, toys, small metal patterns, organ pipes, etc.	$^5/_8$–1	170–200	$2^1/_2$ (5 lb per pr.)
Medium tinware, light roofing; gutters, ventilating flues; electrical, airplane and other medium manufacturing; ship repairs	$^7/_8$–$1^1/_8$	225–250	3 (6 lb. per pr.)
Roofing, refrigerators, copper and galvanized iron, heavy tinware, metal patterns, ship, auto and airplane building	$1^1/_8$–$1^3/_8$	300–350	4 (8 lb per pr.)
Heavy roofing and cornices, vats, tanks, ventilating flues, auto radiators, armature, plumbing and ship building	$1^3/_8$–$1^3/_8$	350–650	5 (10 lb per pr.)
Extra heavy duty work	2	1250	10 (20 lb. per pr.)

NOTE: Above sizes of tip diameters vary according to the make of electric irons and size used depends upon the working space available.

Table 3—ASTM Specifications for Soft Solder Metal (B 32-49) Properties of Soft Solder Alloys

—Nominal composition, %— Tin	Lead	Antimony	Specific gravity*	—Melting ranges, ° F.— Solidus	Liquidus	Uses
70	30	...	8.32	361	378	For coating metals.
60	40	...	8.65	361	374	"Fine solder." For general purposes, but particularly where the temperature requirements are critical
50	50	...	8.85	361	421	For general purposes. Most popular of all
45	55	...	8.97	361	441	For automobile radiator core and roofing seams
40	60	...	9.30	361	460	Wiping solder for joining lead pipes and cable sheaths. For automobile radiator cores and heating units.
35	65	...	9.50	361	477	General purpose and wiping solder
30	70	...	9.70	361	491	For machine and torch soldering
25	75	...	10.00	361	511	For machine and torch soldering
20	80	...	10.20	361	531	For coating and joining metals. For filling dents or seams in automobile bodies
15	85	...	10.50	440†	550	For coating and joining metals
10	90	...	10.80	514	570	For coating and joining metals
5	95	...	11.30	518	594	For coating and joining metals
				Tin-Lead-Antimony Alloys		
40	58	2	9.23	365	448	Same uses as (50-50) tin-lead but not recommended for use on galvanized iron
35	63.2	1.8	9.44	365	470	For wiping and all uses except on galvanized iron
30	68.4	1.6	9.65	364	482	For torch soldering or machine soldering except on galvanized iron
25	73.7	1.3	9.96	364	504	For torch and machine soldering, except on galvanized iron
20	79	1	10.17	363	517	For machine soldering and coating of metals, tipping and like uses, but not recommended for use on galvanized iron
0	97.5	2.5 Silver	11.35	579	579	For use on copper, brass and similar metals with torch heating. Not recommended in humid environments due to its known susceptibility to corrosion
1	97.5	1.5 Silver	11.28	588	588	For use on copper, brass and similar metals with torch heating

* The specific gravity multiplied by 0.0361 equals the density in lb/cu in.
† For some engineering design purposes, it is well to consider these alloys as having practically no mechanical strength at 183 C (361 F).

Table 4—ASTM Standard Solders, B32-48T*

		—Chemical composition, %—				
			Antimony			
Grade No.	Tin	Lead (approx. %)	Class A, max.	Class B, max.	—Class C— Min.	Max.
70	70	30	0.12	0.50	No Class C	
60	60	40	0.12	0.50	No Class C	
50	50	50	0.12	0.50	No Class C	
45	45	55	0.12	0.50	No Class C	
40	40	60	0.12	0.50	1.8	2.4
35	35	65	0.25	0.50	1.6	2.0
30	30	70	0.25	0.50	1.4	1.8
25	25	75	0.25	0.50	1.1	1.5
20	20	80	No Class A	0.50	0.8	1.2

* For elements other than those shown in the table the maximum permissible amounts are as follows: Bismuth 0.25%, copper 0.08%, iron 0.02%, zinc 0.005%, aluminum 0.005%, others (total) 0.08%. The deviation from the nominal tin content for the alloys shown in the table shall not exceed 1.00% in a composite sample of fabricated metal or 0.50% in cast metal.

Table 5—United States Federal Specification for Soft Solder. QQ-S-571b

	Percentage composition*				Approximate melting range, ° F.	
	—Tin—		Lead,	Antimony,		
Grade	Min.	Max.	max.	max.	Solidus	Liquidus
Sn 70	69.5	71.5	Rem.	0.50	360	378
Sn 60	59.5	61.5	Rem.	0.50	360	372
Sn 50	49.5	51.5	Rem.	0.50	360	420
Sn 40	39.5	41.5	Rem.	0.50	360	460
Sn 35	34.5	36.5	Rem.	1.6–2.0	360–365	490–500
Sn 30	29.5	31.5	Rem.	1.4–1.8	360	500–510
Sn 20	19.5	21.5	Rem.	8–1.2	360	525–545
Sb 5	94.0	..	0.2	4.0–6.0	450	464

* For all the tin-lead solders the maximum permissible impurities are as follows: Copper 0.08%, bismuth 0.25%, zinc 0.005%, iron 0.02%, aluminum 0.005%, others (total) 0.08%.

Table 6—ST Soft Solders

Alloy	Analysis by percentage: Tin	Silver	Antimony	Indium	Lead	Liquidus, °F	Tensile strength, psi	Spread 1/2 g on copper, sq in.
ST-5	5.0	1.50	0.5	...	Bal.	565	5260	0.23
ST-10	10.0	1.50	0.5	...	Bal.	554	5335	0.28
ST-15	15.0	1.25	0.5	...	Bal.	532	6180	0.30
ST-20N	20.0	1.25	1.25	...	Bal.	508	7800	0.27
ST-20D	20.0	..	0.5	5.0	Bal.	504	4410	0.54
ST-25	25.0	..	1.25	...	Bal.	500	7100	0.29
ST-30	30.0	1.25	0.5	...	Bal.	482	7625	0.79
ST-30H	30.0	1.25	2.0	...	Bal.	475	8125	0.45
ST-30D	30.0	..	0.5	5.0	Bal.	464	4700	0.85
			Tin-lead solders					
10Sn-90Pb	10	..	0.12	...	Bal.	568	4850	0.20
30Sn-70Pb	30	..	0.12	...	Bal.	495	5390	0.75
40Sn-60Pb	40	..	0.12	...	Bal.	460	5660	1.30
50Sn-50Pb	50	..	0.12	...	Bal.	414	5790	1.23

ing operations that demand freedom from corrosion and conductive flux residues. These are recommended for radio, electronic, television and electrical work. Rosin type fluxes used in the core can be powdered rosin, plastic rosin or activated rosin. The plastic rosin cored solders are relatively weak in fluxing action, but protect the metal from oxidation during the heating. Their use is limited to easily soldered base metals such as are found in tinplate containers and most radio and electrical parts. Pretinning is a distinct aid.

The activated rosin cored solders supply a fluxing action which is more active than plain rosin but still retain the noncorrosive and nonconductive characteristics of rosin. Most activating agents are decomposed at the soldering temperature and are either inactive in the flux residue or are unable to penetrate through the impervious surface of the rosin. Activated rosin cored solder satisfies the need for high production speeds. Practical tests should be conducted to assure that this type of solder meets the requirements for the specific application.

In ordering flux cored wire solder, the following specifications should be specified:

1. Strand Size. The most popular strand size ranges from 0.040 to 0.125 in. diam. Sixty or seventy strand sizes varying from 0.009 to 0.250 in. are available. State strand size desired.

2. Core Size. The core size determines the ratio of solder to flux. One manufacturer supplies six core sizes containing from 0.55 to 6.0% flux. Core sizes containing 2 to 3% flux are preferred for general use.

3. Alloy Composition. The most generally useful compositions are found in the 30 to 60% range. Specify the desired composition from among the possible combinations in the entire range of tin-lead alloys.

4. Flux Core. Indicate on the order whether the acid type, organic type, rosin or activated rosin type flux is required.

5. Spool Weight. Available in 1-, 5-, 20-, 25- and 50-lb spools marked distinctly as to strand, core, alloy and flux specification.

Table 7—Special Solders

Nominal composition, %: Tin	Lead	Antimony	Others	Application
30	70	...	.....	Slip end can solder. Body filler tinning
2–4	Bal.	4–5	0.6 arsenic	Body filler solder
2	98	....	.....	Side seam can solder
90	..	....	10 zinc	Aluminum solder
70	..	....	30 zinc	Aluminum solder
37.5	37.5	....	25 indium	Alkali resistant solder
60	..	....	40 bismuth	Low-melting solder
22	22	....	56 bismuth	Low-melting solder
..	..	5 silver	95 cadmium	High-temperature solder

M. Reference

Lewis, W. R., "Notes on Soldering," Tin Research Institute (1948).

Plan—to attend the *all-welding* meeting and exposition at the famed Shamrock Hotel and connecting Hall of Exhibits—*both* fully air conditioned for your comfort—

in Houston—June 16–19, 1953

(see page 989)

New Rules for Welding Low-Alloy Ferritic Pipe Material

Historical background of the new rules for high-pressure, high-temperature marine piping and the principal provisions of these new rules

by Commander Charles F. Perry, USCG

IT IS of historical interest to note that the first set of Rules for Welding Piping in Marine Construction promulgated by the AMERICAN WELDING SOCIETY, covered carbon steel and were issued in tentative form in April 1938. These early Rules consisted only of 10 paragraphs. At the time of their initial publication they were used for maximum steam conditions aboard merchant vessels of about 450 psi and 750° F. Some minor revisions were made and the Rules reprinted in 1944. Further experience indicated that some relaxations could be made in sofar as temperatures were concerned, so in May 1948 the Rules were revised to permit increased temperatures for gases, vapors and liquids for piping operating at pressures not exceeding 150 pounds per square inch. This eliminated the necessity for stress relieving and nondestructive tests for certain services which had been required heretofore, also clarification was made as to the material specifications which were to be welded under the Rules.

The Rules for Welding Carbon Steel were again revised in 1952, and are in the process of being reprinted. When reissued the Rules will consist of 19 paragraphs so that they will be in the same format as the alloy steel Rules. Relaxation has been made for both pressure and temperature in so far as Class II Piping conveying water is concerned.

The steady increase in steam temperatures rendered carbon and carbon-molybdenum piping materials unsuitable for the higher temperatures being used in the more advanced marine designs of steam propulsion plants because of the low physical properties of the former material at elevated temperatures and the susceptibility of both materials to graphitization, thus necessitating the use of the more complex alloy steels which created problems not heretofore present in pipe welding. The Rules for Welding Carbon Steel Material were not suitable to govern the

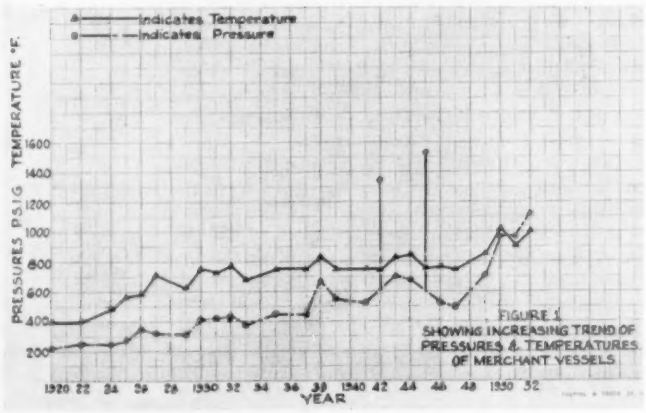

FIGURE 1
SHOWING INCREASING TREND OF PRESSURES & TEMPERATURES OF MERCHANT VESSELS

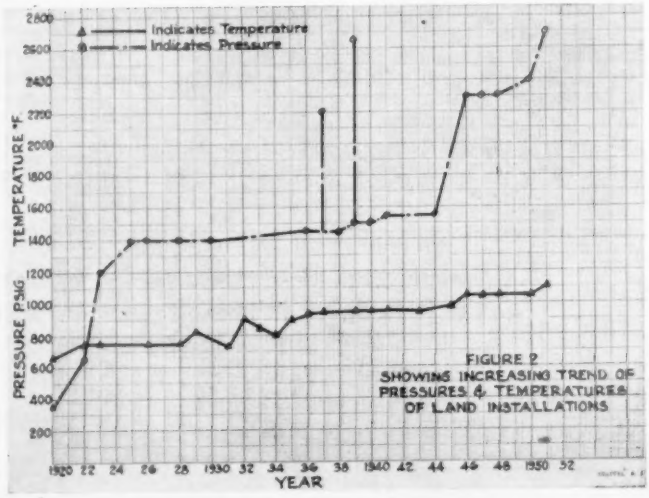

FIGURE 2
SHOWING INCREASING TREND OF PRESSURES & TEMPERATURES OF LAND INSTALLATIONS

Charles F. Perry is Commander with the United States Coast Guard.

Scheduled for presentation at the Thirty-Third National Fall Meeting, AWS, Philadelphia, Pa., week of Oct. 20, 1952. Closing date for discussion Dec. 15, 1952.

welding of these complex alloy steels which necessitated that new rules be developed.

The records indicate that the SOCIETY was formally requested in December of 1948, to have the Committee on Welding in Marine Construction prepare Rules covering the welding of low-alloy ferritic materials such as pipe, tubing, forgings and castings, namely, the component materials normally employed in fabricating a high-temperature piping system. The Coast Guard was particularly interested in the development of such Rules because of discussions about this time with marine engineers indicating the intent of using higher temperatures for new vessels in the planning stage than had been previously employed in merchant vessel practice. Heretofore, the maximum design temperature that had been used in a merchant vessel of American Registry was 910° F which was built for the Atlantic Refining Co. Because of the successful operation of this class of vessel, the first being the *E. J. Henry*, the Atlantic Refining Co. again pioneered in still higher temperature design conditions. The highest design temperature used up to the present time in a merchant vessel of American Registry is 1020° F used in the "Atlantic Seamen" class of vessels built for the same owner. The first of this class of vessels was delivered in 1950. Available information indicates that the performance of these vessels to date has been very successful and has met the expectation of their owner.

As a matter of interest to you engaged in the marine industry and those interested in the trend of increasing pressures and temperatures used in merchant vessels, Fig. 1 gives the increasing trend of pressure and temperature of vessels covering the past 32 years.

Those who have kept abreast of increases in stationary practice over the same period of time as covered by the figure, know that the public utility industry has outdistanced the marine industry as to both pressure and temperature, which can be seen from the data presented in Fig. 2 furnished through the courtesy of the Babcock & Wilcox Co. This lag was due to problems which had to be solved by the marine industry and to economics involved. The marine propulsion problems will be discussed later in this paper.

As was noted in the data presented in Fig. 1, it was after 1925 that steam pressures materially increased above those which were in use during World War I. However, upswings in pressure and temperature created problems in marine plants which were not present heretofore.[1] The economic advantage which could be obtained by use of the higher pressure and temperatures could not be utilized until the problem of obtaining a satisfactory reduction gear to reduce the high speed of the turbine sufficiently for the utilization of a low-speed efficient propeller was solved. Experience gained from operation of the early reduction gear designs, intensive research and development, plus improvement in machine-tool design, eliminated early restrictions and made possible the use of higher pressure and higher temperature steam so that high-speed turbines connected to low-speed propeller shafts by means of reduction gears could be employed.

[2] Another deterrent to the use of high-temperature steam was the fear of a number of engineers in the marine industry that in the operation of geared turbines, overheating of ahead turbines blading would occur when the vessel was going astern. Experience indicates that this fear was practically baseless and today temperatures of above 1000° F are being employed with satisfactory performance indicated in some designs of merchant vessels.

Another obstacle which retarded the use of higher pressures and temperatures was the availability of suitable marine auxiliaries. When the first geared turbines were installed, the same type of marine auxiliaries previously used with reciprocating machinery had to be employed, thereby minimizing the economic gains which would have accrued if the large volume of exhaust steam could have been profitably utilized in feedwater heating. The excess exhaust steam was by-passed to the condenser which caused a decrease in the vacuum and resulted in poor turbine economy. This problem could not be solved until a different type of auxiliaries was used, as all effort was negated in trying to improve the vacuum due to the greatly increased quantity of excess exhaust steam from the auxiliaries. The use of electrically driven auxiliaries with power supplied by an auxiliary turbogenerator operating condensing was found to be the solution of the problem, as the excess exhaust steam from reciprocating auxiliaries resulting in a low vacuum was no longer an obstacle in limiting the usage of turbines for propulsion.

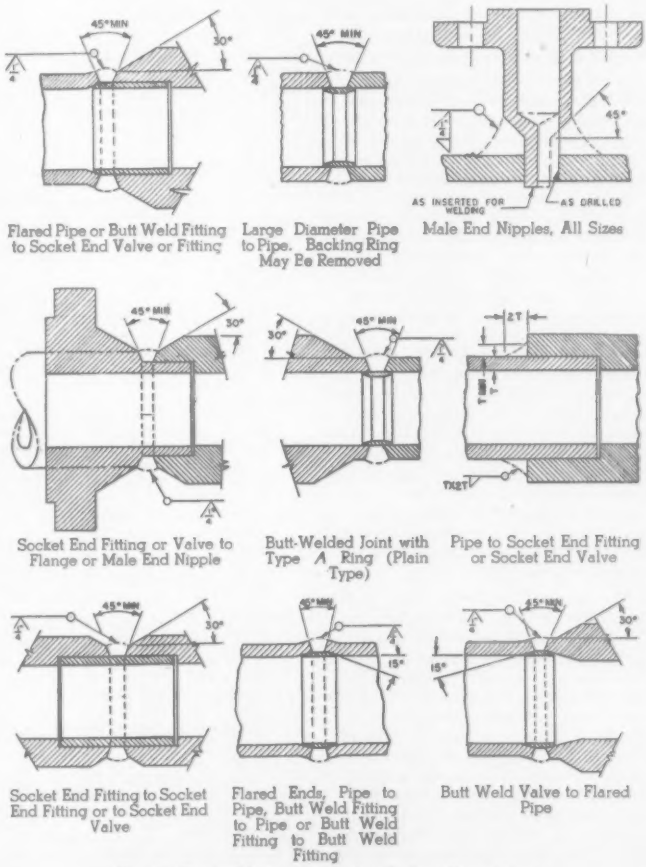

Flared Pipe or Butt Weld Fitting to Socket End Valve or Fitting

Large Diameter Pipe to Pipe. Backing Ring May Be Removed

Male End Nipples, All Sizes

Socket End Fitting or Valve to Flange or Male End Nipple

Butt-Welded Joint with Type *A* Ring (Plain Type)

Pipe to Socket End Fitting or Socket End Valve

Socket End Fitting to Socket End Fitting or to Socket End Valve

Flared Ends, Pipe to Pipe, Butt Weld Fitting to Pipe or Butt Weld Fitting to Butt Weld Fitting

Butt Weld Valve to Flared Pipe

Fig. 3 Typical joint design details for alloy piping

During this period of the evolution of the marine turbine, progress was being made by the boiler industry in the development of new marine boiler designs incorporating automatic combustion control, thereby eliminating manual firing. This forward step resulted in decreasing fuel consumption and stimulated the desire to employ on shipboard still higher pressures and temperatures to achieve the economies that were obtainable.

The motivating factor causing the marine engineer to be so interested in the utilization of higher pressures and temperatures is the same incentive which has caused increased pressures and temperatures to be used in central generating stations, namely, better economy. During the period of approximately 30 years, the reward for increased pressures and temperatures in marine propulsion plants has been an increase in economy which has resulted in large savings in fuel consumption. Today, with the larger horsepower, efficient high-pressure and -temperature marine propulsion plant installations, we expect and get a fuel consumption of about 0.5 lb/shp-hr for all purposes, which is about 50% less than the fuel consumption of about 25 yr ago.

As recognized by those who are familiar with high-pressure and -temperature piping design, welded piping is employed wherever possible aboard ship because of lighter weight, reliability, lower initial and maintenance cost and freedom from joint leakage. To secure good performance it is, of course, essential that proper fabrication be employed which necessitates that correct welding procedure be used. The welding procedure must be carefully established and controlled to insure the production of high-quality welds which will perform satisfactorily in service. To some who have not been involved in the welding of high temperature piping, the procedure established may seem unnecessary, restrictive and resulting in high fabrication costs. In the welding of high-temperature piping the highest class of workmanship must be employed to insure satisfactory service performance because failures and unnecessary troubles cannot be tolerated due to the resultant economic loss caused by the vessel being laid up for repairs and maintenance.

The foreword states the Rules were formulated by the Subcommittee on Machinery Construction of the Committee on Welding in Marine Construction. This subcommittee includes representatives from the shipbuilding industry, the ship owners and regulatory bodies such as the Bureau of Ships, U. S. Navy, U. S. Coast Guard and the American Bureau of Shipping. These regulatory bodies, generally referred to as "Enforcement Authorities" issue their own specifications, regulations or rules. However, the subcommittee, in formulating the minimum acceptable fundamental requirements, has performed the function of coordinating the requirements of the individual bodies.

It should be understood that nothing contained in the Rules supersedes the requirements of the Enforcement Authority; therefore, the Rules are essentially recommended practices.

These Rules were developed for the welding of piping aboard ship, however, they are equally applicable for any high-temperature welding piping application whether it be afloat or ashore. It is to be noted that these Rules cover welding only. Many additional problems exist in connection with the design and fabrication of high-temperature piping. Some requirements are specified by the Code governing the particular installation which must be met. A search of the literature or information obtained from the material manufacturer is frequently also necessary to insure the use of proper fabrication procedure.

In the development of the Rules, various requirements which should be met were considered so as to insure the production of high-quality welded joints for ferritic piping materials suitable for high-temperature application that would perform satisfactorily in service. Below will be discussed the more important items taken into consideration in establishing welding procedure as covered by the Rules.

Table 1

ASTM designation	*Grade*	*Nominal composition*
Pipe material		
A335	P1	Carbon-0.50 Mo
A335	P2	0.60 Cr-0.50 Mo
A335	P3a	1.75 Cr-0.50 Mo
A335	P3b	2.00 Cr-0.50 Mo
A335	P11	1.25 Cr-0.50 Mo
A335	P12	1.00 Cr-0.50 Mo
A335	P22	2.25 Cr-1.00 Mo
A213	T3	1.75 Cr-0.75 Mo
A213	T12	1.00 Cr-0.50 Mo
A213	T14	2.00 Cr-0.50 Mo
Forgings		
A182	F1	Carbon-0.50 Mo
	F2	1.0 Cr-0.50 Mo
	F22	2.25 Cr-1.00 Mo
Castings		
A217	WC1	Carbon-0.50 Mo
A217	WC6	1.25 Cr-0.50 Mo
A217	WC9	2.25 Cr-1.00 Mo

Scope

The ferritic alloy materials which most likely would be used in the temperature range of 800 to 1050° F, listed in the Rules, are covered by ASTM designations given in Table 1 above. As the Rules pertain to welding only, the discussion will not go into detail regarding the selection of material with reference to temperature limitation which is imposed by Enforcement Authorities.

Table 2—Backing Rings and Weld Metal Compositions

Base Materials (ASTM Designation)	Backing Ring Materials* (ASTM Designation)	Weld Metal Composition
A-335 P1 to A-335 P1, A-335 P2, A-335 P12 or A-213 T12, A-335 P11, A-335 P3a or A-213 T3, A-335 P3b or A-213 T14, A-213 T22	A-209 T1, A-335 P1, A-192, A-210, A-53A, A-106B	0.40–0.65 Mo
A-335 P2 to A-335 P2, A-335 P12 or A-213 T12, A-335 P11, A-335 P3a or A-213 T3, A-335 P3b or A-213 T14, A-213 T22	A-209 T1, A-335 P1, A-192, A-210, A-53A, A-106B	0.50–0.70 Cr, 0.40–0.65 Mo
A-335 P12 or A-213 T12 to A-335 P12 or A-213 T12, A-335 P11, A-335 P3a or A-213 T3, A-335 P3b or A-213 T14, A-213 T22	A-335 P12 or A-213 T12, A-335 P11, A-335 P3a or A-213 T3, A-335 P3b or A-213 T14	0.80–2.00 Cr, 0.40–0.65 Mo
A-335 P11 to A-335 P11, A-335 P3a or A-213 T3, A-335 P3b or A-213 T14, A-213 T22	A-335 P11, A-335 P3a or A-213 T3, A-335 P3b or A-213 T14	1.00–2.00 Cr, 0.40–0.65 Mo
A-335 P3a or A-213 T3 to A-335 P3a or A-213 T3, A-335 P3b or A-213 T14, A-213 T22	A-335 P3a or A-213 T3, A-335 P3b or A-213 T14	1.50–2.00 Cr, 0.45–0.80 Mo
A-335 P3b or A-213 T14 to A-335 P3b or A-213 T14, A-213 T22	A-335 P3b or A-213 T14	1.60–2.25 Cr, 0.45–1.00 Mo
A-213 T22 to A-213 T22	A-335 P3b or A-213 T14, A-213 T22	1.60–2.50 Cr, 0.80–1.10 Mo

* These designations are used for the purpose of illustrating chemical analysis only. Backing rings may be manufactured from pipe or bar steels of similar composition.

Types of Joints

Butt joints are required for pipe over 2-in. size for carbon-molybdenum and chromium-molybdenum alloys containing up to 0.70% chromium. Butt joints are mandatory for pipe over 1-in. size where the alloy is of higher chromium content. Socket welded joints are permitted for sizes and chromium content below the limitations given above. The limitations were selected to provide for better stress distribution through the joint and to preclude the possibility of weld cracking as a result of hardness because of high chromium content or large thermal gradient due to metal mass.

Joint Preparation

The material edges are required to be clean and free of foreign matter. Any means that will provide a suitable surface reasonably smooth and free of gouges may be used for the preparation of the welding edges. Some acceptable joint details which have given satisfactory performance in service are shown in Fig. 3.

Backing Rings

Backing rings are specified to be of weldable quality free of foreign material and of approximately the same chemical composition as the base metal. Material designations for backing rings is given in Table 2. It was recognized that carbon-steel backing rings have been used in the welding of materials such as covered by these Rules; however, in view of the limited knowledge regarding the effects of weld dilution, it was deemed desirable for the backing ring to have approximately the same chemical analysis as the base metal until more information is available regarding the effects of dilution for high-temperature application.

Electrodes

It was known that some data existed indicating that weld metal of similar chemical composition was superior to that of wrought or cast base material. However, to prevent dilution from occurring it was decided to require that welds have equal or better heat-resisting properties than the base metal, until further research is conducted regarding heat-resisting properties of lower alloy weld metal as compared to base metal. Chemical composition for electrodes is given in Table 2. The Rules specify that low-hydrogen XX15 or XX16 electrodes should be used if the chromium content is 1% or higher, and that maximum sizes of electrodes should not exceed $^5/_{16}$ in. for flat position and $^3/_{32}$ in. for all other positions, to minimize the likelihood of weld cracking and to prevent the use of too large a size electrodes which causes unnecessary difficulties especially where all position welding is likely to be involved.

Welding Process

The manual shielded arc process was considered to be the type of welding which is the most commonly used and which would produce acceptable welds. Provision, however, is made for the use of oxy-acetylene welding of carbon-molybdenum pipe not exceeding 1 in. in size, and the use of other welding processes which may be approved by regulatory bodies contingent upon a satisfactory procedure test being conducted.

Qualification of Welding Procedures and Welders

To insure that the procedure is satisfactory and that welders are capable of producing acceptable welds, compliance with the latest Standard Qualification Procedures of the AMERICAN WELDING SOCIETY is required.

Preheat and Interpass Temperatures

To minimize the likelihood of cracking during welding, preheat and interpass temperatures are specified based upon the chemical composition. It is stipulated that a higher preheat is usually necessary where the carbon content exceeds 0.18% or complex joints are involved. This precaution is stated, of course, to minimize the likelihood of weld cracking caused by high hardness or unusual joint geometry. Provision is made for lower heating if procedure qualification demonstrates that with the welding procedure employed acceptable joints can be produced.

Weld Quality

Either stringer beads or weaving may be used contingent upon the type used in the qualification procedure. Weld layers should not exceed $^1/_4$ in. in thickness to insure high-quality deposit and minimize the likelihood of defects. The customary

Table 3—Preheat Interpass, Preliminary Postheat and Stress-Relief Temperatures

Base Materials (ASTM Designation)	Minimum Preheat and Interpass Temperatures, ° F.		Preliminary* Postheat Temperatures, ±25° F.		Stress-Relief Temperatures, ±25° F. All Wall Thicknesses
	$^3/_4$ In. and Under Wall Thickness	Over $^3/_4$ to $1^1/_2$ In. Wall Thickness	$^3/_4$ In. and Under Wall Thickness	Over $^3/_4$ to $1^1/_2$ In. Wall Thickness	
A-335 P1 to					
A-335 P1	150	250	Not reqd.	1225	1225
A-335 P2	150	250	Not reqd.	1225	1225
A-335 P12 or A-213 T12	300	400	Not reqd.	1225	1225
A-335 P11	300	400	Not reqd.	1225	1225
A-335 P3a or A-213 T3	300	400	1225	1225	1225
A-335 P3b or A-213 T14	300	400	1225	1225	1225
A-213 T22	300	400	1225	1225	1225
A-335 P2 to					
A-335 P2	150	250	Not reqd.	1225	1225
A-335 P12 or A-213 T12	300	400	Not reqd.	1225	1225
A-335 P11	300	400	Not reqd.	1225	1225
A-335 P3a or A-213 T3	300	400	1225	1225	1225
A-335 P3b or A-213 T14	300	400	1225	1225	1225
A-213 T22	300	400	1225	1225	1225
A-335 P12 or A-213 T12 to					
A-335 P12 or A-213 T12	300	400	Not reqd.	1350	1350
A-335 P11	300	400	Not reqd.	1350	1350
A-335 P3a or A-213 T3	300	400	1350	1350	1350
A-335 P3b or A-213 T14	300	400	1350	1350	1350
A-213 T22	300	400	1350	1350	1350
A-335 P11 to					
A-335 P11	300	400	Not reqd.	1350	1350
A-335 P3a or A-213 T3	300	400	1350	1350	1350
A-335 P3b or A-213 T14	300	400	1350	1350	1350
A-213 T22	300	400	1350	1350	1350
A-335 P3a or A-213 T3 to					
A-335 P3a or A-213 T3	300	400	1350	1350	1350
A-335 P3b or A-213 T14	300	400	1350	1350	1350
A-213 T22	300	400	1350	1350	1350
A-335 P3b or A-213 T14 to					
A-335 P3b or A-213 T14	300	400	1350	1350	1350
A-213 T22	300	400	1350	1350	1350
A-213 T22 to					
A-213 T22	300	400	1350	1350	1350

* When preliminary postheat treatment is applied by a manually controlled torch, precautions should be taken to avoid exceeding the specified temperature range and causing partial transformation of the steel.

precautions are stated that dirt and slag are to be removed after each pass and that starts and stops are to be made in such a way as to avoid entrapment of gas and slag. Provision is made for the use of either chipping or grinding in the removal of defects. Peening is prohibited unless specifically approved. The usual requirements are specified for providing reinforcement and eliminating unnecessary reinforcement.

Postheat Treatment

Based upon mass and hardness, a postheat treatment is required immediately upon completion of welding if the thickness at the joint exceeds $^3/_4$ in. or the base material contains more than 1.50% chromium or 0.75% molybdenum. The same heat treatment is specified in all other cases unless the interpass temperature is maintained until final stress relief, the wall thickness does not exceed $^3/_4$ in., or the hardness of the heat-affected zone in the as-welded state does not exceed 32 Rc. The heat treatment necessitates that the weld area be heated uniformly for a minimum period of 10 min and cooled at a slow, uniform rate within the temperature range as specified in Table 3. The preliminary postheat treatment is not a substitute for final stress relief unless the heat soaking period is based upon a length of 1 hr per inch of thickness as specified for stress relieving.

Stress Relief

All joints exceeding $2^1/_2$ in. pipe size are required to be stress relieved at the temperatures given in Table 3, and if the chromium content exceeds 0.70% all joints exceeding 1 in. are required to be stress relieved. The period of stress relief is as previously stated but in no case is the soaking period to be less than $^1/_2$ hour. Heating and cooling rates shall be within 200–400° F/hr with the weldment allowed to be removed from the furnace when 600 F is reached. Controlled temperature heating is mandatory.

Marking for Identification

The use of a steel die for stamping is permitted but its use is discouraged because the indentations are stress raisers which may cause a crack to develop. The use of paints containing lead, zinc or sulfur compounds are prohibited because of the possible deleterious metallurgical effect these chemical elements may have on steel at elevated temperatures.

Nondestructive Testing

All joints exceeding $2^1/_2$ in. are required to be nondestructively tested and joints of pipe exceeding 1 in. are to be nondestructively tested if the chromium content exceeds 0.70%. Radiographic examination is mandatory if the wall thickness exceeds $^3/_8$ in. which was considered to be about the upper limit for which paramagnetic particle testing was satisfactory. Only 60% of the pipe circumference is required to be examined for sizes below 4 in. when radiography is employed. If paramagnetic powder testing is used the entire joint must be tested.

Because of the marked increase in temperatures over the past decade and the large number of low-alloy ferritic steels available as piping materials, it was considered necessary that standards be established for welding the materials so as to insure that welding failures would be eliminated.

Each installation has problems which must be considered, as follows: selection of suitable material that will not graphitize in service, has good resistance to creep and good stress to rupture properties at the operating temperature, and presents little or no difficulties in fabrication. Other considerations are: can the material be cold bent, or must hot bending be employed? If cold bending can be used, what heat treatment is necessary to restore the necessary ductility and to produce the grain size desired?

If the requirements as specified in the Rules are met, dependable welds will be obtained and a degree of standardization achieved which was the purpose of the Rules.

References

1. *General Electric Review* of December 1945.
2. Kessler, Geo. W., "Procedures on Influencing Factors in the Design of Marine Boilers," *Trans. Soc. Naval Arch. and Marine Engrs* (1948).

CURRENT WELDING LITERATURE

Agricultural Machinery, Manufacture. Production of Mechanized Farm Equipment. Welding & Metal Fabrication, vol. 20 no. 6 (June 1952), pp. 196–202.

Airplane Manufacture. Aluminum Fuel Tanks Are All-Welded. Steel, vol. 131, no. 4. (July 28, 1952), pp. 81–82.

Airplane Manufacture. Huge Fuel Tanks for Stratojet Bomber, L. M. Limach. Machy. (N. Y.), vol. 58, no. 11 (July 1952), pp. 204–208.

Airplanes, Fuel Tanks. Ryan Simplifies Fabrication of Giant Wing Tanks Requiring 30,000 Spot Welds, J. Litell. Western Metals, vol. 10, no. 5 (May 1952), pp. 41–42.

Aluminum Brazing Sheet Used in Radiator Studies. Steel, vol. 131, no. 1 (July 7, 1952), pp. 96–97.

Beryllium-Copper Useful for Large Machine Parts, J. T. Richards. Matls. & Methods, vol. 35, no. 6 (June 1952), pp. 97–99.

Brazing with Metal Powder, H. W. Greenwood. Machy. (Lond.), vol. 81, no. 2070 (July 17, 1952), pp. 98–99.

Bridges, Steel. Are We Ready for All Welded Railroad Bridges, R. N. V. Brodie. Civ. Eng. (N. Y.), vol. 22, no. 6 (June 1952), pp. 25–27.

Bridges, Steel. Designing World's Longest All Welded Highway Structure, W. F. Pond. Roads & Streets, vol. 95, no. 4 (Apr. 1952), pp. 61–65.

Bridges, Steel. Welded Steel Box Girders Used for Three Bridges in Washington. Roads & Streets, vol. 95, no. 5 (May 1952), pp. 47–50.

Buildings. Welded Multi Story Structures Save Steel and Money. B. S. Myers. Civ. Eng. (N. Y.), vol. 22, no. 4 (Apr. 1952), pp. 43–45.

Compressed Air Lines. How to Care for Air Lines in Welding Shop. Industry & Welding, vol. 25, no. 6 (June 1952), pp. 42–44, 47.

Electrodes. Ferritic Welding Electrodes Save Alloy, Give Better Welds, Z. J. Fabrykowski. Iron Age, vol. 170, no. 4 (July 24, 1952), pp. 93–97.

Electrodes. Low-Hydrogen Electrodes Now Used for Welding Armour Plate, R. J. Thomas, Jr. Industry & Welding, vol. 25, no. 6 (June 1952), pp. 48, 51, 69.

Electrodes, Testing. New Double-Fillet Test for Hot-Cracking, E. G. P. Hinds. Welding Research (Brit. Welding Research Assn.), vol. 6, no. 1 (Feb. 1952), pp. 27r–28r.

Electroplating Shops. Fabricated Plastics in Plating Industry, R. B. Seymour and E. A. Erich. Metal Finishing, vol. 50, no. 6 (June 1952), pp. 117–119.

Magnesium and Magnesium Alloys. Weldability and Weld Strength of Some Magnesium Alloy Sheet Materials, J. G. Ball and A. E. L. Tate. Welding Research (Brit. Welding Research Assn.), vol. 6, no. 1 (Feb. 1952), pp. 13r–26r.

Materials Testing, Nondestructive. Radiography in Engineering, L. M. Mullins. Instn. Production Engrs.—J., vol. 31, no. 6 (June 1952), pp. 265–284.

(*Continued on page 930*)

Corrosion of Structural Spot Welds

An investigation of the corrosion phenomena in spot-welded joints of low-alloy, high-strength steel and an evaluation of the beneficial effects of protective weld sealers

by B. Karnisky, E. Kinelski and E. Gruca

Abstract

Structural spot welds frequently are subjected to corrosion by conditions encountered in service, and unless preventive measures are taken, spot-welded joints may fail far short of their expected service life. This paper is concerned with an investigation to gain basic knowledge on the corrosion phenomena in spot-welded joints of low-alloy, high-strength steel, and to evaluate the beneficial effects of protective weld sealers.

Laboratory tests were made to simulate actual service failures. Factors such as corrosion fatigue, preferential attack by acid solution, stress corrosion cracking, alternate immersion in acid and salt solutions were considered in preliminary tests. Subsequently, a procedure was evolved in which various types of spot-welded specimens, either stressed or unstressed, were subjected to industrial atmospheric exposure. Test data have been accumulated over the past four years and numerous spot weld failures have been obtained in the atmospheric corrosion specimens. Metallographic examination of the failed welds revealed additional information on the corrosion failure phenomena in spot welds.

In service, various physical and chemical actions take place which may start corrosion in the faying surfaces, and the alternate wet and dry conditions tend to build up the rust layer causing ultimate failure. The results of the test indicate that spot welds may start to fail by corrosion cracking in as little as one year's time unless proper weld sealers are used in the joint and some form of periodic maintenance is performed.

B. Karnisky is Welding Research Engineer, **E. Kinelski**, Materials Engineer, and **E. Gruca**, Head, Welding and Materials Section, Pullman-Standard Car Manufacturing Co., Research and Development Department, Hammond, Ind.

Scheduled for presentation at the Thirty-Third National Fall Meeting, AWS, Philadelphia, Pa., week of Oct. 20, 1952. Closing date for discussion Dec. 15, 1952.

INTRODUCTION

THE subject of "corrosion" should be of interest to all engineers and fabricators of welded consumer or industrial goods because billions of dollars are spent annually in applying protective coatings on new products, preventing corrosion of the products in service and replacing products destroyed by corrosion. This economic aspect of the corrosion problem is ably stated by Uhlig, who prefaces the *Corrosion Handbook* by stating: "The tax imposed by corrosion of metals on industry, the community, and the nation is an appreciable proportion of our national income." In spite of the fact that the corrosion phenomena is encountered daily, few people are cognizant of the numerous chemical, metallurgical and physical factors involved in the corrosion process.

This paper is concerned with a study of the mechanism of corrosion occurring to spot welds used in primary or secondary structures and in the effectivness of corrosion prevention practices. For the past 17 years Pullman-Standard Car Manufacturing Co. has been analyzing this problem, and the paper highlights the results of the program thus far. The impetus for the research program was related directly to the change from riveted to spot-welded design and by the introduction of low-alloy high-strength steels in the company's products. The objectives of the initial program in 1935 were simple—to observe the effects of outdoor exposure on riveted and spot-welded joints. In the years since then the program has been instrumental in the development of specifications for weld-through primers and sealers* to be used for the protection of spot welds in carbon or low-alloy steels which would not interfere with the quality of the welds.

In summary this paper will: (1) show how spot welds may fail in service by corrosion; (2) describe various laboratory tests made to simulate service corrosion failures and (3) present data to illustrate the effectiveness of specific protective coatings in stressed spot-welded joints exposed to industrial atmospheres.

CORROSION FAILURES IN SERVICE

In order for corrosion to take place, the spot-welded joint must be exposed to a corroding medium. Railroad equipment,

* By definition, weld-through primers are coatings applied to sheet metal prior to spot welding which (*a*) enables the joint to be welded without affecting weld quality and (*b*) offer corrosion inhibition to the coated faying surfaces. Weld-through sealers are also applied prior to welding and act as a viscous barrier in preventing corrosive environments from reaching the faying surfaces. Sealers may also provide chemical resistance to corrosion.

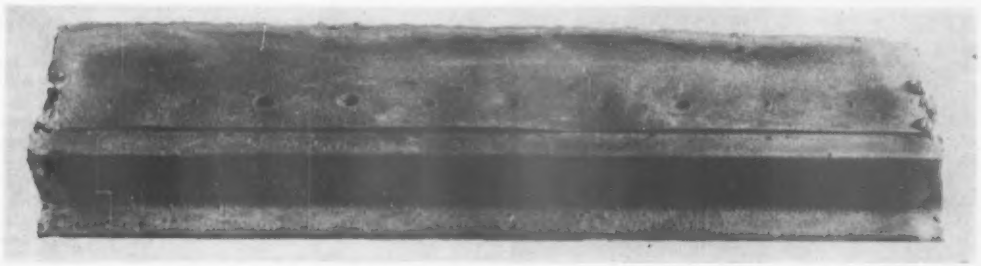

Fig. 1 Spot-welded joint which has failed in service from atmospheric corrosion because of the lack of maintenance. Note the holes in the steel sheet around the periphery of the spot welds

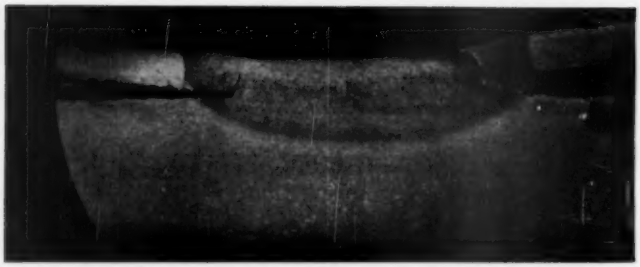

(a) Plug type failure which may occur in joints between sheets and heavy sections. 9 ×

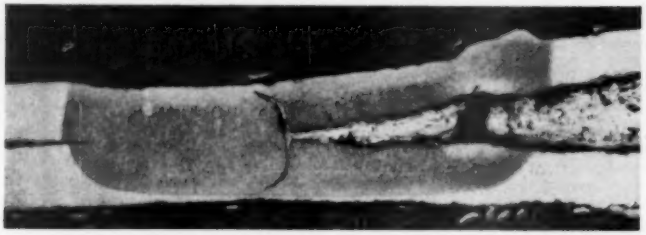

(b) Partial shear type failure which occurs in joints between sheets of approximately the same thickness. 9 ×

(c) Shear type failure. 6 ×

Fig. 2 Types of failures of spot-welded joints which occur after an extreme exposure to atmospheric corrosion. The expansion from corrosion products and the resulting cracks through the welds are shown. These spot welds were originally satisfactory, but the joints were not properly protected from corrosion

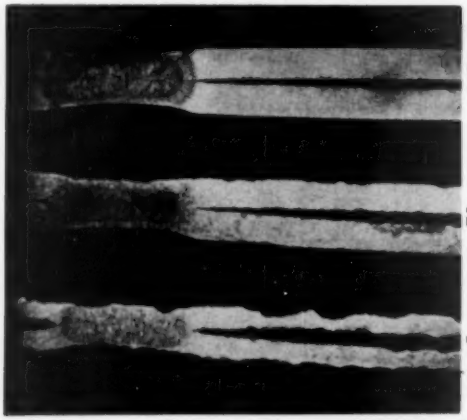

(a) 0.064-in., low-alloy high-strength steel. 5 ×

(b) 0.064-in., copper-bearing mild steel. 5 ×

(c) 0.064-in. plain mild steel. 5 ×

Fig. 3 Appearance of unprotected spot-welded joints after 9-yr atmospheric exposure in Chicago. Variation in amount of corrosion of the three types of steel which were tested and relative expansion of the joints are illustrated

for example, may be exposed to acid solutions, alternate wetting and drying, coal-ash, lime, salt, cinders, etc. In addition, all ranges of humidity, cold and heat are encountered in the different climates of the country. Corrosion rates are also increased by the residual stresses in welded joints and by fatigue stresses in service. The net effect of all these conditions constitutes an ideal setup for the occurrence of corrosion. Proper maintenance through periodic painting programs can help minimize potential corrosion. When this protective measure is not taken, then trouble can start.

Figure 1 illustrates a typical example of a spot-welded joint which has failed in service. In this type of joint, consisting of a light-gage steel sheet spot welded to a heavy member, corrosion failure occurred by pulling a hole in the light-gage sheet around the periphery of the weld. This plug type of corrosion failure is illustrated in Fig. 2 (*a*). Between steel sheets of approximately the same thickness, a partial shear failure may occur as shown in Fig. 2 (*b*), or a complete shear failure as shown in Fig. 2 (*c*). In each of these instances, the original spot welds were satisfactory, but after severe corrosive action, it is sometimes difficult in shear type failures to prove that the joint was even welded. These examples of spot weld failures illustrate the effects of corrosion, and the following pages will describe the techniques and results of the research program undertaken to better understand and control the corrosion problem.

ATMOSPHERIC CORROSION TESTS OF LOW-ALLOY STEEL SPOT WELDS

During the middle thirties, low-alloy high-strength steels having excellent weldability and improved strength and corrosion resistance properties were developed. A research program was thereupon instituted in 1935 to compare the atmospheric corrosion resistance of spot-welded and riveted joints made from a proprietary low-alloy steel with two other steels—copper-bearing and mild steels. The joints were made without the benefit of any protective primer or sealer at the faying surfaces. The externally exposed surfaces of the specimens were given a coat of black lacquer.

Figures 3 and 4 show the appearance of the samples after being exposed to Chicago industrial atmosphere for a period of nine years. During that time they were periodically examined, and measurements were taken of the expansion of the joints caused by build-up of corrosion products. The test results indicated that the mild steel joints expanded much more than the other two types of steel and that the riveted joints expanded slightly more than the spot-welded joints. It is readily apparent by the amount of pitting and joint ex-

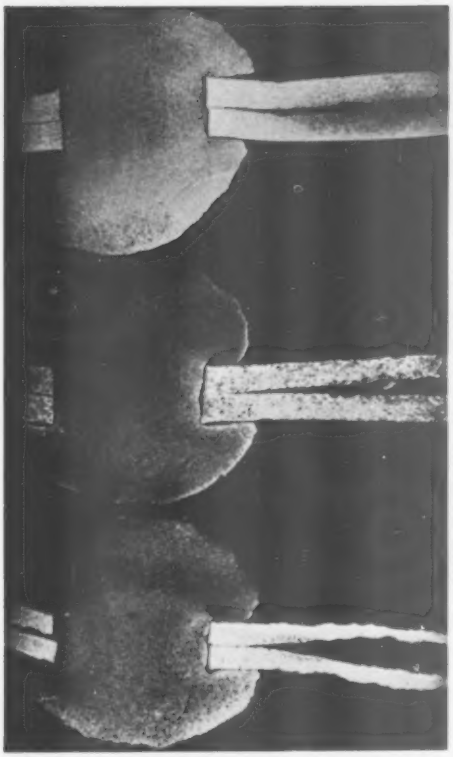

(a) 0.064-in., low-alloy steel spot weld. Note crack in weld nugget at right side. 5 ×

(b) Progress of crack shown in (a) into weld nugget and slight pitting from corrosion. 5 ×

(c) 0.064 inch plain mild steel 5 ×

Fig. 4 Appearance of unprotected riveted joints after 9-yr atmospheric exposure in Chicago. Variations in amount of corrosion of the three types of steel which were tested and the relative expansion of the joints are illustrated

pansion that the spot-welded and riveted low-alloy steel joints have much better corrosion resistance than the other two steels. The lacquer was intact only on the surface of the low-alloy steel. Later results by Larrabie[1] have shown that low-alloy high-strength steels have about two or three times the atmospheric corrosion resistance of structural-steel containing a 0.2% copper.

Upon microscopic examination, as shown in Fig. 5, some cracks were found in the low-alloy steel spot welds, in spite of the slight amount of corrosion and expansion of the joint, whereas no cracks were found in the copper-bearing and mild steel welds. The interdendritic penetration and slightly branched appearance of this type of crack, coupled with the slight amount of general corrosion existing, indicated that the mechanism of failure might be stress corrosion cracking.[2] The requirements for stress corrosion are present because of the inherently high residual stress in the spot weld and the concentrated stresses applied at the faying surfaces by the wedge of corrosion products.

However, the mechanism of failure of these spot welds may be purely mechanical. A small zone of partial fusion, commonly called the corona fusion zone, exists around the spot-weld periphery at the faying surfaces of the sheets. The expansion of the sheets from the wedge of corrosion products readily cracks the corona fusion zone, providing a sharp notch for entrance into the weld nugget. Since spot welds are actually castings with weak planes along the dendritic structure, the crack can enter the weld along these planes. Spot welds in low-alloy steels are much harder and less ductile than spot welds in copper-bearing or plain mild steels and this characteristic would aid cracking.

PRELIMINARY ANALYSIS OF THE MECHANISM OF CORROSION CRACKING

In an effort to determine which of the two theories of the mechanism of failure described above was the most plausible, a number of preliminary laboratory tests were made to develop corrosion cracks in spot welds. These included corrosion fatigue tests, immersion in acid solutions, stress corrosion cracking tests and alternate immersion and drying in a salt solution. Only one type of low-alloy steel was used, having chromium, nickel, copper and phosphorus as the major alloying elements. Specimens were prepared with various sized spot welds, in the as-welded, tempered and furnace stress relieved conditions, so as to vary the factors of residual stress and weld hardness.

Corrosion Fatigue Tests

In determining the factors which influence spot weld corrosion, the combination of cyclic flexure and corrosion on spot welds appeared to offer more severe deterioration than either condition separately. Therefore, corrosion fatigue tests were used as a part of this investigation. Simnad and Evans,[3] in their study of the mechanism of corrosion fatigue of steel in acid solutions, conclude that the bottom of a sharp pit becomes anodic due to concentration of stresses and this anodic material is dissolved away to form a crack. During the formation of a spot weld, high internal stresses are introduced by the rapid heating and cooling cycle. Consequently, the weld is anodic to the surrounding parent metal. The sharp notch produced by the faying edges at the weld constitutes a pit which is anodic at the bottom, as described above. It was therefore reasoned that the effect of fatigue stresses combined with acidic solutions in the joint could conceivably produce the type of spot weld failure encountered in service. Certain protective coatings can be destroyed at locations where acid solution may drain and collect. These locations may be either spot-welded or riveted lap joints which can retain moisture and acid solutions by capillary attraction. For this reason, it was decided to conduct corrosion fatigue tests in sulfuric acid solutions, running water and in air.

Krouse flexural fatigue specimens were prepared from cold-rolled, 0.075-in. low-alloy steel, and the endurance limit was determined in air, running tap water and in a 0.5% sulfuric acid solution. The effect of the corrosive environment was to drastically decrease the fatigue life without changing the manner of failure. Specimens tested under identical load conditions showed a life of 10,000,000 cycles in air, 3,500,000 cycles in water and only 700,000 cycles in the acid solution. Each failure was initiated at the notch formed at the periphery of the corona fusion zone, as shown in Fig. 6, and proceeded around the weld nugget to the surface. Since corrosion did not begin to take effect in the short time required for failure, the fatigue life at high loads was approximately the same in all environments. At extremely low loads, failure occurred by severe pitting of the surface.[4]

The flexural type of fatigue test does not truly represent the actual load on a spot weld in service where both shear and fatigue stresses are combined. By using the tensile fatigue type of machine, which produces a direct shear load on the spot weld, more representative results may be obtained.

Immersion in Acid Solutions

Once corrosion is initiated by any of the corrosive mediums, the expansion of rust in the joint obviously might fracture the spot welds. Iron reacts with oxygen and water to produce a precipitate of ferrous hydroxide which reacts with more oxygen to form ferric hydroxide resulting in a large increase in volume.[5] In order for this reaction to continue, the solution must be acidic so that it will have a large solubility for ferrous hydroxide. This was demonstrated by immersing spot-welded low-alloy steel specimens in water to which bubbling air was introduced. A thick bead of rust soon formed a tight seal completely around the joint and prevented further corrosion in the joint.

Following this test, spot-welded specimens of low-alloy steel were immersed in an aqueous solution of 0.5% sulfuric acid with bubbling air introduced. The dilute acid solution was used in order to increase the galvanic attack at the spot welds, which are anodic to the parent metal. Since iron ions tend to go into solution at anodic areas when steel is placed in an electrolyte, it was reasoned that stressed spot welds would corrode preferentially. However, the tests by immersion in the 0.5% sulfuric acid solution showed that the parent metal of a spot-welded joint would be corroded away without any corrosion attacking the spot welds at the faying surfaces. Most of the corrosion at the joint was confined to the parent metal at the outside edges of the joint as shown in Fig. 7 (*a*). Some of the specimens were spot welded with a proprietary sealer in the joint. This sealer gave complete protection in the joint and reduced the amount of corrosion at the outside edges of the joint as shown in Fig. 7 (*b*).

Concentrated salt solutions, because of their good electrical conductivity, increase corrosion by galvanic and concentration cell attack.[6] Sodium chloride is highly soluble in water and tends to produce soluble corrosion products; therefore, the solution remains in contact with the metal. A slight amount of acidity and oxygen in saline solutions increases the corrosive action on metals. Spot-welded low-alloy steel specimens immersed in an aqueous solution of sodium chloride and perchloric acid were attacked around the periphery of the surface indentations at the welds and at the extreme edges of the joint. The latter, illustrated by Fig. 8, is a typical oxygen concentration cell attack which did not affect the spot weld.

The results of these series of tests, while yielding additional information as to the effectiveness of the sealers, did not produce the desired corrosion cracking of the spot welds. Other tests of corrosive attack were therefore considered.

Stress Corrosion Cracking

The service conditions of high static stresses combined with corrosion led to this portion of the investigation; namely, determination of stress corrosion as the main factor in promoting cracking in structural spot welds. Failures by corrosion fatigue result from simultaneous corrosion and fatigue stresses, while stress corrosion cracking failures occur from simultaneous corrosion and high static stresses. These static stresses ordinarily occur in metals from the strain of cold work, but they may be produced by fabrication methods such as welding or riveting. Cracking may be prevented by annealing to remove the stresses.

The failure of boiler steel by caustic embrittlement has been related to stress corrosion cracking by Waber and McDonald.[2] They were able to produce failure in mild steel with an applied static stress in a solution of mixed nitrates. These corrosion cracks were mostly intercrystalline and slightly branched, similar to the cracks in spot welds which are shown in this article. Stress corrosion cracks occur without a significant amount of general corrosion on the surface. This condition was also present in spot-welded specimens which had cracked after atmospheric exposure. Corrosion cracking of mild steel is related to the strain aging and precipitation of iron nitride in the grain boundaries of the steels and may be prevented by removing the nitrogen. The corrosion process is electrochemical since the application of an anodic current prevents cracking.[7]

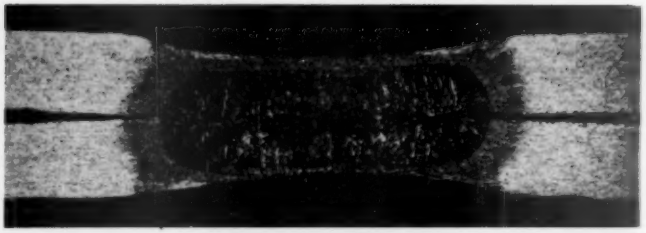

(*a*) .064-inch low-alloy steel spotweld. Note crack in weld nugget at right side. 10 ×

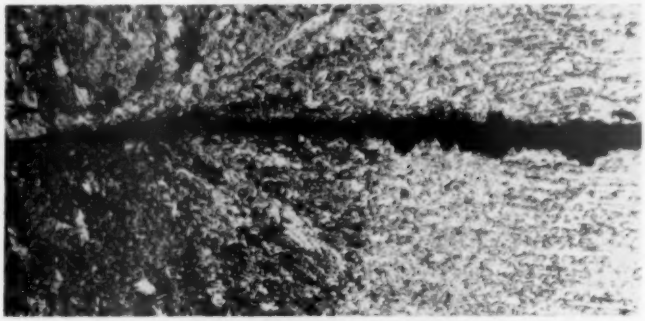

(*b*) Progress of crack shown in (*A*) into weld nugget and slight pitting from corrosion. 50 ×

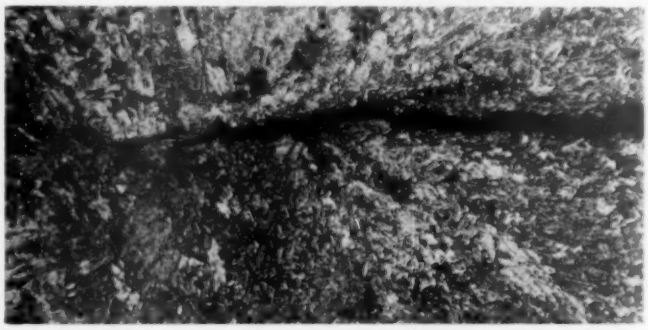

(*c*) End of crack in weld nugget showing branched and interdendritic path. 100 ×

Fig. 5 Corrosion cracking of a low-alloy high-strength steel spot weld after 9-yr exposure to industrial atmosphere in Chicago

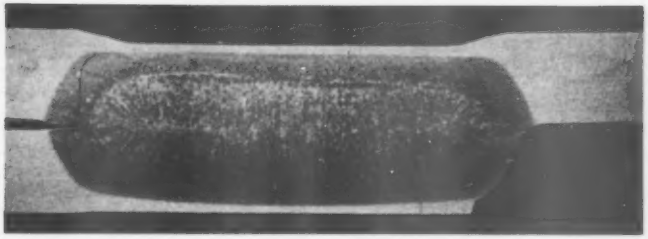

(a) Fatigue failure in air. 8 ×

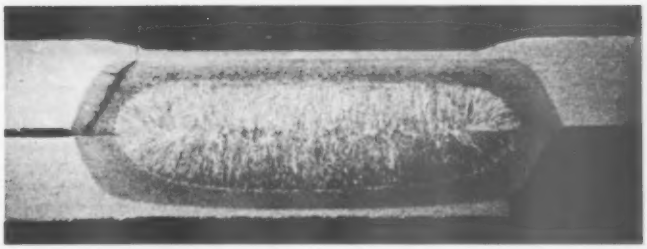

(b) Corrosion fatigue failure in 0.5% sulfuric solution. 8 ×

Fig. 6 Corrosion fatigue failures of spot-welded 0.075-in. low-alloy steel. With flexural loads, failure initiates at the periphery of the corona fusion zone and circumvents the weld

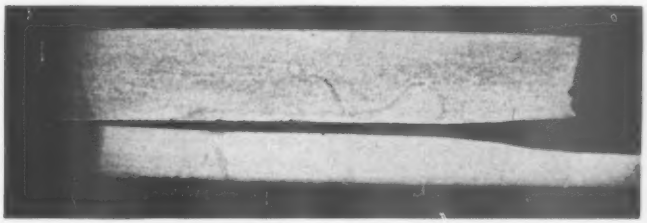

(a) Without sealer in the joint. 6 ×

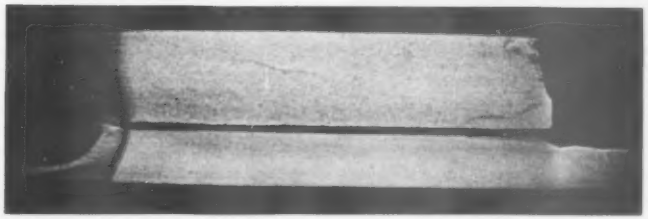

(b) With sealer in the joint. 6 ×

Fig. 7 Corrosion of low-alloy steel spot welds by immersion in a 0.5% sulfuric acid solution for 504 hr. The protection at the edge of the joint provided by the proprietary sealer in the joint is shown by (b)

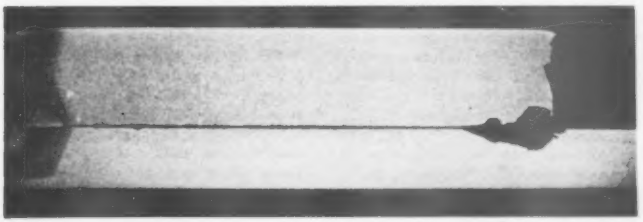

Fig. 8 Concentration cell attack at outside edges of low-alloy steel joint after 836-hr immersion in an aqueous solution of sodium chloride and perchloric acid

Samples, 1½ by 6 in., with three spot welds spaced 2 in. apart were prepared from 0.075 in. and combination of 0.075 and 0.125 in. low-alloy steels. A number of these specimens were given a tempering treatment in the spot-welding machine. The samples were immersed in a boiling solution of calcium nitrate and ammonium nitrate as recommended by Waber and McDonald.[8] This solution produces very little actual corrosion of the steel. However, it does produce rapid cracking in steels subject to corrosion cracking when tensile stresses approaching 90% of the yield strength are present.

All of the spot-welded specimens cracked in the solution, indicating that the low-alloy steel was sensitive to stress corrosion cracking, and that extremely high-tensile stresses were present in the spot welds. In the spot welds made at low welding currents, the highest stresses were in the heat-affected zone as shown in Fig. 9 (*a*). Standard sized spot welds made at average welding currents cracked completely across the weld in a plane normal to the sheet surface as shown in Fig. 9 (*b*). The tempering process reduced the stresses in the weld nugget sufficiently to prevent cracking of the weld as shown in Fig. 9 (*c*), but the stresses in the parent metal between welds remained high so that cracking occurred outside of the welds. Since none of these samples cracked in the weld parallel to the faying surfaces of the joint, additional tests were made by applying a shear load on a single spot-weld specimen immersed in the mixed nitrates solution. These specimens started cracking in the faying surfaces adjacent to the weld and cracked around the periphery of the weld, similar to the corrosion fatigue failures shown in Fig. 6.

Although the failures of spot welds in a mixed nitrate solution indicated that these welds in low-alloy steels were susceptible to stress corrosion cracking, the types of failures did not resemble the shear or plug type failures experienced in actual service of structural welds.

Alternate Immersion in Salt Solution

Since salt solutions have good electrical conductivity and offered possibility of accelerating the corrosion of spot welds, the next phase of the investigation was the exposure of spot welds to an alternate immersion test in 0.1 normal sodium chloride solution. The test began with an immersion into the salt solution for four days at room temperature. Then the salt solutions with the specimens were placed on a hot plate and heated at 150° F for two days, at which time the water had completely evaporated. The specimens remained in the beaker on the hot plate for

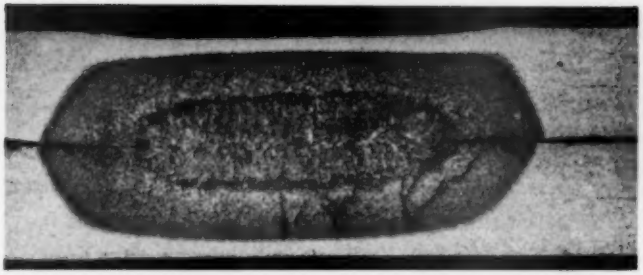

(a) Spot weld made with low welding current. Cracks appear in the heat-affected zone. 10 ×

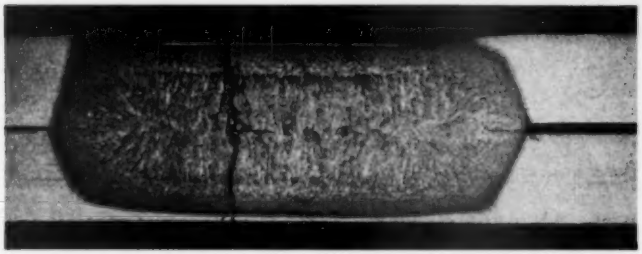

(b) Spot weld made with average welding current. Cracks through center of weld because of high shrinkage stresses. 8 ×

(c) Tempered spot weld reduces internal stresses in weld but high stresses remain in the parent metal between welds. 8 ×

Fig. 9 Stress corrosion cracks resulting from residual stresses in low-alloy steel spot welds and exposure in boiling mixed nitrates solution

an additional day for thorough drying. Each week the cycle was repeated.

Specimens 2 by 6 in. having three spot welds were made using 0.075-in. low-alloy steel, a combination of 0.075 and 0.125-in. low-alloy steels, and also a combination of 0.075-in. 18-8 stainless and 0.075-in. low-alloy steel. With the last named combination of materials, the weld nugget consisted of a mixture of the two dissimilar metals and was hard and rather brittle when conventional spot welding techniques were used. By using short impulses of welding currents and electrodes designed to give the proper current distribution, it is possible to fuse the dissimilar metals together without forming a nugget. Both types of specimens were made. In addition, a complete set of specimens was spot welded with the proprietary sealer in the joint, and another set was stress relieved at 1150° F.

Thickness measurements were made at regular intervals on each specimen in order to record the expansion from corrosion products in each joint. The sealer in the joint prevented expansion for about sixty days, and then the expansion rate was the same as the other specimens. There was very little difference in the expansion rates of the 0.075 in. specimens compared to the specimens of 0.075 in. spot welded to 0.125-in. steel. Likewise, there was no significant difference between the expansion rates of the as-welded and the stress-relieved specimens. The combination stainless steel and low-alloy steel specimens expanded at a rate approximately one-half of the low-alloy steel specimens.

Representative samples of the salt solution corrosion tests were cross sectioned for examination after exposures of six months and one year. At the end of six months exposure, the corona fusion zone around the periphery of the as-welded low-alloy steel spot welds had cracked and extended a very short distance into the weld nugget. This is illustrated by Fig. 10 (*a*) of a spot weld joining the 0.075- and 0.125-in. low-alloy steels. At the end of one year's exposure, these cracks had extended a considerable distance into the weld as shown in Fig. 10 (*b*). A similar failure, shown in Fig. 11 (*a*), occurred in the combination stainless steel and low-alloy steel joint which was purposely made with a brittle type weld. However, the fusion type weld joining the stainless steel to low-alloy steel was free of any cracks even after one year's exposure as shown in Fig. 11 (*b*).

Of the stress-relieved specimens, only the brittle-type stainless steel and low-alloy steel weld cracked after one year's exposure. The stress relieved low-alloy steel spot welds had cracked in the corona fusion zone, but none of the cracks actually penetrated the welds. The hardness of the low-alloy steel spot welds was lowered from Brinell 340 to Brinell 210 by the stress-relieving treatment, but the brittle dissimilar metal spot weld remained at Brinell 350. Evidently the soft weld with a low yield strength could elongate under the stresses induced by rust expansion. However, it could also mean that the planes of weakness along the dendritic pattern of the spot weld were partially eliminated by the stress relief treatment. In addition, stress relieving reduced the residual stresses in the welds and joints and thereby reduced the susceptibility to stress corrosion cracking.

ATMOSPHERIC CORROSION TESTS

It was concluded at the end of the above laboratory tests, that a satisfactory analysis of the mechanism of spot weld failures could be made by controlled atmospheric corrosion tests only. The selective attack by atmospheric corrosion was impossible to duplicate by short time laboratory tests. Since applied stress is an important factor in service failures, it is desirable to apply a load to the exposed specimens. In addition, the phenomenon of stress corrosion cracking is directly related to the amount of stress in the specimen exposed to the corrosive environment. Therefore, an atmospheric test program was established which included unstressed samples and stressed samples under constant deflection, constant bending load and constant shear load in order to observe whether or not the added stresses on the spot welds would accelerate the rate of corrosion cracking.

The samples were spot welded in the same manner, and with the same materials, as the specimens in the alternate immersion tests in salt solutions. These included low-alloy steel joints and combination stainless steel and low-alloy steel joints. They were spot welded with low, average, and high welding currents in order to have a range of residual stresses.

A chemical analysis of the three steels which were used and descriptions of the types of joints with shear strengths of the spot welds are listed in Tables 1 and 2, respectively. The Type C specimens joining the stainless steel and low-alloy steel were purposely made to produce a brittle weld nugget. The Type D specimens were made by the special spot welding procedure mentioned previously in which the dissimilar metals were fused without forming a nugget. In addition, one complete set of specimens was prepared with the proprietary sealer in the joint. A general view of the testing site is shown in Fig. 12. Exposure was started in August 1947, at the Pullman-Standard Plant in Chicago. The atmosphere is predominantly industrial with railroads, chemical plants, general industrial plants, etc., in the area.

Unstressed Atmospheric Corrosion Tests

This group consisted of specimens 2 x 6 in. with three spot welds spaced 2 in. apart. They were inclined at an angle of 30 deg. facing south. At the end of one year's exposure, there was a slight pitting of the low-alloy steel and rust accumulation in the unprotected joints. The corona fusion zone around the low-alloy steel Type A and Type B spot welds had cracked and penetrated the weld nugget a very short distance as shown in Fig. 13 (*a*). No cracks were present in the Type C and Type D combination stainless steel and low-alloy steel spot welds shown in Figs. 13 (*b*) and 13 (*c*).

In the specimens made with spot-weld sealer, the fillet of sealer which had squeezed out around the faying edges of the joints while welding still remained intact at the end of one year's exposure. However, the thin layer of sealer inside the joint had shrunk leaving thin veins of exposed metal. No corrosion occurred inside the faying surfaces, and the spot welds were completely protected as shown in Fig. 14 (*a*).

A similar type of low-alloy steel weld with sealer in the joint was examined after 56 months exposure. In this case, there was no apparent attack of the faying surfaces of the joint, but the corona fusion zone had cracked and started to penetrate the weld. This is shown in Fig. 14 (*b*) with an enlarged view of the crack in Fig. 14 (*c*). There was visible rusting at the tiny porous spots in the sealer inside of the joint. However, the joint was still intact after 56 months exposure, while similar low-alloy steel joints without sealer had failed completely after 41 months exposure. For best results, the combination of spot-weld primer and sealer would be recommended.

Stressed by Constant Deflection

The constant deflection specimens included the Types A, B, C and D joints prepared in the same way with identical material as the unstressed atmospheric corrosion samples described above. However, they were approximately 18 in. long and $1^1/_2$ in. wide, with six spot welds spaced 3 in. apart. In addition, one stressed specimen of each type of joint was welded with average current with a proprietary sealer in the joints. The specimens were clamped as a cantilever beam in a horizontal plane with a special fixture, as sketched in Fig. 15, and deflected on the other end by means of a stainless steel wire and turnbuckle arrangement. The bottom member of each specimen, which is on the compression side, was slightly longer and wider than the top member in

(a) Small crack has started into right side of weld nugget after 6-mo exposure. 7 ×

(b) Appearance after 1-yr exposure. 7 ×

Fig. 10 Corrosion cracks in low-alloy steel spot welds resulting from alternate immersion and drying in a salt solution

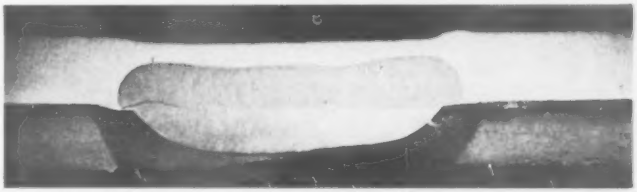

(a) Corona fusion zone and weld cracked. 7 ×

(b) No cracks present. 7 ×

Fig. 11 Spot welds joining stainless steel to low-alloy steel after 1 yr of alternate immersion and drying in a salt solution. The weld shown in (a) was purposely made to mix the dissimilar metals in order to obtain a brittle weld. The weld shown in (b) is made by a special procedure developed for dissimilar metal joints

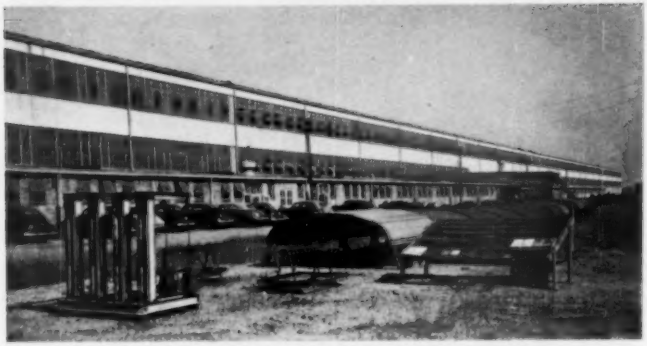

Fig. 12 General view of atmospheric corrosion site at the Pullman-Standard Car Manufacturing Co.'s Chicago Plant

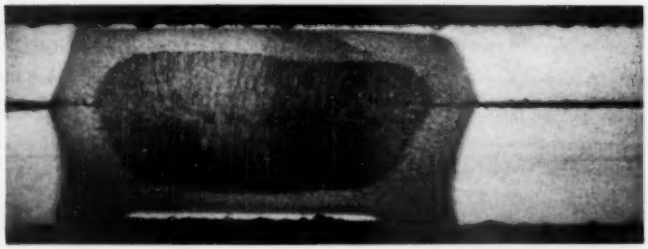

(a) A small crack has just started into the right side of the low-alloy steel, Type B-2 spot weld. 7 ×

(b) No cracking present in combination stainless steel and low-alloy steel, Type C-2 joint, spot welded to purposely produce a brittle weld. 7 ×

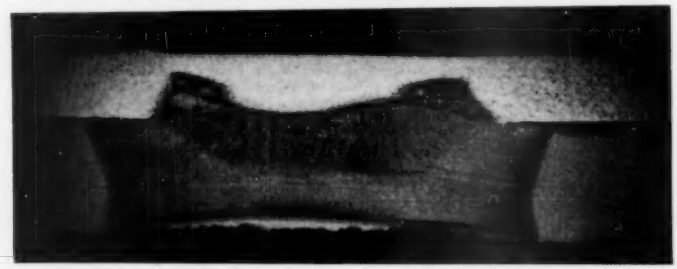

(c) No cracking present in combination stainless steel and low-alloy steel, Type D-2 joint, spot welded by special procedure to produce in a fusion type of weld. 7 ×

Fig. 13 Appearance of unstressed atmospheric corrosion specimens after 1-yr exposure. Spot welds were made without any sealer in the joints. A slight pitting of the low-alloy steel and accumulation of rust in the joint are shown

order to locate the faying surfaces of the spot welds above the neutral axis. The deflecting force was applied to the end of the bottom member, so that there was a tendency to pull the specimen apart. This permitted the top member to expand freely. The wider bottom member served as a ledge to trap and retain moisture in the joint.

One specimen of each type of joint welded with average current was placed horizontally in the rack without any bending load applied to the end. This was done in order to observe the rate of corrosion cracking with and without externally applied loads on the specimens. The desired load was determined with SR-4 strain gages placed on the material before spot welding. For the specimens made of 0.125-in. material on the bottom and 0.075-in. material on top, the residual tensile stress between the spot welds on the top surface was 2200 psi. A deflection of 2 in. produced a maximum stress of 55,000 psi at the point of bending which is the yield strength of the material. A deflection of $2^3/_4$ in. produced the same maximum stress in the specimens of 0.075- to 0.075-in. materials.

At the end of one year's exposure, none of the constant deflection specimens showed any sign of separation or failure. A dark reddish-brown rust covered all of the low-alloy steel surfaces sufficiently to obliterate the spot weld indentations, and the faying edges appeared rusted shut. The underneath side was covered with a loose flaky rust.

At the end of 15 months exposure, the Type A-1 and the Type B-1 low-alloy steel joints spot welded with a low welding current failed completely by separation. The same types of joints welded with average current failed at 41 months of exposure, while those welded with high current had not failed after 57 months of exposure. Evidently, the rate of failure is proportional to the size of the welds, which are listed in Table 2. On the other hand, with the exception of one weld on the Type C-3 joint, none of the combination stainless steel and low-alloy steel joints had failed after 57 months exposure, indicating that the bimetallic couple does not accelerate the corrosion rate. The unstressed specimens reported earlier failed after approximately the same length of time as the specimens with a bending load; so the rate of corrosion is controlled more by residual stresses in the weld and the wedging action of the rust in the joint than the external load. None of the specimens with sealer in the joint had failed after 57 months exposure. These results are summarized in Table 3.

The Type B-2 low-alloy steel joint which was unstressed but failed by separation or shear across the weld after 41 months exposure was examined for corrosion cracks. A failed weld was polished on the fractured surface, which was the cross-

sectional plane between the faying surfaces. The corrosion cracks radiating from the periphery toward the center of the weld nugget are shown unetched and etched in Fig. 16. Again the resemblance to stress corrosion cracks reported in the literature is readily apparent.

A combination stainless steel and low-alloy steel Type C-2 joint which had not separated after 57 months of atmospheric exposure was cross sectioned for examination. Cracks were found in the welds and one weld was almost completely cracked as shown in Fig. 17; therefore, the entire joint would have failed soon. An adjacent spot weld was cross sectioned at the faying surfaces in order to show the stress corrosion cracks in Fig. 18(*a*) and Fig. 18(*b*). The similarity with the cracks in low-alloy steel welds in Fig. 16 is readily apparent. Even though the dissimilar metal spot weld is highly alloyed, the composition of the weld did not prevent cracking but only retarded the rate of corrosion cracking.

Table 1—Chemistry and Approximate Physical Properties of Steels for Spot-welded Atmospheric Corrosion Specimens

Steel No.	1	2	3
Type	Low-alloy, hot-rolled, pickled	Low-alloy, hot-rolled, pickled	AISI Type 302, 18–8 stainless
Thickness, in.	0.082	0.124	0.072
Yield strength, psi	50,000 min	50,000 min	55,000 min
Tensile strength, psi	70,000 min	70,000 min	100/130,000
Elongation, %	20	20	30
Analysis, %			
C	0.118	0.12	0.103
Mn	0.37	0.39	0.70
P	0.133	0.111	0.026
S	0.033	0.031	0.006
Si	0.398	0.370	0.393
Cu	0.372	0.364	...
Ni	0.471	0.336	9.18
Cr	0.816	0.844	19.03

Stressed by Constant Bending Load

These specimens were of identical size, welded the same and mounted in a fixture similar to the constant deflection test specimens. However, a weight was hung on the end to deflect the specimen and thus maintain a constant force as the specimen corroded. Actually, two sizes of weights were used on each type of specimen; one weight gave the same deflection as the constant deflection specimens and the other was lighter in order to provide a maximum fiber stress of approximately 80% of the yield strength. However, the results of these tests were difficult to assess because of their erratic behavior. As corrosion progressed, the specimens kinked instead of maintaining a uniform bow.

Table 2—Types of Spot-Welded Joints for Atmospheric Corrosion Tests and Average Shear Strength of Individual Spot Welds

Joint type	*Combination of steels*	*Weld current*	*Shear strength, lb*	*Weld diameter, in.*	*Type of failure*
A-1	No. 1 and No. 1	Low	3620	0.218	Partial plug
A-2		Average	5720	0.359	Double plug
A-3		High	6970	0.468	Double plug
B-1	No. 1 and No. 2	Low	4640	0.218	Shear
B-2		Average	6340	0.359	Double plug
B-3		High	7320	0.453	Double plug
C-1	No. 1 and No. 3	Low	3930	0.250	Shear
C-2		Average	4990	0.312	Double plug
C-3		High	5700	0.343	Double plug
D-1	No. 2 and No. 3	Low	6000	0.359	Shear
D-2		Average	6340	0.359	Partial plug
D-3		High	7580	0.421	Partial plug

Table 3—Atmospheric Corrosion of Spot-Welded Joints Stressed by Constant Deflection

Joint type	*Weld current*	*Deflection, in.*	*Test results*
	(A) As-welded, without spot-weld sealer		
A-1	Low	2 3/8	Shear failure, 15 months
A-2	Average	2 3/8	Shear failure, 41 months
A-3	High	2 3/8	No failure, 57 months
B-1	Low	2	Shear failure, 15 months
B-2	Average	2	Shear failure, 41 months
B-3	High	2	No failure, 57 months
C-1	Low	2 3/8	No failure, 57 months
C-2	Average	2 3/8	One spot weld failed, 57 months
C-3	High	2 3/8	No failure, 57 months
D-1	Low	2	No failure, 57 months
D-2	Average	2	No failure, 57 months
D-3	High	2	No failure, 57 months
	(B) As-welded, with spot-weld sealer		
A-2	Average	2 3/8	No failure, 57 months
B-2	Average	2	No failure, 57 months
C-2	Average	2 3/8	No failure, 57 months
D-2	Average	2	No failure, 57 months
(C) As-welded, without spot-weld sealer, and without external stress applied to specimens			
A-2	Average	0	Shear failure, 41 months
B-2	Average	0	Shear failure, 41 months
C-2	Average	0	No failure, 57 months
D-2	Average	0	No failure, 57 months

Stressed by Constant Shear Load

In order to apply a more direct load at the faying surfaces of the spot weld, a tensile shear specimen rack was designed and used to test spot welds in atmospheric exposure. The load fixture and specimens are shown in Fig. 19. Lap shear specimens, 1 1/2 in. wide, of the same material combination used in the constant deflection tests were spot welded at low, average and high welding currents to obtain a group of specimens with average shear strengths as shown in Table 2. None of these specimens contained a spot weld sealer. Three lapped shear specimens of

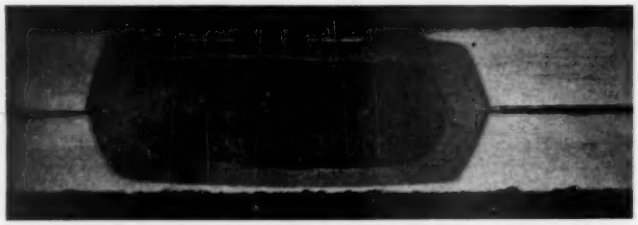

(a) Low-alloy steel, Type A-2 joint after 1-yr exposure. There is a slight pitting on the external surfaces but no apparent corrosion of the faying surfaces. 7 ×

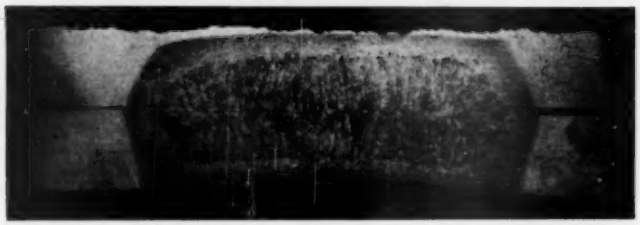

(b) Low-alloy steel, Type A-2 joint after 4½-yr exposure. Very slight corrosion attack of the faying surfaces has cracked the corona fusion zone and started to penetrate the weld

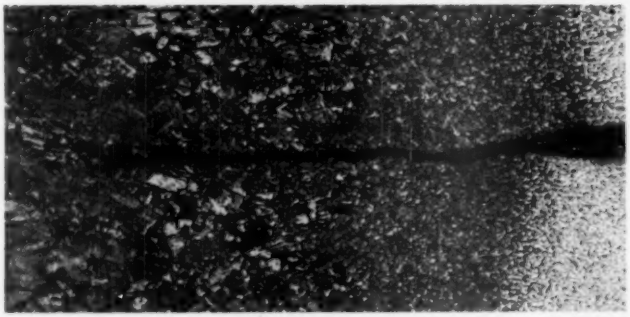

(c) Enlarged view of corrosion crack entering the corona fusion zone of the weld in (b). 100 ×

Fig. 14 Appearance of unstressed atmospheric corrosion specimens spot welded with sealer in the joints

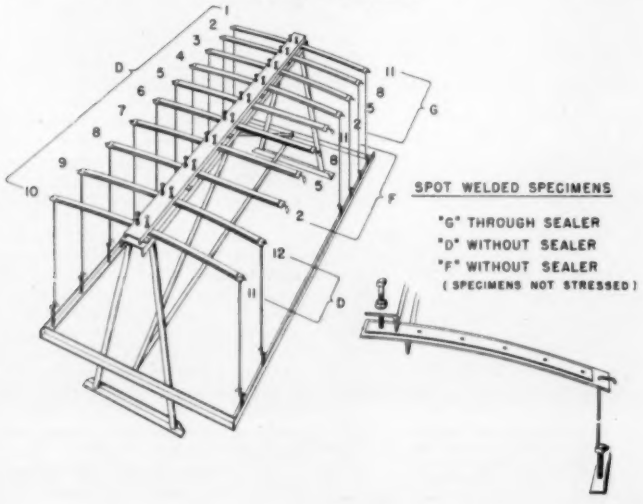

Fig. 15 Test fixture for atmospheric corrosion specimens stressed by constant deflection

each material combination were connected together and placed in a vertical position in the corrosion fixture. Since the lowest average shear strength was 3620 lb, a shear load of 3000 lb was selected as the stress load for the spot-welded samples. Actually, a calculated load of 3036 lb was applied by weights on a lever arm, balanced on a knife edge and vee arrangement, and transmitted to the samples through a universal joint arrangement in order to obtain a direct tensile shear load.

The low-alloy steel joints made with low welding currents, Types A-1 and B-1, failed by shearing after an exposure of 2 months and 7½ months, respectively. The appearance of the shear failure at the faying surface of the weld in Specimen A-1 is shown in Fig. 20. The corrosion attack had completely penetrated the corona fusion zone around the weld and entered for a slight distance into the weld nugget before weakening the weld sufficiently to fail by shear.

In the shear loaded specimens, the vertical position and a tendency for the joint to open around the single spot weld prevented the build-up of corrosion products sufficiently to cause failure. Therefore, the time required for failure was increased as evidenced by Table 4. For example, Specimen A-2 failed after 52 months exposure and B-2 had not failed after 57 months, while similar joints exposed under constant deflection failed after 41 months. However, the plug type of failure which occurred in the shear loaded specimens may be another reason for the increased life. The plug type of failure involves considerably more material than the shear type of failure. This can be seen in Fig. 21 showing photographs of a plug type of failure in Specimen A-2.

The combination stainless steel and low-alloy steel joint, Specimen C-3, also separated after 52 months exposure while stressed with a constant shear load. This was a plug type failure, as shown in Fig. 22 which pulled a hole out of each member. This hole in stainless steel member was cross sectioned in order to examine the path of the fracture. As shown in Fig. 23, the crack entered the weld nugget for a short distance and then traveled up through the weld at right angles to the faying surface.

Since the cracks follow an intercrystalline path through the weld as illustrated in Fig. 23 (*b*), the mechanism of fracture is believed to be stress-corrosion cracking. These cracks followed preferential paths which are believed to be anodic with respect to the adjacent areas. In addition to the intercrystalline corrosion, stress was applied to the weld by residual stresses induced during welding and by externally

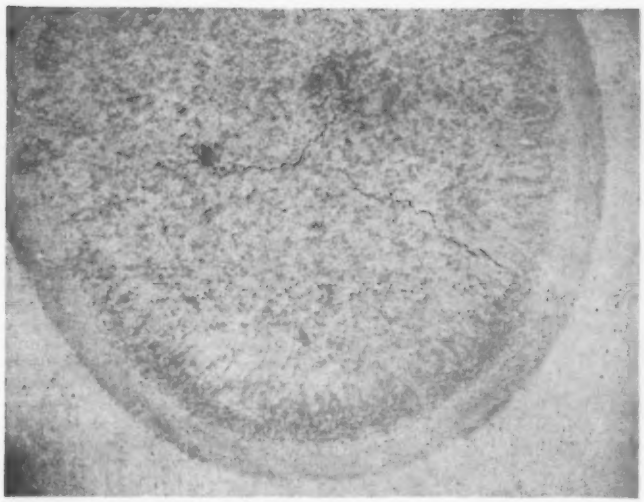

(a) Appearance of corrosion cracks radiating from the periphery to the center of the weld nugget. Fractured surface of weld which failed by shear was polished at the faying edges. 10 ×

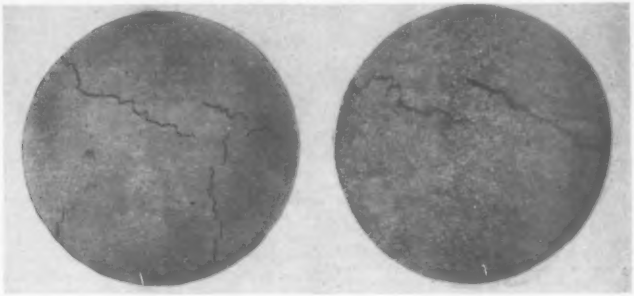

(b) Same as (a) but unetched. 18 × (c) Enlarged view of cracks. 60 ×

Fig. 16 Stress corrosion cracks in low-alloy steel spot weld which failed by shear across the weld after 41-mo atmospheric corrosion. Type B-2 joint without sealer welded with average current and tested unstressed to compare rate of corrosion cracking with stressed specimen

applied stresses. Furthermore, since both the cracks involved in shear and plug type failures of structural spot welds are similar in appearance, both are believed to be a result of stress corrosion.

SUMMARY AND DISCUSSION

Service failures of structural spot welds from atmospheric corrosion are usually represented by a plug type failure. Occasionally, the welds fail by shearing at the faying surfaces of the joint. These failures may be attributed to inadequate joint preparation and improper maintenance in service.

The superior corrosion resistance of spot-welded joints in low-alloy high-strength steel was shown by the atmospheric corrosion tests of spot-welded and riveted joints in low-alloy steel, copper-bearing mild steel and plain mild steel. An advantage of the superior corrosion resistance is manifested by much better adherence and life of protective coatings.

Unprotected low-alloy steel joints, without any spot-weld primer or sealer, may start to crack at the edge of the welds after one year of atmospheric corrosion, and fail completely after 3½ years exposure. A proprietary sealer in the joint retards the start of corrosion cracking beyond 4½ years. The ultimate in protection is the use of both spot-weld primer and sealer in each joint. Additional protection may be provided by a tempering treatment in the spot-welding machine as described in the report. This treatment reduces the hardness of the weld and its susceptibility to stress corrosion cracking. Another method of reducing susceptibility to cracking is the fusion procedure for spot-welding stainless steel to low-alloy steel without producing a brittle weld nugget. Incidentally, there was no increase in corrosion rate as a result of the bimetallic couple produced by the dissimilar metals.

The data reported here serve as a standard for comparing the resistance to atmospheric corrosion of various spot-weld primers and sealers which are currently being tested. These include tests of sealers with zinc dust pigment and synthetic lacquer vehicle. According to Mayne,[9] maximum cathodic protection is afforded only by zinc dust in paints, since the formation of a nonconducting oxide skin on aluminum pigment and magnesium dust in paints prevents the necessary metallic contact.

The mechanism of the corrosion process resulting in the failure of low-alloy steel spot welds involves many factors. The effect of corrosive solutions which may drain and collect at spot-welded joints is not simply the dissolution of the metal at the joint by chemical attack. The most serious effect is the destruction of certain protective paint and caulking compounds. It was demonstrated that a dilute acid solution would not penetrate into a welded joint sufficiently to corrode the spot weld periphery without first weakening the parent metal to the point of failure. However, once the protective coating at the edge of the joint is destroyed, ordinary atmospheric exposure can produce sufficient corrosion in the joint to cause failure of the welds.

Table 4—Atmospheric Corrosion of Spot-Welded Joints, Stressed by Constant Shear Load

Joint type	*Weld current*	*Shear load, lb*	*Test results*
	(A) As-welded, without spot-weld sealer		
A-1	Low	3036	Shear failure, 2 months
A-2	Average	3036	Plug type failure, 52 months
A-3	High	3036	No failure, 52 months
B-1	Low	3036	Shear failure, 7½ months
B-2	Average	3036	Plug failure starting, 57 months
B-3	High	3036	No failure, 57 months
C-1	Low	3036	No failure, 52 months
C-2	Average	3036	No failure, 52 months
C-3	High	3036	Plug type failure, 52 months
D-1	Low	3036	No failure, 57 months
D-2	Average	3036	No failure, 57 months
D-3	High	3036	No failure, 57 months

Once rusting has started in the joint, this rust is capable of holding moisture for ong periods of time. In all probability, the actual process of corrosion in the joint is by an oxygen concentration cell action. The moisture in the rusting joint is saturated with oxygen at the outside and low in oxygen inside the joint. The metal in contact with the solution at the low oxygen concentration is anodic to the high oxygen concentration portion, and therefore, corrodes preferentially.

The process of wetting and drying accelerates the spreading of the joint. The rust formed during wetting expands and hardens during drying, so that the joint is spread a slight amount. The next wetting penetrates farther into the joint. Thus a thin, hard wedge of rust drives itself up to the spot weld. The low-alloy steels form a hard, tight rust which is a primary reason for their good atmospheric corrosion resistance. However, this property is harmful inside a joint because of the extra pressure developed.

A small zone of partial fusion, commonly called the corona fusion zone, exists around the spot weld periphery at the faying surfaces of the joint. The expansion of the joint resulting from the wedge of corrosion products readily cracks the corona fusion zone. Thus, a sharp notch is formed providing entrance into the weld nugget. The concentrated stresses at this location combined with a corrosive medium, develops a stress corrosion crack. If the stresses are developed only by the expansion of rust, the crack enters the weld to produce a shear type of failure. If additional stresses are applied, then the cracking may circumvent a portion of the nugget to produce a plug type failure. In either case, cracking occurs by preferential corrosive attack along the dendritic planes in the weld structure.

In general, the rate of corrosion failure of low-alloy steel welds is proportional to the size of the welds. The effect of an external stress applied as a bending load was negligible on the rate of corrosion.

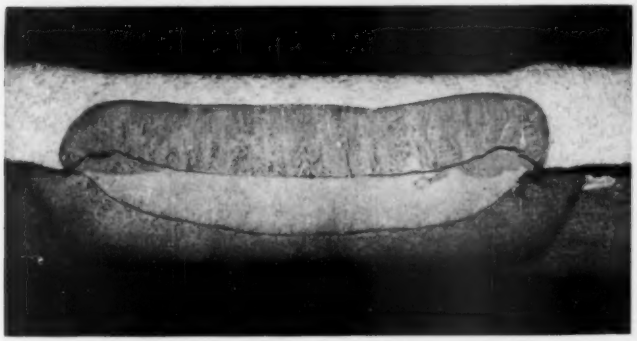

(a) Corrosion cracks almost completely across weld. 10 ×

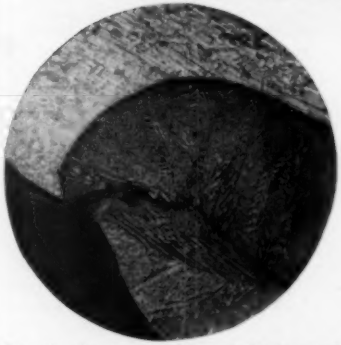

(b) Enlarged view of crack shown above at edge of weld. 25 ×

Fig. 17 Stress corrosion cracks in combination stainless steel and low-alloy steel joint which had not failed completely after 57-mo of atmospheric corrosion. This is a Type C-2 joint without sealer and stressed by constant deflection. Eventual failure could be expected in a short time

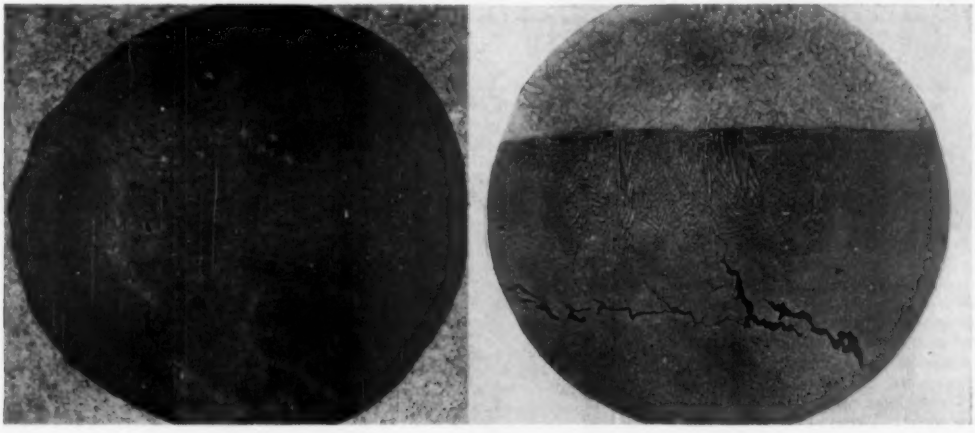

(a) 10 ×

(b) Enlarged view. 37 ×

Fig. 18 Stress-corrosion cracks in combination stainless steel and low-alloy steel spot weld similar to Type C-2. The weld was cross sectioned at the faying surface in order to show cracks similar to those found in low-alloy steel weld in Fig. 16. This weld was adjacent to the one illustrated in Fig. 17

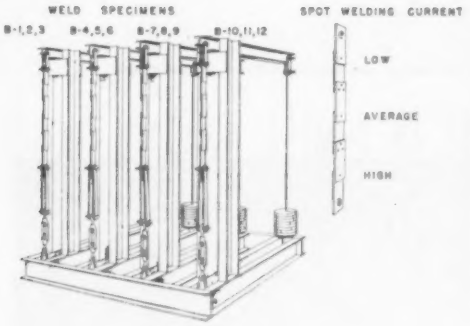

Fig. 19 Atmospheric corrosion of spot-weld specimens stressed by constant shear load

The same is true of the externally applied shear load except in the case of undersize welds made with low currents. Evidently, the residual internal stresses resulting from the rapid quenching of the weld are sufficiently high to induce stress corrosion cracking without an external stress. Corrosion fatigue probably plays an important part in the failure of spot welds in service, but it was impossible to determine this with the flexural type of fatigue test. In the dissimilar metal spot welds joining stainless steel to low-alloy steel, the highly alloyed weld nugget reduced the rate of corrosion cracking to some extent but did not prevent it. However, the fusion type of weld joining these dissimilar metals showed no sign of corrosion cracking after 4 1/2 years of exposure.

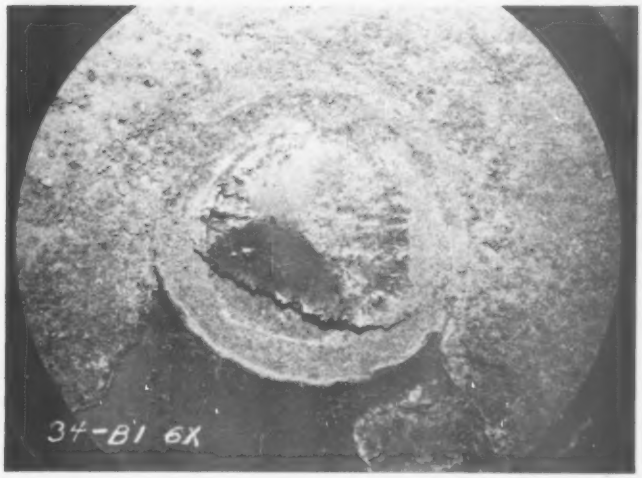

Fig. 20 Corrosion cracking of low-alloy steel spot weld after 2-mo atmospheric exposure while stressed by a constant shear load. This is Type A-1 specimen looking at the faying surface. Corrosion penetrated the weld a short distance until it was weakened sufficiently to fail by shear

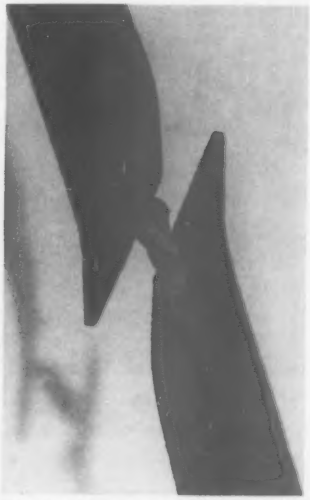

Fig. 21 Plug type of failure after 52-mo atmospheric corrosion while stressed by constant shear load. Specimen A-2, low-alloy steel spot welded with average current without any sealer

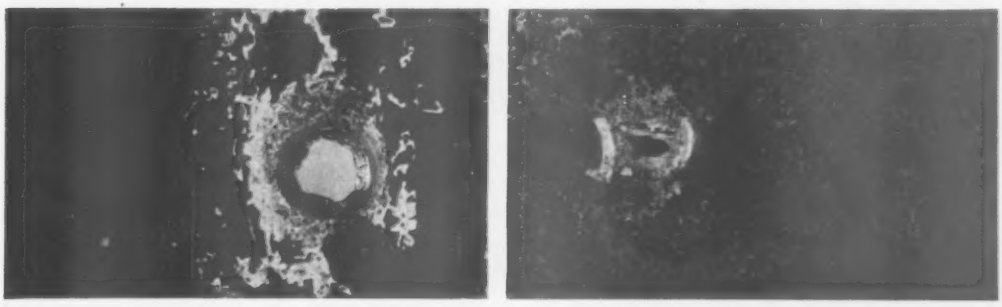

(a) Hole pulled in stainless steel by plug type failure. Faying surface is shown

(b) Faying surface of low-alloy steel portion of joint with plug type of failure

Fig. 22 Plug type of failure after 52 mo of atmospheric corrosion while stressed by a constant shear load. This is specimen C-3, combination stainless steel and low-alloy steel, spot welded with high current without any sealer

(a) Path of fracture through stainless steel portion of weld

(b) Enlarged view of fracture at right showing preferential path of crack. 1000 ×

(c) Enlarged view of (a) showing fracture following the dendritic pattern in corner of weld. 100 ×

Fig. 23 Path of fracture of the plug-type stress corrosion failure shown in Fig. 22

CONCLUSIONS

The difficulty of protecting spot-welded joints to withstand many years of atmospheric corrosion in service is well recognized. This problem becomes increasingly difficult with the sporadic and insufficient maintenance which is provided. Its solution involves the improvement of protective coatings, sealers and caulking compounds. Other approaches are to design the joints for automatic submerged arc welding or mash seam welding to eliminate lap joints. The use of more corrosion resistant materials may be desirable in some applications. Emphasis must be placed on good shop practice to insure the proper production of spot-welded joints with the correct primers and sealers.

References

1. Larrabee, C. P., "Effect of Composition and Environment on Corrosion of Iron and Steel," from *Corrosion of Metals*, American Society for Metals, Cleveland, Ohio, 1946.
2. Waber, J. T., and McDonald, H. J., "Stress Corrosion Cracking of Mild Steel," THE WELDING JOURNAL, **26** (6), Research Suppl., 362-s (1947).
3. Simnad, M. T., and Evans, U. R., "The Mechanism of Corrosion Fatigue of Steel in Acid Solution," *Jnl. Iron and Steel Inst.*, 531–539 (August 1947).
4. "Prevention of the Failure of Metals Under Repeated Stress," Battelle Memorial Institute, 161 (1941).
5. Speller, F. N., *Corrosion, Causes and Prevention*, McGraw-Hill Book Co., New York, p. 223 (1935).
6. Mears, R. B., Brown, R. N., and Dix, Jr., E. H., "A Generalized Theory of Stress Corrosion of Alloys," Symposium on Stress Corrosion Cracking of Metals, American Society for Testing Materials, 1945, p. 325.
7. Waber, J. T., and McDonald, H. J., "Relation of Strain Aging to the Stress Corrosion Cracking of Mild Steel," THE WELDING JOURNAL, **25** (4), Research Suppl., 223-s to 233-s (1946).
8. Waber, J. T., and McDonald, H. J., "Report on Stress Corrosion Cracking of Boiler Plate Steel," *Ibid.*, **24** (5), Research Suppl., 268-s to 273-s (1945).
9. Mayne, J. E. O., "Metallic Pigments, Electrolytic Functions in Protective Paints," *Paint Manuf.*, **XVLL**, 11, 380–382 (November 1947).

See—the Welding Industry's *newest* products designed to *cut* cost and speed production—

in Houston—June 16–19, 1953

(see page 989)

Hard-Facing Alloys of the Chromium Carbide Type

Engineering properties of deposits of high-chromium iron in which carbon and chromium combine to provide a considerable volume of hard carbides

by Howard S. Avery and Henry J. Chapin

Abstract

High-chromium irons, in which carbon and chromium combine to provide a considerable volume of hard carbides of the Cr_7C_3 type, have long been used for wear resistance as castings and as welded overlays. They may have pearlitic, martensitic, austenitic or mixed matrix structures.

This paper summarizes data on their engineering properties, including hardness, abrasion resistance, erosion resistance, oxidation resistance, hot hardness, creep resistance, compression strength and behavior under impact.

The austenitic 30% Cr hard-facing alloy is usually gas welded with a reducing flame that tends to increase carbon in the deposit. These welds have excellent resistance to erosion or low-stress scratching abrasion. They are only mediocre in resisting high-stress grinding abrasion. The chromium level provides good scaling resistance and their fair hot hardness up to 1000° F also makes them suitable for some hot wear applications. This grade is relatively insensitive to minor composition changes and nearly all gas weld deposits will have a hardness of Rockwell C56 ± 5 and erosion resistance from 20 to 50 times that of mild steel.

The martensitic irons of the HC250 type can be heat treated for machining and then rehardened, which makes them especially adapted to certain hard facing and casting applications where the austenitic grades that do not respond to heat treatment cannot be used. The hardness range is greater than that of the austenitic grade while erosion resistance is about the same. Where high-stress abrasion is involved the hardened HC250 is superior. However, the welding behavior of the austenitic grade is preferred by many operators.

Except where hot hardness above 1000° F and creep resistance are needed, or where high stress abrasion occurs, the austenitic chromium irons are desirable substitutes for the 2.5% carbon chrome-cobalt-tungsten hard-facing alloys. They cost less and frequently will out perform the latter.

INTRODUCTION

CHROMIUM carbide hard-facing alloys occupy an important place in the hard-facing field. They are the preferred materials for solving many wear problems, but since they give poor or mediocre performance in other situations, it is well to understand them thoroughly. This paper describes these alloys and presents many of their pertinent properties to aid those who wish to select wear-resistant alloys effectively.

The compositions in this group are essentially high-chromium cast irons and have been used for wear resistant castings as well as for hard facing. This is worthy of note, since such interchangeability provides engineering flexibility that sometimes leads to important savings.

The most common grades contain from 25 to 32% chromium with several per cent of carbon. Their structures contain considerable amounts of the trigonal chromium carbide, $(Cr, Mn, Fe)_7C_3$. The matrix structures of these irons may be austenitic, pearlitic or martensitic. The matrix has considerable influence on wear resistance, especially if high stresses are imposed on the micro-constituents. For low-stress abrasion (erosion) the volume and hardness of the carbides are important and the austenitic grade with carbon near 5% has been quite satisfactory. This is exemplified by field use on agricultural machinery working in sandy soil.

However, if high microstresses are imposed on the hard but brittle carbides, the wear resistance may be poor unless they are supported in a strong matrix. Only the martensitic type seems to provide this. High-stress grinding abrasion then requires that heat treatment of a high-chromium iron produce martensite for good wear resistance. The hardenable type is designated as HC250 herein, following the Alloy Casting Institute system. The austenitic and the hardenable alloys will be discussed in separate sections, though in some applications they are interchangeable.

AUSTENITIC CHROMIUM IRON

The austenitic high-chromium iron, covered by AWS designation I-C-1 (1950 WELDING HANDBOOK), characteristically carries about 6% manganese and 2% silicon. These alloys contribute to welding behavior but produce such stable austenite that the alloy is not considered amenable to heat treatment. The original patent on this hard facing type* recommended 2.0% carbon,

Howard S. Avery is Research Metallurgist and **Henry J. Chapin** is Metallurgist with the American Brake Shoe Co., Mahwah, N. J.

Scheduled for presentation at the Thirty-Third National Fall Meeting, AWS, Philadelphia, Pa., week of Oct. 20, 1952. Closing date for discussion Dec. 15, 1952.

* U. S. Patent 1,671,384 dated May 29, 1928.

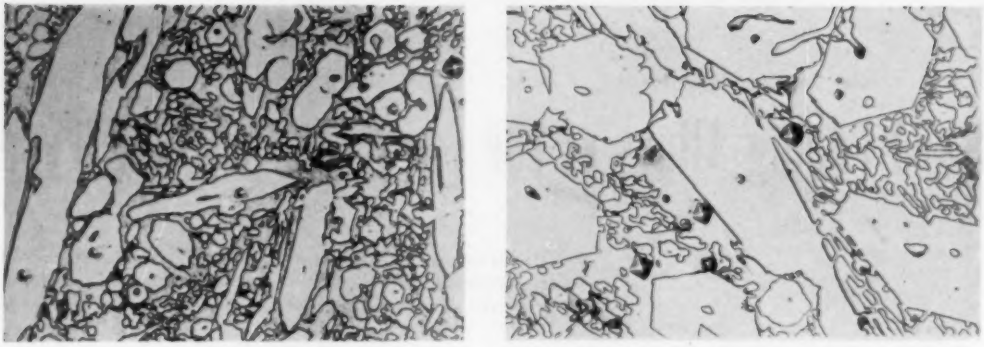

(a) (b)

Fig. 1 Austenitic 30% chromium iron hard facing. Etchant: 1% picral and 5% HCl. 500 ×

(a) Four-layer, 3/16 to 1/4-in. thick oxy-acetylene weld deposit of 3.30% carbon, 6% Mn, 2% Si and 30% Cr alloy. The constituents are Cr_7C_3 type carbides (VPN about 1770) in a matrix of austenite and smaller carbides. Rockwell hardness: C53. Area shown is 0.125 in. above weld junction with base metal.
(b) Three-layer, 1/4-in. thick oxy-acetylene weld deposit of 5.00% C, 6% Mn, 2% Si and 30% Cr alloy. The constituents are Cr_7C_3 type carbide. (VPN about 1690), smaller carbides and an austenite matrix (VPN about 360). Note the greater volume of large carbide crystals at this carbon level. Rockwell hardness: C60. Area shown is 0.063 in. above weld base.

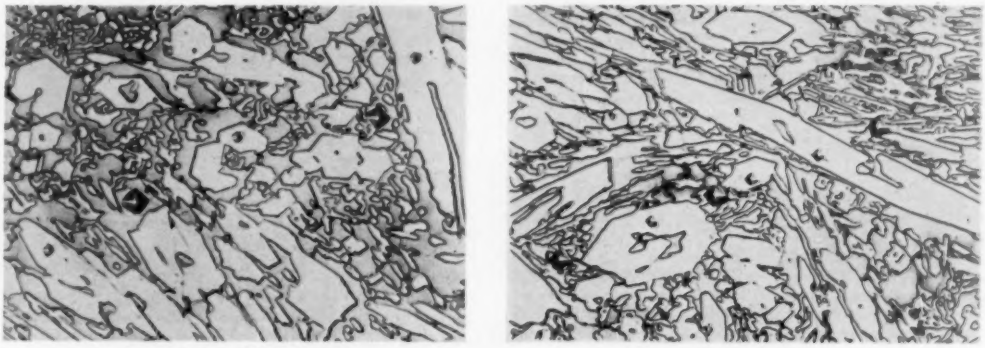

(a) (b)

Fig. 2 Austenitic 30% chromium iron hard facing. Etchant: 1% picral and 5% HCl. 500 ×

(a) Three-layer, 3/16-in. thick oxy-acetylene weld deposit. Rockwell hardness: C55. Area shown is 0.1075 in. above weld base.
(b) Six-layer, 3/8-in. thick oxy-acetylene weld deposit. Rockwell hardness: C57. Area shown is 0.375 in. above weld base. Rod composition: C 4.43%, Mn 6.9%, Si 2.1% and Cr 30.4%. Constituents are Cr_7C_3 type carbides (VPN 1730) and austenite containing smaller carbides. The Vickers diamond impressions demonstrate the relative hardness of the constituents.

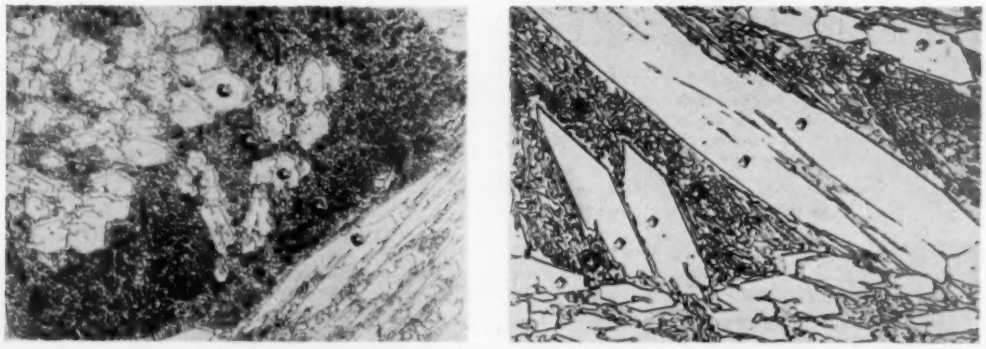

(a) (b)

Fig. 3 Austenitic 30% chromium iron hard facing. Etchant: 1% picral and 5% HCl. 500 ×

(a) Three-layer, 3/16-in. thick, 28-v, 150-amp, arc weld deposit. Rockwell hardness: C54. Area shown is 0.190 in. above weld base.
(b) Six-layer, 3/8-in. thick, 28-v, 150-amp, arc weld deposit. Rockwell hardness: C57. Area shown is 0.187 in. above weld base. Rod composition. C 4.43%, Mn 6.9%, Si 2.1% and Cr 30.4%. Constituents are Cr_7C_3 type carbides (VPN 1535) and a granular matrix of austenite and fine carbides. The Vickers diamond impressions demonstrate the relative hardness of the constituents.

8.0% manganese, 2.0% silicon and 29.5% chromium. Subsequent experience has operated to raise the carbon to near 5%, thus increasing the volume of the hard carbides present and slightly raising the over-all hardness. An important effect of the higher carbon levels is a relatively long melting range within which the alloy is mushy. This makes possible high bead contours and shaping of the deposit by hot wiping. When surfacing near edges, this effect is helpful in precisely positioning the deposit.

Metallography

Weld deposit structures typically consist of roughly hexgonal shaped spines of chromium carbide set in a matrix of austenite that also contains many smaller carbides. Figure 1 shows these and something of the relative volume of the large carbide crystals in relation to carbon content.

Figures 2 and 3 show structures of an intermediate carbon level as affected by weld deposit thickness and welding method. The most obvious difference is the finer texture of the matrix aggregate of austenite and fine carbides in arc welds, which is attributed to their usually more rapid cooling rate. There is also an opportunity for dilution from base metal admixture, which causes fewer of the large carbide crystals to appear, as in Fig. 3 (*a*). The first layer of an arc weld may differ considerably from the nominal hard facing composition.

These structures were obtained from welds made on $1^1/_2$ x $2^1/_4$ x $1^1/_8$-in. blocks of SAE 1020 steel using $^5/_{16}$ in. diameter rods and represent a standardized test condition. It is obviously impractical to duplicate all of the various field conditions in describing the metallography, but those that appear here are reasonably representative of gas welds and of arc deposits that have suffered little or only moderate dilution.

Identification of the large carbides was based on X-ray diffraction patterns, which match best with the $(Cr, Fe)_7C_3$ carbides of Goldschmidt's reference data.[1] Manganese carbide, Mn_7C_3, is reported to be virtually identical in structure and it seems likely that iron, chromium and manganese are all present in the compound, with chromium as the dominant element. The diffraction patterns showed little or no evidence of the other possible carbides, Cr_4C (or $Cr_{23}C_6$) and Cr_3C_2.[2] The chromium carbide Cr_7C_3 is quite stable at all temperatures below its melting point; there is no tendency to graphitize as is the case with some others such as tungsten carbide (WC) and cementite (Fe_3C).[3] However, Cr_7C_3 will react with steam above 1025° F.[4]

The $(Cr, Mn, Fe)_7C_3$ carbides have a VPN* hardness of perhaps 1730. Various determinations have given averages of $VPN_{25\ gm}$ 1676 ± 106 and 1638 ± 127 on longitudinal faces; and 1860 ± 101 and 1743 ± 66 on cross sections of the carbides in Fig. 1 (*a*) and 1 (*b*), respectively. The plus-minus values indicate the 95% confidence interval as calculated statistically from the observed range of seven observations. The scatter bands are such that the differences between averages may not be significant. This carbide hardness is above that of quartz and thus confers resistance to scratching abrasion by most common materials.[1] The hard carbides are brittle and fracture readily.

The austenitic matrix is softer [about 360 VPN in Fig. 1 (*b*)] and somewhat plastic. Precise hardness determination is difficult because of the closely associated small carbide crystals. However, the austenite can be eroded from around the carbides and may not give them competent support under conditions of high-stress abrasion.

The austenite, as welded, is rich in dissolved carbon. Much of it separates out as spinelike crystals of Cr_7C_3 during cooling, some crystallizes as smaller carbide particles, and some remains in solid solution. The effect of the high chromium content together with that of the manganese or nickel is to so stabilize the austenite that it does not transform by usual steel hardening reactions. It can precipitate some additional carbide in dispersed form during aging heat treatments above 1400° F, but this hardening is minor and is neglected in practical hard facing. A casual check on a gas weld indicated an insignificant change in hardness after 24 hr at 1400° F, an increase of about 6Rc points after 24 hr at 1600° F, and in increase of 1.6Rc points after 24 hr at 1800° F. The hardness tests were replicated sufficiently to establish the statistical significance of these small changes.

Hardness

The as-welded hardness when deposited by the oxy-acetylene method will vary with carbon content. The average of 104 production quality control tests was Rc56.1 with a standard deviation of 1.5 and an observed range of Rc51 to 62, representing a range of 4.3 to 5.2% carbon. Macrohardness values such as Rockwell or Brinell numbers will increase slowly as carbon increases. Such figures reflect the greater proportion of the hard carbides in the softer matrix but do not reliably indicate abrasion resistance.

The variables in arc welding lead to a greater range in deposit hardness. The base is melted and mixes with molten electrode metal; the low-carbon, low-alloy base may easily be half of the first weld bead. Such dilution can markedly affect the properties of the deposit. In multiple layers this effect is progressively diminished. Some hardness values from three layer deposits appear in Table 1.

Note that the weld deposit compositions of the five lots differ appreciably, which may be attributed to the fact that there is as yet no standardized specification, to the probable differences between individual heats and to the variables of welding. The data were

* Vickers Pyramid Numbers (from hardness tests with a Vickers diamond pyramid indenter) have the same mathematical basis as Brinell Hardness Numbers, but with light loads (25 gm in this case) can measure hardness well beyond the 700 BHN limit of the Brinell test.

Table 1—Hardness of Some Arc-Weld Deposits of High-Chromium Irons (Ref. 5)

	Chemical analysis of weld deposit, %					Brinell* hardness, ° F		Average hardness Rockwell C*			Average hardness Rockwell C†		
Mfgr.	C	Mn	Si	Ni	Cr	70	850	1st layer	2nd layer	3rd layer	1st layer	2nd layer	3rd layer
A	*3.17	4.30	4.01		29.1	614	583	52	55	56			
											56	57	55
D	*4.16	5.44	2.02	0.78	27.7	541	455	53	55	55			
E	*3.42	4.32	2.69	0.73	29.3	489	413	47	53	54			
											42	55	51
G	*3.45	0.51	0.46	4.57	28.7	461	404	46	50	50			
											48	52	52
Hb	*2.58	0.44	0.22	1.32	24.7	436	368	41	49	51			
	†2.12	0.50	0.19	0.30	28.5						35	51	51
	Average of five lots:												
	First layer					448	386						
	Second layer					520	456						
	Third layer					557	492						
								From all deposits					
	Estimated standard deviation					30.4	77.8	5.2					
	Triplicate coupons std. deviation					43.0		7.5					

* Data from U. S. Naval Engineering Experiment Station.
† Data from Theodore Gaynor of Bethlehem Steel Co.

subjected to statistical analysis by B. B. Day, who concluded that the BHN (at 70° F) differences between lots, except E and G, were probably significant. Lot A is unusually high in silicon, lot G uses nickel instead of manganese as an austenite stabilizer and lot Hb belongs to the hardenable HC250 type described later.

The average hardness increases with each of the three layers. However, experimental errors were so large that only the difference between the third layer BHN and the others is statistically significant. The Rockwell hardness trends are inconclusive. The observed scatter emphasizes the variability of arc weld deposits.

Besides dilution, electric welding may change composition by oxidation of carbon and other elements in the arc. These changes are serious for some alloys but are usually unimportant for this class. However such variability can best be avoided by using oxy-acetylene welding.

Since dilution is not expected in normal gas welding, the chief variable is carbon absorption from the flame. With the recommended 3X feather to cone or 3:1 ratio flame*,[6] adjustment, a pick-up of 0.4% carbon has been observed if the rod is on the low side of the carbon range. With the rod near 5% carbon a neutral flame can slightly decarburize the deposit.

* Swenson's paper provides sketches illustrating flame adjustment, tip size considerations and general welding technique instructions.

Hot Hardness

Hardness falls slowly with temperature up to about 800–900° F and thereafter falls rapidly and also becomes strongly affected by creep. At 900° F the instantaneous hardness is about Rc43 and 3 min under load will cause an apparent drop to near Rc37. At 1200° F the instantaneous value may be no higher than Rc5 and the apparent loss due to creep in 3 min may be as much as 45 points on the "C" scale. However, the loss of hardness due to tempering is negligible in comparison with many martensitic alloys, and the drop in hardness shown by hot testing is practically recovered on cooling to ordinary temperatures.[7]

Some hot hardness charts appear in a previous publication.[7] Recent tests on gas and arc welds appear in Table 2. In noting the marked difference between gas and arc welds, it should be recognized that arc welding is usually associated with loss of some carbon as well as over-all dilution by fused base metal.

The marked loss in hardness above 1000° F should be remembered in selecting hard-facing alloys. At and above 1200° F the chrome-cobalt-tungsten alloys[7] have a well-established superiority. Below 1000° F they seldom can outperform the austenitic chromium iron or other more appropriate and less expensive alloys.

Table 2—Hot Hardness of Austenitic High-Chromium Iron Weld Deposits

Chemical composition of welding rod: C 4.43%, Mn 6.90%, Si 2.09%, Cr. 30.4%

Specimen status (all specimens stabilized by holding at test temperature for 2½ hr before testing)	Rockwell "C" scale hardness: At 70° F before and after hot test	At 1000° F, minutes under load: 0	1	2	4	At 1200° F, minutes under load: 0	1	2	4
Six-layer gas weld, 3/8 in. thick	57/57	40	37	36	34				
	58/57					25	7	1	−4
Three-layer gas weld, 3/16 in. thick	57/57	38	35	34	33				
	55/54					14	−6	−12	−15
Six-layer arc weld, 3/8 in. thick	58/56	37	27	25	22				
	57/52					6	−27	−31	−33
Three-layer arc weld, 3/16 in. thick	58/55	29	23	21	18	Too soft for valid measurement			
	48/48								

NOTE: Structures of these deposits are shown in Figs. 2 and 3.

Impact

This alloy may withstand very light impact without cracking, but if blows produce plastic deformation, cracks will form readily. It seldom is used under conditions of medium impact and is considered quite unsuitable for heavy impact. Dynamic compression stresses above 60,000 psi should be avoided.

As an example of behavior under impact, $^7/_8$ in. diam by $^7/_8$-in. high cast specimens from 4.15% C and 5.0% C alloys were subjected to repeated impact blows.[11] Cracking appeared after 1000 ft-lb of impact on the 5.0% carbon alloy and after 4500 ft-lb on the 4.15% carbon specimen. Complete failure occurred after 1650 and 7000 ft-lb respectively. The specimens were permanently reduced in height by 0.52 and 1.54% at the point of failure. This effect of carbon has motivated the use of two ranges within the broad specification range, the higher carbon for agricultural service and the other for industrial use. Where an even stronger material of the cast iron type is required, the martensitic irons are more appropriate.

Compression

The effect of carbon on compression properties is parallel to the impact evidence. Table 3 includes detailed evidence that explains why the limit of 60,000 psi is suggested. This is an arbitrary yield strength value corresponding to about 0.05% permanent deformation. A number of such stresses can be absorbed before the plasticity in compression is exhausted, but stresses higher than this will accelerate cracking by quickly using up the ductility available. Also, it should be remembered that the tensile yield strength may be similar to that in compression.

Surface Stability

The high chromium content confers excellent oxidation resistance up to 1800° F and it can be considered for hot wear applications if its hot plasticity is not objectionable.[8] The matrix chromium content is comparatively low, however, and is thus not very effective in providing resistance to liquid corrosion. The alloy will rust in moist air and is not stainless, but it is more stable than ordinary iron and steel.

Abrasion

Since this alloy is quite sensitive to several factors, it is essential that variables in the field of abrasion be recognized. These include abrasive hardness, angularity, particle size and the stresses involved.

Almost any cast iron will perform well against soft minerals and rocks such as calcite, kaolin (in clay), fluorite, limestone and dolomite. Steels also wear well against these. However, the commonest abrasive encountered is quartz, which is harder than hardened steel and thus wears it rapidly. Quartz may even be responsible for most of the wear blamed on softer material because its presence is not realized. Very fine quartz is usually present in clay for example.

The common occurrence of quartz justifies its use as a standard test abrasive. With it, differences due to angularity, size and stress can be demonstrated. Two standardized laboratory tests[8,9] have been employed to produce quantitative data.

One uses a loose wet abrasive that is ground between a circular copper lap and the face of the alloy being tested. The chief purpose of the water used is to help the flow of abrasive to the wearing face, but it also prevents frictional heat from becoming a variable. The other test feeds loose dry abrasive to a rubber wheel bearing against the specimen. The wheel yields to the abrasive, preventing loads from rising above the elastic limit of the rubber. The effective abrasive undergoes little change in this test, whereas in the copper lap device it is ground finer at a significant rate. These two wear patterns have been tentatively designated as wet sand grinding abrasion and dry sand scratching abrasion (or erosion). The grinding abrasion test is more severe by a factor of 1.4 for mild steel and of 20 for gas welds of austenitic chromium iron.

The grinding test correlates well with ball mill service.[10] The rubber wheel test correlates with the erosion seen in rotary shot and sandblast machine blades, and is related to plowing in sandy soil.

Particle size makes a marked difference in the response of some materials. For example, the abrasiveness (in the wet grinding test) of a 50 mesh* sand was 10.4 times that of silica flour against gas welds of austenitic chromium iron. In contrast, the coarse sand was only 1.5 times as abrasive to 1020 steel. Parallel tests with coarse sand show a definite superiority of Cr-Mo or Cr-Ni martensitic irons over this austenitic type, but as abrasive particle size decreases this pattern changes until the performance is reversed for silica flour and for mixtures of fine sand and clay that simulate "wheat

* Mesh size is rated by American Foundryman's Society Grain Fineness Number (GFN).

Table 3—Compression Test Data for Austenitic Chromium Irons

(1.5- × 0.400-in. diam specimens from $^1/_2$-in. castings)

C, %	Yield strength, 0.05% set, psi	Yield strength, 0.10% set, psi	Ultimate compressive strength, psi	Deformation* Elastic %	+	Plastic %	=	Total, %	RC
4.09	62,000	86,000	286,500	1.01		3.42		4.43	55
4.09	62,000	87,000	274,000	0.92		3.40		4.32	54
4.76	96,000	122,000	207,000	1.04		1.17		2.21	50
4.76	70,000	92,000	152,000	0.72		0.37		1.09	52

* Values at failure as determined from stress-strain diagram.

belt" soils.† This change is attributed to the lowered stress on the abrasive contact point, since four times as many particles are theoretically available to carry the load when particle size is halved.

In loose abrasive grinding tests initial angularity is not so important since the grinding action quickly produces many sharp edges. However, the abrasiveness of quartz can be increased by a factor of about three by using crushed flint, which is tougher as well as more angular than quartz sand, though its hardness and composition are identical. With much lower stresses that cannot crush the abrasive, angularity becomes a potent variable. With the rubber wheel abrasion test, the abrasiveness of angular quartz particles may be 4 or 5 times that of rounded sand grains.

A fundamental difference in the two abrasion tests that provided the data herein is the stress that is applied on a microscopic scale to the abraded surface. The cushioning of the rubber wheel keeps this stress low while in the grinding test with 50 GFN sand the stress rises to at least the crushing strength of the abrasive. Under low-stress abrasion ordinary white cast irons perform well, though not as well as the austenitic chromium iron. Under high-stress grinding abrasion they are poor and are inferior to a variety of hard and soft steels. Some general comparisons are summarized in Fig. 4.

Wear in these tests is reported as an abrasion factor, which is a ratio of weight loss to that of a standard of annealed (SAE 1020) mild steel. Small factors indicate a low rate of wear. To indicate relative merit of the different materials the abrasion factor scale is inverted in Fig. 4. Also, on the right margin, a ratio of merit versus SAE 1045 steel, which is frequently recommended as a base for hard facing, is plotted for convenience.

While the two conditions differentiated in Fig. 4 involve wet and dry testing, this difference should not be considered distinctive. Both of the tests can and have been operated with and without water. The important distinction is the strength of the back-up face and the level of stress at the abrasive points that it permits.

Austenitic high-chromium iron has its most important field of usefulness where the dominant wear factor is abrasive erosion or low-stress scratching abrasion. Successful field applications involving such conditions are found in screw conveyors, chutes, feed spouts and pipe-line fittings of all kinds where wet or dry abrasive

† Soil samples from northern Oklahoma and Southern Kansas were analyzed to provide these formulations for "soil" abrasion tests.

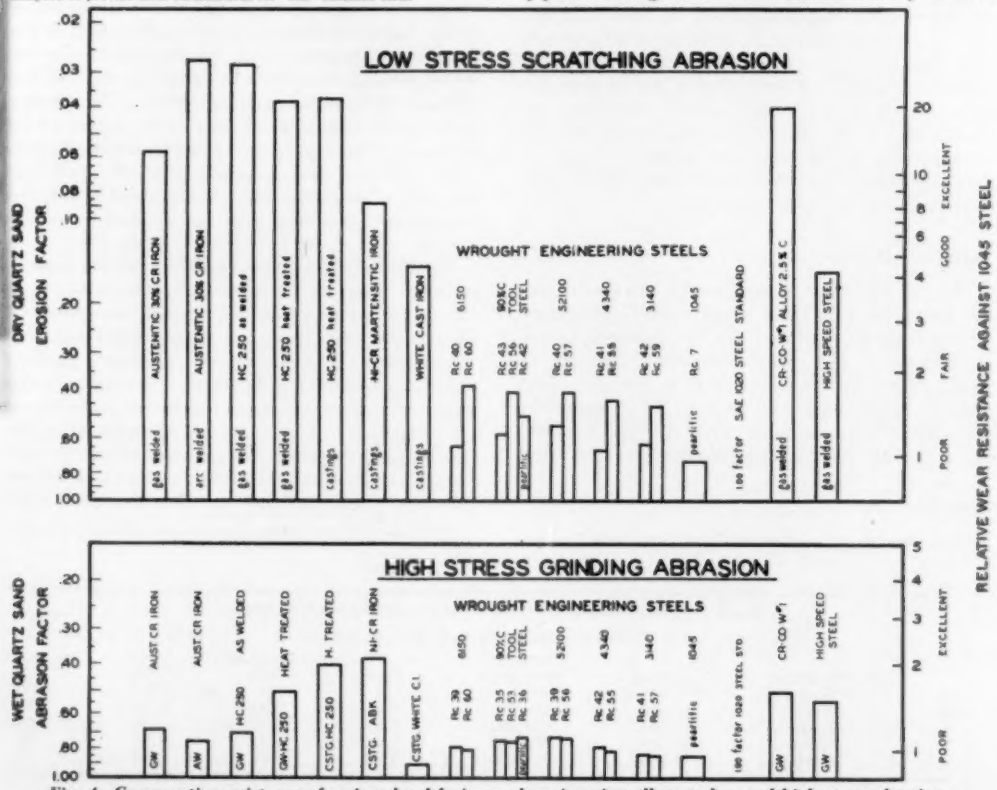

Fig. 4 Comparative resistance of various hard facing and engineering alloys to low and high stress abrasion

particles are handled. Most agricultural machinery parts that wear from soil erosion can be effectively protected with this alloy. Pump runners, flotation mill impellers, brick and clay plant machine parts, and cement mill parts provide many places where such hard facing leads to important economies. However, the austenitic iron should be selected cautiously if impact, grinding or crushing conditions are present. As these factors become important the martensitic irons are likely to be a better choice, and they in turn should give way to martensitic or austenitic steels as the impact or stress conditions become more severe.

The employment of arc welding, with its reduction in volume of hard carbides as shown in Figs. 2 and 3, and as reflected in hardness data in Table 1, may affect both abrasion resistance and toughness. Haworth, who developed the rubber wheel testing technique,[11] reports a weight loss spread of 2.6 to 0.35 gm in a standardized test with crushed quartzite, the arc welds showing inferior wear resistance.[12] As carbon is reduced by dilution, the less expensive arc welds are expected to be tougher than oxy-acetylene deposits. Understanding of this pattern is helpful in exercising engineering judgment.

Some test data from an experimental aluminum oxide grinding wheel test are of interest in relation to carbide volume in these high-chromium irons. Though the test is not yet well standardized and correlated with field performance, it demonstrates a performance pattern different from that of the other abrasion tests used in this work and suggested an area where the austenitic chromium iron is distinctly superior to the hardenable HC250 type that is described later.

The test employs a 38 grit $^1/_2$-in. wide, 10-in. diam. alundum grinding wheel at 92 rpm abrading a 0.35 sq in. surface on a small brake-shoe type specimen. Abrasion factors are reported versus a 1020 steel standard as in the other tests. Table 4 contains pertinent data.

Table 4—Resistance of High-Chromium Irons to Grinding Wheel Abrasion

Material tested	*Hardness, BHN*	*Alundum grinding wheel abrasion factor*
Annealed SAE 1020 Steel (test standard)	107	1.00
Annealed HC250 casting	375	0.44
	375	0.47
Hardened HC250 casting (air cooled from 2000° F)	683	0.25
	683	0.28
Austenitic chromium iron casting (4.15% C, 32% Cr)	477	0.066
	477	0.065

This type of wear is probably related to the gouging[13] abrasion frequently observed in the field. However, gouging abrasion is so commonly associated with heavy impact, that the high-chromium irons are generally unsuitable because of the brittleness.

Metal to Metal Wear

Frictional wear on metal faces is quite difficult to predict or to measure in the laboratory. Most data are from devices that involve some lubrication, which has a profound effect. If the mating faces are dry, rub in a way that removes dirt, oxide films and the like, and are under enough pressure to insure intimate contact, there is likelihood of welding. This leads to seizing, scoring, galling, scuffing and similar manifestations of welding wear. Low yield strength constituents, such as austenite, are easily forced into intimate contact and thus weld easily. External or frictional heat, because it lowers the yield strength, promotes such welding but may not be necessary to it.

The austenite of the chromium irons is thus relatively susceptible to welding wear, but in contrast the hard carbides resist deformation, intimate contact and seizing. Thus the practical result may not be predictable. If abrasives are present the surfaces tend to polish well and a low friction coefficient is expected. The carbides are likely to stand slightly in relief and thus carry the frictional load unless it is too high. Provided the microscopic roughness from this relief effect is not objectionable good performance is expected as long as the abrasive is fine enough to avoid the high-stress grinding pattern discussed above.

Among the metal to metal applications where this alloy has been acceptable are tractor clevis connections and the like, high-speed drive sprockets; cement mill drive shaft bearings and bushings; drag chain links, pins, rider blocks and idlers; friction clutches on lumbering equipment, railway car retarder parts, steel mill guides of various kinds, barrels for wire coilers, pinch rolls, wire straightener rolls and piercing points. However, this grade is not always best for such parts, and critical judgment and careful comparisons are advisable when possible.

Incidentally, mill scale or iron oxide on metal surfaces is a common abrasive. It is not so hard as quartz, and its form usually does not allow it to produce high-stress abrasion, thus permitting effective use of the austenitic chromium irons. In Fig. 5, the protection afforded by this alloy permitted handling 63,000 tons of bar steel whereas the normal life of an unfaced guide

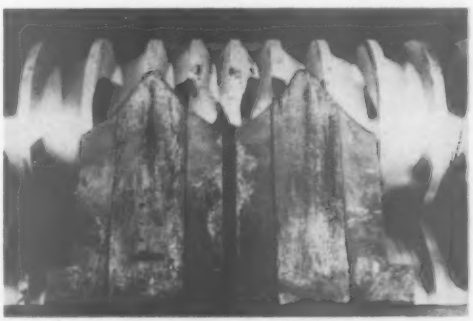

Fig. 5 Worn faces of bar mill guides hard surfaced with an austenitic high chromium iron. Service life was about 63,000 tons of bars handled. Normal life of an unfaced guide is about 1200 tons

was about 1200 tons. Some cracking from thermal fatigue has occurred, but this is not serious here.[8]

For estimation of welding wear behavior, compression data seem to be among the pertinent engineering properties. The yield strengths of these austenitic irons (Table 3) are lower than those of the martensitic irons and steels, about equal to the high-carbon cobalt base type, and superior to austenitic steels or the low-carbon cobalt and nickel base varieties.[14]

Machinability

The deposits are considered commercially unmachinable with cutting tools and are also very difficult to grind. For machine shop use the grinding wheels recommended by their manufacturers are aluminum oxide abrasive with a 24 grit size, hard (Q) and medium spaced resinoid bond for off-hand high-speed work and a slightly softer (P) vitrified bond, for off-hand low speed use. It has not been clarified why the harder silicon carbide abrasive wheels are not recommended.

Identification

When welding rods are mixed, this grade can frequently be identified by (*a*) brittleness of the cast rod, (*b*) nonmagnetic behavior, (*c*) its very dull, lifeless spark that is short and produced with difficulty, (*d*) sometimes by the presence of fine needlelike Cr_7C_3 crystals on a fracture section, and (*e*) a spot test for cobalt will distinguish it from the somewhat similar Cr-Co-W welding alloys. The magnetic permeability of rod specimens is about 1.03 with a magnetizing force of 24 oersteds. The specific gravity is about 7.48.

Welding Procedure

Flat position welding with a 3× carburizing or 3:1 ratio flame[6] is recommended. The coefficient of thermal expansion is about 50% greater than that of carbon steels and irons (in round numbers, 10 millionths of an inch per inch per degree Fahrenheit). Contraction stresses are prone to crack the deposit, and while these cracks may do no harm, they can be minimized by preheating and postheating techniques. The use of a flux may be helpful in dealing with dirt, scale and other undesirable surface contamination, but on a clean bright metal surface, such as grinding produces, flux is ordinarily unnecessary. A peculiarity of the 6% Mn, 2% Si, 28% Cr alloy is that fluid oxides form on the surface of the weld bead during oxy-acetylene welding. This slag exerts a mild fluxing action against light surface oxides, and assists in multiple-layer welds. It appears to be ineffective on a dirty oxidized surface. A good bond can be produced on all iron base materials provided the base metal is not damaged by the high temperature conditions of welding and weld cooling. The melting point of the alloy is near 2450° F.

This alloy has proved very popular for facing agricultural machinery parts. Plow shares can be considered as a typical successful application because the alloy flows well enough to produce a thin-edge deposit and the wear conditions in sandy soil are typically those of erosion or low-stress scratching abrasion. It is significant that it becomes unsuitable in very rocky soils because of the associated impact.

HARDENABLE CHROMIUM IRONS

In addition to the austenitic type already described, many chromium-iron-carbon alloys have been used for hard facing, including those comparable to various tool steels. They do not readily develop the Cr_7C_3 type of carbides, however, unless chromium is above about 20% and considerable carbon is present. These steels will, therefore, be omitted from this discussion. Beginning with perhaps 2% carbon and 20% chromium, a series of alloys that may range to 5% carbon and 35% chromium is pertinent.

The basic patent on these irons was issued in 1917 (U. S. Pat. 1,245,552). They have since proved successful[13] for many applications involving abrasion. The alloy casting industry has averaged yearly (1945 to 1949) about 190,000 lb[14] of castings of this type. Data from castings are thus a valuable source of information pertinent to the use of the alloys for hard facing. The HC250* composition, with the ranges of

C, %	2.25–2.85
Mn, %	0.50–1.25
Si, %	0.25–1.00
Cr, %	24–30
Ni, %	Minimum

has been more popular in cast form but its useful properties make it well adapted for hard facing.

The alloy can be used as welded, but best all around wear resistance is obtained by a hardening heat treatment that produces a martensitic structure in the matrix. In this condition the alloy combines the advantages of martensitic irons with the hardness of the associated chromium carbides. This susceptibility to hardening transformations by heat treatment differentiates this group from the previously described austenitic irons. The 40 to 74% improvement in high-stress abrasion resistance as shown in Table 7 is significant. The compressive strength after heat treatment is also high (Table 11).

Metallography

These alloys usually carry only small amounts of other alloying elements and stable austenite is, therefore, abnormal. This means that the matrix may exhibit pearlite, martensite or metastable austenite, depending on the thermal history and especially upon cooling rates. The associated Cr_7C_3 carbides are in smaller volume than the usual austenitic grade because of the difference in carbon content.

* This is an Alloy Casting Institute type designation, the H signifying a heat-resistant alloy, the C indicating the 26–30% chromium range, while 250 is the nominal carbon content (2.5% carbon) with the decimal omitted.

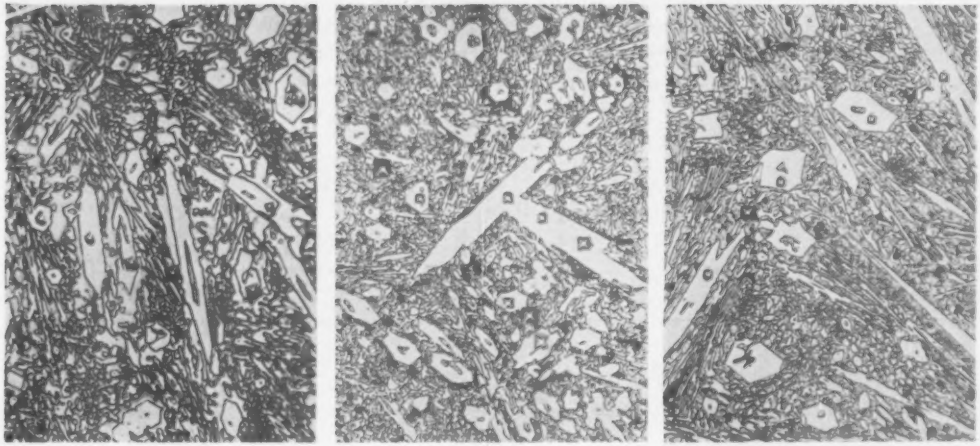

(a) As-welded (b) Annealed (c) Hardened

Fig. 6 Hardenable HC250 chromium iron hard facing. Etchant: 1% picral and 5% HCl. 500 ×

Single-layer weld deposit of HC250 hard-facing alloy after oxy-acetylene deposition (*a*), after annealing for 24 hr at 1400° F and furnace cooling (*b*) and after hardening (the annealed structure) by air cooling from 2 hr at 2000° F (*c*). The matrix of (*c*) is martensitic, and this has the greatest hardness and resistance to high-stress abrasion of the three structures.

Pearlite formation requires very slow cooling, such as occurs with heavy castings, unless dilution (from arc welding) has considerably altered the normal composition. Faster cooling is likely to produce a fine, granular aggregate of metastable austenite and carbides that is commonly seen in weld deposits and small castings. However, by reheating in the range from 1600 to 2200° F, carbides can be precipitated from or dissolved in the austenite, depending on the temperature involved. The lower ranges precipitate carbon, thereby changing austenite composition, and subsequent cooling produces some martensite. The higher temperatures increase the proportion of austenite retained after cooling. This pattern permits hardening by making the matrix martensitic through heat treatment.

In appearance under the microscope the as-welded structure [(Fig. 6 (*a*)] may be similar to that after annealing [Fig. 6 (*b*)] or after hardening [Fig. 6 (*c*)]. The matrix character changes, however, as evidenced by hardness. The true matrix hardness is difficult to determine because of the closely associated carbide particles, but the values below indicate the trend:

Table 5—Microhardness of HC250 Constituents

	*Gross hardness, Rockwell "C" composite structure**		*Microhardness,* Vickers VPN, 25 gm*	
			Carbide	*Matrix*
As-welded	54	L	1707 ± 108	400 – 539
		X	1684 ± 87	....
Annealed	40		1453 ± 194	456 ± 48
Hardened	63	L	1268 ± 125	935 ± 56
		X	1759 ± 92	

* See Fig. 6. L = longitudinal section
X = cross section

Except where an actual range is shown, the values given are averages plus-minus a 95% confidence interval, usually based on the range of seven readings.

The difference between gas welds, as illustrated in Fig. 6 and arc welds may be profound. Arc weld behavior cannot be predicted with assurance because of the variables, such as arc power, bead size and deposition technique, that are in the hands of the welder, but an example can show the trend, as in Fig. 7. Here the weld carbon content has been so reduced by dilution and oxidation that the massive Cr_7C_3 type crystals do not appear. Instead islands and masses of austenite occur in the granular matrix of fine carbides and austenite. In effect, a soft constituent has been substituted for the hard carbides, with a loss of abrasion resistance and an increase in toughness. How far this effect goes, or whether it is good or bad depends on circumstances. This is an area where good judgment is an asset, since it can weigh the relative importance of abrasion and

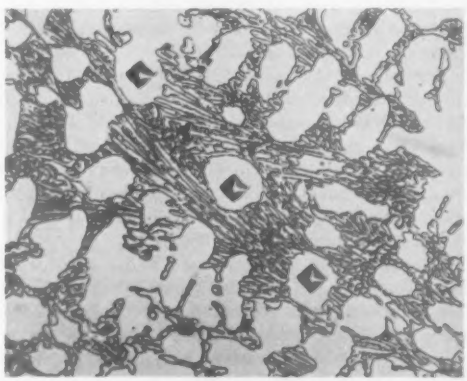

Fig. 7 Hardenable HC250 chromium iron hard facing. Etchant: 1% picral and 5% HCl. 500 ×

Two-layer arc weld deposit of HC250 chromium iron, as-welded on SAE 1020 Steel. The white areas in the granular matrix are austenite with a VPN 25 g. microhardness of about 420. The replacement of the usual Cr_7C_3 crystals by austenite is the result of dilution and oxidation during arc welding. Area shown is 0.017 in. from the base metal.

Table 6—Typical Hardness Ranges of HC250 Weld Deposits

Gas welds on 1- x 4- x 3/8-in. blocks of SAE 1020 Steel					Arc welds on 2- x 2½ x 3/8-in. blocks of SAE 1020 Steel			
Layers	Thickness, in.	Cooling	Rockwell hardness Range	Avg.	Layers	Status	Rockwell hardness Range	Avg.
1	1/16	Air	C53.5–58	C56	1	As-welded	C36–45.5	C43
2	2/32	Air	C52–57	C54	2	As-welded	C53.5–56	C55
3	1/8	Air	C53–55.5	C53.5	4	As-welded	C51–55	C54
4	2/16	Air	C51–54	C52.5				
1	1/16	Water	C48–55	C51	1	1800° F, 2 hr, furnace cool	C32.5–35	C33.5
2	2/32	Water	C48–54	C51	2	1800° F, 2 hr, furnace cool	C37.5–40	C39
3	1/8	Water	C48–55	C51	4	1800° F, 2 hr, furnace cool	C39–41	C40
4	2/16	Water	C46–53	C51				
1/8-in. deposition 2- x 2½ x 3/8-in. block					1	2000° F, 2 hr, air cool	C58–61	C60
					2	2000° F, 2 hr, air cool	C58.5–61	C60.5
As-welded			C52–55	C53	4	2000° F, 2 hr, air cool	C58.5–61	C60
Annealed, 1800° F—2 hr—Fce. Cooled			C48–53	C50.5				
Hardened, 2000° F—2 hr—Air Cooled			C57–60	C59				

impact in the service conditions as well as influence deposition technique.

Hardness

The hardness as gas welded may range from Rockwell 51 to C59. Annealing at 1400° F can lower this to C36–C47. Arc welds can range lower because of carbon loss in the arc and dilution by base metal. (Table 1, item Hb, and Table 6) Rehardening should raise the hardness to C54–C62 and produce the mixture of austenite and martensite of the matrix structure shown in Fig. 6 (*c*).

Heat Treatment

The HC250 alloy can be softened somewhat for machining, which is unusual for high-carbon hard facings. The success of the annealing treatment (12 to 24 hr at 1400 to 1450° F, followed by cooling in the furnace or in still air)[13] depends largely on the carbon content. If gas welding with a carburizing flame has added carbon to the deposit, annealing may reduce hardness only to about 400–450 BHN. Arc welding, if it burns out carbon (as is usually the case) may permit annealing down to below 340 BHN.

The annealed structures of HC250 are more machinable than these hardness levels would indicate. Tungsten carbide tools are employed where possible, since the hard Cr_7C_3 carbides present can cause rapid wear of steel tools, but the chips from cutting break readily and cause a minimum of trouble. Lathe tooling is common, while drilling and tapping can be done at the 2.5% carbon level if hardness is near 350 BHN.

After machining, the alloy should be hardened for use by cooling from the range between 1750 and 2100° F. Liquid quenching is not necessary. Cooling in free air is sufficiently rapid and tends to minimize distortion. The hardened structure is so abrasion resistant that even machine grinding is likely to be uneconomical and a strong effort should be made to establish precise dimensions in the annealed condition.

The critical temperature for hardening is 1450–1550° F. Above this, austenite is stable and a similarity in behavior between HC250 and the 6% Mn-2% Si austenitic types is expected. From 70 to 2000° F the average expansion coefficient on heating is 0.000009 in. per inch per ° F, which corresponds to a total expansion of 1.8%. This includes a lower rate from 70 up to 1500° F, an arrest from 1500–1700° F and a higher rate for the austenite from 1700 to 2000° F. Upon cooling the contraction was observed as 0.0000128 in./in./° F until transformation occurred and 0.0000072 in./in./° F thereafter. The effect of chromium is to lower the rate of expansion. At the 0.35–0.40% carbon level, coefficients of 0.0000084, 0.0000073 and 0.0000067 in./in./° F for 0, 7.7 and 18.9% Cr, respectively, have been reported[17] for the range from 70–1300° F. It should be recognized that the matrix of these cast iron types is a steel containing perhaps 7% Cr and something above 0.40% carbon.

Upon quick cooling the martensitic hardening transformation (Ms) usually occurs between 560 and 150° F. This causes a volume change and can lead to serious stresses. To help avoid them it is desirable to preheat before welding. This is done incidentally to gas welding, but must be included by intent in arc welding practice if it is important to minimize cracking.

Without heat treatment there is no obvious superiority of the HC250 alloy over the 6% Mn 2% Si austenitic type, while the lower carbon may sometimes reduce wear resistance (Table 4). However, when hardened, HC250 may have several advantages. It can attain a compressive yield strength above 150,000 psi and thus can resist light impact effectively.[13] This also contributes to galling resistance. Hardened weld deposits have been successfully used as bushing surfaces in highly stressed sleeve bearings operating under conditions where ordinary lubrication is impractical.

Sometimes HC250 arc welds of favorable composition cool rapidly enough to approach the properties of a heat-treated structure. It is also possible by arc welding on a carbon steel to produce a fusion product that develops martensite. However, unless heat treatment is planned, it is better to obtain air-hardening martensitic structures from other alloys specifically balanced for the purpose.

Table 7—Resistance of High-Chromium Irons to High-Stress Grinding Abrasion

(Wet quartz sand in American Brake Shoe Co. laboratory test, Ref. 9)

Material	*Condition*	*Lab No.*	*Wet sand abrasion*		
			Rc	*BHN*	*Factor*
Austenitic 30% Cr Iron	3/16-in. thick gas weld	R1843	55	...	0.69
Austenitic 30% Cr Iron	3/8-in. thick gas weld	R1844	57	...	0.67
Austenitic 28% Cr Iron	1/2-in. thick casting	R605	58	600	0.88
Austenitic 30% Cr Iron	3/16-in. thick arc weld	R1845	54	...	0.75
Austenitic 30% Cr Iron	3/8-in. thick arc weld *	R1846	57	...	0.74
Austenitic 31% Cr Iron Deposited on austenitic manganese steel	Arc welds	S1496	55	...	0.75
		S1497	58	...	0.67
HC250 as-welded	Gas weld	T2897	60	600	0.69
HC250 as-welded	Gas weld	T2898	57	592	0.69
HC250 as-welded	Gas weld	T3653	56	566	0.72
HC250 heat treated*	Gas weld	T3654	62	639	0.47
HC250 heat treated*	Gas weld	T3662	62	713	0.53
HC250 as-welded	1/2-in. thick arc weld	T2310	57	600	0.56
HC250 heat treated*	3/8-in. thick arc weld	T2311	61	652	0.32
HC250 as-welded	1/2-in. thick gas weld	T2312	59	717	0.65
HC250 heat treated*	1/2-in. thick gas weld	T2313	62	600	0.38
		Standard of annealed 1020 Steel		107	1.00

* Heat treatment was 1400° F, 3 hr, air cool, followed by 2100° F, 2 hr, air cool.

NOTE: The standard error of the abrasion factors from this test is 0.028; thus a 95% scatter band (average ±2 S.E.) includes an abrasion factor range of 0.11. In comparing factors from various materials or conditions a difference greater than 0.11 is therefore significant. The effect of heat treatment on the performance of HC250 is thus well substantiated by these data.

Abrasion Resistance

The as-cast or as-welded structures of both austenitic and hardenable high-chromium irons are much alike in abrasion resistance. The difference in performance due to welding technique is as great or greater than variations that can be assigned to composition. Table 7 permits a comparison under wet high-stress abrasion. Note that the range from 0.65 to 0.75, which can be considered a ±2 standard deviation scatter band, contains all but one of the as-welded specimens. The significant improvement by a hardening heat treatment is obvious. Insistence on statistical significance is pertinent because there are many cases where greater hardness of hard-facing alloys does not provide better abrasion resistance.

The matrix structure seems to have much less effect on low-stress abrasion, as shown in Table 8. At the low abrasion factor range involved, the experimental error shown by duplicate welds may be 100%. The differences between as-welded and as-hardened tests with sand are neither consistent nor significant, and the slight apparent superiority of HC250 over the austenitic grade cannot be accepted as real.

Note that the weight loss from abrasion in Table 8 is not seriously affected by changing to a coarse flint abrasive, but the factors are lowered. This is the result of much greater wear on the steel standards. The flint is Joplin grit, a chert gangue mineral from the Tri-state lead and zinc mining district, and has the reputation of being one of the most abrasive ores on the

Table 8—Resistance of High-Chromium Irons to Low-Stress Abrasion or Erosion (Dry Quartz Abrasives)

Material	*Condition*	*Lab No.*	*Subangular No. 50 sand, dry quartz sand erosion*			
			Rc	*BHN*	*Wt. loss, gm*	*Factor*
Austenitic 30% Cr iron	Gas weld	R3058	56		0.065	0.055
Austenitic 4.1% C, 29% Cr iron	Gas weld	R3060	58		0.080	0.047
Austenitic 4.2% C, 33% Cr iron	Gas weld	R3062	60		0.087	0.075
Austenitic 4.4% C, 28% Cr iron	Gas weld	R3061	57		0.075	0.060
Austenitic 5.0% C, 30% Cr iron	Gas weld	R3063	60		0.053	0.046
HC250 as welded	3/16-in. thick gas weld	T2319	54		0.040	0.026
HC250 heat treated*	1/8-in. thick gas weld	T2320	50		0.085	0.058
HC250 as-welded	Gas weld	T2909	56		0.035	0.021
HC250 as-welded	Gas weld	T2910	57		0.050	0.036
HC250 heat treated*	Gas weld	T2954	56		0.050	0.033
HC250 heat treated*	Gas weld	T2955	59		0.035	0.024
HC250 as-welded	3/16-in. thick arc weld	T2317	48		0.315	0.22
HC250 heat treated*	1/8-in. thick arc weld	T2318	57		0.040	0.027
	SAE 1040 Steel, normalized			164	0.915	0.725
	SAE 1020 Steel, annealed (standard)			107	1.23	1.000

Material	*Condition*	*Lab No.*	*Angular No. 30 flint abrasive, dry Chert erosion*			
			Rc	*BHN*	*Wt. loss, gm*	*Factor*
Austenitic 4.1% C, 29% Cr iron	Gas weld	R3060	53		0.065	0.014
Austenitic 5.0% C, 30% Cr iron	Gas weld	R3063	58		0.095	0.020
HC250 as-welded	Gas weld	U168	51		0.055	0.009
HC250 as-welded	Gas weld	U169	51		0.045	0.008
HC250 heat treated*	Gas weld	U170	58		0.050	0.009
HC250 heat treated*	Gas weld	U171	58		0.050	0.009
	SAE 1045 Steel, normalized			164	4.39	0.821
	SAE 1020 Steel, annealed (standard)			107	5.35	1.000

* Heat treatment was 1400° F, 3 hr, air cool, followed by 2100° F, 2 hr, air cool.

American continent. It is probably similar to some of the jaspilite rock encountered in taconite mining.

Haworth[11] has provided an interesting series of chromium-iron-carbon alloys that shows the beneficial effect of carbon and chromium on resistance to low-stress abrasion. Carbon is especially potent, leading to the conclusion that carbide volume is important. His data also indicate that in the high-carbon, as-cast alloys about 30% Cr may reduce wear by quartz to from one-half to one-fifth that associated with 13% Cr. Heat treatment (1900° F., oil quenched and drawn at 300° F) increased the hardness of the high-chromium irons and sometimes greatly benefited their wear resistance.

Service tests in clay plant operation[18] have confirmed the wear resistance of the HC250 type. In a test of 42 pug mill knife alloys, specimens of 2.53% C, 0.74% Mn, 0.66% Si and 28.14% Cr iron at 460 BHN (no heat treatment) were next to the top in performance, being surpassed only by a heat-treated Cr-Mo iron. Of four muller tire alloys, the iron with 2.62% C and 26.73% Cr was second, a martensitic Ni-Cr iron of the Ni-Hard type being first. Of eight alloys tested as dry pan runner plates the HC250 was best. Clay handling is believed to be chiefly low-stress abrasion and, while the tests were made on castings, the results are considered applicable to oxy-acetylene and undiluted arc-weld deposits.

Heat Resistance

HC250, whose designation stems from its production by heat and corrosion-resistant alloy foundries, is a good heat-resistant iron. It resists softening up to 800° F[7] and has good creep properties (Table 9) in comparison with the common 27% Cr steel. Because it becomes austenitic above 1550° F the volume change from transformation may cause cracking if rapid repeated heating and cooling are involved.

Table 9—Elevated Temperature Properties of HC250 26% Cr Cast Iron*

	Temperature, ° F		
	1400	*1600*	*1800*
Yield strength, psi	9,600	10,200	5,800
Ultimate tensile strength, psi	28,000	30,000	14,000
Elongation in 2 in., %	8	8	30
Reduction in area, %	8	6	24
Stress for 100-hr life, psi		5,900	2,600
Stress for 1000-hr life, psi		3,400	1,400
Limiting creep stress (for 0.0001% per hour), psi		1,300	450
Elastic modulus, million psi	18.8	8.6	6.8
Properties of HC30 (0.30% C, 27% Cr steel) for comparison			
Ultimate tensile strength, psi	10,500	5100	2450
Elongation in 2 in., %	65	94	110
Reduction in area, %	81	93	98
Stress for 100-hr life, psi	3,400	1700	840
Stress for 1000-hr life, psi	2,200	1150	630
Limiting creep stress (for 0.0001% per hour), psi	1,400	760	375

* Cast specimens, annealed before machining.

Scaling from oxidation is quite slow, a surface metal loss rate of 0.005 in. per year penetration being obtained in ten 100-hr test periods at 1600° F. Burgess[19] reports surface stability equivalent to 0.12% C, 27% Cr heat-resistant steel at 1000° C (1832° F) and the level of 25% chromium is expected to maintain useful oxidation resistance to at least 1800° F.[20]

The hot hardness pattern is similar to that of the austenitic type if casual exposure between 600 and 1000° F is involved (Table 10). Creep likewise becomes important at 1000° F. However, with continued exposure a marked drop in hardness occurs, which is due to tempering of the matrix. Stabilizing the structure by tempering for 24 hr at the test temperature before testing lowers the instantaneous hot hardness from 15 to 25 Rockwell "C" points, and under sustained loading creep causes even more softening. In contrast, the effect of tempering on the austenitic companion grade is negligible.

Table 10—Effect of Alloying Elements on the HC250 Hardenable Chromium Iron

		Rockwell "C" hardness, ° F									*Wet sand abrasion*		
		70	*800*		*1000*		*1100*		*1200*				
Heat No.	*Alloy*		*0m*	*3m*	*0m*	*3m*	*0m*	*3m*	*0m*	*3m*	*Lab No.*	*Rc*	*BHN*	*Factor*
46-198	HC250													
As-cast														
2050° F, 3 hr, air cool		..	..	..	..	..	..	..	..	..	N912	60	652	0.35
1950° F, 6 hr, oil quench		65	54	52	48	41	..	..	−5	−53	46-198-3	65	783	0.31
1950° F, oil quench + 1200° F, 24 hr†		43	36	32	27	13	..	..	−4	−47				
49-039*	HC250 4Mo (3.87% Mo)													
As-cast		56	48	47	41	39	37	27	19	−4	R304	54	477	0.67
2000° F, 2 hr, air cool		61	49	48	45	43	39	24	21	−3	R490	62	600	0.30
49-040*	HC250 4W (3.95% W)													
As-cast		56	46	45	42	40	35	24	20	0	R305	54	495	0.56
2000° F, 2 hr, air cool		61	52	50	47	44	33	14	20	−8	R491	62	626	0.34
49-041*	HC250 4V (3.68% V)													
As-cast		56	52	50	46	42	22	4	−2	−26	R306	56	555	0.78
2000° F, 2 hr, air cool		59	53	51	48	45	27	11	7	−18	R492	62	652	0.47

* Hot hardness specimens stabilized 24 hr at the test temperature before testing.
† Hot hardness specimens tempered at 1200° F for 24 hr regardless of test temperature.
NOTE: The 0m and 3M columns under hot hardness indicate the effect of time of loading on apparent hot hardness, corresponding to 0 and 3 minutes under load. The drop in hardness noted is due to creep (plastic flow).

Table 11—Properties of High-Chromium, Hard-Facing Alloys

	Test Temperature	Austenitic type* Oxy-acet. gas welds	Austenitic type* Small castings	Austenitic type* Electric arc welds	Hardenable type† Oxy-acet. gas welds	Hardenable type† Small castings	Hardenable type† Electric arc welds
Hardness—Rockwell							
As-welded	70° F	C56	C56	...	C55	C56	...
or as-cast	600° F	C55	C50	...	...	...	...
	800° F	C48	C47	...	...	...	...
	1000° F	C40	C36	C37	...	...	...
	1200° F	C25	...	C6	...	...	...
Annealed at 1400° F	70° F	...	...	...	C42	...	...
Hardened from 1950° F	70° F	...	...	...	C59	C65	C60
Hardened from 1950° F	800° F	...	...	...	...	C54	...
Hardened from 1950° F	1000° F	...	...	...	...	C48	...
Hardened from 1950° F	1200° F	...	...	...	...	C5	...
Resistance to flow	Under repeated impact	Good	Good	Good	Excellent	...	Good
Resistance to cracking	Under repeated impact	Low	Low	Low	Fair	Fair	Fair
Tensile toughness	Under repeated impact	Low	Low	Low	Fair	Low	Fair
Average compression properties							
Yield strength, 0.05% set, psi			72,500			145,000‡	
Ultimate strength, psi			260,000			404,000‡	
Elastic deformation, %			0.9			1.2‡	
Plastic deformation, %			2.2			2.5‡	
Resistance to wet quartz sand grinding abrasion (high stress)		Fair	Fair	Fair	Excellent‡		Good‡
Resistance to dry quartz sand scratching abrasion (low stress)		Outstanding		Good	Outstanding		Good
Oxidation resistance		Excellent		Excellent	Excellent		Excellent
Useful up to		1800–2000° F			1800–2000° F		
Thermal expansion coefficient							
70–1500° F		0.0000103 in./in./° F			0.0000081 in./in./° F		
1700–2000° F		0.0000138 in./in./° F			0.0000143 in./in./° F		

* Nominal chemical composition: C 4.5%, Mn 6%, Si 2%, Cr 30%.
† Nominal chemical composition: C 2.5%, Mn 1%, Si 1%, Cr 28%.
‡ Hardened by air cooling from 2 hr at 2000° F.

The addition of other alloying elements such as molybdenum, tungsten or vanadium serves to increase hot hardness, but their extra cost does not seem to be justified by abrasion resistance (Table 11).

Though HC250 is a brittle iron at room temperatures, it becomes surprisingly ductile at red heat (Table 9). When it is used as an oxidation and wear-resistant overlay on steels that soften and creep when they become red hot, this plasticity may prevent cracking.

Identification

The spark tests of the austenitic and the hardenable chromium irons are similar. HC250 rods are usually magnetic and this property can be used to distinguish between the two. The response of weld deposit hardness to heat treatment is also indicative.

The melting point of HC250 is near 2320° F. It has a shorter melting range and at the same temperature may appear to be more fluid than the austenitic grade. The higher manganese and silicon of the latter may confer a more pronounced self-fluxing action.

SUMMARY

Two commercially available high-chromium, hard-facing irons have been described in detail. The austenitic type is excellent for conveyor mechanisms handling loose abrasives, all sorts of agricultural equipment subject to erosion by soil, clay, brick and cement plant parts, and some metal to metal and hot wear problems. The hardenable HC250 type has many of the same virtues together with amenability to heat treatment that permits some machining and also a hardening reaction that confers good wear resistance in some additional areas.

To better distinguish these types, abrasion resistance has been differentiated by two levels of stress at the wearing face.

Table 11 permits a quick comparison of the two alloy types. No attempt has been made to list all of the successful applications of the well-known austenitic type; extensive tables of these have appeared in trade literature. The field performance of HC250 hard facing is less well documented and use of the data given here may be expected to expand its areas of recognized usefulness.

Both types can be gas and arc welded, but HC250 is more sensitive to composition changes from oxidation and dilution in arc welding. These changes tend to increase machinability and decrease wear resistance.

In general, the hardenable 29% chromium irons can substitute, with or without heat treatment, for the related austenitic type. After a hardening heat treatment it has resistance to both high- and low-stress abrasion and can substitute for the other martensitic irons. If some machinability is required the annealed HC250 grade is unique among the hard-facing irons.

The influence of heat treatment is apparently not widely known, and field experience with treated HC250 is scant in comparison with the austenitic iron that has been popular for many years. One purpose of this paper is to provide engineers with greater insight when selecting alloys and to encourage the exercise of judg-

ment rather than a dependence on the experience of others. The latter can be misleading, especially when field conditions are poorly defined. As an example, the austenitic iron may be excellent as a facing for power shovel dipper teeth working in sandy soil, but could be entirely unsuitable if the dipper is to work in heavy boulders where impact is severe.

The two alloys are logical substitutes for the more expensive high-carbon Cr-Co-W alloys provided corrosion resistance or hot strength above 1000° F are not critical requirements. At atmospheric temperatures these iron-base surfacing materials are less expensive and frequently superior to the cobalt base type in performance.

ACKNOWLEDGMENT

The authors are indebted to John W. Gleassey for the photomicrographs, to Harry C. Satterlee for invaluable aid with welding and microhardness determinations, to the Metallurgical Department of the American Manganese Steel Division for technical data, welding rod and test specimens, to R. C. Carruthers, H. A. Fabert, J. A. Fellows, N. A. Matthews and L. B. Haughwout for helpful criticism and to the American Brake Shoe Co. for permission to publish this paper.

The authors also wish to thank Bela Ronay of the U. S. Naval Engineering Experiment Station and Theodore Gaynor of Bethlehem Steel Co. for making available some of the tabular data.

Bibliography

1. Goldschmidt, H. J., "Interplanar Spacings of Carbides in Steels," *Metallurgia*, 103 (June 1949).

2. Bloom, David S., and Grant, N. J., "The System Chromium–Carbon," U. S. Navy Bureau of Ships, Research Memorandum No. 4–49 (1949).

3. Boericke, F. S., "Equilibria in the Reduction of Chromic Oxide by Carbon, and Their Relation to the Decarburization of Chromium and Ferrochrome," U. S. Bureau of Mines Publication R.I. 3747, March 1944.

4. Kelley, K. K., Boericke, F. S., Moore, G. E., Huffman, E. H., and Bangert, W. M., "Thermodynamic Properties of Carbides of Chromium," U. S. Bureau of Mines Technical Paper 662, 1944.

5. Communication from Bela Ronay to the AWS-ASTM Surfacing Filler Metal Sub-Committee. These data are from a cooperative program of this committee and the Navy Department Bureau of Ships. The Navy tests were performed at the Annapolis U. S. Naval Engineering Experiment Station.

6. Swenson, Oscar E., "Hard Facing of Steam Valve Seats and Disks," THE WELDING JOURNAL, 29 (12), 1053–1058 (1950).

7. Avery, Howard S., "Hot Hardness of Hard-Facing Alloys," *Ibid.*, 29 (7), 552–578 (1950).

8. Avery, Howard S., "Hard-Facing Alloys for Steel Mill Use," *Iron and Steel Engr.*, September 1951, Vol. XXVIII, No. IX, pp. 81–106.

9. Avery, Howard S., "Hard Surfacing by Fusion Welding," American Brake Shoe Co., New York (1947).

10. Norman, T. E., Loeb, C. M., Jr., Avery, Howard S., discussion of "Wear Tests on Grinding Balls," *Trans. AIME*, 176, 521–523 (1948)

11. Haworth, R. D., Jr., "The Abrasion Resistance of Metals," *Trans. ASM*, 41, 819–854 (1949).

12. Haworth, R. D., Jr., "Effect of Welding Practice on Abrasion Resistance of Hard Facings," *Iron Age*, 83–87 (Oct. 7, 1948).

13. Avery, Howard S., "Hard Facing for Impact," THE WELDING JOURNAL, 31 (2), 116–143 (1952).

14. Avery, Howard S., "The Selection of Hard Facing Alloys," *Product Engrg.*, XXIII, No. 3, 154–157 (March 1952).

15. Alloy Casting Institute "Statistical Reviews, Production Castings," issued yearly.

16. *Abrasion Resistant High Chromium Iron*, a booklet by Electro Metallurgical Division of Union Carbide and Carbon Corp., 1950.

17. Jones and Heselwood, "The Effect of Chromium and Carbon Contents on the Coefficients of Thermal Expansion of Chromium Steels," *Jnl. Iron and Steel Institute* (British), CXXXVII, No. 1, 361–382 (1938).

18. Dierker, Arthur H., and Everhart, J. D., "Wearing Properties of Some Metals in Clay Plant Operation, Part I. Pug Mill Knives, Muller Tires, Runner Plates, Screen Plates," Ohio State University Engineering Experiment Station *Bull. No. 87* (November 1937).

19. Burgess, C. O., "Influence of Chromium on the Oxidation Resistance of Cast Iron," *Proc. ASTM*, 39, 604–622 (1939).

20. Anon., "Chromium in Cast Iron," Electro Metallurgical Co. of Union Carbide & Carbon Corp., 1939. This includes a 33-reference bibliography.

(*Continued from page 902*)

Molybdenum and Molybdenum Alloys. Jet Engines Push Welded Molybdenum Study. Iron Age, vol. 170, no. 2 (July 10, 1952), pp. 145–148.

Oxygen Cutting. More About Carbon-Arc Cutting and Gouging, H. Chappie. Industry & Welding, vol. 25, no. 6 (June 1952), pp., 70, 73–79.

Pipe Lines. Let Oxy-Acetylene Make Your Pipe Work Easier, E. P. Auler. Power Eng., vol. 56, no. 3 (Mar. 1952), pp. 74–76.

Preheating. How Preheating and Controlled Cooling Improve Weld Quality. Industry & Welding, vol. 25, no. 6 (June 1952), pp. 62–64, 66.

Pressure Vessels. Fabricating Modern Pressure Vessels. Welding & Metal Fabrication, vol. 20, no. 4 (Apr. 1952), pp. 120–129; No. 6 (June), pp. 207–212.

Rails, Welding. Report of Special Committee on Continuous Welded Rail. Am. Ry. Eng. Assn.—Bul., vol. 53, no. 500 (Feb. 1952), pp. 683–693.

Refrigerating Machinery Manufacture. Welding Facilitates Construction of Refrigerated Carbonating Equipment. Refrig. Eng. vol. 60, no. 2 (Feb. 1952), pp. 153, 190.

Resistance Welding Applications Increase. Steel, vol. 131, no. 3 (July 21, 1952), pp. 91–96, 98.

Shipbuilding. Factors Involved in Welded Shipbuilding, E. W. Ansell. Welding & Metal Fabrication, vol. 20, no. 6 (June 1952), pp. 213–218.

Shipbuilding. New Tugs for Old, C. Richardson. Mar. Eng. & Shipg. Rev., vol. 57, no. 5 (May 1952), pp. 72–74.

Shipbuilding. Prefabricated Ship Construction, C. Stephenson. Brit. Motor Ship, vol. 33, no. 387 (June 1952), pp. 106–107.

Shipbuilding. Welding in Ship Repairs, J. W. Coulthard. Inst. Mar. Engrs.—Trans., vol. 64, no. 4 (Apr. 1952), pp. 2–5; no. 5 (May), pp. 1–5.

Soldering Aluminum. Sheet Metal Worker, vol. 43, no. 8 (May 1952), pp. 46–48.

Steel Hardening. Flame Hardening by Oxy-Town Gas. Shipbldr. & Mar. Engine Bldr., vol. 59, no. 526 (June 1952), pp. 415–416.

Tanks. Tall Aluminum Chemical Tank Grows Upward as Shell Plates Are Welded on from Below, W. B. Dunwoody, J. A. Rademaker, and J. D. Wilson. Construction Methods & Equipment, vol. 34, no. 4 (Apr. 1952), pp. 88–90.

Tanks, Military, Manufacture. Tanks Roll on Welded Wheels, L. Maas. Am. Mach., vol. 96, no. 12 (June 23, 1952), pp. 106–107.

Welding, Electric Resistance Titanium. Titanium Alloys Flash Welded Easily, I. A. Oehler. Steel, vol. 131, no. 2 (July 14, 1952), pp. 84–85.

Tubes. Continuous Tube Forming and Welding. Welding & Metal Fabrication, vol. 20, no. 6 (June 1952), pp. 204–206.

Welded Steel Structures. New Look in Structural Steel. Industry & Welding, vol. 25, no. 6 (June 1952), pp. 33–34, 67.

Welded Steel Structures. Ore Bridge Span Uses Arc Welding for First Time, H. E. Cable. Iron & Steel Engr., vol. 29, no. 6 (June 1952), pp. 116, 118, 120.

Sheet Metal. Electric Arc Welding of Light Gauge Sheet Metal Fabrications, R. Gardener. Mech. World, vol. 131, no. 3390 (Jan. 1952), pp. 12–13.

Welding, Electric Resistance. "Dot Weld" Process, J. A. Cooper. Welding & Metal Fabrication, vol. 20, no. 6 (June 1952), pp. 218–219.

Welding, Electric Resistance. Scientific and Mass Production Aspects of Resistance Welding, A. J. Hipperson. Instn. Production Engrs.—J., vol. 31, no. 8 (Aug. 1952), pp. 337–358.

Welding, Electric Resistance. Applying Projection Welding to the Product, R. H. Warring. Mech. World, vol. 131, no. 3391 (Feb. 1952), pp. 70–71.

Welding Jigs and Fixtures. Special Fixtures Speed Sheetmetal Fabrication, G. C. Farrington. Iron Age, vol. 170, no. 2 (July 10, 1952), pp. 142–144.

Welding Machines, Control. Slope Control for Resistance Welding, W. B. Hills. Electronics, vol. 25, no. 5 (May 1952), pp. 124–125.

Welding Machines. Triple Multi-Point Welding Machine for Automobile Seats, R. M. Herbert. Machy. (Lond.), vol. 80, no. 2066 (June 19, 1952), pp. 1079–1080.

Welding. Thorough Analysis Plus Necessary Tests Makes Production Runs Pay Off at Automatic Welding, F. M. Burt. Western Metals, vol. 10, no. 5 (May 1952), pp. 49–51.

Welding vs. Casting. Redesign Eliminates Castings, Cuts Costs 50%, R. Zeh. Industry & Welding, vol. 25, no. 6 (June 1952), pp. 36–37.

Welds, Testing. Correlation of Weldability Tests with Structural Joints, C. L. M. Cottrell and P. H. R. Lane. Welding Research (Brit. Welding Research Assn.) vol. 6, no. 1 (Feb. 1952), pp. 2r-12r.

The Expression of Spot-weld Properties

Empirical solutions involving weld characteristic interrelations of carbon and manganese steel spot welds within the ordinary thickness strength and composition ranges

by Julius Heuschkel

Abstract

A series of empirical solutions involving weld characteristic interrelations has been secured which permits direct expression of the commonly determined properties of carbon-manganese steel spot welds for materials within the ordinary thickness, strength and composition ranges. Using the formulas presented for this purpose, weld properties in torsion, in tension, and in shear were found to be expressible 80% of the times within 15° of the test twist angle, within 33% of the normal tension strength and within 20% of the tension-shear strength values. The derived empirical expressions thus permit the direct conveyance of a large amount of test experience in a simple, terse, usable form. This information should be useful to design, production, inspection and quality control personnel.

The data analysis supports the soundness of production procedures which use weld nugget diameter, secured from representative etched sections, as a criterion of weld quality. It provides the users of this procedure with an approach for correlating such a simply determined value with the probable physical properties of a single weld if tested under standard conditions.

The most useful spot-weld property, its strength (S) under tension-shear loading, is shown to be a function of five essentially independent variables which may be numerically expressed: stock thickness (T), tensile strength (U), carbon and manganese contents (C and Mn) and the weld nugget diameter (D). These variables have different affects as thickness varies across the range, as indicated by the shifting magnitudes of derived coefficients in the basic equation, $S = TUD[\alpha - \beta(C + 0.05Mn)]$.

In a similar manner it is shown that the strength (N) of a weld loaded normal to the sheet interfaces is related to the same five variables in a differing manner but, because of the sensitivity to nonuniformity of stress conditions, a close correlation is more difficult to establish. The basic equation form is:

$$N = TUD\left[\frac{a}{U - b} + c - (fC + gMn)\right]$$

Angle of twist at rupture is shown to relate to stock analyses only for materials over 0.03 in. thick and to both prewelded ductility and stock analyses for thinner sheets. One common equation form did not apply across the entire thickness range.

The presented equations apply only to conventional single impulse spot-welding procedures on welds stressed at normal temperatures. Within these limits, by using the derived and presented coefficients for any specific stock, the basic equations provide the average probable weld property, as known from available test data.

Julius Heuschkel is connected with the Westinghouse Research Laboratories of the Westinghouse Electric Corp., East Pittsburgh, Pa.

Scheduled for presentation at the Thirty-Third National Fall Meeting, AWS, Philadelphia, Pa., week of Oct. 20, 1952. Closing date for discussion December 15, 1952.

Nomenclature

T = single sheet or stock thickness, in.
U = ultimate tensile strength of prewelded stock, psi
E = tensile elongation of prewelded stock, %
C = carbon content of stock, %
Mn = manganese content of stock, %
D = weld nugget diameter, in.
A = rupture angle of twist of weld, deg, Fig. 3
N = normal tensile rupture strength of weld, lb, Fig. 3
S = shear tensile rupture strength of weld, lb, Fig. 3
W = width of specimen, in., Fig. 3
W_N = width of strip in weld diameters for which weld loaded normal to interface will develop the full tensile strength of the stock; a dimensionless number
W_S = width of strip in weld diameters for which weld loaded in tension shear will develop the full tensile strength of the stock; a dimensionless number
Y_A = ordinate used to indicate angle of twist relations
Y_N = ordinate used to indicate normal strength relations
a = component of normal strength formulas, psi
b = component of normal strength formulas, psi
c = component of normal strength formulas, no dimension
f = component of normal strength formulas, no dimension
g = component of normal strength formulas, no dimension
z = component of angle of twist formulas
x = component of angle of twist formulas
u = component of angle of twist formulas
A_c = calculated angle of twist, deg
N_c = calculated normal tensile strength, lb
S_c = calculated shear strength, lb
α = component of shear strength formulas, no dimension
β = component of shear strength formulas, no dimension
σ = bending stress on extreme fiber, psi
e = base of natural logarithm, 2.7183

INTRODUCTION

THE strength and ductility of spot welds in carbon steels, the most widely used commercial metal, have previously been shown to be related in a general way to the thickness, strength and analysis of the steel.[1-3] However, there is no published reference which provides a means for expressing a specific

probable average value of strength or ductility for a spot weld in any particular lot of steel, either before or after it is made, except by destructive test techniques.

The unique object of this presentation is to provide a method for the expression of the average properties of any carbon-manganese steel spot weld made, or to be made, by conventional single impulse techniques. A related object is to point the way toward a universally acceptable method for this purpose. The basis of the proposed system applies across the entire common thickness range for the ordinary commercial steel analyses and tempers.

The procedure effectively used for achieving the first of the listed objectives was to collect together all available data wherein nine specific items were reported for well-proportioned weld nuggets, while using comparable test specimens. The weld property items were then related to the steel properties and to weld diameter when that factor was important. The information required included:

1. Thickness of stock, T, in.,
2. Ultimate tensile strength of prewelded stock, U, psi.
3. Elongation or ductility of prewelded stock under tension loading, E, %
4. Carbon content of stock, C, %
5. Manganese content of stock, Mn, %
6. Diameter of spot-weld nugget, D, in.
7. Rupture angle of distortion of spot weld, A, deg
8. Rupture strength of spot weld loaded in normal tension, N, lb
9. Rupture strength of spot weld loaded in tension shear, S, lb

From 186 lots of steel selected to cover a wide range of material conditions and for which such weld data were available, the three most useful engineering weld properties, Items 7, 8 and 9, were correlated with the listed variables, Items 2–6. From these correlations the expression giving the average of each of the three weld properties was secured for each thickness of material, Item 1, in equation form. From the 10 thicknesses for which data were available the resulting equations were then cross correlated with material thickness so that the several derived coefficients could in turn be obtained for all thicknesses within the range studied. This enabled the writing of equations giving the average value of twist, normal strength and shear strength for any thickness of material within the limits of 0.008 to 0.500 inch.

To indicate the potentials of such correlations, all the individual test results were lastly checked against the values calculated from the equations and the defections found were expressed in terms of degrees for the twist data and percentages for the strength data. It was found that 80% of the calculated shear strength values were within 20% of the test values. This is particularly remarkable when considering that the strength of any given well-proportioned weld is shown to be a function of five-dimensional and analysis variables, and these do not encompass other known sources of difference such as variations in grain size and inclusion distribution.

One of the present needs of industry is that the uncertainty of performance of welded structures be reduced. Until the results from a simple laboratory test specimen can be expressed and predicted with reasonable certainty, it is not possible to provide a sound engineering basis for the performance of the spot-welded structure. The correlations presented here are offered as a step in the procedure of securing a sounder basis for judging spot-welded performance.

The spot weld is ordinarily to be used only in shear, the load being applied in either tension or compression. This limitation applies because of the weakness of the weld in torsion and its possible weakness in direct tension. Nevertheless it is important that the properties in torsion and direct tension be known for any proposed material so that improper conditions of usage or application may be avoided.

MATERIALS AND DATA

Comparative data were available within the author's experience from 186 lots of steel. More than 4000 individual welds were involved covering the ranges listed in Table 1.

The test values were segregated for each of the 10 thicknesses for which data were available. The presented correlation is made possible not alone by the number of steels and welds involved but by the broad range of variables covered. To secure as complete a pattern as practical in the higher thicknesses stock from selected heats was specially purchased in the form of $^1/_2$-in. bar stock for weld testing purposes.

Table 1—Limits of Material and Weld Size Variables Studied

T, in.	U, psi	E, %	C, %	Mn, %	D, in.
0.008	47,000/128,000	32/1.4	0.01/0.16	0.29/1.31	0.12/0.15
0.012	47,700/131,900	36.8/1.5	0.04/0.14	0.28/0.75	0.13/0.16
0.018	47,200/163,800	37.5/1.0	0.04/0.21	0.25/1.31	0.12/0.18
0.030	37,500/137,800	40.6/1.5	0.02/1.03	0.05/1.31	0.15/0.25
0.060	42,900/128,300	44.3/2.4	0.01/1.00	0.04/1.27	0.19/0.30
0.125	41,000/148,800	47.5/19.8	0.04/1.02	0.03/1.37	0.37/0.60
0.188	44,500/96,000	44/28	0.05/1.09	0.36/1.29	0.51/0.69
0.250	42,300/94,500	...	0.01/0.40	0.04/0.82	0.80/0.86
0.375	42,300/92,500	...	0.01/0.47	0.05/0.74	1.09/1.16
0.500	59,500/101,000	...	0.15/0.58	0.38/0.87	1.28/1.50

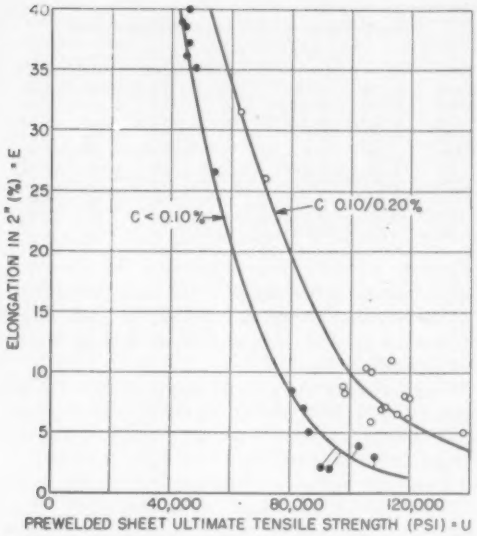

Fig. 1 Typical interrelationship between steel sheet strength, ductility and analysis. (Increased strength from cold working)

Also included in the 186 item correlation, however, are the data from two prior papers,[1, 2] which total 77 items.

It is not within the scope of this paper to consider detail affects of variations in microstructure or possible affects of differing causes of origin of fracture.

STEEL PROPERTY RELATIONSHIPS

Severely cold reduced low-carbon steels progressively increase in strength and decrease in ductility with the cold work, Fig. 1. Ductility here is evaluated as inches per inch of plastic elongation at rupture stress, in per cent, and was obtained from standard ASTM tensile specimens. For any given ultimate tensile strength the elongation may be increased by increasing the alloying content, Fig. 1, because under those conditions less cold reduction is necessary to secure a particular ultimate strength. It is not intended that the data presented here be proof of these steel property relations, they merely serve to remind of their existence.

The importance of alloy additions, limited here to carbon and manganese, lies in the fact that spot-weld properties are related both to prewelded tensile strength or ductility of stock and to postwelded hardness. The inverse relations between stock strength and ductility which exist for a specific analysis complicates the problem of segregating the causes of variations in weld strengths. For example, one cannot determine here the fundamental factor of whether the welds subject to normal tension loading were weaker for high strength stock because higher notch stresses were imposed or because the unaffected stock was less able to flow plastically and hence afforded less ability to distribute the imposed loads across a larger area, or whether rupture was due to notch brittleness resulting from metallurgical changes alone.

Because the conventional single impulse spot-welding methods involve drastic quench rates, particularly on thin sheets,[3] the increased alloy contents rapidly tend to reduce weld ductility, and sometimes even the weld strength. Alloy content affects were accordingly necessarily incorporated into the equations derived for expression of weld properties.

WELD PROPORTIONS

The welds correlated here include only those having reasonably suitable proportions, Table 1. The relations existing between weld diameter and sheet thickness are shown in Fig. 2, both directly in the lower curve and as a relative value in the upper curve. Weld diameters decrease with sheet thickness but not in direct proportion and therefore, relatively speaking,

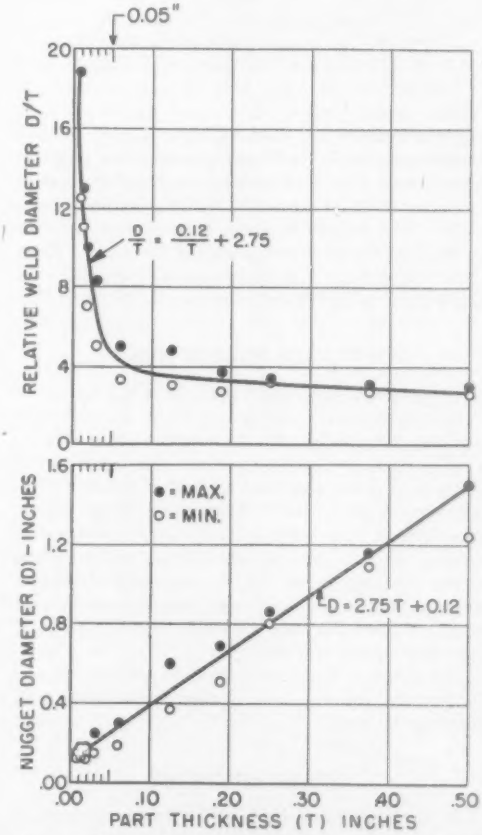

Fig. 2 Relations between material thicknesses and weld diameters

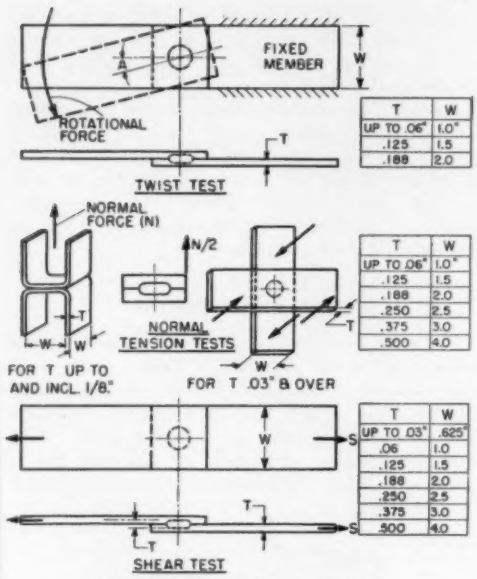

Fig. 3 Details of test specimens

larger diameters are used on thin sheets. It will become apparent in the following presentation that this relative weld size influences the form in which the weld properties may be expressed when loaded in torsion.

Only those nuggets having a fusion penetration of 30 to 80% into the sheet are included in this study. Electrode indentations in general never exceeded 10% of a single sheet thickness and were commonly much less.

SPECIMEN PROPORTIONS

The specimen dimension standards of the AMERICAN WELDING SOCIETY were used in so far as they were available for making all tests correlated here, Fig. 3. Uniformity of specimen proportions is important since it has been shown that weld strength is also related to specimen width.[2] Both shear and normal tensile properties of spot welds are also subject to eccentric loading, which in turn introduce stress concentrations at the weld edge notch, Fig. 3. Any such correlation as attempted here automatically includes an evaluation upon all other pertinent variables including those of specimen making and testing.

The values in Table 2 show how the section area, and its potential influence upon average stress, varies with material thickness.

ANGLE OF TWIST

In the twist test a single weld between two parts is tested by holding one part firmly and forcefully rotating the second member, in its original plane, around the natural center of the nugget. The angle of rotation (A) at rupture is recorded. There is often some uncertainty as to when rupture occurs and the test is not a precision test.

Table 2—Pertinent Specimen Relationships

T, in.	W, in.	WT, sq in.	$1/WT$, sq in.	W/T, sq in.	$D(avg)$, in.	W/D
0.008	0.625	0.005	200	78	0.14	4.46
0.012	0.625	0.0075	133	52	0.15	4.16
0.018	0.625	0.011	91	35	0.18	3.48
0.030	0.625	0.019	52	21	0.20	3.12
0.060	1.00	0.060	17	16	0.29	3.45
0.125	1.50	0.189	5.3	12	0.46	3.27
0.188	2.00	0.375	2.7	11	0.64	3.13
0.250	2.50	0.625	1.6	10	0.81	3.09
0.375	3.50	1.312	0.6	9	1.18	2.97
0.500	4.00	2.000	0.5	8	1.50	2.67

Examination of the data for angle of twist (A) at rupture from 142 lots of steel, led to the conclusion that for thin sheets, up to and including 0.030 in. in thickness, the rupture angle is related both to sheet ductility and to sheet analysis. It is recognized, Fig. 1, that sheet ductility here is also related to sheet strength. The angle of rupture values available could be algebraically related to sheet ductility and analysis to secure a series of expressions which provided calculated angles within 15° of the test values 80% of the time.

The methods used for final derivation of the twist angle formulas are given in Figs. 4 and 5.

The procedure followed was to plot, for thin sheets, prewelded sheet tension elongation (E) as abscissae, Fig. 4, against an ordinate value "Y_A" which is arithmetically equal to the sum of the rupture angle of twist in degrees, and a number which is equal to a coefficient multiplied by the sum of the carbon and modified manganese contents. When all data points were

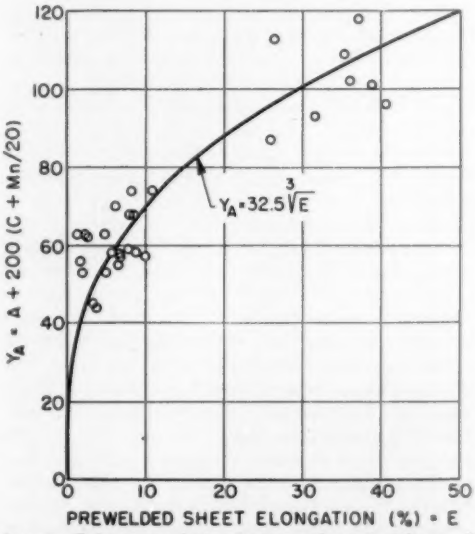

Fig. 4. Cube root relation between sheet ductility and twist angle for thin sheets. (Example: T = 0.030 inch)

plotted in this fashion, for 0.030-in. stock for example, it was observed that a smooth curve could be plotted through the points which provided a reasonable fit to the equation:

$$Y_A = 32.5 \sqrt[3]{E}$$

But since by definition,

$$Y_A = A + 200(C + 0.05\,Mn),$$

it follows that

$$A = 32.5 \sqrt[3]{E} - 200(C + 0.05\,Mn)$$

This equation expresses and defines the average angle of twist secured for the 0.030-in. sheets. It shows the angle to increase with the cube root of the sheet elongation, as previously defined, and to decrease linearly with each increment of added carbon and manganese. This is the algebraic expression of the observation that higher angles of twist are secured with high-ductility sheet, which are the low-strength sheets, Fig. 1, and are low with low-ductility sheets, which are the high-strength sheets. Further, it teaches that the angles of twist are higher when the stock analysis is lower and lower when the stock analysis is higher. The specific average angle of twist for welds of the quality being studied is provided for any given sheet by substitution of the corresponding values of E, C and Mn in the equation and making simple slide rule and mental calculations.

The same procedure applied to all the other thin sheet data with minor variations in magnitudes of coefficients. It is considered to be of basic significance that this method is applicable to all thin sheet data, Table 3. Returning to Fig. 2, it can be seen that this form of expression holds only for the sheets having a high weld diameter to sheet thickness ratio wherein, as a result, failure occurs by twisting out a slug from the sheet. The described form of equation did not hold for sheets 0.060 in. and thicker. For sheets thicker than 0.060 in. the angle of rupture is more nearly relatable to analysis of sheet alone, and failure generally occurs in the weld nugget. A sample derivation of twist angle formulas for 0.125-in. sheets is given in Fig. 5. The average curve is a rectangular hyperbola of the general form

$$Y_A = \frac{z}{x - v} + u$$

In the Fig. 5 example,

$$Y_A = A_c = \frac{10}{C + Mn/10 + 0.05} - 10$$

where

A_c = calculated angle of twist
u = -10
v = -0.05
x = $C + Mn/10$
z = 10
C = number which is equal to carbon content of sheet
Mn = number which is equal to manganese content of sheet

The summary of the several equations for giving average angle of twist is given in Table 3.

Table 3—Summary of Weld Twist Angle Formulas

T, in.	A
0.008	$A_c = 35\sqrt[3]{E} - 250\,(C + Mn/20)$
0.012	$A_c = 35\sqrt[3]{E} - 250\,(C + Mn/20)$
0.018	$A_c = 35\sqrt[3]{E} - 200\,(C + Mn/20)$
0.030	$A_c = 32.5\sqrt[3]{E} - 200\,(C + Mn/20)$
0.060	$A_c = \frac{8}{C + Mn/20 + 0.05} - 10$
0.125	$A_c = \frac{10}{C + Mn/10 + 0.05} - 10$
0.188	$A_c = \frac{10}{C + Mn/10 + 0.05} - 15$

The limits of variation of the calculated values obtained from the use of these equations with respect to the actual test angles secured are listed in Table 4.

While the correlations presented in Table 4 for angle of twist are not of precision quality, neither is the test method. Nevertheless, in spite of its defections, the procedure described permits an expression of experience with the twist test in which for 114 of the 142 available cases, or 80% of the time where data were available, the rupture angle results are provided within 15 degrees. Also there were no reversions, that is, in no case did the use of the equations give either a low or high result unless the test data were also either low or high. While one cannot be completely satisfied with the best correlation secured to date, these studies indicate a definite possibility that with further careful study, by securing now unpublished data, by improvements in testing technique and possibly by examining other factors neglected here, an even more precise method of expressing these data will ultimately be made available for engineering usage.

NORMAL TENSION STRENGTH

Normal tension strength data were available for 181

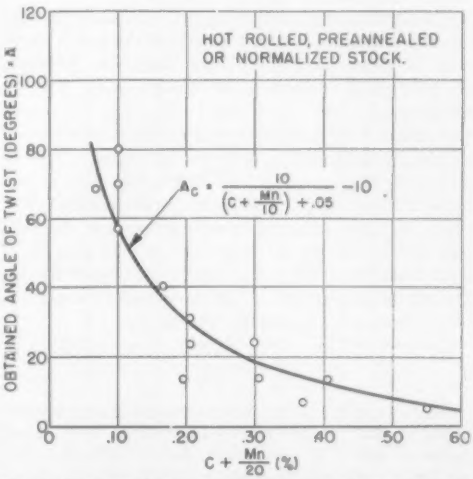

Fig. 5 Inverse relation between sheet analysis and twist angle for thicker sheets. (Example: T = 0.125 inch)

Table 4—Summary of Comparisons of Calculated and Actual Weld Twist Angle Values

Material thickness, T, in.	Total no. of obs.	Distribution of calculated from actual — Direction (no. of each) Low	Equal	High	Limits of variation, deg ±5	±10	±15	±20	±25	Range of angles for actual test specimens, deg
					% of total within each group					
0.008	24	13	1	10	42	71	71	92	100	8/83
0.012	17	6	0	11	35	71	88	100	100	14/96
0.018	39	15	1	23	39	72	82	87	97	9/108
0.030	32	15	1	16	38	72	81	91	94	10/109
0.060	14	9	0	5	43	64	64	72	72	10/115
0.125	12	6	0	6	50	75	83	100	100	5/80
0.188	4	2	0	2	75	100	100	100	100	4/46
7	142	66	3	73	41	72	79	90	95	4/115 MIN/MAX
		TOTALS			WEIGHTED AVG					

lots of steel. Correlation of these data, wherein the individual weld test strengths ranged from 40 to 39,720 lb involved a considerably more complicated approach than was required for the twist data. Final correlation was achieved by arriving at the general five-variable equation of the form:

$$N_c = TUD\left[\frac{a}{U-b} + e - (fC + gMn)\right]$$

wherein

N_c = calculated normal tensile strength of weld, lb
T = material thickness, in.
U = prewelded steel strength, psi
D = weld nugget diameter, in.
C = number equal in magnitude to the material carbon content, %
Mn = number equal in magnitude to the material manganese content, %
a, b, e, f and g = coefficients which vary in an orderly manner with material thickness, Figs. 9 and 10

The derivation of these general formulas and the establishment of the values of the five thickness variable coefficients involved the making of several thousand individual calculations based upon principles which can be simply explained.

The basic concept is to imagine that the normal load applied to the spot weld is transmitted through a single strip of metal having the same thickness, strength, elongation and analysis as the welded metal, that is, an identical piece of the metal. The rupture tensile strength of a strip of this metal having a width equal to the weld diameter is then calculated. This is simply the product of T, U and D, which are each known from the test data. The dimensionless number, W_N, being the quotient of the normal strength of the weld (N) divided by the TUD product or the number of weld diameters for which the load (N) would develop the full tensile strength (U) of the prewelded stock was then obtained for each of the 181 items:

$$W_N = \frac{N}{TUD}$$

This procedure reduced the magnitude of variation of the quantity to be correlated from a 40- to 39,720-lb range, or 994:1, to one which varied from 0.01 to 3.7 or 370:1. It was observed that the magnitude of W_N tended to become low when high sheet analyses or strengths were involved, that is, when the welds would be hardest and most brittle, and when the surrounding sheet ductility was lowest but when the elastic and plastic characteristics were such that highest potential bending stresses could be imposed upon the weld edge notch.

The next step involved relating the now primary variable W_N to a suitable ordinate so that an equation of relation could be secured. Such a relation based upon sheet analysis alone, or elongation alone or the two in combination was not too satisfactory, although it demonstrated the general trend of the data. An example is shown in Fig. 6.

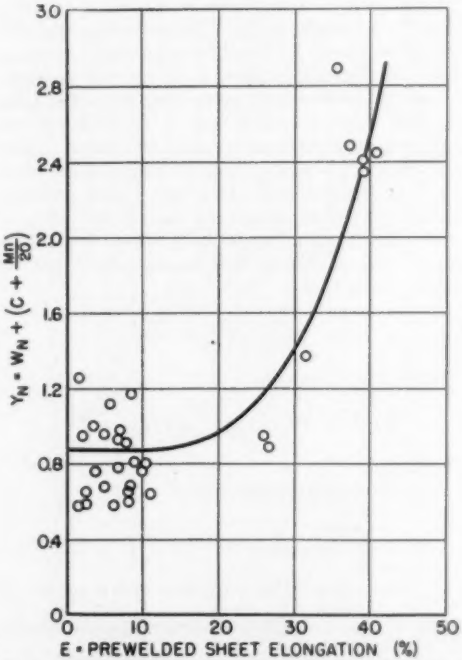

Fig. 6 Relation between prewelded sheet ductility, sheet analysis and spot-weld strength. (Example: T = 0.030 inch)

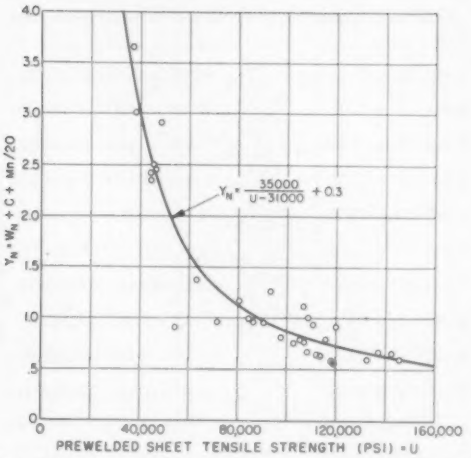

Fig. 7 Derivation of formulas for calculation of normal strength on thin sheets. (Example: T = 0.030 inch)

Best correlations were finally secured by relating W_N as a component part of a "Y_N" ordinate to the prewelded sheet tensile strength as abscissas, Fig. 7. This followed from the observation that a reasonable correlation could be secured by this means when using a value of "Y_N" equal to the sum of W_N and suitable coefficients multiplied by sheet analysis. For example, with 0.030-in. sheets, by selecting $Y_N = W_N + (C + 0.05\ Mn)$ and plotting this as the ordinate against the value of U as abscissas provided a distribution whose average could be expressed by a smooth curve of the form

$$Y_N = \frac{35{,}000}{U - 31{,}000} + 0.30$$

From these two independent relations of Y_N, the expression of W_N is derived as

$$W_N = \frac{35{,}000}{U - 31{,}000} + 0.30 - (C + 0.05\ Mn)$$

But since by derivation, or rather by definition:

$$W_N = \frac{N}{TUD}$$

therefore $N = TUDW_N$.

It follows that:

$$N_c = TUD\left[\frac{35{,}000}{U - 31{,}000} + 0.30 - (C + 0.05\ Mn)\right]$$

This equation provides the expression of the normal strength of the spot welds for 0.030-in. sheets. The strength is given in terms of five variables: thickness (T), prewelded strength (U), carbon (C) and manganese (Mn) contents of sheet, and the weld diameter (D).

Another example of data agreement is given in Fig. 8 for $^1/_2$-in. plates and bars. It is believed to be significant that the same treatment of available data for all ten material thicknesses provided similar correlations, differing only in the magnitudes of the determined

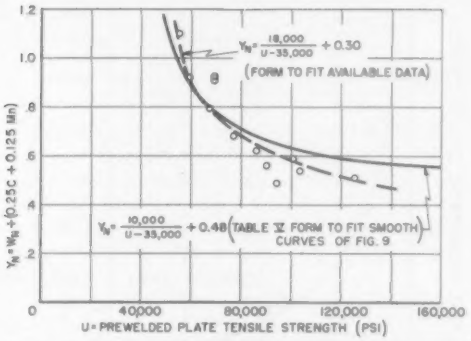
$Y_N = W_N + (0.25C + 0.125\ Mn)$
$Y_N = \frac{18,000}{U-35,000} + 0.30$
(FORM TO FIT AVAILABLE DATA)
$Y_N = \frac{10,000}{U-35,000} + 0.48$ (TABLE Σ FORM TO FIT SMOOTH CURVES OF FIG. 9)
U = PREWELDED PLATE TENSILE STRENGTH (PSI)

Fig. 8 Derivation of formulas for calculation of normal strength of spot welds in $^1/_2$-in. plates

coefficients, which were found to vary with thickness of material in an orderly manner, Figs. 9 and 10. The summary of the derived formulas is given in Table 5.

Discontinuities are shown in Fig. 10 and the only explanation offered for the relation of the carbon and manganese coefficients to material thickness is that in a prior paper[3] it was shown that the thin sheet welds were quenched to the full hard condition. For those conditions carbon content dominated weld performance and amount of manganese had little affect. For the

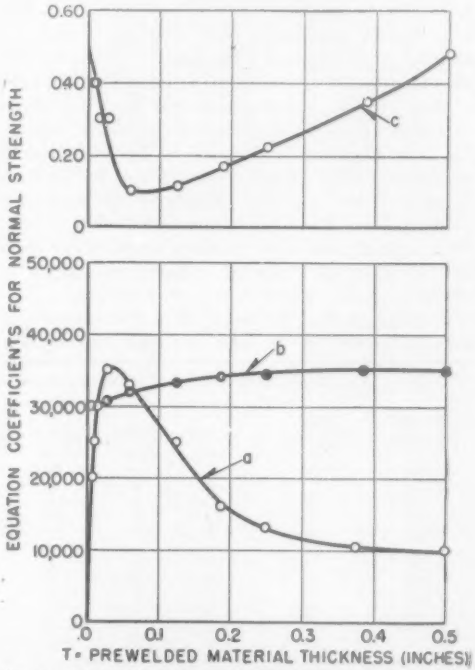

Fig. 9 Relation between material thickness and equation coefficients for normal spot-weld strength

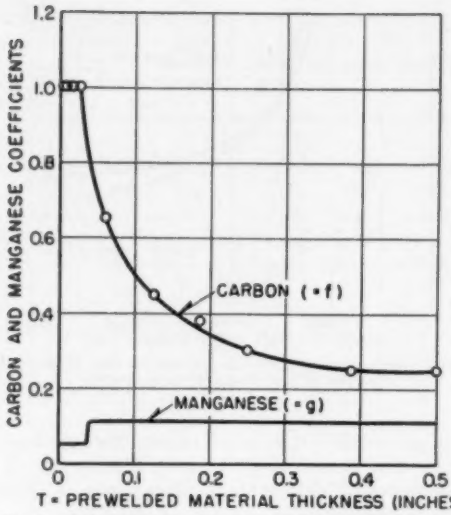

Fig. 10 Relations between material thickness and analysis coefficients for normal spot-weld strength equations

thicker stock not quenched to full hardness the effect of manganese was relatively more important.

The distribution of the variation of the values calculated by use of the listed formulas from the obtained test values is given in Table 6. Again this is not precision agreement, but neither is the normal tension test method a precision test. It has been shown, and it is further emphasized here, that spot welds are sensitive to direction of applied load. It follows that they are sensitive to degrees of variation in application of load. In the normal tension test there are either two or four zones of major stress concentration, depending upon whether the square U or the cross type of specimen is used. Both were employed in the data being correlated. In either case rupture can be affected at much lower loads by uneven distribution of load. This could be caused, for example, by off-center spots or by nonuniform jigging. Drastic reductions in strength can be secured by one-point loading.

Considering that the test-applied stress conditions are not necessarily uniform and that the rupture

Table 5—Summary of Weld Normal Strength Formulas

T, in.	N
0.008	$N = TUD\left[\frac{20,000}{U-30,000} + 0.40 - (1.0C + 0.05Mn)\right]$
0.012	$N = TUD\left[\frac{25,000}{U-30,000} + 0.40 - (1.0C + 0.05Mn)\right]$
0.018	$N = TUD\left[\frac{30,000}{U-30,000} + 0.30 - (1.0C + 0.05Mn)\right]$
0.030	$N = TUD\left[\frac{35,000}{U-31,000} + 0.30 - (1.0C + 0.05Mn)\right]$
0.060	$N = TUD\left[\frac{33,000}{U-32,000} + 0.10 - (0.65C + 0.125Mn)\right]$
0.125	$N = TUD\left[\frac{25,000}{U-33,000} + 0.11 - (0.45C + 0.125Mn)\right]$
0.188	$N = TUD\left[\frac{16,000}{U-34,000} + 0.17 - (0.38C + 0.125Mn)\right]$
0.250	$N = TUD\left[\frac{13,000}{U-34,500} + 0.22 - (0.30C + 0.125Mn)\right]$
0.375	$N = TUD\left[\frac{10,500}{U-35,000} + 0.35 - (0.25C + 0.125Mn)\right]$
0.500	$N = TUD\left[\frac{10,000}{U-35,000} + 0.48 - (0.25C + 0.125Mn)\right]$

strength is a function of five independent variables, T, U, D, C and Mn, it is believed to be significant that 74% of the 181 lots of welds, wherein the test strengths ranged over approximately a 1000:1 range, can be individually expressed within 33% of the average pattern value by use of the equations derived. The deficiencies in the derived expressions point toward the need of greater care in the use of this type of test specimen and possibly in the design of the specimen itself. Also they point toward the need for more precise data and improvements in data analysis.

In spite of possible deficiencies of either the test method or the employed correlation techniques however, the data firmly point up the fact that normal weld strength tends to increase linearly with sheet thickness and weld diameter, to decrease from any existing level with increased carbon and manganese contents and to actually decrease, but not linearly, with prewelded sheet strength.

The product of the one component of the general normal weld strength equation, $aU/(U - b)$ is a hyperbolic form which decreases in value as the value of "U" exceeds "b," that is, as U becomes large. The fact that this product approaches an infinite value as U decreases to equal the value of b is of no concern because in the softest annealed condition steel cannot

Table 6—Summary of Comparisons of Calculated and Actual Normal Strength Values

Material thickness, T, in.	*Total no. of obs.*	*Distribution of calculated from actual — Direction (no. of each) Low*	*Equal*	*High*	*Limits of variation, % ±10*	*±20*	*±33*	*±50*	*Range of strengths of actual test specimens lb*
					% of total within each group				
0.008	24	11	0	13	38	58	83	92	40/88
0.012	17	8	0	9	29	65	82	100	66/173
0.018	39	25	0	14	23	50	74	97	91/303
0.030	35	14	1	20	34	49	77	89	156/735
0.060	18	7	0	11	17	33	33	50	10/2030
0.125	19	10	0	9	21	47	74	84	220/6610
0.188	10	5	0	5	40	60	70	70	1090/8520
0.250	6	3	0	3	17	33	83	100	3300/12,500
0.375	3	1	0	2	33	67	67	67	12,970/18,680
0.500	12	5	0	7	25	67	92	100	21,270/39,720
10	183	89	1	93	28	54	74	87	40/39,720 MIN/MAX
		TOTALS			WEIGHTED AVG				

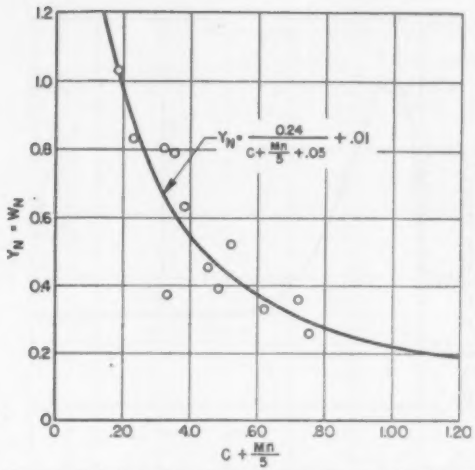

Fig. 11 Relation of analysis to normal strength of spot welds in $^1/_2$-in. plates

be produced having strengths as low as the equation values of the coefficient b.

The general equation also specifically expresses the increased effect of added carbon and manganese contents on high strength steels. For a given value of U, T and D in any of the equations, more and more strength potential is subtracted as increases in these values increase the TUD $(fC + gMn)$ product.

Efforts were made to relate normal strength directly to material analysis. While this could be done in general, as shown for example in Fig. 11 for $^1/_2$-in. plates, the spread of data from the average curve was wide. Also it was possible to relate the value W_N in combination with an alloy content influence to prewelded material strength by the use of exponential functions, as shown in Figs. 12 and 13 for $^1/_8$- and $^1/_{16}$-in. stock. This procedure would lead to an expression of the normal strength N in terms of T, U, D, C, Mn and a power of the natural logarithm base. However, in general, the agreement of the data to such curves was no better than when using the simpler hyperbolic functions just described.

SHEAR STRENGTH

Expression of the most important design value, spot-weld shear strength, was a relatively simple matter compared to the normal strength determinations. The form of this general equation was derived by modification of the original concept[2, 3] by correcting for material thickness and analysis affects. The general form found was:

$$S = TUD[\alpha - \beta(C + Mn/20)]$$

Again as for normal tension the weld shear strength is found to be a function of five test variables but only two thickness-affected coefficients.

The general derivation was reached following an examination of the W_s values, which were calculated in a manner identical to that described for W_n except that the shear strength S was used in their determinations. This value, W_s, was then related to sheet analysis for each thickness as illustrated in Fig. 14 for $^1/_8$-in. stock and in Fig. 15 for 0.018-in. stock. The projected ordinate intercept for zero values of alloy content, the equivalent of steel without carbon or manganese, provided the magnitude of the dimensionless constant "α." The negative slope of the curve, using a straight line relation, provided the value of β. The effect of manganese did not appear to be too great and a constant factor of $^1/_{20}$ was used throughout.

The individual equations for each of the 10 test material thicknesses are given in Table 7 and the manner in which the coefficients α and β vary with T are shown in Figs. 16 and 17.

The distribution of the calculated from the actual data are summarized in Table 8. With individual test values which varied from 126 to 79,170 lb in magnitude it was possible to express the shear values for the 186 test lots within 20% of their obtained values 80% of the time.

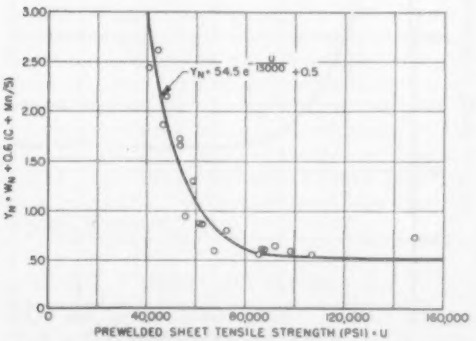

Fig. 12 Derivation of formulas for calculation of normal strength on $^1/_2$-in. sheets

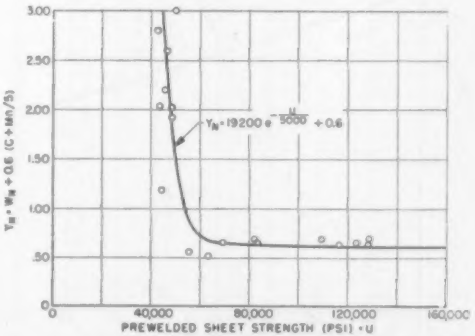

Fig. 13 Relations between prewelded sheet strength, and weld strength factor on $^1/_{16}$-in. sheets

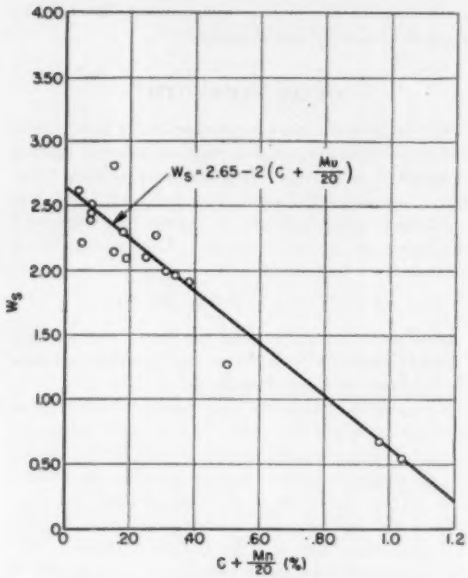

Fig. 14 Relation between W_S and analysis for 1/8-in. sheets

Table 7—Summary of Weld Shear Strength Formulas

T, in.	*S*
0.008	$S_s = TUD[2.65 - 0.80\,(C + Mn/20)]$
0.012	$S_s = TUD[2.75 - 2.00\,(C + Mn/20)]$
0.018	$S_s = TUD[3.22 - 4.12\,(C + Mn/20)]$
0.030	$S_s = TUD[3.35 - 3.50\,(C + Mn/20)]$
0.060	$S_s = TUD[3.50 - 2.65\,(C + Mn/20)]$
0.125	$S_s = TUD[2.65 - 2.00\,(C + Mn/20)]$
0.188	$S_s = TUD[2.00 - 1.35\,(C + Mn/20)]$
0.250	$S_s = TUD[1.75 - 1.20\,(C + Mn/20)]$
0.375	$S_s = TUD[1.70 - 1.20\,(C + Mn/20)]$
0.500	$S_s = TUD[1.70 - 1.20\,(C + Mn/20)]$
All	$S_s = TUD[\alpha - \beta\,(C + Mn/20)]$

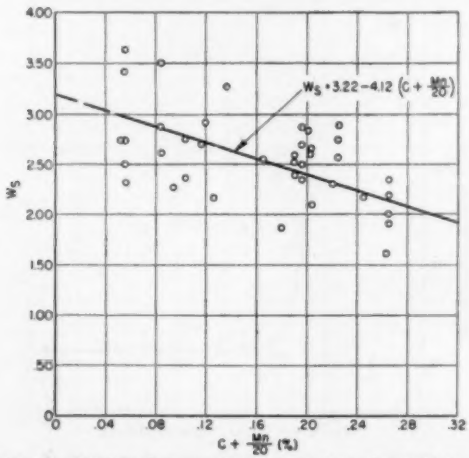

Fig. 15 Relation between W_S and analysis for 0.018-in. sheets

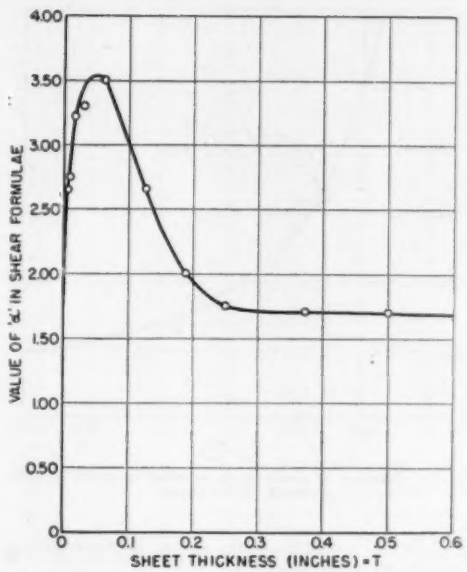

Fig. 16 Relation between sheet thickness and "α" value in shear formulas

A system containing five independent variables will operate within an established range of satisfaction only one-half the time if each individual value is within

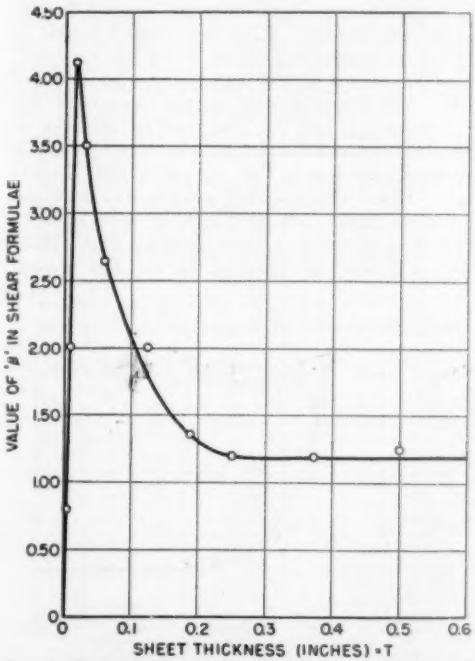

Fig. 17 Relation between sheet thickness and "β" value in shear formulas

Table 8—Summary of Comparisons of Calculated and Actual Shear Strength Values

Material thickness, T, in.	Total no. of obs.	Distribution of calculated from actual: Direction (no. of each) Low	Equal	High	Limits of variation, % ±10	±20	±33	±50	Range of strengths of actual test specimens, lb
					% of total within each group				
0.008	24	9	4	11	63	88	100	100	126/375
0.012	17	7	1	9	71	82	100	100	211/527
0.018	39	18	1	20	54	87	100	100	363/907
0.030	36	13	2	21	42	58	81	95	405/2921
0.060	19	8	3	8	63	84	95	100	667/4565
0.125	19	7	2	10	79	84	100	100	3740/13,580
0.188	10	4	0	6	50	80	80	90	5610/20,600
0.250	7	4	0	3	57	86	100	100	13,390/26,560
0.375	3	0	0	3	67	67	100	100	26,520/40,180
0.500	12	6	0	6	50	83	92	100	51,920/79,170
10	186	76	13	97	58	80	97	99	126/79,170 MIN/MAX
		TOTALS			WEIGHTED AVG				

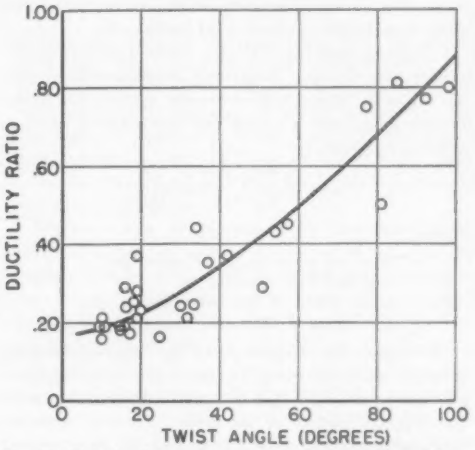

Fig. 18 Relation between twist angle at rupture and ductility ratio. (Example: T = 0.03 inch)

limits just 87% of the time. The 80% fit, within the 20% tolerance, means that all observations must have been nearly correct 96% of the time. The statistical requirement is that if the average weld strength is dependent upon five distinct properties and probability of defection is independent and equal for each property, in order to secure a probability of total success of expression equal to "p," the probability of accuracy of each property must be $\sqrt[5]{p}$. The correlation secured across the range of steel thicknesses, strengths and compositions is good when considering this fact. It provides a firm basis for expressing the values of spot-weld shear strength in terms of five measurable values, four of which may and should be known before the metal reaches the welding machine, at the discretion of policy personnel.

DUCTILITY RATIO

The ratio of normal strength (N) to shear strength (S) is commonly taken as an index of weld ductility (N/S). The provision of independent means for expressing the values of N and S provides, at the same time, the method for estimation of this ductility ratio. The direct ratio of the two general equations for N and S results in a cumbersome expression which could be directly used for this purpose, although there is no apparent reason for doing so in practice. It does show that the "ductility ratio" is independent of weld diameter and is largely independent of material thickness. It also summarizes that the higher the sheet strength and the higher the carbon and manganese contents the lower the ductility ratio:

$$N_e/S_e = \frac{a}{(U-b)(\alpha - \beta C - 0.05\beta\, Mn)} + \frac{c - eC - fMn}{\alpha - \beta C - 0.05\beta\, Mn}$$

There is a general but rough relation between the numerical magnitudes of the rupture angle of twist in degrees "A" and the test secured ductility ratio N/S.

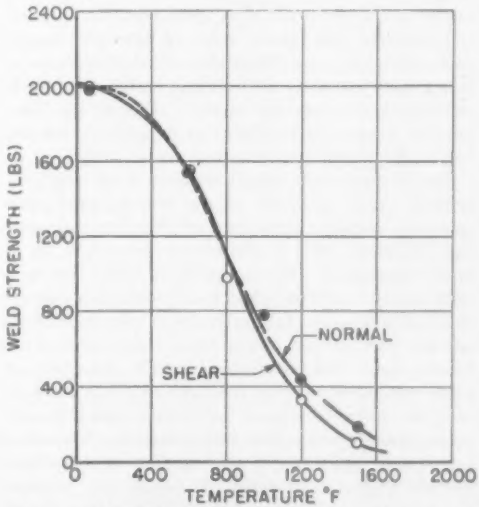

Fig. 19 Relation between spot-weld strength and test temperatures. (Example: T = 0.06 in., C = 0.05%, Mn = 0.39%, U = 50,900 psi)

High angles of twist were secured when high ductility ratios were secured and vice versa. Very few reversions were observed for the 142 lots for which data were available An illustration of these relations is shown in Fig. 18.

SERVICE TEMPERATURE

The correlated data apply only to normal atmospheric temperatures. The strengths of the welds and the directional affects of loading are also influenced by test temperature. A single set of data secured from 0.060-in. low-carbon steel may be used to illustrate this point, Fig. 19 While the strengths of the welds decrease rapidly with increases in temperatures above 500° F, the degeneration is somewhat less rapid under normal tension than in shear. All fractures in this particular instance for both types of loading were in the sheet, that is, they were of the button type.

DISCUSSION

The analysis of data presented here confirm that there is a sound basis for judging production quality of spot welds in the carbon-manganese steels on the basis of weld diameter alone, provided both the prewelded tensile characteristics and the analysis of the material are known. Unless these values are within satisfactory established tolerances for the particular application requirements there is little that can be done by the welder except to completely alter the welding technique.

Thus, just as strongly, this study demonstrates that when using the conventional single-impulse spot-welding method, spot weld diameter is the only variable that influences weld properties which is within control at the point of welding. This statement applies to welds similar to the test welds upon which the proof is based and includes only those welds of tolerable nugget penetration, electrode indentation and sheet separation. It is known that some of the higher carbon-steel welds reported here contained cracks.[3] Except for these cases all nuggets were reasonably sound but were not necessarily wholly free of nugget center voids.

The fact that weld nugget diameter is the only controllable factor available to the welding production operators, assuming again the single impulse nontempering treatment with well-proportioned welds, is of broad significance. For one thing, it means that spot weld quality cannot be judged by any known nondestructive technique unless full knowledge of steel characteristics are also known. When those characteristics are known, only weld penetration, nugget diameter and some reasonable freedom from porosity and cracking need be known to express the average probable weld properties. It means that firm control must be maintained over uniformity of steel quality, or the welded product quality may suffer. It means that, knowing the steel analysis and tensile properties only, a simple etched cross section is all that is needed to establish weld quality. This practice has been followed by some plants. The correlations presented here substantiate and document the validity of this procedure.

An explanation of the variations in the magnitudes of the two constants in the shear equations as thickness changes should be available if the relations have any logical basis. This explanation is provided by an analysis of the stress pattern under the tension loading conditions, Fig. 3.

The magnitude of α in the shear equation would be expected to approach unity as the weld diameter became infinitely large with respect to sheet thickness as would occur when sheet thickness approaches zero. This would approach the condition of a continuous seam weld wherein the upper limit of strength of the joint is the product TUD, where D would be the length of the weld seam. The closeness with which this occurs, Fig. 16, lends added confidence to the usefulness of the magnitudes of the derived coefficients.

A bending moment ST also exists because of the eccentric conditions. Neglecting stress concentrations due to weld shape the uniformly distributed inner fiber bending stress (σ), using the conventional bending moment formulas, is:

$$\sigma = \frac{ST \times T/2}{WT^3/12} = \frac{6S}{WT}$$

where

σ = bending stress on inner fiber, psi
S = imposed load on weld, lb
W = total width of specimen, in.
T = thickness of material, in.

The higher the magnitude of the imposed bending stress the less is the margin remaining from the inherent rupture stress U of the material which can absorb the imposed load S on the weld. Since S increases with the product of T and D and D can be expressed as a function of T, it follows that σ is a function of T/W. Since the value T/W increases with T, Table 2, the

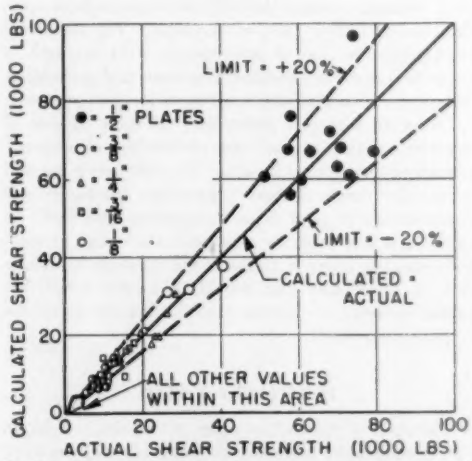

Fig 20 Graphical relation between actual test and calculated shear strength values

strength margin for resisting applied load decreases with increased thickness. Obviously no such simple stress pattern exists. Nevertheless the orderly manner in which the entire series of data fit a single mathematically describable pattern, without too many drastic exceptions, has prompted the presentation of this material. The important property of weld shear strength has been calculated and expressed within the limits shown in Fig. 20 over a range of 125 to 79,200 lb, or 633:1, without misclassification in a single instance. It remains to be determined whether either supporting or contradictory data now exist or will be secured later.

All welds included in the study were made with conventional procedures and it is well established that procedures employed may influence results obtained.[4]

SUMMARY

Relations between average spot-weld properties, weld dimensions and material characteristics have been reduced to a specific basis. This makes it possible to express existing experience with the common weld properties in terms of generally available information. Such procedures should ultimately enable the engineer to render design judgments upon a rational basis for any specific instance.

While it may be necessary to later modify the coefficients derived as more and more data are subsequently secured on this subject, it has been shown that the commonly determined weld properties are directly related to prewelded material properties and to weld diameter. Therefore, one of the most effective ways to assure uniformity of weld quality is to assure that only steels of the same grade are furnished to the welder. In practice this simply means uniformity of steel application, because steel properties are controlled at the source, and the production of welds of uniform configuration. The determination of the existence of a particular weld dimension alone has no significance unless the material is under such uniformity control. However, when the material characteristics are known only the weld diameter need be measured to establish probable weld properties, provided adequate nugget penetration exists together with reasonable freedom from porosity and cracking.

Twist angle at rupture is related to sheet ductility and the alloy content for thin sheets and to alloy content alone for thicker stock, above 0.06 inch. Angle of twist appears to be independent of weld diameter but is a reliable index of ability of weld to withstand distortion and the application of concentrated stress.

Tensile shear and normal tension strengths are related to prewelded stock strength, thickness and alloy content and to weld diameter. In both instances a single general form of relation can be applied across the entire thickness range by using suitably adjusted coefficients. Thus while data were provided for only 10 thicknesses, by interpolation these values can be secured for any thickness. In no case are precision correlations secured, but nevertheless the studies have much practical value.

The data presented apply only to carbon-manganese steels, but it is not beyond the realm of possibility that similar correlations may be shown to exist for other commercial metals.

References

1. Bibber, L. C., and Heuschkel, J., "The Spot Welding of Low-Carbon and Other Aircraft Steels," THE WELDING JOURNAL, 22 (12), Research Suppl., 616-s to 632-s (1943).
2. Heuschkel, J., "Selecting Spot-Welding Schedules for Low-Carbon Steel," *Ibid.*, 25 (10), Research Suppl., 700-s to 726-s (1946).
3. Heuschkel, J., "Some Metallurgical Aspects of Carbon-Steel Spot Welding," *Ibid.*, 26 (10), Research Suppl., 560-s to 582-s (1947).
4. Heuschkel J., and Bitzer, H., "Spot-Weld Consistency Studies," *Ibid.*, 28 (10), Research Suppl., 477-s to 483-s (1949).

Display—your products to the Southwest's highly diversified industrial market—which *knows* welding—*wants* welding—and *buys* welding—

in Houston—June 16–19, 1953

(see page 989)

PRACTICAL WELDER AND DESIGNER

Improved Welds for Galvanized Metal

GALVANIZED angle iron can be welded without losing the galvanized coating by using the inert gas-shielded arc welding process and an Everdur filler rod. This method has been accepted as "perfectly satisfactory" for frames supporting air-conditioning coils in the new Prudential Insurance Co. building in Houston, Tex.

Inert-gas-shielded arc welding did not decrease appreciably the resistance to corrosion, even though there was some loss in the thickness of the zinc coating. The slight loss noted next to the weld was due to direct vaporization under the heat of the arc.

Least disturbance of galvanized coating and most efficient tinning of the base metal was obtained when the arc cone was directed as much as possible on the weld deposit. Welding was done from both sides of the angle. A $^1/_{16}$-in. gap left between the legs of the angle allowed filler rod to tin more than halfway through the thickness. Efficiency of the joint was tested by attempting to shear an angle clip from the frame using a 4-lb. hammer. No failure occurred in the weld even though the legs of the angle were beaten flat.

Previous welding jobs on galvanized iron were done by other methods which destroyed the corrosion-resistant coating and left unsightly welds. Grinding the weld area and redipping the entire section produced extreme distortion. Subsequent straightening operations cost an estimated two or three times the cost of the assembly. Elimination of this distortion and necessary straightening work by inert-gas-shielded arc welding represents a considerable saving.

As in other welding operations on zinc-coated metals, the operator in this process should be provided with adequate ventilation or approved breathing equipment.

Fig. 1 Portable Heliarc apparatus such as used for welding of galvanized iron frames. (Courtesy of The Linde Air Products Co.)

Fig. 2 Clean, strong weld produced by inert-gas-shielded arc welding with Everdur filler rod. No finishing operation was necessary. (Courtesy of The Linde Air Products Co.)

Flame-Plating

Flame-Plating, a new process developed by Linde Air Products Co., a Division of Union Carbide and Carbon Corp., was announced at an editors' meeting held on Aug. 20, 1952

GENERAL DESCRIPTION

FLAME-PLATING is a method of applying powdered metals—like tungsten carbide—to metal parts. The deposit is made in the form of a coating, and is normally applied in thicknesses ranging from 0.0005 to 0.020 in. The coating is not diluted in any way.

One of the biggest advantages of this new process is that the temperature of the base metal does not exceed 400° F during the plating operation—even when tungsten carbide is being deposited. The low-temperature deposition practically eliminates any possibility of a change in the properties of the metal being plated, and reduces to a minimum the chance that the part might warp.

The process is adaptable. Flat areas, cylinders, holes and parts having various shapes and contours can be coated. Surfaces up to 6 in. wide and 40 in. long can be handled with present facilities. The plated part can be used as-coated or ground to a mirror finish.

In the majority of applications listed to date, parts Flame-Plated with tungsten carbide have shown wear resistance equal, or superior, to the sintered tungsten carbides—and vastly superior to cast alloys, hard chrome-plating and tool steels. Parts Flame-Plated with tungsten carbide have all of the desirable properties of sintered tungsten carbide such as resistance to abrasion and frictional wear and, in addition, have a lower modulus of elasticity and greater resistance to impact and thermal shock.

Metals other than tungsten carbide have been deposited by this new method. However, the bulk of the development work, and greater portion of the field testing, has been accomplished with tungsten carbide. Consequently, this report is limited to the results obtained with this material.

The Potential Market

There is a large field of application for Flame-Plating. It will be used wherever an undiluted coating of tungsten carbide is required to protect metal parts from severe abrasion and frictional wear. Cotton picking spindles, dies, seaming rolls and burnishing tools are good examples of parts exposed to this type of wear. Up until now, the tungsten carbide applied to these parts was diluted either by the base metal or the steel welding rod used as a binder.

Flame-Plating will be in demand for protecting precision parts—where the wearing away of a few thousandths of an inch of metal would make the part useless. Up until now, many of these parts were made of sintered tungsten carbide. When the surface wore away, the entire part had to be scrapped. Flame-Plating a steel part will prove to be an economical solution to this problem. Some of the parts that fall into this category are plug and thread gages and arbors.

Up until now tungsten carbide could not be deposited

Some Facts about Flame-Plate Tungsten Carbon Coating Currently Being Applied

Composition	92% tungsten carbide; 8% cobalt	
Hardness	1200 to 1500 Vickers (300 gm. load)	
Coating Thickness	Maximum - 0.020 in.; Minimum - 0.0005 in.	
Surface (As Coated)	125 microinches rms (Brush Analyser)	
Surface (After Finishing)	2 microinches rms (Brush Analyser)	
Base Materials	Tool steels, cast iron, aluminum, copper, brass, bronze, titanium, magnesium	
Temperature of Base Piece during Application of Coating	Less than 200 deg. centigrade	
* Size of Base Piece	Round: O.D. - from 1/8 in. to 6.0 in. Length - to 40 in.	Flat: As coated - 6 in. by 40 in. Finish-ground - 3/4 in. by 40 in.
* Shape of Base Piece	Externally -- any area at no greater than 45° from a horizontal datum 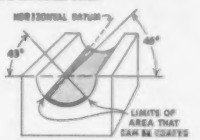 Inside cylinder walls -- Coating can be deposited to a depth equal to the diameter of the hole.	

* Other sizes and shapes can be handled with special jigs and fixtures.

Figure 1

on many metal parts because the heat required for the facing operation would distort the part or change its metallurgical properties. Flame-Plating eliminates this problem. Now saw teeth and paper slitter knives can be protected by a hard coating.

Flame-Plating will fit into the picture where some degree of toughness is required in a wearing part. Core rods used in powder metallurgy, for example, are excellent applications for Flame-Plating.

The decision as to when to use this process will have to be based on a number of factors. The cost of Flame-Plating a part, in actual dollars and cents, will fall somewhere between the cost of a hard-faced part and a sintered tungsten carbide. A Flame-Plated plug gage, for example, will cost more than a gage made of a cast alloy, but less than one made of sintered tungsten carbide. Of course, the outlay of dollars must be balanced against the service life. Very often the time and money a long-wearing part saves by reducing down-time for maintenance and repair more than offsets its initial cost.

What Metals Can Be Coated

Through the use of Linde's Flame-Plating process, tungsten carbide can be deposited on almost any base metal. Steels of all types, cast iron, aluminum, copper, brass, bronze, titanium and magnesium have all been coated successfully by this new method.

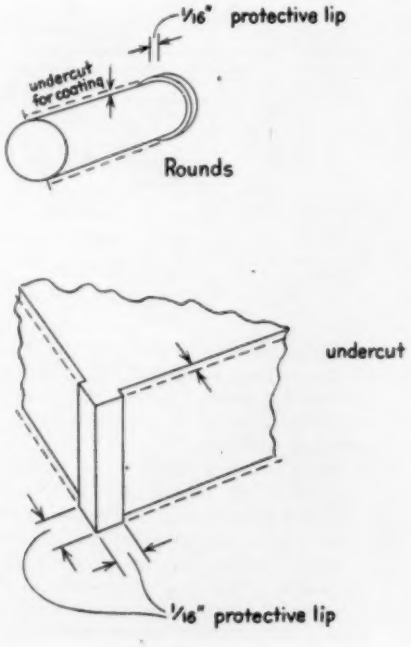

Fig. 2 Preparation of parts for Flame-Plating

This wide selection of base metals should make this process especially interesting to the design engineer. He may, for example, require a part that has good electrical conductivity but at the same time must resist surface wear. He can now obtain both properties by Flame-Plating copper. Or, he may have a problem of reducing the weight of a wearing part. Flame-Plating aluminum with tungsten carbide might be his answer. Any number of problems can now be solved by combining the desirable properties of a base metal with the extremely hard Flame-Plated coating.

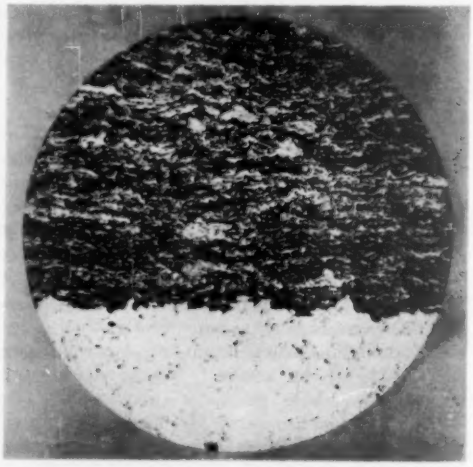

Fig. 3 Photomicrograph of a Flame-Plated tungsten carbide coating at 300 magnifications

The applied coating is the dark area. The lighter zone shows the mild steel base. The jagged bond line between the two materials indicates the cleaned, slightly roughened surface that was coated. Notice the excellent interlocking mechanical bond. There is no mixing or dilution of the coating with the base. The coating has a fine-grain, dense, laminar structure with negligible porosity.

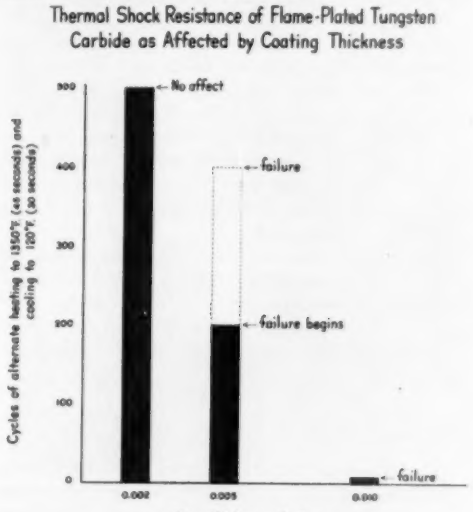

Figure 4

Size Limitations

The size of the parts that can be Flame-Plated are limited by the handling equipment available at the present time. These limitations will be relaxed as the equipment is improved. The areas that can be coated vary with the shape of the part. Here is a quick summary of just what can be done right now:

Flat surfaces 6 in. wide and up to 40 in. long can be Flame-Plated in thicknesses up to 0.020 in., providing the part is to be used in the as-coated condition. If the part is to be finish-ground, the width limitation is $^3/_4$ in.

Cylindrical objects from $^1/_8$ to 6 in. in diameter can be handled with present equipment. Smaller or larger diameters may be plated but these would require special handling. The limitation on length is 40 in.

Holes or internal areas of cylinders can be plated to a depth equal to the diameter. A 1-in. hole can be plated to a depth of 1 in.

Irregular-shaped objects can also be handled. The width and length limitations are the same as for cylindrical and flat areas. The rule on irregular-shaped objects is that any area can be covered directly from the horizontal plane to an angle no greater than 45 deg from the horizontal can be successfully Flame-Plated.

Preparation of Parts

The parts to be Flame-Plated should be undercut just deep enough to allow for the desired thickness of the coating. It is advisable to leave a small protective lip at any edge where the part may be subjected to

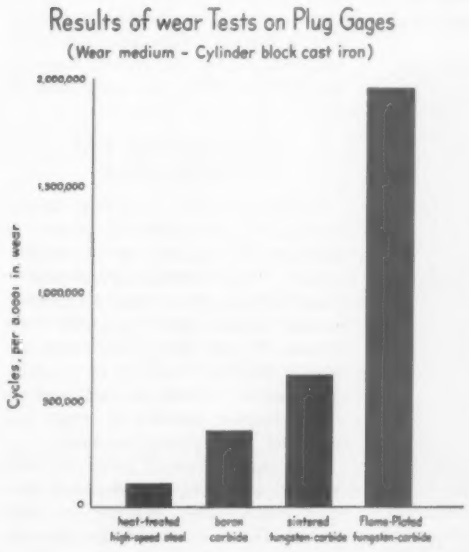

Figure 5

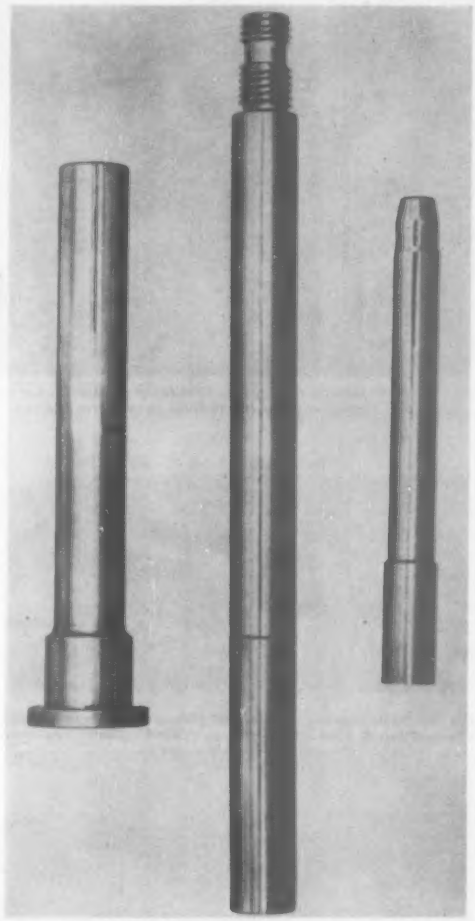

Fig. 6 Core rods must resist severe abrasion and be tough enough to withstand a certain amount of loading and deformation. A hard coating of Flame-Plated tungsten carbide over a strong steel base provides the ideal combination of properties for this application

Fig. 7 Flame-Plating is well suited to burnishers. The cutting areas of the buttons are coated so that they will maintain close tolerances for thousands of precise operations

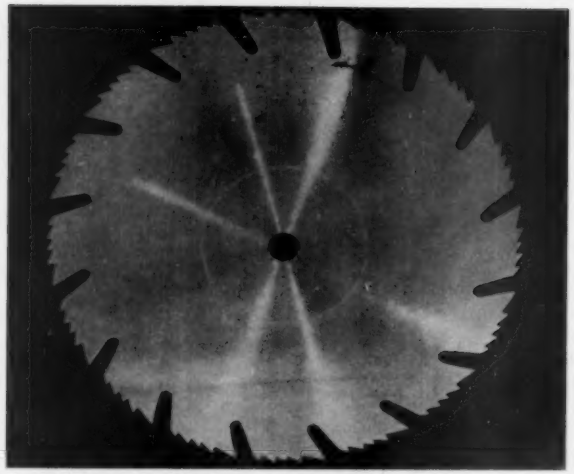

Fig. 8 The teeth of this 10-in. circular saw blade have been Flame-Plated to help them keep their "bite" longer

abuse or where two Flame-Plated surfaces are at right angles to each other. This is especially important on plug gages, shafts, spindles and core rods.

How Thick Should the Coating Be

Although the maximum thickness obtainable with a Flame-Plated coating now offered is 0.020 in., few applications would require a thickness of over 0.005 in. A coating thickness of a few thousandths of an inch will resist mechanical and thermal shock to a much greater degree than will a thickness of 0.010 or 0.020 in. A coating thickness of 0.001 in. over the allowable wear tolerance is sufficient in most instances.

If the part is to be finish-ground an excess coating of 0.004 in. is deposited. However, it may be desirable to use the as-coated surface. This surface is 125 microinches rms, as measured by a Brush Analyzer.

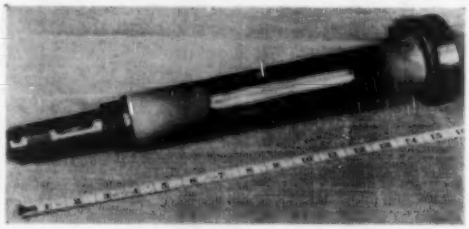

Fig. 9 Both bearing surfaces of this machine spindle are Flame-Plated, and are shown as coated. These coatings will be finish ground

Finish Grinding

A Flame-Plated surface can be ground to a finish of approximately 2 microinches rms. The surface of a coating that has been finish-ground appears to have a certain amount of microscopic porosity. These surface pores are extremely shallow and do not have a detrimental effect on the wear qualities of the coating.

Resinoid bonded diamond wheels are the only grinding wheels suitable for finishing a Flame-Plated surface. A 100-mesh wheel should be used for rough-grinding and a 400-mesh wheel for finish-grinding when no more than 0.0005 in. is to be removed. Before grinding, the flow of coolant should be adjusted so that the part is flooded. Fifty per cent water and 50% soluble oil, or 50% kerosene and 50% spindled oil are good coolants.

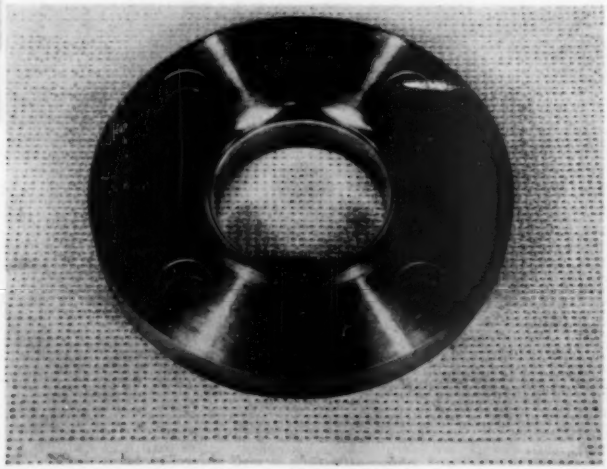

Fig. 10 The inner lip of this cup drawing die has a small area, but must resist an extraordinary amount of wear. This surface has been Flame-Plated. For this application, a 0.003-in. thick coating is used

COMPOSITION AND METALLURGY

Tungsten carbide currently applied by Linde's Flame-Plating process is composed of tungsten, carbon and 8% cobalt. These elements are present in forms differing from sintered tungsten carbide. There are two predominate phases, WC and M_6C. The latter represents Co_2W_4C, Co_3W_3C or Co_4W_2C. Most of the cobalt is combined in these complex carbides of cobalt and tungsten. There is no free cobalt.

The particles which form the coating are elongated and flattened into thin disks. The diameter of each particle is many times larger than its thickness.

The photomicrograph, Fig. 3, shows the coating at 300 magnifications. The tungsten carbide is the dark area while the steel base is relatively white. The jagged bond line between the two indicates the cleaned and slightly rough surface prior to coating. An excellent interlocking mechanical bond is in evidence.

The lighter colored material in the coating is tungsten carbide, while the very dark material is composed of the complex carbides of tungsten and cobalt. The laminar structure is clearly evident.

Microscopic examination indicates that the bond between the parent metal and the coating is not a welded bond. It can be seen that there is no mixing or dilution of the coating material with the base. Even though there is a distinct boundary between the coating and the base, there is no void or visible oxide layer. Currently it is believed that in order to separate the coating from the base, the base must be deformed. If the coating is thin when the base is deformed, the coating will crack vertically, but will adhere to the base between the cracks. If the coating is thick, the coating will tend to separate from the base.

The critical thickness above which separation occurs depends on the nature of the base, its hardness and surface preparation. The bond is better with the softer metals such as aluminum than with extremely hard metals such as chromium. Practically all commercial metals and alloys including hardened tool steel can be coated satisfactorily. Chromium plate, sintered tungsten carbide and ground Flame-Plated surfaces cannot as yet be coated with good adherence.

The fact that the coating does not mix with the base metal is important because the properties of both the base and the coating are retained.

PROPERTIES OF FLAME-PLATED COATINGS

Hardness

Tungsten carbide is one of the hardest, best-wearing metals known. The hardness of Flame-Plated tungsten carbide coatings (92% tungsten carbide; 8% cobalt) averages about 1350 Vickers pyramid number (VPN). This is equivalent to 89.3 Rockwell (A scale). Almost all of the hardness tests on coatings give values of from 1200 to 1500 VPN, using a 300-g load.

Actually, the particles that make up a Flame-Plated coating are harder than indicated by the Vickers test. The difference between actual (particle) hardness and apparent (coating) hardness is due to the type of bond between particles. This bond, though it lowers the *apparent* hardness, improves wear resistance.

Modulus of Elasticity

Within the limits of elasticity, the modulus of elasticity is the ratio of unit load (stress) to corresponding unit deformation (strain). The modulus of elasticity of Flame-Plated tungsten carbide is surprisingly low,

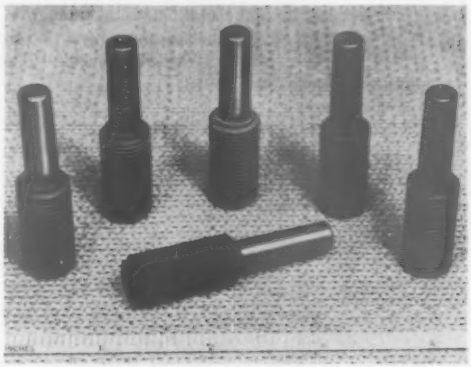

***Fig. 11** These thread gages are Flame-Plated, but must be finish ground before being put to use*

being only 15,000,000 psi as compared to 85,000,000 to 90,000,000 psi for sintered tungsten carbide. This extreme difference in stress-strain relationship is also attributed to the unique bond between the individual particles in a coating.

A low modulus of elasticity is advantageous for materials used to resist frictional and abrasive wear. It means that even a light load will cause slight deformation of the coating. The load will, therefore, be distributed over a larger portion of the bearing surface. This, in effect, means a smoother wear surface.

The modulus is desirable for another reason: any load applied to a ductile base material will cause de-

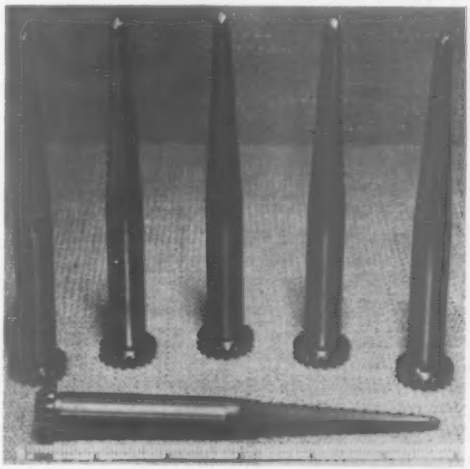

***Fig. 12** When these cotton-picker spindles rotate at about 2000 rpm, the barbs on each conical surface pluck cotton at an amazingly fast rate. Sand in the bolls wears steel barbs down. A 0.001-in. thick Flame-Plated coating protects the barbs from this unusual wear condition. In this application, no grinding or polishing is necessary*

formation. A low modulus coating will also deform—to a limited degree—rather than tend to retain its original shape and crack. As the coating deforms, it uniformly distributes the load to the base metal.

Porosity

In contrast to many other types of coatings, Flame-Plated tungsten carbide has a negligible amount of porosity—less than 0.5%.

Tensile Strength

Sintered tungsten carbides are inherently weak in tension. Due to the thinness of Flame-Plated coatings (from 0.005 to 0.020 in.), no accurate measure of their tensile strength has been made. The coating material is supported, however, by the base metal over which it is applied.

Corrosion Resistance

Reagents that attack tungsten carbide or cobalt will attack Flame-Plated coatings. These reagents include most acids and strong alkalies. Mild alkalies, detergents in lubricating oils and atmospheres free from acid fumes have no detrimental effect on the coating.

Thermal Shock Resistance

Because of the unique bond between individual particles, low modulus of elasticity and thinness of coating, the stresses induced in Flame-Plated tungsten carbide by a given temperature differential are low. Thermal shock of a moderate rate and below about 2000° F has little or no effect on thin coatings. Most satisfactory resistance is obtained with thicknesses not greater than 0.003 in. (after grinding).

Results of laboratory tests, which indicate the effect of coating thickness on thermal shock resistance of strip samples, are shown in Fig. 4. The samples were preloaded in tension to 15,000 psi, heated to 1350° F in 45 sec, and then cooled with an air jet to 120° F in 30 sec. The heating-cooling cycle was repeated 500 times, or until failure of the coating was observed.

Mechanical Shock Resistance

Although a tungsten carbide coating has the inherent brittleness of tungsten carbide in any form, the coating can absorb a moderate amount of deformation. For mechanical shock resistance, the coating thickness should not exceed 0.003 in. after finish grinding. Any shock or impact that causes permanent distortion of the base piece, impairs Flame-Plated coatings regardless of coating thickness.

Flash Welding of Titanium Alloys

by Dr. I. A. Oehler

OUR experience at the American Welding & Manufacturing Co. in Warren, Ohio, has shown us that the flash butt welding of titanium alloys is one of the lesser problems in the fabrication of these alloys. Satisfactory welds that closely approach parent metal properties are being regularly produced on conventional hydraulic machines.

Our initial work was done early in 1949 on samples of commercially pure $^1/_2$-in. diameter rod supplied to us by the Remington Arms Division of Dupont. Excerpts from our report at that time follow:

Dr. I. A. Oehler is Director of Metallurgy and Research with the American Welding and Manufacturing Co., Warren, Ohio.

Paper was presented before the Titanium Fabrication Conference, Minerals and Metals Advisory Board, National Academy of Sciences, National Research Council at the Hotel Carter, Cleveland, Ohio, June 19, 1952.

1. No protective atmosphere was used.
2. Specimens tested to destruction had ductile fractures adjacent to the weld in the parent material.
3. The weld zone in the as-welded condition was acicular in structure.
4. Annealing at 1650° refined this structure.
5. All welds appeared sound with no inclusions or voids apparent in the microstructure.

Flashing travel of $^1/_4$ in., upset travel of $^7/_{16}$ in. and final die opening of $^1/_4$ in. was used. The total welding cycle consumed 5 sec at a voltage setting of 2.9 v. Speed of upset was of particular importance, and fast speeds, comparable to those used for aluminum, were employed.

Following these initial tests, small production runs of RC70 bars were fabricated into rings and the joint flash welded. The weld burr is chipped off while hot. Cross sections up to 2 sq in. have been welded, and we see no reason that several times this area cannot be welded.

The introduction of the higher strength alloys such as RC-130B and TI-150A presented a problem not normally encountered in working with other ferrous and nonferrous materials. This was the apparent sensitivity of these materials to cracking in areas of surface or structural discontinuities. We found that on bars which had surface defects removed by grinding just prior to shipment from the mill, cracking occurred

when the bars were clamped in the welding machine. One lot, which had been checked for hardness at the mill, fractured through the Brinell impressions. If fracture did not occur at these points immediately upon clamping, it was noted that cracks appeared sometime after the weld was completed. The additional stresses set up by the thermal gradient during the welding cycle apparently are sufficient to cause failure. When bars were annealed at the mill after surface preparation, no trouble was encountered. In our own processing, it was found that a rough chip or grind mark resulting from burr removal could give rise to cracks, but cracking could be avoided by getting the rings into a furnace at 1300° F immediately after welding.

A typical weld cycle for 2 x $^5/_{16}$-in. bars of RC-130B flash welded into a ring consumes 8 sec. with the voltage (open circuit) at 6.2. Flashing travel was $^3/_4$ in., upset travel $^3/_8$ in. and final die opening $^1/_2$ in. That cycle produced welds of 152,000 ts, 146,500 yield and 15% elongation in 2 in. with a reduction in area of 46%.

Occasionally we noted that welds of good strength exhibited very low ductility—elongations of 1–7%. Investigations in our customer's laboratory, as well as in our own, showed this to be associated with a banded structural condition in the bars. Additional welds made in the same banded bar always showed low values. A similar condition is encountered on heavily banded dirty steels that are flash welded. The upset portion of the welding cycle turns the fibers at the weld outward so they lie transverse to the bar axis and the inclusions present in the material act as notches which produce brittle failures. In the titanium alloys, a banded structure, without any apparent inclusions as such, is sufficient to produce failure. This condition is now well known to the alloy manufacturers and so should not be encountered in the future on flash welding applications.

Titanium alloys have been flash welded to aluminum alloys and to carbon steels. This work was carried on only as a curiosity, with no present practical applications in mind. On such joints, failure occurs outside the weld when tested in tension or bending.

In summary, flash welding of titanium alloys can be readily accomplished provided:

1. Material is of good quality and uniform structure.
2. Techniques similar to those used for aluminum are employed.
3. Welded parts are annealed or otherwise furnace treated immediately after welding.

Powder-Cutting Halves 5 Billets per Minute

WHEN a hot saw at a billet mill could not keep up with mill production, an oxy-acetylene powder cutting setup was installed to cut double-length billets in half. This billet cutting installation now makes an average of 900 to 1000 cuts per turn—better than three times the production formerly obtained.

Figure 1 shows the installation. It consists of three beds and a carriage cab which mounts the equipment. While billets are being cut on one bed, the second is unloaded and the third, loaded. In this view, as soon as the bed at right is cut, the carriage will move down to the bed at extreme left, which is ready for cutting. In the center bed, cut billets are being unloaded.

The carriage cab mounting the cutting equipment runs on tracks alongside the billet beds. An Oxweld cutting machine travels on a 10-in. machined I-beam which is fastened to the cab. The cutting machine cuts through the billets at 15 in. per minute.

An iron-rich powder is used in the oxy-acetylene flame to get quick starts. The operator, in the cab, controls the cutting operation.

When the cuts on one bed have been completed, the operator disengages a clutch on the cutting machine and returns it to the starting position by a pulley and cable drum arrangement. Then he moves the cab to the next bed and starts the operation all over again.

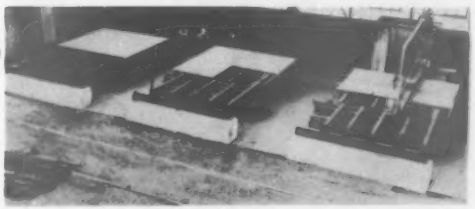

Fig. 1 Powder-cutting installation for cutting billets enables mill to keep up with production in seamless mills by operating only one turn per day

Fig. 2 Cutting machine cuts through 3 in. billets at 15 in. per minute

Four men make up the billet cutting crew: the operator, two chain men who load and unload beds and a crane operator. When all four men are kept busy, top production has gone as high as 1500 cuts per turn.

Welded Build-Up of Worn Spoke Surfaces of Tractor Trailer

Bronze application plus grinding quickly put wheel assembly back on job

Data and photos courtesy Air Reduction Sales Co.

Figure 1

by L. J. MacLennan, Jr.

AS AN example of how a welding torch helps to "keep 'em rolling" let's look in on a welding shop where we see, in Fig. 1, an operator working on the wheel assembly of a larger tractor trailer.

As he rolled on toward his destination, the driver of this tractor trailer noticed an unusual "wheel bearing" noise that warranted immediate attention. An inspection of the trailer wheels revealed that due to loose lugs —not wheel bearings—the tire and rim assembly was on the verge of falling off entirely.

The loose lugs had permitted the tire and steel rim assembly to slide back and forth, laterally, across the bearing surface of each of the six wheel spokes. This lateral movement, over a prolonged period of time, caused excessive wear on these six wrought iron spoke surfaces. The wear was so extensive at several of these points that the lug bolt recesses were completely worn through and the lug bolts sheared. So here was a tire problem that neither a spare tire nor a mechanic—without welding equipment—could remedy.

In order again to support and mount the tire and rim, the bearing surfaces of each spoke arm had to be built up to their original dimensions. This job was success-

L. J. MacLennan, Jr., Dealer Sales Dept., Air Reduction Sales Co., A Division of Air Reduction Co., Inc.

Figure 2

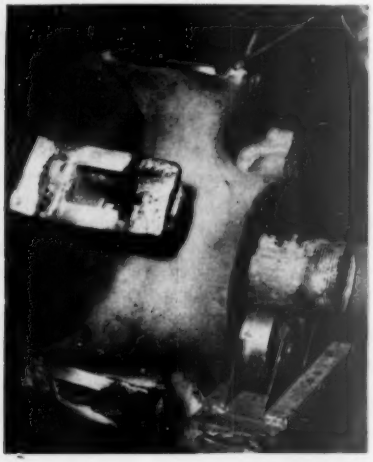

Figure 3

Figure 4

fully accomplished in short order with a welding torch, bronze rod, Marvel Flux, a grinding wheel and an abrasive disk.

The surface of each spoke, where build-up was necessary, was lightly ground (Fig. 2). This clean surface was then smoothly braze welded with bronze rod. One lug recess, as can be seen in the illustration, was completely worn through.

How two spoke sections were built up prior to the disk surfacing is shown in Fig. 3. A third section is receiving its application of bronze.

Figure 5

The method of final surfacing to bring the spoke sections back to their original dimensions is illustrated in Fig. 4. In the lower section of Fig. 5 can be seen the finished spoke surface, again as good as new.

With a little "barreling along" on the last leg of the haul the driver was able to complete his run almost on schedule—thanks to the heat of the oxyacetylene flame and a skilled welding operator.

Portable Sigma-Welding Equipment

BY MOUNTING equipment for sigma welding high up out of the way, welding production may be speeded by making it possible to slide equipment from one part of the shop to another. At the same time, the mounted equipment practically elimi-

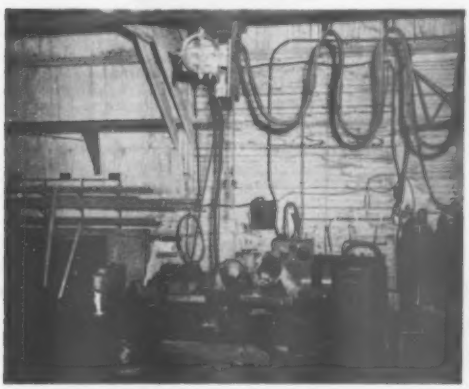

Fig. 1 By hanging equipment on track, sigma welding can be done at several welding stations

Fig. 2 Mounting of equipment showing the roller-type hangers which permit the equipment to slide easily

nates wear and tear on argon and water hoses, and welding cable.

This setup is used by one manufacturer to fabricate aluminum window frames. Figure 1 shows the operator making a weld in a window frame. The sigma rod feed and control unit have been pulled into position above the work. The unit can be used at several welding stations, by merely sliding it along the rail to the station.

A close-up of the way the control unit and hose assemblies ride the rail is shown in Fig. 2.

Principles of Braze Welding

by H. K. Schmuck

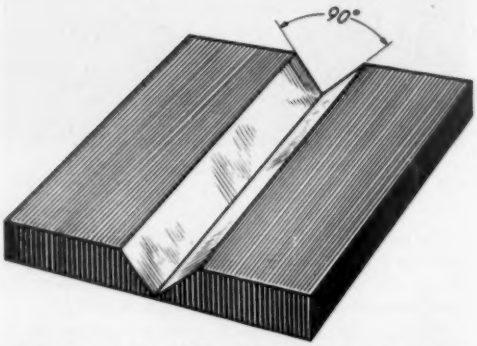

Fig. 1 For metal over 1/4 in. thick, bevel to make an angle of about 90 deg. A coarse file can be used. For heavy sections of cast iron a grinder will be needed; for steel castings, a cutting blowpipe or gouging nozzle

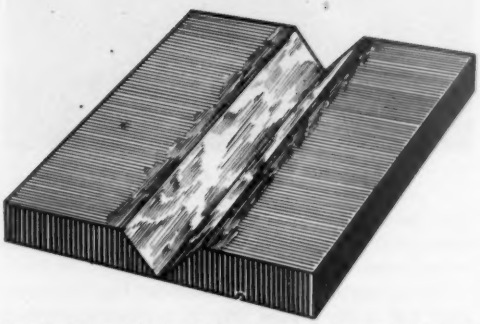

Fig. 2 Thorough cleaning is one of the secrets of a good weld. Remove all oil, grease, scale, rust or oxide from the beveled edges. Clean the top surface for about 1/2 in. back from the edges. Use a grinder, stiff wire brush, file, emery cloth or steel wool

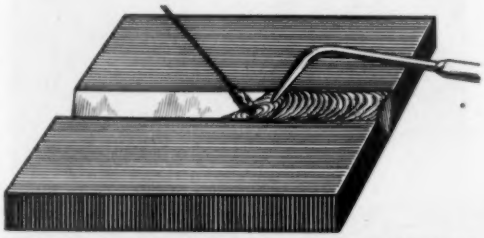

Fig. 3 The beveled surfaces must also be cleaned by using a liberal amount of flux. Add the flux by dipping the end of the hot rod into the flux can. A bronze rod precoated with flux helps, because you are sure of getting exactly the right amount

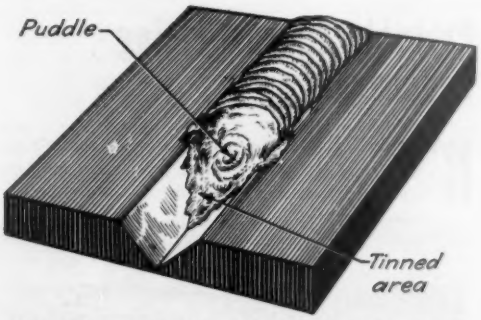

Fig. 4 Tin the surface ahead of the main rod deposit when the metal is at the right temperature and thoroughly clean. If the metal is not hot enough the bronze rod will form into drops. If the metal is too hot the bronze rod will boil and form into little balls

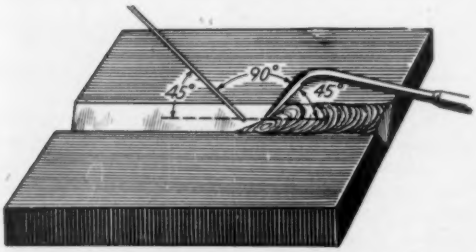

Fig. 5 Position of blowpipe and rod is another secret for making good bronze welds. For a weld in the flat position, hold both rod and blowpipe at an angle of about 45 deg to the workpiece

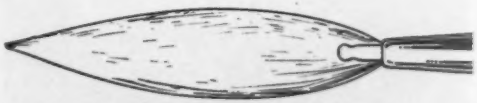

Fig. 6 Adjust the flame until there is a slight excess of oxygen. The oxidizing flame has a bluish outer envelope and shorter inner cone than the neutral flame. There is no secondary flame or feather

H. K. Schmuck is connected with Linde Air Products Co., Denver, Colo.

the AMERICAN WELDING SOCIETY

activities • related events

1952–53 National Nominating Committee

H. W. Pierce, Past-President and member of the Board of Directors, has been appointed Chairman of the 1952–53 National Nominating Committee by President Jennings and his appointment approved by the National Board of Directors.

There will be an open meeting of the Nominating Committee during the National Fall Meeting of the SOCIETY. All members of the SOCIETY have the privilege of presenting their recommendations to the National Nominating Committee at this open meeting.

The meeting will be held in Philadelphia, Pa., at the Bellevue-Stratford Hotel, on Wednesday, Oct. 22, 1952, at 2 to 4 P.M., in the Blue Room. The Committee will be in open session to receive recommendations from the membership between the hours of 2 and 4 P.M. At 4 P.M. the open meeting will be closed and the Committee will retire into a closed session for deliberation and working program.

Other members of the committee are: J. L. Forand, District No. 1 Representative, J. H. Humberstone, District No. 2 Representative, R. E. Lorentz, Jr., District No. 3 Representative, G. O. Hoglund, District No. 4 Representative, H. Baldwin, District No. 5 Representative, J. B. Davis, District No. 6 Representative and C. M. Styer, District No. 7 Representative.

American Welding Society Announces A. F. Davis Undergraduate Welding Awards

The AMERICAN WELDING SOCIETY has selected the winners of the 1951–52 A. F. Davis Undergraduate Welding Awards which include cash prizes of $700 and award certificates. This annual program is named for its sponsor, A. F. Davis, Vice-President and Secretary of the Lincoln Electric Co., Cleveland, Ohio.

Two Cornell University undergraduate engineers, Paul J. Wisniewski and David A. Thomas, won the first prize of $200 with their paper entitled "Metal Transfer in Arc Welding" which appeared in the April 1952 issue of *The Cornell Engineer*. Both were juniors this past year in Metallurgical Engineering. *The Cornell Engineer* will also receive a $200 cash prize for publishing the winning paper.

A Wisconsin University senior, Norman Fletcher, has been selected as winner of the second prize. His prize-winning paper on the subject of "Arc Welded Machine Jigs" was published in the November 1951 issue of *The Wisconsin Engineer*. Mr. Fletcher and the publication will each receive $150 for second prize.

The award certificates will be presented to the winners on Monday, Oct. 20, 1952, at special ceremonies during the National Fall Meeting of the AMERICAN WELDING SOCIETY at Philadelphia. The Award winners have already received the cash prizes.

Prize Winning Papers Selected by RWMA Jury of Award, 1952

At its Aug. 25, 1952, meeting in Troy, N. Y., the 1952 RWMA Jury of Award made the following selection of prize winning papers:

GROUP I, Papers from Industrial Sources—1st Prize: "A Case of Power," by J. Geralds, P. Duker and M. Zucker. 2nd Prize: "Quality Control for Spot Welding in a Job Shop," by P. G. Poetto. 3rd Prize: "Corrosion of Structural Spot Welds," by B. Karnisky, E. Kinelski and E. Gruca.

GROUP II, Papers from University (Staff) Sources—1st Prize: "Temperature Distribution During the Flash Welding of Steel," by E. F. Nippes, W. F. Savage, J. J. McCarthy and S. S. Smith. 2nd Prize: "Projection Welding of Steel in Heavy Gages and in Dissimilar Thicknesses," by E. F. Nippes and J. M. Gerken.

These papers were selected from a total of 19 papers entered in the Industrial Class and four papers entered in the University (Staff) Class. There were no papers entered in the University (Undergraduate) Class.

AWS Aircraft and Rocketry Panel Tours Solar Plant

More than 120 Southern California welding engineers visited San Diego recently to view one of the largest arrays of production welding equipment in the United States.

Touring the San Diego plant of Solar Aircraft Co. members of the Aircraft and Rocketry Panel of the AMERICAN WELDING SOCIETY saw demonstrations of many of the Solar plant's 275 welding installations which are certified to turn out work for the armed forces, plus numerous other welding installations.

Many types of Solar-designed welding equipment were demonstrated in action to the guests, who represented most of the leading metalworking plants of Southern California. The Solar-made machines included butt welders, special purpose spot and seam welders, sigma welders and submerged arc welders.

Before the tour, the engineers were guests of Solar at a dinner and heard Frank Harkins, Solar's chief welding engineer, and Al Bennett, superintendent of the Solar flux department, describe the company's advances in the welding of stainless and other alloy steels.

Frank Harkins, Chief Welding Engineer of Solar Aircraft Co. in San Diego, demonstrates a Solar-built butt welder to Francis H. Stevenson, center, Welding Engineer of Aerojet Engineering Corp., & Bernard Gross, Dir. of Labs. at Rohr Aircraft Corp.

Library Service Again Featured at the National Metals Exposition

Metallurgists and scientists who attend the National Metal Congress at Philadelphia, October 20–24, should make it a point to visit the exhibit in Booth No. 1020 where the Special Libraries Association will reproduce a working library. A metals librarian in constant attendance will quickly locate the answers to your reference questions. New books and periodicals will be on display. Special Libraries booth has nothing to sell. It is simply a demonstration of service.

The Monday afternoon session of the Special Libraries Association Metals Section will feature reports on the new metallurgical classification and mechanical methods for literature handling now in the experimental stage. Tuesday's meetings will be of special interest since they will deal with the availability of research reports, unclassified government material and foreign language literature.

All visitors are cordially invited to attend and join in the discussions which follow these papers.

AWS Annual Dinner

The Thursday evening, October 23rd, highlight is the Banquet or Annual Dinner in the Ballroom of the Bellevue-Stratford. At 6:30 a "pay-as-you-go" bar will be opened adjoining the ballroom for the convenience of those who wish to assemble prior to the dinner. At 7:15 P.M., *prompt*, the famous "Bellevue" Roast Beef dinner will be served in proper "Stratford" style.

Frank Schluth, famous mimic, will be a "Master Welder" headliner, supported by the "Selendias" with their topical satires in dancing; and sextette of shapely Welderettes; Dave Monahan with his "Black-Light" and puppet novelty musical feature; the melodius and fast-swinging duet of Fred Smith and June Sayre with their amazing repertoire of the best loved American Aires. All this to the accompaniment of Art Jordan's popular orchestra for ladies and gentlemen, the low price of $10 per plate (taxes and gratuities included)! Write: K. Wm. Ostrom, Chairman, c/o K. Wm. Ostrom & Co., 3717 Filbert St., Philadelphia 4, Pa., phone Ev 2-5444 or J. E. Norcross, Arcos Corp., 50th & Paschall Ave., Philadelphia, Pa., phone Sa 7-1500 or L. D. T. Berg, Arcway Equipment Co., 49th & Grays Ave., Philadelphia 43, Pa., phone Sa 7-3000. Tickets sold singly, by group or for complete tables.

Meet Government Specifications With

NEW SINGLE PHASE NON-SYNCHRONOUS UP-DOWN SLOPE CONTROL with

Robotron "CUSHIONED POWER" WELDING TIMERS

Now . . . with this new concept of Non-Synchronous SINGLE PHASE Control you can weld all types of Brass, Aluminum, Monel Metal, Stainless and Nickel Alloy Steels, Coated or Plated Metals or any combination of Dissimilar Metals and meet U. S. Government Specifications. Welding is accomplished with minimum surface indentation, and electrode pick-up, maximum ductility and constant uniformity. The Robotron Non-Synchronous SINGLE PHASE Control Unit has the simplicity of a single phase circuit instead of the present complicated and difficult-to-maintain multiple circuits.

HI-CONDUCTIVITY
LO-CONDUCTIVITY

Robotron's "Cushioned-Power" welding cycle begins with a PREHEAT, or up slope, stage that assures proper seating of electrodes, cutting down surface resistance and increasing WELD heat where it's needed. It also decreases surface indentation, spewing of metal and lengthens the life of the electrodes. The TEMPER stage, or down slope (Trailing Current), controls rate of heat flow into the surrounding metal after weld is over, definitely controlling brittleness and in case of Coated Metals, allows coating or plating to resurface the weld.

Non-Synchronous "UP-DOWN" Slope Welding Control Unit is the least expensive unit on the market today, and it still assures better welds under a greater variety of welding conditions.

And best of all . . . Robotron's well-known plug-in feature gives you quick, easy installation and maintenance, plus complete versatility and adaptability in operation.

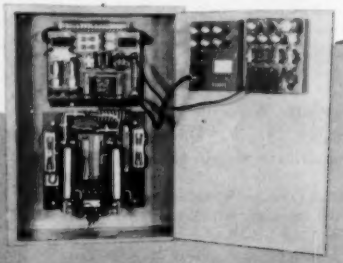

W361-H3C4
NEMA 3B WITH "UP-DOWN" SLOPE CONTROL —600 AMP. IGNITRON CONTACTOR AND SIZE "B" IGNITRON TUBES

THE FINEST IN INDUSTRIAL ELECTRONICS

Ask about our on-the-job approval plan. (NO OBLIGATION)

Robotron* CORP.

21300 W. Eight Mile Rd., Detroit 19, Mich.

7883 *T. M. Registered

Cut Welding Time 40%!

GET { fewer rejects! / no burn-throughs! / 100% penetration! / X-ray quality!

Use a P&H AC Welder

— the only welder with Instantaneous Control

Ideal for use with inert gas. Lets you handle "hard-to-weld" metals with ease — aluminum, magnesium, brass, copper, stainless, high carbon, high alloy, and low carbon steels

A touch of your toe instantly gives you the exact heat you need — there's no time lag! That's how this P&H AC Welder gives you the instantaneous control you don't get with other welders.

When you use it on high frequency with inert gas, you can fabricate to close tolerances. And there's no burn-back to oxidize the metal before you get started.

The P&H Inert Gas Welder saves production time these five ways — no other welder makes the work so easy:

1. **Foot switch automatically starts power, high frequency, gas, water.**
2. **Arc starts instantly without touching work.**
3. **Foot control instantly provides exact heat needed *while* welding.**
4. **Foot switch cuts power and high frequency immediately or gradually at completion of weld.**
5. **Automatic time delay shuts off gas and water.**

There are other outstanding P&H AC Welder features: P&H Dial-lectric Control that eliminates moving parts — for lower maintenance cost, easier operation. Built-in high-frequency unit that eliminates additional external equipment. Stepless amperage regulation. Unusual arc stability. Selector switch that gives operator choice of standard or high frequency.

Cut *your* welding time for non-ferrous and "hard-to-weld" metals. Get faster, easier, sounder welds — fewer rejects. Use a P&H AC Welder.

Ask your P&H representative for further information — or write us.

P&H WELDING DIVISION
HARNISCHFEGER CORPORATION
4551 WEST NATIONAL AVE. • MILWAUKEE 46, WISCONSIN

POWER SHOVELS • CRAWLER AND TRUCK CRANES • OVERHEAD CRANES • HOISTS • ARC WELDERS AND ELECTRODES • SOIL STABILIZERS • DIESEL ENGINES • PRE-FABRICATED HOMES

NEWS OF THE INDUSTRY

ASTE International Area Meeting

An International Area Meeting of the American Society of Tool Engineers, the 21,000-member technical society of American and Canadian production experts, will be held in the Statler Hotel in Buffalo, N. Y., on Oct. 10 and 11, 1952.

Twelve chapters from Ontario, Canada, New York and Pennsylvania representing a total membership of more than 2100 members are cooperating in the meeting which will feature four technical papers, plant tours and special activities.

40th Annual National Safety Congress

The 40th Annual National Safety Congress will be held in Chicago on Oct. 20–24, 1952. It is expected that 12,000 safety people from all over the world will attend. More than 600 speakers will appear at 200 sessions, covering every phase of safety. In addition, the Congress exposition will contain about 250 exhibits covering all types of safety aids.

Theme of the 40th Congress will be the need for cooperation in the safety movement.

Twelfth Annual Meeting of Society for Non-Destructive Testing

The Twelfth Annual Meeting of the Society for Non-Destructive Testing will be held at the Hotel Sylvania in Philadelphia, on Oct. 20-23, 1952. It occurs simultaneously with the National Metals Show and the annual meetings of the American Welding Society, American Society for Metals and the American Institute of Mining and Metallurgical Engineers.

According to the sponsors, the program for this meeting is directed to one of the most important problems facing industrial management, inasmuch as it shows the basic ways in which non-destructive testing can lower production and operating costs.

$30,000 Mechanical Design Award Program

A new competition for designers, engineers and manufacturers of machinery of all types has just been announced by The James F. Lincoln Arc Welding Foundation of Cleveland, Ohio. The new $30,000 Mechanical Design Award Program offers $30,000 in 101 cash awards, as well as national recognition, for the best papers describing the mechanical design and construction of any type of machine or machine component which is designed for arc-welded steel fabrication.

Any machine or component whose performance or appearance has been improved or whose cost has been reduced through the use of arc welding in its construction can be described. Any person who has participated in the designing, planning or manufacturing of the machinery can compete in the program by describing his work. A total of $20,100 will be given in 54 awards in 18 different divisions comprised of 18 first awards of $500, 18 second awards of $250 and 18 third awards of $150, plus 39 Honorable Mention awards of $100. Each division offers a separate competition. A total of $9900 will be given in grand awards to the 8 best-of-the-program papers. All papers are eligible for both divisional and grand awards. Top award is $2000, plus $500 first divisional award.

Papers may describe machinery in any of the following 18 classifications: Metal cutting, metal forming, electrical, conveying, pumping and compressing, prime moving, jigs, fixtures and tooling, processing, construction and mining, petroleum and gas, metalmaking and refining, textile and clothing, farming and ranching, food and fiber products, woodworking, lumbering and milling, household, printing and, machinery not otherwise classified.

The Foundation states in the rules brochure for the program that it is sponsoring the program to stimulate the scientific advance of machine design through the wider use of arc-welded construction. According to A. F. Davis, Secretary of the Foundation, "When correct welded design is applied to machinery, performance and appearance are improved, strength and rigidity are increased, service life extended and savings up to 50% can be made."

Papers will be judged by a Jury of engineers, educators, designers and fabricators selected from men prominent in industry and education. The program closes July 27, 1953. The rules and conditions brochure is available from The Lincoln Foundation, Cleveland 17, Ohio.

Welding Classes for Fall Months

A regular schedule of weekly classes in advanced welding techniques starting with the week of September 15th with a new session commencing every two weeks thereafter through the end of the year has been released for the Eutectic Welding Institute by Eutectic Welding Alloys Corp., Flushing, N. Y.

Detailed course outlines, schedules of courses, and similar additional information may be obtained by writing to Eutectic Welding Alloys Corp., 172nd St. at Northern Blvd., Flushing 58, N. Y.

Electrode Comparator Slide Rule Available

A new, 9-in. welding electrode comparator slide rule which permits a comparison of General Electric welding electrodes with those of other electrode manufacturers is available at G-E Welding Distributors.

Designated GEN-37B, the handy slide rule provides an electrode comparison in a matter of seconds as the operator designates a choice for comparison.

P&H Appoints New Distributor

The Harnischfeger Corp. of Milwaukee, Wis., is pleased to announce that the General Welding Equipment Co., 2106 N. Broadway, St. Louis 6, has recently been appointed distributor for the metropolitan St. Louis area to handle the complete line of P&H arc welders, electrodes and welding positioners.

At the same time, the General Welding Equipment Co. announces plans for a modernized sales and show room, and an enlarged loading dock. They also plan expanding their service and repair department to provide emergency and maintenance repair work on all types of welding equipment.

Color and Sound Movie on Inside Story of Welding Electrode Manufacturing

First showing of a new 22-min motion picture in full color and sound, revealing the "inside story" on how arc-welding electrodes are manufactured, will be held at the National Metal Exposition in Philadelphia, October 20–24, by the Alloy Rods Co., York, Pa., as the central feature of their exhibit in Booth No. 448.

Entitled "No Finer Electrodes Made. . . Anywhere," the film was made by professional movie crews in the Alloy Rods Co.'s plant at York, and will be exhibited every hour on the hour at the Metal Show in a small theater that will form the central attraction of the manufacturer's exhibit.

Magnetic? OR Electronic? WELDER CONTROL — WHICH WILL DO YOUR JOB BEST?

Square D makes them all... for simplest or most exacting applications!

CLASS 8992 Type BBG-1

Magnetic — **for General Purpose Machines**

For applications requiring widely varying welding conditions, normal welding speeds and maximum simplicity.

Electronic (SYNCHRONOUS) — **for Precision Welding**

For welding aluminum, other non-ferrous and ferrous metals requiring precision weld times; stepless heat control; slope or taper control.

CLASS 8993 Type BCG-2

Electronic — **for High Speed Welding**

For production line (gun or stationary) welders and other applications where high speed, high currents or dual gun control are factors.

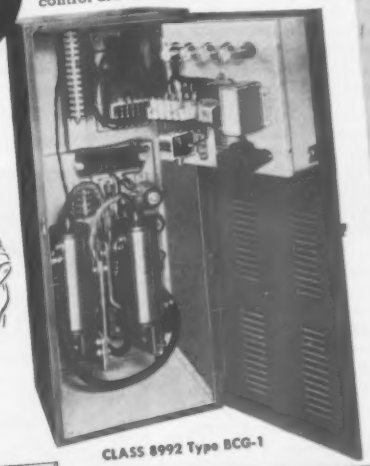

CLASS 8992 Type BCG-1

You'll find your nearby **Square D** *Field Engineer a source of sound counsel in selecting the welder control best suited to your application.*

SQUARE D COMPANY

DEPEND ON DURABLE DOCKSON REGULATORS

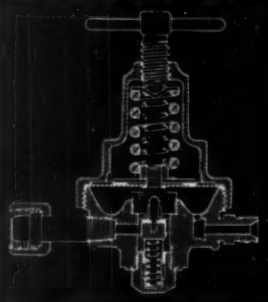

in types for Oxygen, Acetylene, CO_2, Air, Fuel Gases.

"BUILT FOR BETTER SERVICE" with improved diaphragms, replaceable, self-aligning seats; sturdier construction; shatter-safe gauges; alert safety valves and other advantages.

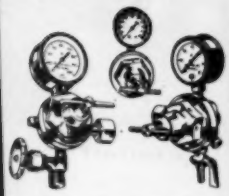

THERE IS A DOCKSON DISTRIBUTOR NEAR YOU—Let us send you his name and our complete catalog of DOCKSON WELDING and CUTTING EQUIPMENT.

Dockson CORPORATION
3839 WABASH • DETROIT 8, MICH.

Coating of Electrodes

According to company officials, this film is not a typical "sales movie" or promotional device, but was purposely photographed and edited to be an instructional and technical pictorial story intended mainly for showing before welding societies, engineering groups, metalworking industry organizations, college and university classes, and others interested in arc-welding techniques. It comprises about 45 scenes "shot" on the Alloy Rods Co. production lines and is believed by the company to be the first pictorial story of the manufacture of alloy arc-welding electrodes showing actual manufacturing processes, procedures and research close-ups. These matters, it is said, have always been carefully guarded trade secrets heretofore.

The picture proceeds from the initial step—cold drawing of hot rolled rod—on through the many manufacturing, research and quality control processes to the Alloy Rods Co.'s method of packing finished electrodes in sealed all-metal, moisture-proof containers. Along the way, the viewer is taken via the camera right up beside production workers, laboratory technicians and quality control specialists in a series of "close-ups" which are explained by a narrator who interprets what is going on in easily understandable terms.

After its premiere at the Metal Show, 16-mm prints of the entire movie will be made available to any reputable organization or group which desires to show the film. Arrangements may be made by writing Department M of Alloy Rods Co., York, Pa. In addition to the film, the company has published a 24-page brochure (Bulletin AR52-7) showing the key "stills" of the picture for distribution to viewers and other interested parties.

The McKay Co. Chicago Representative

Thomas S. Collins has been appointed electrode representative for the Chicago territory of The McKay Co., Pittsburgh, Pa. From headquarters at 1500 S. Western Ave. in Chicago, Mr. Collins will cover northeastern Illinois and northwestern Indiana. He will handle sales and service for the entire line of McKay mild steel, stainless steel and special-purpose arc-welding electrodes.

Mr. Collins is a veteran of World War II, having served 42 months in the Navy. A graduate of Loyola University, he earned a Bachelor of Science Degree in the School of Commerce. He recently became a member of the AMERICAN WELDING SOCIETY.

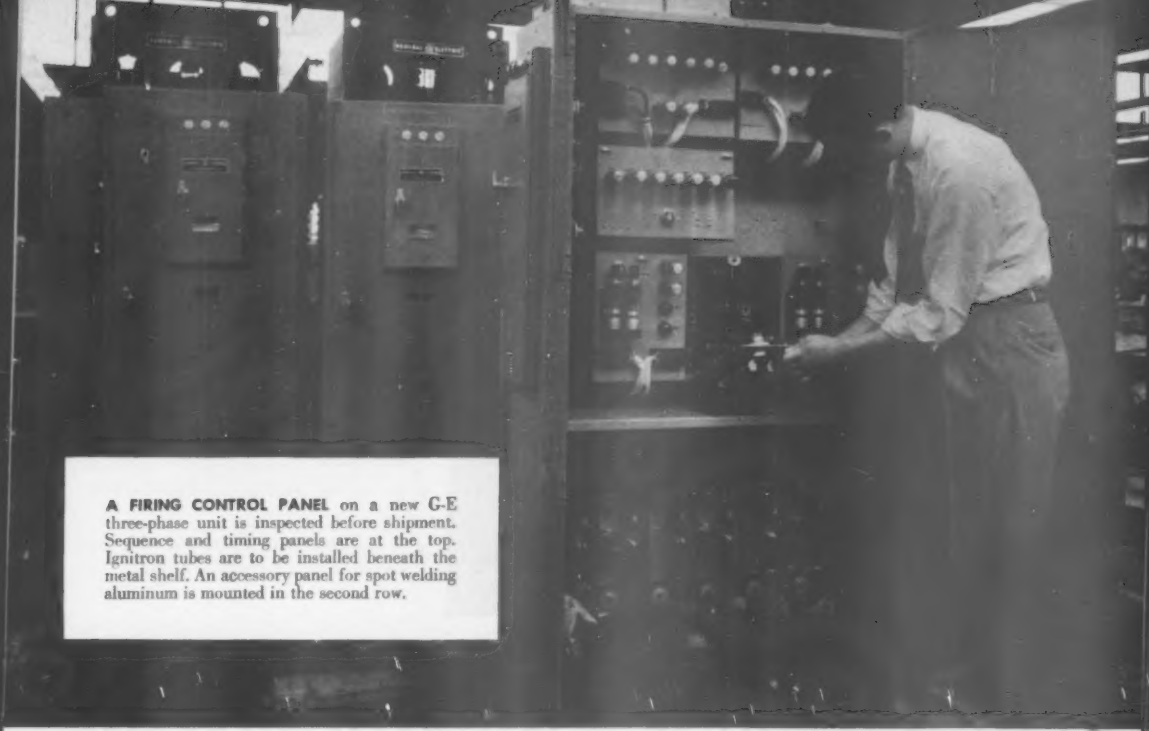

A FIRING CONTROL PANEL on a new G-E three-phase unit is inspected before shipment. Sequence and timing panels are at the top. Ignitron tubes are to be installed beneath the metal shelf. An accessory panel for spot welding aluminum is mounted in the second row.

New Maintenance and Modification Features on G-E Three-phase Resistance Welding Control

The picture above shows the new G-E three-phase sectionalized control with hinged panels for each control process, permitting quick inspection and servicing. To you, this new G-E control means:

DEPENDABLE OPERATION

The new G-E three-phase resistance welding control provides lower maintenance because just one relay on the main panel operates each time the solenoid valve relay operates. All resistors, transformers, capacitors, and other components are conservatively rated for long life.

VERSATILE DESIGN

Circuit points are easy to reach. There is room in the cabinet for accessories or modifications when job requirements change. For example, if you are changing from welding $\frac{3}{32}$-inch to $\frac{1}{4}$-inch or thicker metal, you can get the added power simply by changing Size C ignitron tubes to Size D. A special kit is available containing the larger bus bars that can be quickly installed by your own service crew.

SERVICE FACILITIES NEAR YOU

Factory-trained G-E service engineers are on call 24 hours a day. There is one in your area ready to help you keep production going.

For more information on G-E three-phase welding control, fill out and send in the attached coupon today. General Electric Company, Schenectady, New York.

GENERAL ELECTRIC

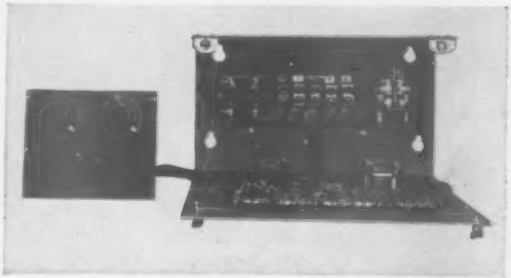

A SEAM-WELDING AUXILIARY PANEL, like other panels, is easily mounted in the cabinet because of keyhole mounting slots. Spade terminals are easily connected to the terminal boards on the main panel. Dials are mounted on front of cabinet.

General Electric Company
Section F 645-56
Schenectady, New York
Gentlemen:

Please send me bulletin GEC-491 on G-E three-phase welding control. I would like to have this for:

☐ **reference material** ☐ **an immediate project**

NAME .....

COMPANY .....

ADDRESS .....

.....

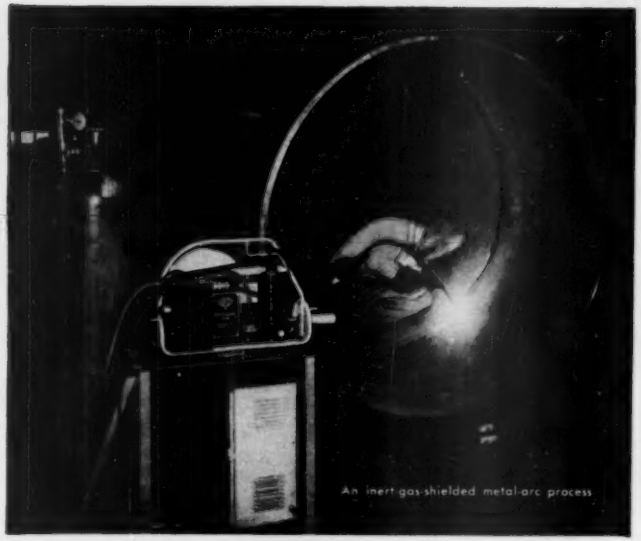

An inert-gas-shielded metal-arc process

AIRCOMATIC® WELDING

for hard-to-join metals

- Continuous high-rate deposition of filler metal
- Welds aluminum, bronze, nickel, stainless & carbon steels
- No flux required — no slag removal
- Minimum plate-edge preparation
- Heavy section welding with little or no preheat
- No "blind" welding — always a visible arc
- A semi-automatic operation with the versatility of all-position welding

AIRCO

PRESENTS THE LATEST

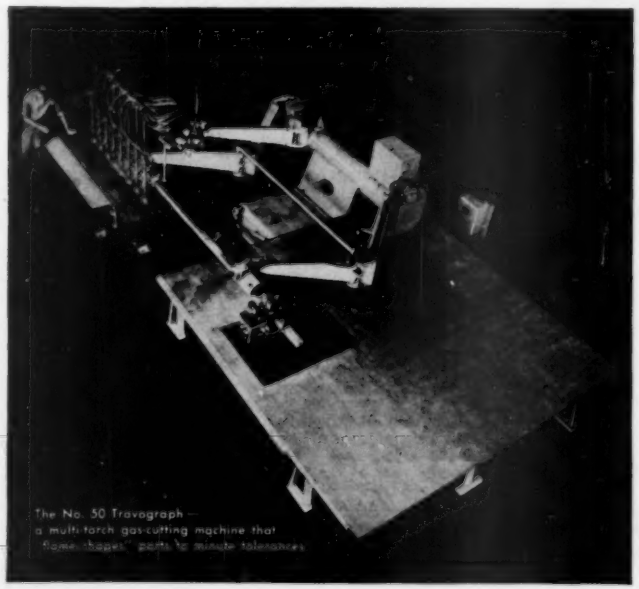

The No. 50 Travograph — a multi-torch gas-cutting machine that "flame-shapes" parts to minute tolerances

TRAVOGRAPH® CUTTING

for mass producing intricate shapes

- "Electronic bloodhound" tracing device accurately reproduces template or outline drawings
- Handles light plates, heavy slabs, billets or forgings
- Straight cutting, beveling or squaring
- All-welded construction for durability and precision
- Torch arm will support up to 8 cutting torches
- Precision shapes up to 102" x 144" — circles up to 12' in diameter — with one 16' set of rails. Cutting length extended with additional rail

at CONVENTION HALL
in PHILADELPHIA

Airco will bring you an "operators-eye-view" of the Aircomatic welding process . . . a continuous "live" demonstration of the #50 travograph. Here's a rare opportunity to view the latest in welding and cutting equipment! Movies . . . Exhibits . . . Welding Apparatus . . . Stationary and Portable Cutting Machines . . . Gas and Arc Welding Accessories.

IN WELDING AND CUTTING!

SEE 'EM IN ACTION!
THE
NATIONAL METALS
CONVENTION
OCT. 20-24
BOOTH 1623

AIRCO
DEALERS
AND OFFICES IN
MANY PRINCIPAL CITIES

AIR REDUCTION
AIR REDUCTION SALES COMPANY • AIR REDUCTION MAGNOLIA COMPANY • AIR REDUCTION PACIFIC COMPANY
REPRESENTED INTERNATIONALLY BY AIRCO COMPANY INTERNATIONAL
DIVISIONS OF AIR REDUCTION COMPANY, INCORPORATED
at the frontiers of progress you'll find

PERSONNEL

John R. Morrill Joins Gibson Welding Supplies

John R. Morrill has just become a partner and general manager of Gibson Welding Supplies and Inland Oxy-Acetylene Co., Inc., in Spokane, Wash., according to Vern B. Finch, President.

John Morrill was for 11 years a sales executive of The Lincoln Electric Co., Cleveland, Ohio, and for the past two years has been vice-president of the Baker Raulang Co., Cleveland, manufacturers of industrial fork-lift trucks.

Gibson Welding Supplies is the largest supplier of welding equipment in the Northwest Inland Empire, and Inland Oxy-Acetylene Co., Inc., manufactures oxygen and acetylene which is distributed by Gibson.

Norman A. Fletcher

Norman A. Fletcher, author of the paper "Arc-Welded Machine Jigs" which won second prize in this year's A. F. Davis Undergraduate Welding Award Contest, was born in Birmingham, England, on June 19, 1924. He served in the Royal Air Force as a bomber pilot from September 1942 to September 1946, and saw active service in the Burma Theater.

Mr. Fletcher came to the United States in September 1947. He enrolled at the University of Wisconsin and was graduated in June 1952 with the degree of BS (ME). While at Wisconsin, he was elected to Phi Eta Sigma, Pi Tau Sigma and Tau Beta Pi honor societies. He was

awarded sophomore and senior honors, and a share of the fourth prize of the James F. Lincoln Undergraduate Award and Scholarship program in 1951.

Mr. Fletcher's practical experience includes serving progressively as toolmaking apprentice, machinist, toolmaker, tool designer and production manager. He is now Production Manager and Tool Engineer at Kupfer Products, Inc., Madison, Wis.

Obituary

Hugh J. Fraser

Hugh J. Fraser, Vice-President in General Charge of All Plant Operations in the United States of The International Nickel Co., Inc., died at St. Mary's Hospital, Montreal, Que., Canada, Friday, August 22nd, after a brief illness, in his 55th year. He resided at 45 Woodbine Ave., Larchmont, N. Y.

Born in Brockville, Ont., the son of Oliver K. and Margaret A. Fraser, he attended Queen's University at Kingston, Ont., graduating in 1923 with a Bachelor of Science degree.

Mr. Fraser joined the Huntington (West Virginia) Works of The International Nickel Co., Inc., in May 1923, serving in various technical and operating capacities before being promoted to the Company's New York Office in February 1935, as Assistant Manager of the Production Department. He was elected Vice-President in March 1947, and in the following June was made Vice-President in General Charge of All Plant Operations in the United States of International Nickel. He was also an Assistant Vice-President of the parent organization, The International Nickel Company of Canada, Limited, since June 1943.

Mr. Fraser was a member of the Canadian Institute of Mining and Metallurgy, American Institute of Mining and Metallurgical Engineers, American Society for Metals, the Mining and Metallurgical Society of America and The Canadian Society of New York. He was also a member of the City Midday Club, New York, The Mining Club, New York and the Larchmont Yacht Club, Larchmont, N. Y.

Surviving are his widow, the former A. Muriel Dunne, formerly of Ottawa, Ont.; two daughters, Joan and Dorcas, and two brothers, O. B. J. Fraser, of Westfield, N. J., and C. E. Fraser, of Toronto, Ont.

A Solemn High Requiem Mass was celebrated for Mr. Fraser at St. Ignatius Loyola Church in Montreal on Monday morning, August 25th, with interment at Brockville, Ont.

WAGNER
ELECTRODE HOLDERS

The perfect teammate for WAGNER GROUND CLAMPS

RESIST ARC HEAT
Copperhead Tip Insulation operate near 6,000° heat.

COOLER
Patented channel construction flushes heat radiation twice as fast.

FULL CURRENT DELIVERED
Wagnerloy Construction results in high conductivity, longer service.

WAGNER MFG. CO.
350 W. 1st SOUTH ST.
JACKSON, MISSOURI
Weld with Wagner

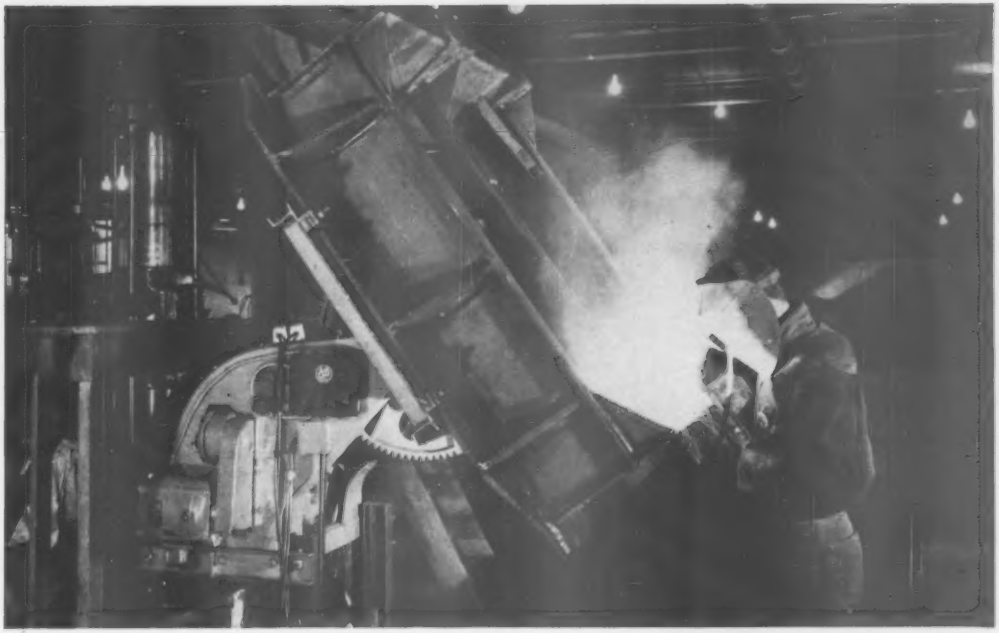

WORTHINGTON WELDING POSITIONER ELIMINATES time-wasting handling of the work-piece . . . increases arc-time by tilting the work into position for continuous, economical downhand welding. Capacities from 100 lbs to 30 tons. Also: Turning Rolls from 3 to 150 tons, stationary and self-propelled.

A way to get more and better welding from your welders

Every minute your welders spend climbing, turning and propping is *lost* welding time.

Turn this waste time into *all arc-time* with Worthington Welding Positioners that tilt or turn all welds into position—*without delay*—for *continuous* downhand automatic or manual welding. Today's labor scarcity makes this increased production more important than ever.

These Positioners lower costs and boost production up to 50%. Downhand welding is *quicker* (only one pass instead of two or three) . . . *better* (deeper penetration with higher current, heavier electrodes, faster deposition of weld metal) . . . *neater* (weld metal levels itself). There's less rod waste, too.

Where can you see a Worthington Welding Positioner at work near you? Just write Worthington Corporation, Plainfield, N. J., for this information or for Bulletin 210D.

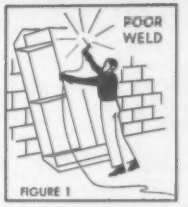

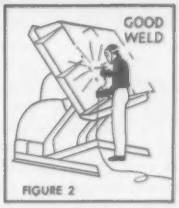

HOW WORTHINGTON WELDING POSITIONERS PRODUCE BETTER WELDS

When the welder has to climb over, prop or flop the work-piece, he may only be able to use downhand welding over a limited area (Figure 1). With a Worthington Welding Positioner, the work is continually tilted or rotated automatically into position for downhand welding (Figure 2).

WORTHINGTON'S UNIVERSAL TABLE TOP makes the Welding Positioner as profitable on job work as mass production. Those "T" slots make the table adaptable to any shape of work-piece and a wide range of sizes. No special jigs or fixtures needed.

Y.2.3

WORTHINGTON

Welding Positioners
Turning Rolls

abstracts of CURRENT WELDING PATENTS

prepared by V. L. Oldham

Printed copies of patents may be obtained for 25¢ from the Commissioner of Patents, Washington 25, D. C.

2,604,936—Method and Apparatus for Controlling the Generation and Application of Heat—William L. Kachni and Frank J. Kachni, Cleveland, Ohio, assignors to Metal Carbides Corp., Youngstown, Ohio, a corporation of Ohio.

This patent relates to controlled heating action and relates to a method comprising the formation of a flame and creating and maintaining a unidirectional electrostatic field between the flame and an adjacent object to be heated. The electrostatic field has a potential gradient in excess of about 1500 v per inch and the flame is utilized as the positive electrode of the electrostatic field.

2,605,376—Welding Transformer—Artur Schuttler, Solingen-Ohligs, Germany, assignor to "Kronprinz" Aktiengesellschaft für Metallindustrie, Solingen-Ohlings, Germany.

The patented transformer is rotatable and comprises an iron core, a primary on the core and a secondary enclosing the primary and part of the core. The secondary has a hollow body open at one end for introducing the core and primary into the hollow body and the core is journaled within the hollow body. Two disks are connected to the core shaft and to a journal therefor, respectively, the disks acting as welding electrodes.

2,605, 379—Automatic Thermal Metal-Joining Tool—Herbert Couchman McKay Eustis, Fla., assignor to Warren Dunham Foster, Eustis, Fla., and himself, as trustees.

McKay's patent is on a hand metal-joining tool which includes a barrel with a base on one end thereof and a first electrode is partially housed within the barrel and movable along its axis to project without the barrel. A second electrode is fixed adjacent another end of the barrel and is disposed to cooperate with a clamp associated with the barrel. Such clamp may position a workpiece. An actuating member is carried by the base and an operating connection extends within the barrel between the actuating member and the movable electrode to move it by movement of the actuating member. Circuit means connect the first and second electrodes.

2,605,448—Electric Welding Control With Phase Shift—Stuart C. Rockafellow, Farmington, Mich., assignor to Robotron Corp.

This patent is on an electronic control circuit including a pair of electric discharge devices used for controlling current conduction. A phase shift circuit also is provided in the control while a pair of ignitron electric discharge devices are present and are connected in back-to-back relationship. The circuit arrangement is such that the conduction and nonconduction of the ignitrons is controlled by a timing circuit provided and the precise point on the wave form at which conduction by the ignitrons is started is determined by the phase shift circuit.

2,605,537—Machine for Forming and Welding Parts—Albert F. Pityo, Clifton, and Harry E. Butterfield, Jr., Maplewood, N. J.

This patent is on a welding machine wherein a turret is mounted upon a support structure and carries devices for holding stems with wires theron. The turret is provided with indexing movement, and means are provided for supporting U-shaped elements adjacent the wire of the stem at one position thereof. Additional means press against the wire and weld it to an arm of the U-shaped element.

2,605,732—Tube Welding Machine—James L. Anderson, Closter N. J., assignor to Air Reduction Co., Inc. a corporation of New York.

This patent discloses a machine for welding the longitudinal seams of tubes. The machine includes a carriage movable along a support and a pair of welding devices are mounted on the carriage for welding the seam of a tube during movement of the carriage. Means are provided on the carriage for moving it along the support and to drive a drive shaft extending from the carriage for supplying motive power to move the carriage on a similar machine.

2,606,067—Acetylene Welding Reel—Leon S. Roark, Shreveport, La., assignor of one-third to Dawson M. Hawkins and one-third to Curtis Kinard, both of El Dorado, Ark.

A specialized welding hose reel is shown in and covered by this patent.

2,606,132—Copper Brazing Compositions—Louis G. Klinker, Griffith, Ind., assignor to The Glidden Co., Cleveland, Ohio, a corporation of Ohio.

Klinker's composition is adapted for use as a brazing paste in furnace-brazing and similar operations. The composition includes a major quantity of cupreous material and a minor quantity of ferruginous material. The total available metallic iron content of the ferruginous material amounts to between about 0.5 and 12% of the total available metallic copper content of the cupreous material. A minor quantity of a noncorrosive, nonmetallic, thermally evanescent plasticity-imparting carrier is mixed with the other materials to make a paste.

2,606,267—Gas Blanketed Metal Arc Welding—Thomas McElrath, Jr., Chatham, N. J., assignor, by mesne assignments, to Union Carbide and Carbon Corp., a corporation of New York.

This patent relates to a gas-blanketed metal arc welding process wherein a high density current is passed between the work and a fusible metal wire at a contact point on the wire spaced from its tip to maintain an arc between the tip and the work. An annular stream containing essentially inert gas is passed along the wire and through an annular nozzle between the contact point and the tip to blanket the arc and molten portions of the wire and the work. During the welding operation, a longitudinal thrust is applied to the wire. Certain specified limits for gas flow in relation to the welding current and rate of feed for the wire are set forth in the patent.

2,606,268—Method of Forming and Welding Pins to Metal Parts—Albert F. Pityo, Clifton, and Harry Butterfield, Maplewood, N. J.

This patent discloses a method of welding in succession substantially radially directed pins to the sides of a metal tube and it includes supporting the metal tube and turning it intermittently upon its longitudinal axis and thereby providing rest periods for the tube. A wire is supported substantially radially with respect to the tube and is moved toward the tube when the tube is at rest. A welding current is applied to the wire to weld it to the

Now You Can Weld Easier and Faster

THESE 5 G-E FEATURES TO HELP YOU

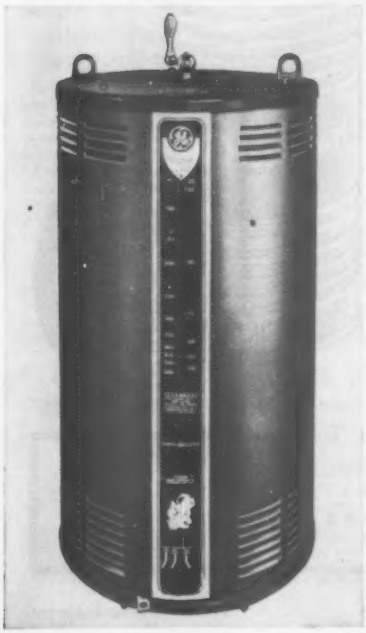

Generous overtravel makes accurate current settings easy.

1. **SMOOTH, FAST WELDS** are simple to make with the steady arc because arc-stabilizing capacitors eliminate popouts.
2. **ACCURATE CURRENT SETTINGS** are easy to make, especially in the low current range.
3. **OPERATING COST IS REDUCED** because less power is used when idling.
4. **INSTANT STARTING** without scratching saves operator's time. The hotstart automatically provides the right amount of starting boost for every setting.
5. **LONG COIL LIFE** is assured with Class H silicone insulation, exclusive with G.E.

TO GET YOUR SHARE of these big welding benefits, call or see your nearest authorized G-E welding distributor! His name is listed in the yellow pages of your telephone directory. Look for General Electric under "Welding Equipment."

Section J711-24, General Electric Company, Schenectady 5, N. Y.

Please send me immediately information on a typical G-E a-c welder, GEC-750.

Name .....

Company .....

Address .....

City ..... **State** .....

GENERAL ELECTRIC

tube and then the wire is severed at a point spaced radially from the tube.

2,606,754—Gas Torch Machine for Cutting Structural Shapes—Joseph M. Tyrner, New York, N. Y., assignor to Air Reduction Co., Inc., a corporation of New York.

Tyrner's patent is on a cutting machine that has a bed for supporting a workpiece and a ram movable horizontally toward and away from the workpiece. A platform on which the ram is movably supported is provided and the ram supports a carriage vertically movable with respect thereto. A cutting torch is carried by the ram and a cutting torch is on the carriage. A probe is carried by the ram for contacting a workpiece and is movable with respect to the ram. Special drive and control means are present and are actuated in response to the degree of movement of the probe on the ram and connected to the drive means of the ram and carriage for moving them independently upon the degrees of movement of the probe.

2,606,988—Arc Welding Electrode Holder—John F. Dove, Lombard, Ill., assignor to National Cylinder Gas Co., Chicago, Ill., a corporation of Delaware.

This patent is on an arc-welding electrode holder wherein a shielding gas is supplied to envelop the arc. The holder includes a metallic body portion having a bore for receiving an electrode therethrough and spaced therefrom to provide an annular gas passageway therebetween. Clamp means, including a collet, is positioned within the body portion and is adapted to position the electrode therein. Other means supply the shielding gas and welding current to the electrode holder.

2,607,310—Welding Fixture—Llewellyn W. Evans, Rivera, Calif., assignor to Rheem Manufacturing Co., Richmond, Calif., a corporation of California.

The patented welding fixture holds a cylindrical hollow element having a longitudinal open seam which is to have a weld formed therealong. A plurality of levers with fingers thereon are provided for being brought into engagement with the elements positioned on the fixture to urge adjacent areas of the element bordering the seam to move relative to each other.

2,607,404—Welding Burner with Detachable Tip—Johan August Osterlind, Malmo, Sweden.

This patent relates to a welding burner which has a tip positioned thereon by special means so that a rapid and easy exchange of the tip can be made without unscrewing a retainer nut from the end of the burner handle.

TWECO TERMINAL CONNECTORS
for Welding Machines

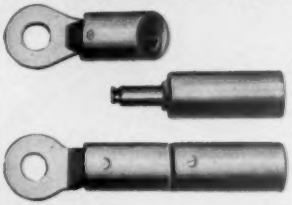

Bolt directly to positive and negative welder studs. Provide easy cable switch to reverse polarity. Simple cable disconnect for quick "Jump-In" of additional cable.
3 Sizes for cables #5 through 4/0

The male plug of TWECO "Sol-Con" and "Mec-Con" Cable Connectors connect with TWECO Terminal Connectors: Sol-Con and Mec-Con Cable Connectors are COMPANION ITEMS.

Write for Tweconey #8 giving data and prices on the complete TWECO line of electrode holders, ground clamps and cable connections for electric welding.

See Your Welding Supply Distributor

Tweco PRODUCTS COMPANY

TWECO PRODUCTS

Boston at Mosley, WICHITA, KANSAS

National Carbide

IN THE RED DRUM

EFFICIENT

ECONOMICAL

DEPENDABLE

FOR WELDING and CUTTING

Use National Carbide in the Red Drum

Write us for information as to nearest available stock.

60 E. 42nd St. NATIONAL CARBIDE COMPANY New York 17, N.Y.

A Division of Air Reduction Co., Inc.

stop CAST IRON brazing & welding failures . . . minimize stress, distortion, warpage with

Low Temperature **EUTECTIC** WELDING ALLOYS

Impossible? That's what the "Steelbilt Company" thought, too, until they actually tried these new entirely different EUTECTIC Low Temperature. WELDING ALLOYS.® Then they came up with the astounding "Case History" shown on the left.

Yes, we not only *claim* this amazing performance — we *prove* that "EUTECTIC" is different . . . *prove* that these new alloys solve metal-joining problems where conventional materials fail!

Let us prove it in YOUR shop, just as we have in over 78,000 other plants and shops throughout America. There's no cost, no obligation involved. Just fill in and mail the coupon, below, for a FREE Consultation-Demonstration from one of our 350 trained District Engineers who stand ready to serve you from coast to coast. **Prove to yourself that there is something new and different in metal-joining . . .**

"IMPOSSIBLE" REPAIR AVOIDS TWO YEAR SHUT-DOWN

"The folding press shown in the photos had been in service a great many years and during that time, cracked one leg of the side frame. Temporary repairs were unsuccessful and cracking of two other legs occurred, making the machine unusable.

After various welding companies had decided against repairing this machine by any welding method, we called for a EUTECTIC Consultation and were told that the repair could be made with EutecTrode 24, your special electrode for welding cast iron "cold".

As recommended, we supported the weld repair by boxing in the complete side frame with steel plate and attaching the closely fitted plate to the frame with fitted bolts. The repair made in this manner was *completely successful* and the machine now operates as efficiently as a new unit.

An idea of the enormous savings we realized by using your unique welding alloys can be had when we tell you that quoted delivery on a new machine was at least two years!"

—Steelbilt Co.*

*Full name and address on request.

FREE

75-PAGE BOOK
"Manual of Welding Design and Engineering" with 50 new photos, 60 new drawings. Send for YOUR free copy TODAY.

MAIL THIS COUPON TODAY

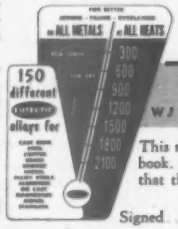

EUTECTIC WELDING ALLOYS CORPORATION
172nd St. & Northern Boulevard
Flushing 58, New York, N. Y.

W J 7

This new manual of yours sounds like a very helpful book. Send me a FREE copy with the understanding that there will be no cost or obligation now or later.

Signed .....

Firm .....

Address ..... Zone .....

City ..... State .....

EUTECTIC WELDING ALLOYS CORPORATION
172nd St. and Northern Boulevard., Flushing 58, New York, N. Y.

AMERICA'S LEADING INSTITUTION DEVOTED TO THE RESEARCH AND MANUFACTURE OF SPECIALIZED METAL-JOINING ALLOYS

LOS ANGELES, CAL. · SAN FRANCISCO, CAL. · CHICAGO, ILL. · MINNEAPOLIS, MINN. · INDIANAPOLIS, IND. · BOSTON, MASS. · BALTIMORE, MD. · DETROIT, MICH. · ST. LOUIS, MO. · OMAHA, NEBR. · CINCINNATI, OHIO · CLEVELAND, OHIO · PHILADELPHIA, PA. · DALLAS, TEXAS · PORTLAND, OREGON · PITTSBURGH, PA. · HOUSTON, TEXAS · MILWAUKEE, WISC.

NEW LITERATURE

Welding and Cutting Units

Victor Equipment Co., 844 Folsom St., San Francisco, Calif., announces a new bulletin, No. 330, containing Victor welding and cutting units. This small, compact and very complete bulletin illustrates and describes Victor Units for flame cutting, heating and welding. For your copy of Bulletin 330, write directly to the company at the above address.

Hard-Facing Alloys

The Wall Colmonoy Corp. announces the availability of their new Catalog No. 77 covering the various hard-facing alloys which the company manufactures. Copies of this catalog may be obtained, free of charge, by writing to Wall Colmonoy Corp., 19345 John R St., Detroit 3, Mich.

Electrode Bulletin

A new, 49-page, pocket-size booklet describing the application, chemical analysis and mechanical properties of General Electric welding electrodes has been announced as available from G-E Welding Distributors.

Designated GED-1634, the new booklet also includes an electrode trouble-shooting chart, a chart which specifies the number of electrodes per pound, and an explanation of the significance of the AWS nomenclature.

AWS Standard on Recommended Practices for Metallizing

One of the newer means for protecting against corrosive atmospheres and sea water is the application of a thin layer of zinc or aluminum by metallizing.

How these metals are best applied, and how much of which metal to use for different conditions is the subject of the latest American Welding Society standard—Recommended Practices for Metallizing: Part IB—Application of Zinc and Aluminum for Protection of Iron and Steel.

The booklet covers in detail the materials and equipment to be used; techniques of blasting and spraying; and inspection procedures for verifying the adequacy of the coating. Also covered is the use of organic coatings as an additional protective measure. The last section of the standard gives typical coatings for various exposures including general atmospheres; salt atmospheres; industrial atmospheres; and fresh and sea water.

This is the first national publication on the subject. The recommendations are based on studies conducted in setting up a test program of actual exposure of specimens under different corrosive exposures.

Copies are available at 50 cents each from the American Welding Society, 33 W. 39th St., New York 18, N. Y.

PFI Standard on Machined Backing Rings for Butt Welds

The Pipe Fabrication Institute announces publication of a standards bulletin having the title *End Preparation and Internal Machining for Machined Backing Rings for Butt Welds*. This is designated as Standard ESI-1952 and supersedes the first standards bulletin issued by the Institute almost four years ago. This revised standard meets present-day high-pressure and high-temperature piping requirements; it includes design changes that minimize the amount of weld metal required and the resultant shrinkage stresses in the weld.

The Engineering and Standards Committee of the Pipe Fabrication Institute has prepared five other Standards of interest to designers, contractors and users of pressure piping. They are: "Method of Dimensioning Welded Assemblies"... "Standard Practice, Shop Hydrostatic Testing of Fabricated Piping"... "Standard Practice Cleaning Fabricated Piping"... and "Built-up Weld Metal Bosses."

Copies of any or all of the PFI Standards are available on request without cost to those concerned with piping. Write to The Pipe Fabrication Institute, 811 Clark Building, Pittsburgh 22, Pa.

Republic Titanium and Titanium Alloys

Republic Steel Corp. has announced that it is producing titanium and titanium alloys at its Canton and Massillon, Ohio, steel plants.

Titanium is only 56% as heavy as alloy steel, yet comparable in strength. This weight advantage, together with its corrosion resistance, makes it especially desirable for use in the aircraft and other industries where both strength and lightness of metals are desired.

Titanium, in many cases, equals or exceeds stainless steel in its ability to resist corrosion. Preliminary results with al-

Faster, Smoother —non-porous welds in all positions

Maybe some E-6010 electrodes are hard to handle. But not the Hobart "10". You'll find that this new and versatile all-position electrode gives you real welding ease—PLUS—deep penetration, high tensile strength and ductility, quick and easy slag removal, a stable arc, and non-porous welds.

The Hobart "10" is widely used in structural work, ship building, pipe line construction, etc. Its penetrating arc makes it ideal for welding galvanized plates.

Yes, the Hobart "10" is years ahead of any electrode you may be using. But don't take our word for it. Instead, write us today for complete information and free samples to try on your next job. You'll be glad you did.

Overhead weld in 3/8-in. plate welded with Hobart No. 10 electrodes.

Vertical fillet weld in 3/4-in. plate welded upward with Hobart No. 10.

Whatever the position . . . the Hobart "10" gives you better, faster welds at lower cost.

HOBART BROTHERS COMPANY
Box WJ-1022, Troy, Ohio
"One of the world's largest builders of arc welders"

Simplify all your welding by using HOBART ELECTRODES

Radiography checks—

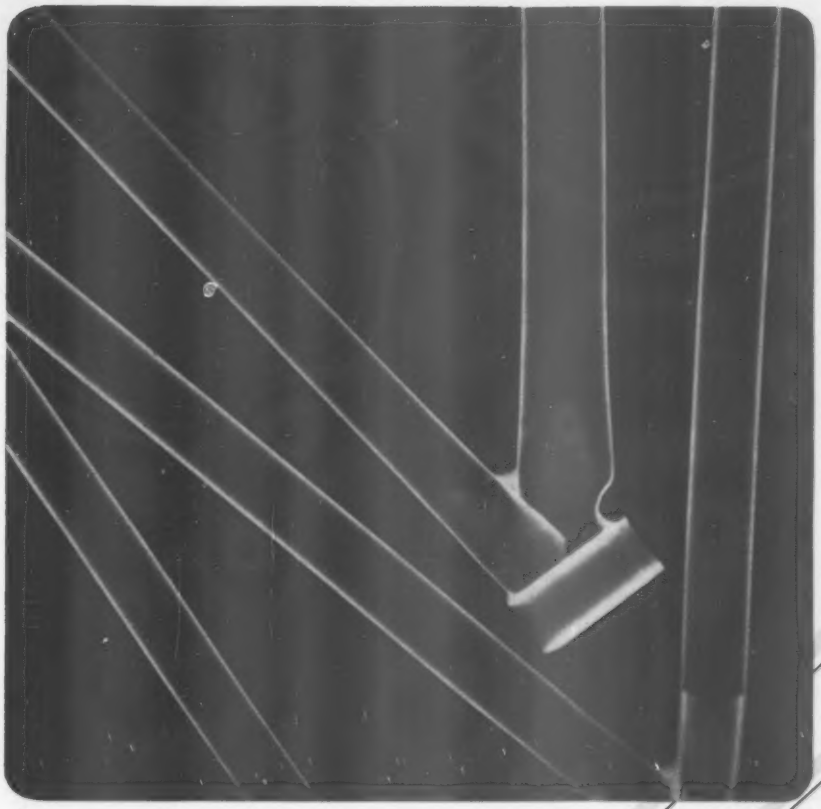

then double checks

LANDING GEAR STRUTS lead a life of punishment. Though light, they must be strong. Their joints must be sound. Radiography is the method used to prove them sound.

A maker of amphibian aircraft goes even further. Though treated and sealed, strut members can develop internal corrosion and become weakened. Radiography alone can provide the required nondestructive examination of these internal surfaces. So it has become routine to x-ray these struts as part of the periodic inspection of the planes.

This is but one example of how radiography is proving a boon to the welding process. It is helping to open new fields for the use of welding—especially in the fabrication of highly stressed products and assemblies.

Look into the ways Radiography can aid your business. Your x-ray dealer will be glad to give you full information and assistance.

EASTMAN KODAK COMPANY
X-ray Division, Rochester 4, N. Y.

Radiography—

another important function of photography

Kodak
TRADE-MARK

Now is the time to investigate the important services your nearby All-State Distributor offers.

1. ONE SOURCE OF SUPPLY

It makes sense to make your A-S Distributor and All-State your one proven source for all alloys and fluxes needed for welding, brazing, soldering, tinning and cutting.

2. BETTER JOBS FOR LESS

A-S Distributors stock a large variety of things you have to have quickly when you want them. They're competitive on price — usually lower if your eye is on the job costs. That comes of their handling All-State Alloys and Fluxes for all metals. They do better jobs for less.

3. TECHNICAL SERVICE

Each All-State Distributor has men especially qualified by training and experience to aid in the proper selection and use of alloys and fluxes for jobs where you might need help. Back of them, and always ready to pitch in on the problem jobs are the All-State regional men and the well-known All-State technical service facilities at White Plains, N. Y.

4. FREE LITERATURE

Ask for 32-page Buyers Guide to the complete line of All-State Alloys and Fluxes for welding, brazing, soldering, tinning and cutting.

A-S DISTRIBUTORS EVERYWHERE

All-State

ALL-STATE

WELDING ALLOYS CO., INC.
White Plains, N. Y.

loyed titanium indicate it has higher strength to weight ratios than any other commercial metal.

Republic said it has been supplying titanium and titanium alloys in ingot, sheet, plate, strip, bar and wire forms for the last two years for aircraft and other defense programs. Production is still limited and is under strict allocation by the government.

Republic revealed its work, on the new metal in a technical book, *Republic Titanium and Titanium Alloys*, now being distributed by its sales offices throughout the country. A copy of this book may also be obtained by writing to Republic Steel Corp., Republic Building, Cleveland 1, Ohio.

Alloy content of titanium alloys probably will not exceed 15%, with most high-strength grades running between 4 and 10%. Included among the alloys are iron, chromium, manganese, aluminum and many others.

Major production is confined to the commercially pure product, but Republic is doing considerable development work on the chromium-iron and manganese alloys. Other alloys can be modified to give variations in properties so that a fairly wide range of physical properties is possible.

All of the common machining operations may be performed on titanium. Commercially pure titanium can be spot welded, seam welded or inert gas welded to itself. Welding of alloy grades by conventional methods has not been too successful, but indications are that hot pressure or flash welding may prove satisfactory. Titanium has been successfully brazed to itself and to other metals.

In its book, Republic said, "While an excellent core of information on titanium has been established, the technology is dynamic. Additional information on fabrication, welding, heat treating, etc., becomes available each day which both supplements and modifies previous data."

"Aluminum Forming" Manual

Metalworking men will find a wealth of information on how to draw and form aluminum sheet, plate, tubing and pipe in *Aluminum Forming*, a new 148-page technical manual just published by Reynolds Metals Co., Louisville, Ky.

The manual points out that the most common mistake is the attempt to work and form aluminum by the identical techniques used for other metals. While similar techniques may be employed in some operations, others require special procedures. Then too, selecting the proper grade of aluminum to use for a specific application is of utmost importance.

It is recognized that readers will generally be familiar with methods and equipment for working the older metals. So the

See for yourself how *Arcair slashes costs for GOUGING and CUTTING**

Many times faster than chipping! Using only carbon arc and compressed air, can be used anywhere on any metal. Simple to operate. Cuts clean, removes defects with pinpoint precision. Now saving thousands of man hours, cutting operating costs for materials up to 80%, and solving many metal removal problems for progressive fabricators, foundries and other users.

The unique Arcair TORCH,* with its air control valve, self-aligning rotating jet and concentric cable is all the equipment needed—at just $87.50 complete.

Prove its saving in your own plant

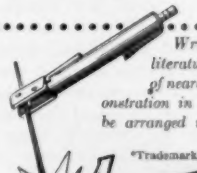

Write today for literature and name of nearest dealer. Demonstration in your plant can be arranged in most areas.

*Trademark

Arcair

2014 Burwell Street BREMERTON, WASH.

Alloy Rods Co.

LOOK FOR THE FLAMING ARC TRADEMARK

ALLOY RODS COMPANY

The Leading Manufacturer of Alloy Arc Welding Electrodes

PRESENTS

THE FIRST "INSIDE STORY" FILM

OF HOW ARC WELDING ELECTRODES ARE MADE

"No Finer Electrodes Made... Anywhere"

A 22-MINUTE SOUND MOTION PICTURE IN FULL COLOR

MADE INSIDE ALLOY RODS' YORK, PENNSYLVANIA PLANT

Never before to our knowledge, since arc welding became of age as a major fabricating tool for American industry in the early 1930's, has any electrode manufacturer permitted the public to see how coated arc welding electrodes are made. The manufacturing processes and procedures have always been carefully guarded trade secrets.

Now, for the first time, *Alloy Rods Company* has filmed its entire manufacturing process in the interests of better trade relations and technical understanding... from the cold drawing of hot rolled rod to the packaging of its finished electrodes in moisture-proof metal containers. You can now see how arc welding electrodes are made.

"No Finer Electrodes Made... Anywhere" is not a sales film or promotional tool. It is technical and instructional... shot on the production lines and in the laboratories ...to show those interested in better arc welding *why* we make electrodes this way. Prints of this film are available, without charge, to any reputable organization or institution.

WRITE, WIRE, OR TELEPHONE to Department M if you would like to use this film for any organizational or educational purpose. We will try to have a print available to fit your next open date.

ALLOY RODS
COMPANY
YORK PENNSYLVANIA

NO FINER ELECTRODES MADE... ANYWHERE

AR-12

WORLD PREMIERE At the Metal Show, Philadelphia, Pa., October 20-24, 1952
... showing every hour on the hour, Alloy Rods' Exhibit, Booth 448, Arena.

. . . an all-position phosphor-bronze electrode that's easy to handle

Phos-Trode is ideally suited for overlay work and for general maintenance and repair welding throughout industry.

In addition you get these 4 important advantages that keep welding costs down.

1. **All position** — Deposit solidifies rapidly — can be used for flat, vertical or overhead welding, operates on reverse polarity DC.

2. **Welds dissimilar metals**— cast iron, bronze, brass, copper, galvanized and malleable iron, etc. and combinations of same. This versatility keeps welding costs down and simplifies your electrode stocking problems.

3. **High deposition rate** — Low spatter loss permits high welding currents for faster welding and lower costs.

4. **Sound deposits, high physicals** — Special ingredients in Phos-Trode coating give properly deoxidized deposits, sound welds and correct bead contour.

Phos-Trode, the most versatile electrode in the phosphor-bronze field, is available in 6 sizes from 3/32" to 1/4". Order your supply now and take advantage of Phos-Trode's 4-way savings.

W-110

AMPCO

AMPCO METAL, INC.

MILWAUKEE 46, WISCONSIN

West Coast Plant: Burbank, California

It's Production-Wise to Ampco-ize!

book is devoted mainly to a detailed explanation of how to form aluminum as it differs from other metals. Thus two important sections are devoted to metallurgical data . . . one on aluminum sheet and plate; the other on aluminum tubing and pipe.

The manual will be sent without charge to engineers, designers, plant personnel and others who request it on company letterhead. Address all requests to Reynolds Metals Co., 2500 S. Third St., Louisville 1, Ky.

Explosive Gas Detector, Indicators and Alarms

Four types of combustible gas protective instruments are cataloged in a new folder, Form FSE1251. Included are:

1. Portable Indicator—a light, convenient unit into which suspected vapor is drawn by means of an aspirator bulb and long probe. Explosive level is read directly from an indicating meter.

2. A Portable Audible Alarm which is used to maintain a continuous guard against the appearance of combustible gas at any field or factory location where welding or other flame or spark-producing activity is carried on. Storage-battery operated, the unit contains its own 115-v charger.

3 and 4. Combustible Gas Alarm for fixed locations. Two types of units with similar operating characteristics but different physical arrangements are designed to guard against the appearance of explosive mixtures in specific areas. Both operate from 115-v lines and display indicator lights to reveal the presence of gas. One type has explosionproof construction to permit mounting directly in the hazardous area—the other is designed for mounting the sensing unit at the hazardous location and locating the controls remotely.

Folder illustrates the various models; describes their style and principles of operation; lists accessories and spare parts; shows typical users and applications; tabulates specifications for the four models. Prices are included. Johnson-Williams, Ltd., 2732 Third St., Palo Alto, Calif.

Ladders

There is no bad luck about ladders if you observe ladder safety, says the September 1952 issue of the *California Safety News*, revealing in an article that nine workers were killed and almost 4000 disabled by ladder accidents in California industry alone last year. The number of home ladder accidents is undoubtedly even greater.

Ladder accidents usually spring from two causes, the article points out: the use of unsafe ladders, and the unsafe use of safe ladders. It describes the three com-

Weldwire Company, Inc.

WIRE FOR WELDING

Weldspool Electrode Wire

FOR INERT GAS WELDING
(Chemically processed-precision wound)

For "QUALITY CONTROLLED" Welds on:

ALUMINUM
STAINLESS STEELS
ALLOY STEELS
BRONZES
CAST IRON or
SPECIAL ALLOYS

USE "WELDSPOOL" ELECTRODE WIRE or "WELDBEST" ELECTRODES

Weldbest Electrodes

FOR MANUAL ARC WELDING

Technical Literature available upon request

You are invited to visit us at The National Metal Exposition Booth #1383

WELDWIRE COMPANY, INC.

N. W. Cor. Emerald & Hagert Sts.

Philadelphia 25, Pa.

PHONE: Garfield 3-1232

BURDOX

made by WELDING *men for* WELDING *men*

When you need safety equipment for welding or cutting work, you'll do far better with BURDOX—both in performance and value. BURDOX has developed its line of safety equipment out of its long experience in the welding field so that each product is best for its purpose. There are no unnecessary extras—every feature is designed for greater comfort, protection and performance! Whatever your requirements in the welding field are—torches or regulators, lenses or helmets—you can depend on BURDOX for the best. Write today for FREE catalog.

Branches
AKRON
MANSFIELD
COLUMBUS

Branches
CINCINNATI
YOUNGSTOWN

THE BURDETT OXYGEN COMPANY

General Offices
3333 LAKESIDE AVENUE
CLEVELAND 14, OHIO

Plants
CLEVELAND & DAYTON, OHIO
LOS ANGELES, CALIFORNIA

THE BURDOX LINE INCLUDES • WELDING AND CUTTING EQUIPMENT AND MACHINES • SOLDERING AND BRAZING OUTFITS • REGULATORS AND GAUGES • INDUSTRIAL GASES • HOSE AND CABLE • ACETYLENE GENERATORS • GOGGLES AND HELMETS • LENSES AND FACE SHIELDS • RODS AND FLUXES • CYLINDER TRUCKS

SPEAKING OF LABELS . . .

HERE'S ONE THAT SHOULD GET EVERY WELDOR'S VOTE!

No matter how you cast your ballot in November, you're sure to pick a winner when you vote for Rexarc. Weldors coast to coast declare these electrodes "Outstanding."

They like their fast build-up, long wearing quality and best of all, the ease with which they are applied. Get on the Rexarc "band wagon"—ask your Distributor for a demonstration!

REXARC IS A PRODUCT OF

THE SIGHT FEED GENERATOR COMPANY

West Alexandria, Ohio, U.S.A.

Manufacturers of Welding Equipment For More Than 25 Years

mon-sense precautions which, if observed, would put an end to virtually all ladder accidents and injuries.

It stresses the need for selecting the right ladder for the job—not using a light household ladder for heavy construction work, for instance; for checking the ladder for missing, broken or otherwise defective rungs, among other things; and for observing the rules it lists for safe use of ladders.

Copies of the article in brochure form are available without charge from the Division of Industrial Safety, 965 Mission St., San Francisco 3, or 357 South Hill St., Los Angeles 13.

Magnesium Finishing

Magnesium Finishing, a new revision of the manual on finishing systems for magnesium products, is available from the Magnesium Department, The Dow Chemical Co., Midland, Mich.

The 128-page manual describes in detail surface stability and surface treatment, including cleaning, mechanical finishing, chemical treatments, electroplating, painting, and assembly protection for magnesium alloy die castings, sand and permanent mold castings and sheet, plate and extrusions.

Rebuilding and Repairing of Crushers

The Stulz-Sickles Co., 134 Lafayette St., Newark 5, N. J., has just released for distribution a folder intended to show how to save time and money by rebuilding and repairing various types of crushers with Manganal, 11–13¼% manganese-nickel steel. The folder is available upon request from Stulz-Sickles Co.

Chemalloy Welding or Soldering Metal

Chemalloy Associates of Santee, Calif., announces the availability of a two-page brochure entitled "Information on Chemalloy Welding or Soldering Metal." According to this company, the Chemalloy development simplifies the soldering or welding of any aluminum or zinc-base metal including aluminum or galvanized coatings. For additional information and photographs wire to Chemalloy Associates, Gillespie Airport, Santee, Calif.

Isotope Newsletter

The Aug. 19, 1952, issue of Isotope Newsletter is devoted to the use of isotopes in the oil industry.

It describes among other things how tanks, new or old, full or empty, are

HOBART 12 electrode (E-6012)

...for use in any position with AC or DC current

What ONE electrode can handle 80% of all your production work? What ONE electrode is today's best buy for all-purpose welding? The answer to both questions is the same—the Hobart "12". It's truly a premium electrode in both quality and performance—yet actually costs you less than any other E-6012 electrode because it gives you more actual weld deposit, increased production, less clean-up time.

YOU CAN STANDARDIZE on Hobart "12"—many of the country's largest fabricators of tanks, automobile frames, agricultural implements, etc., already have. They tell us that the Hobart "12" is the most versatile electrode they have ever used. They tell us, too, that the Hobart "12" goes further—leaves more actual weld deposit per electrode because there's less spatter and less stub loss, even when higher than normal welding currents are used.

You've tried the rest . . . now try the best. Write us today for complete electrode catalog and free samples of the Hobart "12" to try on your next job. You'll be glad you did.

HOBART BROTHERS COMPANY

Box WJ-1021, Troy, Ohio

"One of the world's largest builders of arc welders"

Simplify all your welding by using HOBART ELECTRODES

for the rare gases

argon or helium where accurate flow control is essential

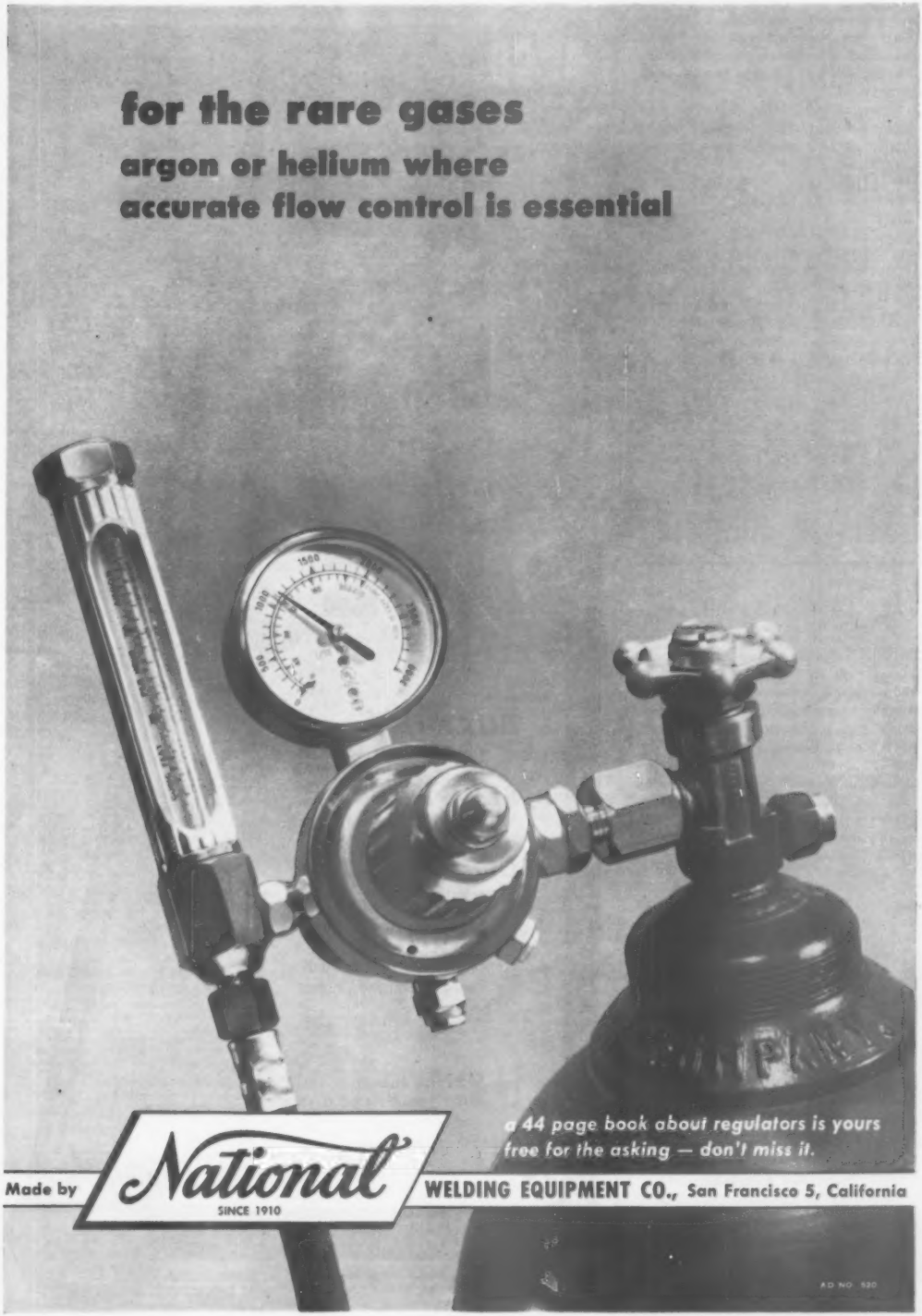

a 44 page book about regulators is yours free for the asking — don't miss it.

Made by National SINCE 1910 WELDING EQUIPMENT CO., San Francisco 5, California

AD NO. 520

tested, inspected and measured. Also, it points out the important role being played by isotopes in che king the quality of welds in oil tank and pipe-line construction.

Copies of Isotope Newsletter may be obtained by writing to Isotope Products Limited, Box 127, Oakville, Ont., Canada.

Welding with Stainless Steel Electrodes

This is a 32-page booklet with heavy paper, covering welding of practically all types of stainless steels. Price $0.25. Published by The Lincoln Electric Co., Cleveland 17, Ohio. It contains reprints of material from the *Procedure Handbook of Arc Welding Design and Practice*, and was published so as to make this information more generally available.

Employment Service Bulletin

Positions Vacant

V-277. Technical Sales Representative for welding equipment and accessory field. Young man 25 to 30 years with some knowledge of metallurgy and welding. After intensive training, to address salesmen's groups and local sections of the AWS on prebeating, postheating, etc. Straight salary and all traveling expenses and a chance to move ahead with growing firm. Give complete résumé of education, specialized training, and business experience in first letter.

Welding Engineers: (1) GS-12, $7040 per annum and (2) GS-11, $5940 per annum. For development of welding and associated procedures, ferrous and nonferrous metals. Requirements include metallurgical training and experience in test procedures. Electrical Engineer: (1) GS-11, $5940 per annum. Requirements include experience in induction heating, instrumentation and electrical testing incidental to development of welding procedures. Welding and Electrical Laboratory, U. S. Naval Engineering Experiment Station, Annapolis, Md. In Baltimore contact: J. H. Siegel, 5150 Edmondson Ave., Wilkens 0428.

Services Available

A-630. Graduate B.S. in E.E.; 7 years' experience as welder, including 4 years' apprenticeship; 1½ years technical experience as Asst. Welding Research Engineer and Chief Inspector. Married. Age 29. Desires Eastern location.

an ACCO product
for Stainless Steel WELDING
AC-DC Electrodes
GAS Welding Rods
made by
PAGE
BURNING...
stable even at lower heats
SLAG...
clean, easily removed
COATING...
resists cracking down to very short stubs
SELECTION...
complete line for welding every type of stainless
Get in touch with your PAGE distributor
ACCO
PAGE STEEL AND WIRE DIVISION
AMERICAN CHAIN & CABLE
Monessen, Pa., Atlanta, Chicago, Denver, Detroit, Los Angeles, New York, Philadelphia, Portland, San Francisco, Bridgeport, Conn.
PAGE Welding Electrodes AND Rods

LINK WELDERS

Engineered . . . FOR HIGH WELDING Output!

LINK SINGLE POINT, AIR-OPERATED PEDESTAL TYPE WELDERS

Above: Model #WM-680 with 75 KVA Transformer, 220-440 volt primary per specifications; 6.6 minimum to 10. maximum secondary voltage. Also available with 70 KVA Transformer, 5.0 minimum to 7.1 maximum secondary voltage.

Also available; Model #WM-629 with 50 KVA Transformer capacity, 220-440 volt primary per specifications, 3.19 minimum to 5.8 maximum secondary voltage.

High speed production is a familiar result wherever Link Spot and Projection Welders are used. In addition, these machines have established outstanding records for safe, dependable performance.

Designed, engineered and built to JIC air and electrical standards, these units offer long life, smooth operation and versatility in application. Moderate in cost, economical in performance and maintenance, convenient in operation . . . these are but a few of the many reasons why a Link unit should be your choice in resistance welding equipment . . . whether your need is spot or projection welding machines.

Complete information available on these and other Link Standard Spot, Projection, Seam, Butt Welders and special welding machines.

Submit your welding problems to Link Welder. You will receive complete, competent recommendations without obligation to you.

LINK LIGHT, MEDIUM, HEAVY DUTY COMBINATION SPOT AND PROJECTION WELDERS

Below: Model #WM-725 Medium Duty Combustion Projection Welder with 150 KVA Transformer.

A broad selection of standard and specially designed Link Welders with Transformer capacities ranging from 70 to 500 KVA are available. Every machine is designed and built to meet the toughest requirement.

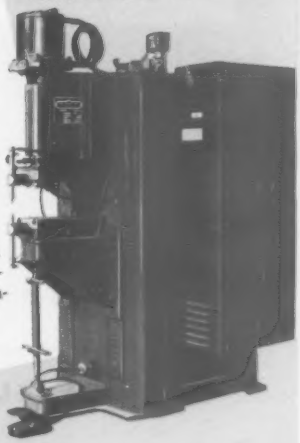

"THE STRONGEST IN YOUR PRODUCTION CHAIN"

LINK

"THE STRONGEST IN YOUR PRODUCTION CHAIN"

LINK WELDER CORPORATION

Designers and Manufacturers of High Production Welding Equipment

13684 WEST BUENA VISTA • DETROIT 27, MICHIGAN

the big '52 metal show

TRADE IN OLD IDEAS FOR NEW...

The most valuable asset of the Big Metal Show beyond its impelling hold on all metals industries people lies in its singular virtue of sparking new ideas and changing old concepts of all things concerning metals. Don't miss this Big Metal Show . . . it'll be jam-packed with stimulating, refreshing, different idea-changers.

OCTOBER 20-24

PHILADELPHIA, PA.

NATIONAL METAL EXPOSITION

NATIONAL METAL CONGRESS

Tempilstiks°

the amazing crayons that tell working temperatures from 113° to 2000° F.

in
welding
flame-cutting
tempering
forging
casting
molding
drawing
straightening
heat-treating
in general

$2 each

gives up to 2000 readings

It's this simple: Mark the workpiece with the proper Tempilstik° When the mark melts, the specified temperature has been reached.

Booth No. 135
National Metal Show
Philadelphia

113	200	288	375	650	1000	1350	1700
125	213	300	388	700	1050	1400	1750
138	225	313	400	750	1100	1450	1800
150	238	325	450	800	1150	1500	1850
163	250	338	500	850	1200	1550	1900
175	263	350	550	900	1250	1600	1950
188	275	363	600	950	1300	1650	2000

FREE SAMPLE PELLETS

Use this coupon. Specify temperatures of interest to you.

TEMPIL° CORP., 11 West 25th St., N. Y. 10, N. Y.

Please send free sample pellets in the following rating_____

Name_____

Company_____

Address_____

INDEX TO ADVERTISERS

Air Reduction . . . . . 962, 963, Outside back cover
Alloy Rods Company 973
All-State Welding Alloys Co., Inc. 972
Aluminum Company of America 999
The American Brass Co. . . . . Inside back cover
American Chain and Cable Co. 978
American Manganese Steel Division 991
Ampco Metal, Inc. 974
Anti-Borax Compound Co., Inc. 990
Arcair Company 972
Arcos Corporation 984, 985
AWS Spring Technical Meeting 989

The Burdett Oxygen Company 975

Dockson Corporation 960

Eastman Kodak Company 971
Erico Products, Inc. 1000
ESAB 994, 995
Eutectic Welding Alloys Corp. 969

Fansteel Metallurgical Corp. 988

General Electric 961, 967

Harnischfeger Corporation 957
Haynes Stellite Company, a Division of Union Carbide and Carbon Corporation 997
Hobart Brothers Company 875, 970, 976

The International Nickel Company, Inc. 880

The Lincoln Electric Company 993
Linde Air Products Company, A Division of Union Carbide and Carbon Corporation . . 878
Link Welder Corporation 979

P. R. Mallory & Co., Inc. 877
Metal & Thermit Corporation 876

National Cylinder Gas Company 986, 987
National Carbide Company 968
National Metals Show 980
National Welding Equipment Co. 977

Page Steel and Wire Division 978
Pennsylvania Optical Company 983

The Reid-Avery Company 1001
Robotron Corp. 956

The Sight Feed Generator Company 976
Square D Company 959
Stulz-Sickles Co. 992

Tempil° Corporation 981
Tweco Products Company 968

Union Carbide and Carbon Corporation
Haynes Stellite Company 997
Linde Air Products Company 878
United States Testing Company, Inc. 1002

Victor Equipment Company . . . . . Inside front cover

Wagner Manufacturing Co. 964
Weldwire Company, Inc. 974
Westinghouse Electric Corporation 990
J. H. Williams & Co. 990
Worthington Corporation 965

NEW PRODUCTS

Arc Welding Thin Material

The Synchro Electronic Corp., 1565 Railroad Ave., Bridgeport, Conn. is now producing a new type of arc-welding equipment (Fig. 1). They are placing this apparatus on the market and are equipped to do development work in their laboratories. The process has been specifically developed for arc welding all types of weldable material in sheet thicknesses below 0.020 in.

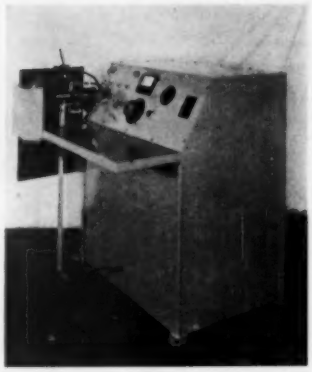

Fig. 1

In the past the difficulties met in welding thin materials with an arc have been to exactly control the amount of energy being utilized. The Synchro Electronic Corp., with its Energy Storage Arc-Welding System, has solved this problem.

The patented system, employing the energy storage principle, is a simple one. Energy is stored in a capacitor bank, then discharged into the arc. This process is repeated at a rate of 60 (or 120) times a second.

The energy stored in the capacitor bank can be uniformly varied from *any desired minimum* to *any desired maximum value*. The control is fully electronic and the uniformity of welding may be held to very close limits. Thus the *exactly correct* and *constantly maintained* energy in the arc which may be required for any given thin section can be easily obtained.

A wide variety of materials can be welded by this process. Among them are: ferrous materials and alloys including stainless steels; aluminum and aluminum alloys; nickel and nickel alloys including Ni-Span C; bimetals; copper, brasses, bronzes, beryllium copper and other alloys; precious metals.

Uniformly high-quality arc welds result from the precision control of all the factors entering into the production of an arc weld made on the Synchro Electronic Corp. units. The linear speed of welding and the length of the arc, for example, are unit adjustments which are not varied during the welding. The welding speed is motor controlled and the work is moved under the stationary welding electrode.

Welds are made at linear speeds ranging from 7 to 15 fpm depending upon gage and type of weld. No metal is added to the weld.

The above speeds are based on a half-way 60-cycle unit. The speed of welding can be increased by applying a full wave unit or increasing the frequency depending upon the speed desired.

Illustrative examples of the work done by this new process are shown in Fig. 2.

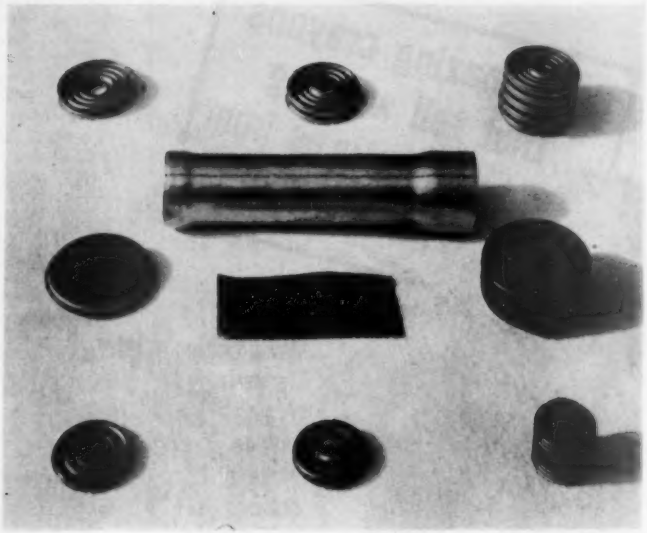

Figure 2

Top row (left to right): (1) Shows operation one; phosphor-bronze diaphragm pieces welded at inner hole junction. (2) Shows operation two; phosphor-bronze diaphragm pieces welded at outer edge. (3) Shows complete assembled phosphor-bronze bellows; phosphor-bronze all-welded bellows produced by combination welding inside and outer edge of diaphragm pieces.
Second row: Aluminum flashlight shell expanded after welding.
Third row (left to right): (1) Ni-Span-C diaphragm. (2) Longitudinal weld on pure nickel. (3) Brass head in phosphor-bronze automobile thermostat bellows.
Bottom row (left to right): (1) Beryllium copper diaphragm as it left the welder. (2) Same as No. 1, tested to 441 psi at which point soldered fittings blew off. (3) Brass head welded in brass thermostat bellows.

Portable X-ray Units

The rapid development in welding technique, particularly in shipbuilding, structural engineering and pressure vessel manufacture, involves a steadily increasing need for reliable and conveniently portable X-ray units for radiographic examination of welds in finished structures.

To meet this demand a prominent European manufacturer of X-ray equipment, Carl Drenck, of Copenhagen, Denmark, has developed the FEDREX units after exhaustive research and experimentation. The result is a product the design of which denotes a distinct departure from traditional lines. One of the most important characteristics of the new FEDREX units is the integral design combining X-ray tube and all other high-tension parts in one single, all-welded steel tank.

A complete FEDREX unit consists of two parts: An X-ray unit containing X-ray tube, high-voltage transformer, filament transformer, cooling pump and control panel comprising instruments, regulating devices, exposure timer, safety relays, etc.

These two units only require to be connected by one single low-tension cable to make the equipment ready for service.

High-tension cables, cooling connec-

PENNSYLVANIA OPTICAL COMPANY

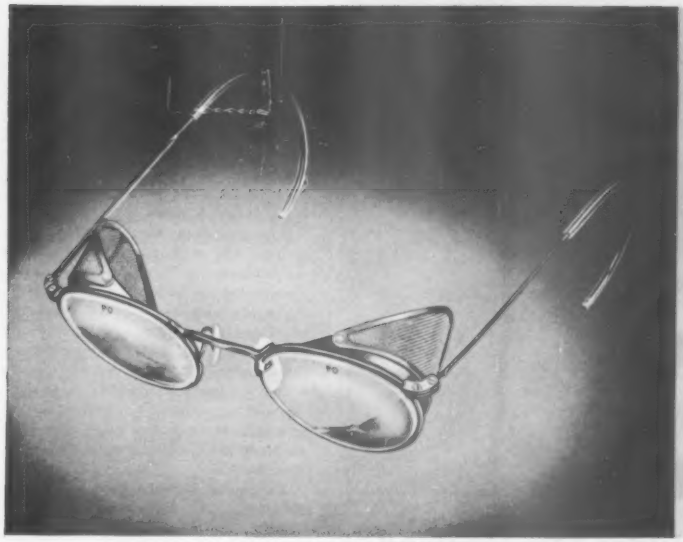

ANNOUNCES ITS NEW LINE OF SAFETY GOGGLES!

The 220 Series Goggles

The new 220 Series Goggles are designed to give the utmost in eye protection. Comfort is assured during continued wear by proper balance combined with lightness of weight. This results in worker approval and a higher factor of safety. Varied combinations make these goggles adaptable to many industrial operations requiring positive eye protection.

- ★ Metal construction combines comfort with strength and long life.
- ★ Designed to permit unobstructed side to side vision.
- ★ Heat treated safety lenses, individually tested for impact resistance, and examined for optical perfection.
- ★ Flat or curved lenses—either clear or absorptive green in medium, dark and extra dark shades.
- ★ Many combinations of side shields, lens sizes and bridge widths.

For illustrated folder, containing prices and detailed information, write directly to Pennsylvania Optical Co., Reading, Penna.

Order Direct and Save!

PENNSYLVANIA OPTICAL COMPANY
READING, PA.
Known for Fine Ophthalmic Products Since 1886

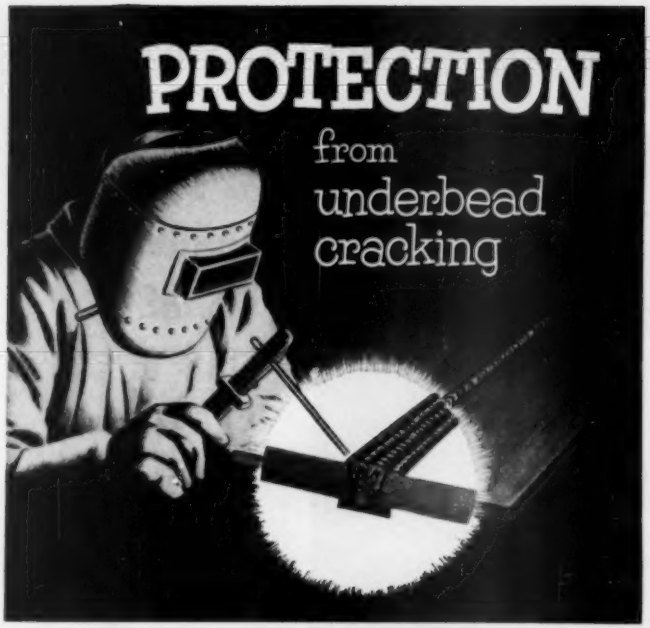

Use ARCOS Low Hydrogen Electrodes

ARCOS GRADE	A.W.S. SPEC.
Tensilend 70	E7016
Tensilend 100	E10016
Tensilend 120	E12015
Manganend 1M	E9015
Manganend 2M	E10015
Nickend 2	E8015
Chromend 1M	E8015
Chromend 2M	E9015

With Arcos Low Hydrogen Electrodes you can produce sound weld metal without the need for preheat or post heat frequently required with mild steel electrodes. Correct selection and blending of coating ingredients, and controlled-cycle, high temperature baking produce a moisture-controlled coating that safely minimizes the gases released in welding.

The moisture-proof wrapping on every 5 and 10 lb. package in a box of electrodes prevents moisture pick-up in shipment and storage.

Added together, these Arcos "quality controls" assure you consistently sound weld metal on every high tensile steel application. ARCOS CORPORATION · 1500 South 50th St., Philadelphia 43, Pa.

WELD WITH

ARCOS

Specialists in Stainless, Low Hydrogen and Non-Ferrous Electrodes

tions, separate transformers and cooling pumps have been completely eliminated.

Exclusive U. S. distributors, Holger Andreasen, Inc., 703 Market St., San Francisco 3, Calif.

Gouging and Cutting of Metals

The "Arcair" process of gouging and cutting all metals, using only carbon arc and compressed air, will be demonstrated to visitors at the National Metal Exposition, Philadelphia, October 18–24. The exhibit is planned to include a working demonstration plus on-the-scene color photographs of the process in use in varied industrial applications.

A new product, the Arcair Torch for gouging and cutting is reported by its manufacturer as having received widespread adoption by fabricators for removing welds, cleaning roots of welds and grooving plate; by foundries for removing casting defects, and by construction firms, railroad shops, oil contractors and others for general purposes. The torch operates on ordinary d-c welding current and features air-control valve, adjustable electrode angle, self-aligning jet and concentric cable.

The Arcair Torch is manufactured by Arcair Co., 2614 Burwell St., Bremerton, Wash.

"Mir-O-Col 45–90 Method" for Rebuilding Tractor Rollers, Etc.

The Mir-O-Col Alloy Co., Inc., 340 N. Avenue 21, Los Angeles 31, Calif., placed on the market a new low cost "Mir-O-Col 45–90 Method" for rebuilding tractor and shovel rollers, idlers and rails. Developed after years of research and field testing, the Mir-O-Col 45–90 Method is described as combining the impact resistance of Mir-O-Col No. 45 wire with the abrasion resistance of Mir-O-Col No. 90 wire into a "build-up" with exceptionally high wear resistance.

The new Mir-O-Col 45–90 Method, states the company, will enable users to cut tractor and shovel roller, rail and idler rebuilding costs to a fraction of new part replacement costs.

Mir-O-Col No. 45 automatic wire has a high nickel content to withstand heavy impact and can be used in multiple-pass operations with no spalling. Hardness of deposit is from 22 to 28 Rockwell C. Mir-O-Col No. 90 automatic wire contains chromium, molybdenum and vanadium, and has a Rockwell C scale hardness of 46 to 48. It is claimed that both wires are readily adaptable to the submerged arc process of welding.

Coupled with the development of these two automatic wires, the Mir-O-Col Alloy Co., Inc., has developed new automatic welding heads and positioners for the Mir-O-Col 45–90 Method.

A new 12-page illustrated brochure, "Mir-O-Col 45–90 Method for Automatic Rebuilding," is available when requested on business letterhead.

Organic Metallic Bonding Agents

An exclusive agreement has been reached by the ChemoTec Division of the Eutectic Welding Alloys Corp., and the Ciba Co., Inc., to exploit the processes developed from a fundamentally important line of new materials that perform unique functions in bonding metals such as: titanium, magnesium, aluminum and all the metals and alloys commonly in use, together with glass, wood, porcelain, plastic, etc. These may be joined to each other or metal may be joined to glass, fabric to metal, or glass to wood.

It is reported that a great deal of research and investigation has been done by Ciba in this field, and ChemoTec intends to continue this preliminary work in its laboratories. ChemoTec will manufacture and market under Ciba license using its basic materials and processes.

Inks for Crack Detection

The Physics Department of Manchester Oil Refinery Ltd. of Manchester, England, announces that it has recently developed two petroleum-based types of ink for nondestructive crack detection for both magnetic and nonmagnetic materials.

The first of these products is Supramor Electro-Magnetic Flaw Detection Ink for the detection of both subsurface and surface flaws in ferrous metals. The second is Glo-Mov Fluorescent Crack Detection Ink for indication of surface cracks in nonferrous alloys and plastics.

Full details of the method of application and the type of indication produced may be obtained by writing to Manchester Oil Refinery Ltd., Twining Road, Trafford Park, Manchester 17, England.

Combination Welder and Charger

Mid-States Welding Manufacturing Co., Chicago, Ill., announces a new combination a-c arc welder and battery charger, reconnectable for 110- or 220-v operation. The new welder, Model 175-BC, lists the following features: 15 to 175 amp output range; 140 amp rated output; arc voltage, 25 v; open circuit voltage, 65 v; power factor correction 75%; duty cycle at rated amperage load, 50%; duty cycle above rated amperage load, 20%; 36 amp draw at 220 v; kva at rated output, 7.9; battery charging rate, 6 d-c amp.

The new Mid-States combination welder and charger handles rods from $^1/_{16}$ to $^3/_{16}$ in. and is also available without battery charging circuit. The new Model 175-BC

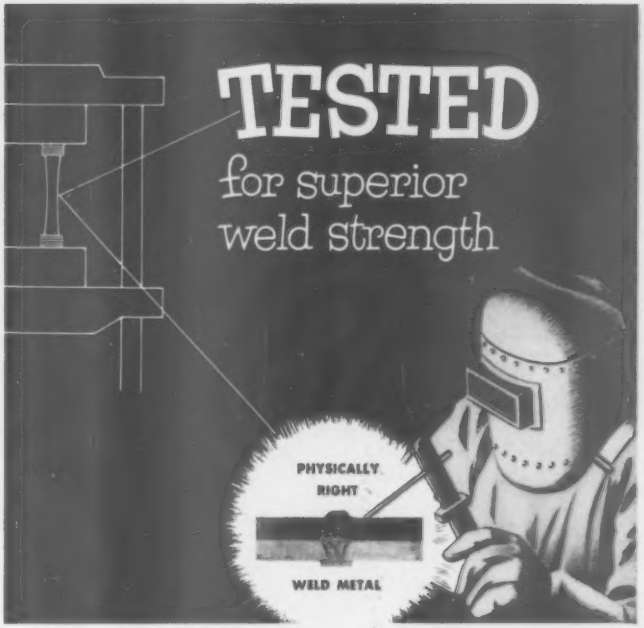

Use ARCOS Stainless Electrodes

Because Arcos applies a series of mechanical performance tests for strength, toughness, and ductility to all types of Stainless weld metal, you can be sure that your deposits with Arcos Stainless Electrodes will be physically "right". Whatever the job requirement—ability to withstand heavy loads, high pressures, or severe shocks—you'll get the results you want.

Other Arcos "quality controls" assure that the weld metal will be chemically and metallurgically "right" as well. That's why it will pay you to depend on Arcos Stainless Electrodes for the correct combination of properties that lead to sound welds on every job. ARCOS CORPORATION • 1500 South 50th St., Philadelphia 43, Penna.

What happens when an aircraft manufacturer turns his talents to house trailers? At Spartan Aircraft Company in Tulsa the result, as you might expect, is a mobile home embodying the best features of aircraft design: light, yet strong, with minimum wind resistance; compact, yet commodious and comfortable. Spartan's mass production techniques bring a completed trailer off the line every 18 minutes. Seven NCG Sureweld A-C Welders, centrally positioned, permit fast, efficient welding of chassis frames. A Sureweld Portable D-C Welder (shown below the A-C machines) is a timesaver for maintenance and repair at Spartan. It can be moved quickly and easily anywhere throughout the big 40 acre plant.

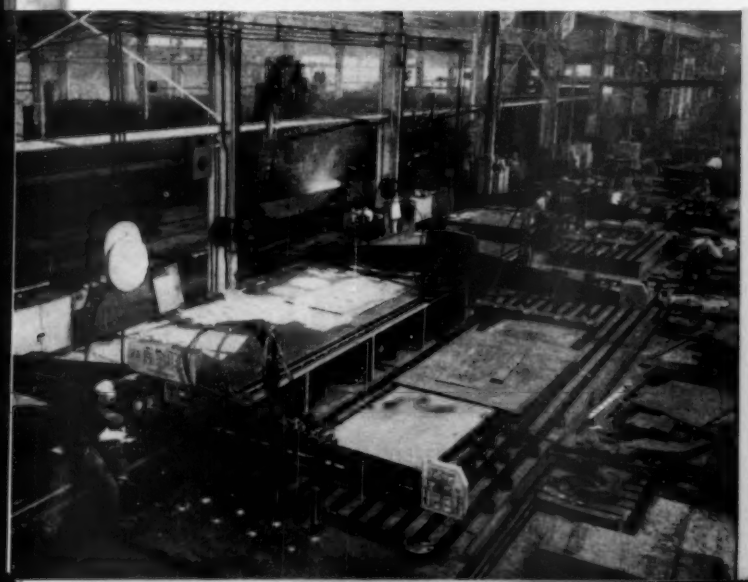

Three NCG automatic flame cutting machines help speed production at the Whiting Corporation, Harvey, Ill., one of the nation's leading producers of foundry and railway equipment, material handling equipment, rotary shears, chemical equipment and special machinery. Two of the machines are mounted on one long table to provide a 40-foot cutting length. Parts being cut in this picture are for Whiting's new "Trackmobile." Whiting has used NCG cutting equipment for ten years.

AT RIGHT: Rego KX Hand Cutting Torches and NCG's Cut-O-Matic and RS Cutting Machines speed production at Welded Steel Shapes, Inc., structural steel fabricators at Coatesville, Pa. NCG's pipe-line system, fed from portable banks, keeps NCG gases flowing conveniently and economically at this modern shop where work ranges from the fabrication of buildings and bridges to farm equipment.

Get it done faster and better with NCG

In plants and shops across the country NCG equipment is proving that it can get work done more profitably

In times like these when all basic costs are high, one of the solutions for profitable production is selecting tools that will help get jobs done easier, faster and better—that can be depended on, too, to stand up under heavy use without costly maintenance.

NCG customers from coast to coast are getting this profitable kind of help from NCG equipment. You can get it, too!

Whatever your needs are for welding or flame cutting equipment, find out what NCG has to offer before you make a choice. Your nearest NCG office or the authorized NCG dealer in your locality is able and anxious to help you. And you'll like the interest they take in making your problems their own.

NCG®

EVERYTHING FOR WELDING

NATIONAL CYLINDER GAS COMPANY

Executive Offices:

840 North Michigan Avenue, Chicago 11, Illinois

© 1952, National Cylinder Gas Co.

See us at the METAL SHOW!

with

WW®

KAPTRODE*

*Trade Mark

SPOT WELDING ELECTRODES

The new WW Kaptrode Electrode is a small cap type electrode which fits into a semi-permanent Kaptrode Adapter Shank. This in turn fits into any standard Morse taper type holder of appropriate taper size. The entire assembly makes a highly efficient watertight and electrically-efficient unit.

- COPPER SAVINGS—75% and more with widespread, careful use.
- ELECTRODE COST SAVINGS—20% and up in ordinary shop operations; careful operators save as high as 50%.
- INVENTORY SAVINGS—30% and up; only small supply of shanks needed; electrodes are interchangeable; one shank with proper care should outlast ten or more.
- TIME SAVINGS—Kaptrodes quickly, easily inserted and removed.
- MAINTENANCE SAVINGS—in majority of cases, the Adapter Shank may be left permanently in the holder, saving maintenance and changeover time.

For the toughest electrode-consuming job in your plant, order a supply of WW-Kaptrode Electrodes NOW!

WW®

22803A

WEILER-WELD & CO., Division of Fansteel Metallurgical Corp. • 11644 Cloverdale Avenue • Detroit 4, Michigan

welder is covered by the Mid-States regular 5-year burn-out proof guarantee.

The announcement states that the new welder meets NEMA Standards and REA Specifications. The amperage range is said to be wide enough to meet any farm, maintenance or repair shop requirement.

Complete details and specifications on the new Mid-States combination welder and battery charger may be obtained by writing Mid-States Welding Manufacturing Co., 6025 S. Ashland Ave., Chicago 36, Ill.

Electric Tubular Heaters

The Edwin L. Wiegand Co., 7500 Thomas Blvd., Pittsburgh 8, Pa., announces that it has developed an electric tubular heater as a new aid in welding steel pipe and plate. The heaters are intended to reduce the temperature differential between the weld area and adjacent metal, with its attendant advantages, such as controlling the "locked-in" stresses that frequently cause failure of welded parts.

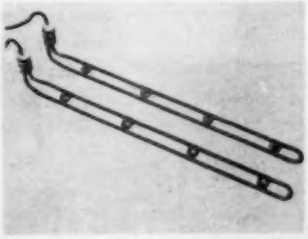

By placing the heaters between the weld line and larger sections of cold metal, a "heat dam" is formed which slows conduction of heat away from the weld. In the case of a straight line weld, heaters are held in place about six inches from the weld line by bolting them to tack-welded studs. Special heater shapes are similarly attached to fit the heat to various weld contours.

The heater elements are triangular in cross section, and one flat side is in contact with the work to give fast and efficient heat transfer. The triangular construction also gives good physical strength to the heater for this rugged type of work.

In operation the heaters are turned on before welding begins until a temperature of 400–500° F is attained in the weld zone —and they are left on after welding is completed. These preheating and postheating periods vary according to type and thickness of the metal.

Head and Tail Stock Positioner

The Aronson Machine Co. announces a new item in their line of welding positioners. As shown in the accompanying photograph, its purpose is to rotate large pieces between centers. The tables are the face plates and the workpiece is attached to them. The rotation is in one plane only, the horizontal rotational axis. The operation is similar to a lathe except the speeds are much slower, 1.13 rpm constant speed, and they are primarily for welding, either manual or automatic.

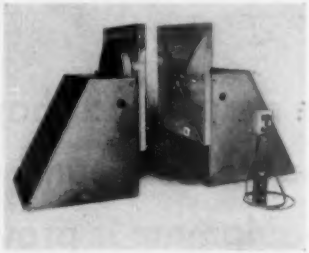

The following features are claimed for the three models HTS5, HTS12 and HTS32 with capacities 5000, 12,000 and 32,000 respectively:

(*a*) Magnetic brake motor operated with magnetic reversing starter.
(*b*) 110-v control circuit on remote push button station.
(*c*) Anti-friction bearing throughout.
(*d*) Mercury grounding on both head and tail stock.
(*e*) Cam yoke roller on table for backup to prevent table deflection under load.
(*f*) Direct drives without belts or chains.

For additional information write to Arsonson Machine Co., Arcade, N. Y.

Acetylene Regulator

The development of a new, Prest-O-Lite acetylene regulator, with ample capacity for the most efficient use of any air-acetylene torch or appliance, has been announced by Linde Air Products Co. This R-411 regulator is designed for small tank apparatus such as paint burning and soldering outfits used by painters, plumbers and refrigerator repairmen.

It is claimed that acetylene at pressures up to 13 psi can be delivered through this

HOUSTON
TEXAS
JUNE 16-19, 1953

Come- to the *welding-minded* Southwest where America has invested billions in creating a *new* industrial empire.

See- the Welding Industry's *newest* products designed to *cut* cost and *speed* production.

Hear- the *latest* news on engineering development from the Industry's *foremost* authorities.

Tour- the tremendous industrial development along Houston's Ship Channel; now *second* in U. S. shipping tonnage.

Marvel- at Houston's welded office, hospital and factory buildings; *more* that in *any* equivalent area in the world.

Display- your products to the Southwest's highly diversified industrial market—which *knows* welding—*wants* welding—and *buys* welding.

Plan- to attend this *all-welding* event at the famed Shamrock Hotel and connecting Hall of Exhibits—*both* fully air conditioned for your comfort.

national
SPRING TECHNICAL MEETING
and
WELDING and
ALLIED INDUSTRY EXPOSITION
in the
air conditioned
SHAMROCK HOTEL and
HALL OF EXHIBITS

Now! - Make Booth Reservations. Rentals and Floor plans on request.

For Additional Information
Communicate with
NATIONAL SECRETARY
AMERICAN WELDING SOCIETY
33 West 39th St. New York 18, N. Y.

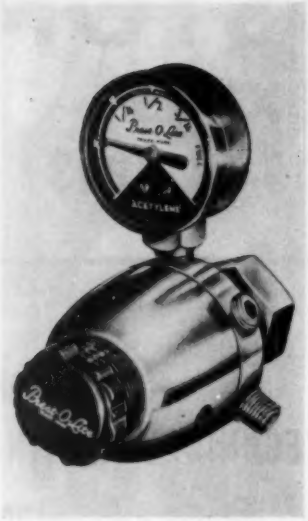

regulator. Once set, the R-411 automatically delivers gas at precisely correct working pressure. It eliminates the need for frequent adjustment of pressure at the tank valve and saves gas since excessive acetylene pressure is never used and wasted.

Additional features attributed to this regulator are simplified replacement of the fabric-reinforced rubber diaphragm, valve seal and filter screw. These are the only parts that will require replacement even after long periods of normal use. The pressure gage shows tank contents at a glance on a dial calibrated at 1/4, 1/2, 3/4 and full, similar to an automobile gasoline gage for easy reading.

New Welding Heads for "Prest-O-Weld" Blowpipes

A series of 13 new welding heads for welding and heating work on practically any metal from 32 gage to more than 1 in. in thickness, is announced by Linde Air Products Co., a Division of Union Carbide and Carbon Corp.

The new heads fit interchangeably on Prest-O-Weld W-121 and W-122 welding blowpipes. All heads are of the snap-in type, and are attached to either blowpipe handle by means of a hand-tightening connection nut. Since no wrench is needed to get a firm, gas-tight seal, head changes take only a few seconds.

Two synthetic rubber "O" rings (see illustration) on each mixer make possible the use of timesaving snap-in type heads.

Head sizes are spaced so that welding ranges overlap. Size numbers, from 2 to

100, are stamped on each head. They indicate the flow rate, in cubic feet per hour, of oxygen and acetylene when heads are used at recommended operating pressures. Knowing the flow rate makes it easy to estimate gas consumption for any job.

Once connected to the front of a blowpipe, the heads can be turned on the handle to point in any direction.

Heavy-Duty Holders and Electrodes for Spot Welding

The new Mallory heavy-duty "Nu-Twist" holders and electrodes represent an entirely new approach to electrode-holder construction for spot welding forces over 6000 lb, according to an announcement by P. R. Mallory & Co., Inc., Indianapolis. They are designed with flat mating surfaces between holder and electrode. This eliminates threaded and tapered connections. The electrode supposedly cannot jam in the holder. The flat surfaces effectively support the highest welding pressures, yet the electrodes can be quickly and easily removed by hand. No tools are required.

Westinghouse Offers Better Brazing for less!

Are you still using costly silver solders to braze copper, brass or bronze? The time-tested Phos-Copper and the sensational new Phos-Silver will braze these metals at a fraction of the cost of silver solder and do the job better and faster with these advantages:

No Flux: On copper-to-copper joints, a flux is not required when using Phos-Copper or Phos-Silver.

Low Temperatures: Phos-Copper permits brazing temperatures as low as 1350° F. Where even lower temperatures are required, Phos-Silver may be used as low as 1225° F.

Perfect Bonds: The high fluidity and excellent wetting properties of Phos-Copper and Phos-Silver assure strong, ductile bonds capable of withstanding repeated shock and vibration.

For further information call your nearest Westinghouse office or write Westinghouse Electric Corporation, Welding Division, Buffalo, N. Y. Ask for Brazing Booklet B-5454. J-21712

Westinghouse
WELDING EQUIPMENT

Buy "PROVEN FLUXES"
Years of GUARANTEED SATISFACTION
behind these GOOD
"ANTI-BORAX" FLUXES
Insist on them — Unequalled Quality

No. 1 Cast Iron Welding Flux
No. 2 Brazing Flux for Brass, Bronze, Steel, etc.
No. 4 Braz-Cast Flux for Bronze Welding Cast Iron
No. 5 & 8 Cast & Sheet Aluminum Fluxes
No. 9 Stainless Steel Welding Flux
No. 11 Tinning Compound
No. 16 Silver Solder Paste Flux

Mfg. By
ANTI-BORAX COMPOUND CO., INC.
Fort Wayne, Ind.

WELDING CONNECTORS

Saxe Welding Connection Units position and secure structural parts to be welded.

Clip K3A permits an adjustable connection.

These widely used units eliminate all hole punching, and, with welding, produce the most economical, safe, and quickly erected structural frame.

Write for 1951 edition, Structural Welding Practice Manual.

J. H. WILLIAMS & CO.
Buffalo 7, N. Y.
AIR REDUCTION CANADA, LTD.
Montreal 2, Canada

Amscoating

The Right Way to Say Hard-facing for every Industrial Use

AMSCO TOOLFACE for metal to metal wear up to 1000 F. Deposits have high abrasion and impact resistance. All diameters bare and coated. Microstructure: martensitic steel.

AMSCO TUBE TUNGSITE (coarse particles) is best suited for applications requiring highly efficient cutting qualities, for hardfacing earth working and drilling equipment used for cutting extremely hard compositions, for hardfacing applications requiring a serrated edge and hard-facing certain types of earth working equipment or parts subject to extreme abrasion.

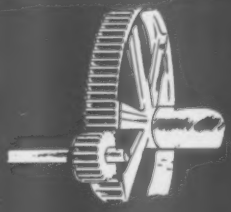

AMSCO HF-60 for moderate impact and abrasion and has outstanding weldability particularly for vertical applications. All diameters, coated only. Microstructure: martensitic steel.

AMSCO FARMFACE or AMSCO CHROMEFACE for farm or industrial use. Excellent resistance to low stress sliding abrasion. All diameters, bare and coated. Microstructure: a high chromium austentitic iron containing manganese and silicon, and consisting of hard chromium carbides in a matrix of austentite.

AMSCO AW-79 will meet most requirements for better control of wear where abrasion and impact are important factors—plus all the advantages of automatic welding. Especially suitable for rebuilding and hardfacing tractor rollers, steel wheels, sheeting rolls, dredge pins, as well as dozens of other automatic applications. [illegible] and [illegible] in 22½" ID., 100 lb. coils.

AMSCO V-MANG, bare or coated, for build up and repair on manganese steel castings exposed to impact; work hardens—[illegible]. Microstructure: austenitic manganese steel.

AMSCO CO-MANG, coated only, for build up and repair of manganese steel castings exposed to severe impact. Deposit has excellent impact resistance; work hardens—[illegible]. Microstructure: austenitic manganese steel.

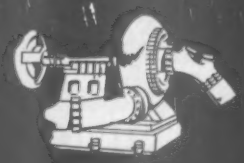

AMSCO TUNGROD (fine particles) is best suited for applications requiring highly efficient cutting qualities, for hardfacing earth working and drilling equipment used for cutting extremely hard surfaces or formations, for hardfacing applications requiring a thin edge or small point, for hardfacing certain types of equipment or parts subject to extreme abrasion.

AMSCO ECONOMY HARDFACE "C" for abrasion resistant service and severe impact. All diameters, coated only. Microstructure: martensitic steel.

AMSCO No. 217 for abrasive service up to 1000 F. All diameters, bare and coated. Microstructure: an air hardening martensitic iron alloy containing chromium and tungsten.

AMSCO HF-40 for severe abrasion, moderate impact. Deposits have excellent weldability. All diameters, coated only. Microstructure: martensitic cast iron.

AMSCO AIR-HARDENING for abrasion and severe impact. Deposit can be forged to sharp edge without loss of hardness. All diameters, bare and coated. Microstructure: martensitic steel.

AMSCO No. 1 and AMSCO No. 6 for combination of corrosion and abrasion or for 1000 F. service and above. No. 1 has greater abrasion resistance. No. 6 is tougher and can be machined. All diameters, bare and coated. Microstructures: No. 6 contains an eutectic carbide mixture in a solid solution matrix, while No. 1 contains large hard wear-resistant chromium carbide crystals scattered through a solid solution matrix.

AMSCO No. 459 for severe abrasion, mild impact. Excellent abrasion resistance. All diameters, bare and coated. Microstructure: martensitic cast iron containing chromium and molydenum, consisting of hard carbides, austentite and martensite.

To get the right answer, detailed analyses, and other pertinent information, concerning your wear problem, write for catalog 650W or contact your nearest Amsco Distributor.

AMERICAN Brake Shoe COMPANY

AMERICAN MANGANESE STEEL DIVISION

399 EAST 14th STREET • CHICAGO HEIGHTS, ILL.

Other Plants: New Castle, Del., Denver, Oakland, Cal., Los Angeles, St. Louis. In Canada: Joliette Steel Division, Joliette, Que. Amsco Welding Products distributed in Canada by Canadian Liquid Air Co., Ltd.

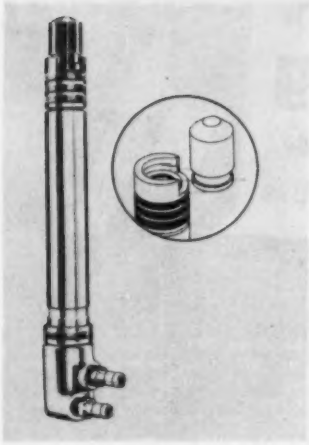

Other construction features claimed for the new holder are: (1) Manually operated electrode locking nut requires no tools. . . permits easy removal and replacement of electrodes. Unique, double grooved construction in bore of locking nut positively aligns electrode centrally in the holder and locks electrode in position. (2) Flat mating surfaces between electrode and holder withstand highest pressures and are silver plated for lowest contact resistance. (3) "O" Ring seal provides watertight connections at all times. Coolant hole and wall thickness of the electrodes are properly proportioned to insure efficient cooling with adequate metal section to carry the higher welding currents without overheating. (4) Retractable coolant head permits retracting adjustable coolant tube when removing or installing electrodes. Coolant tube automatically locks into normal position when coolant head is pushed back into the operating position.

Mallory "Nu-Twist" holders are available from stock in 8- and 12-in. lengths and in $1^1/_4$-, $1^3/_4$-, 2- and $2^1/_2$-in. barrel diameters. Electrodes are available from stock in Elkaloy A, Mallory 3 and Mallory 100 Metal. Complete technical information is available on request. Write P. R. Mallory & Co., 3029 E. Washington St., Indianapolis 6, Ind.

All-Plastic Welding Helmet

A seamless all-plastic welding helmet is announced by The Boyer-Campbell Co., 6540 St. Antoine St., Detroit 2, Mich. The shell is made from a thermo-setting, Fiberglas, reinforced polyester resin by compression molding. It is reported to be exceptionally strong and moisture resistant, will not warp and is lighter than vulcanized fiber. It is easily cleaned and sterilized. A complete insulating glass holder, made from shredded canvas base Bakelite, provides strength and lightness.

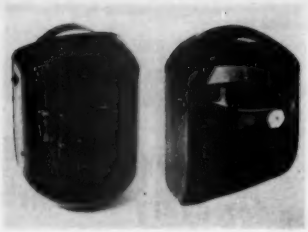

There are four different models: Plastic No. 1130 or No. 1136 Lift front; No. 1085 Insulated Steel or No. 1096 Insulated Dowmetal.

For additional information write to the company at the above address.

Air-Acetylene Outfit

Full capacities of five separate outfits for soldering, heating and light brazing are combined in one new Prest-O-Lite 5-in-1 Precision Outfit being produced by Linde Air Products Co. It is claimed that all work, from very fine soldering in radio and television sets to work requiring a large volume of heat, such as thawing frozen pipes and light brazing, can be handled by this outfit.

Four open-flame torch stems and a pointed copper soldering iron attach interchangeably to a newly designed precision

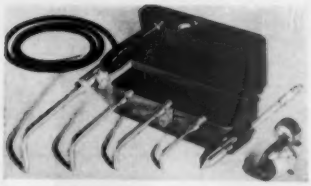

control handle which is equipped with a pilot needle valve contained in the shutoff valve. This valve can be adjusted to keep only a small pilot flame burning, to save gas on intermittent work. A flip of the thumb (one-quarter turn) operates the shutoff valve.

The acetylene pressure regulator included in this outfit is also of the latest design. It is fully adjustable to deliver acetylene at any pressure up to 13 psi as long as usable pressure remains in the tank. No adjustment is needed on the cylinder valve to compensate for decreasing cylinder pressure.

Hose with standard "A" size (left-hand thread) hose fittings and a metal carrying case for all parts complete the outfit.

A 4-in-1 outfit also is being produced in the Prest-O-Lite line of apparatus. This smaller outfit covers the same range of work with the same parts as the larger combination but does not include a soldering iron for working in locations

TRACTOR SHOES LAST LONGER . . . COST LESS

When You . . . Repair Worn TRACTOR GROUSERS with . . .

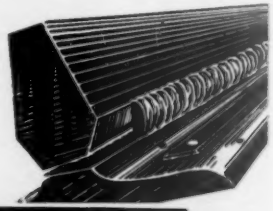

MANGANAL

U.S. Patents 1,876,738—1,947,167—2,021,945

11%-13½% Manganese-Nickel Steel

SPECIAL SHAPE APPLICATOR BARS

- Workharden to 550 Brinell. Tensile strength to 150,000 p.s.i.
- Provide stronger, longer-lasting replacements —cost less than new parts.
- Practically eliminates build-up welding.
- Easily fabricated hot or cold without injury to metal.
- Outlast other steels due to its extreme toughness and high resistance to impact and abrasive wear.

FREE booklet on the newest methods of economical repairs to TRACTOR SPROCKETS, ROLLERS, IDLERS, BLADES, CORNER BITS.

NEAREST DISTRIBUTOR UPON REQUEST

STULZ-SICKLES CO.

SOLE PRODUCERS 92 N. J. RAILROAD AVE. NEWARK, N. J.

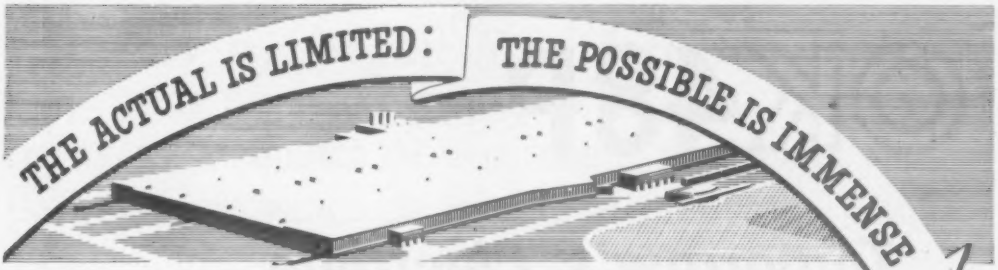

NEW LINCOLN PLANT CREATED BY INCENTIVE INSPIRED CO-ACTION IN DEVELOPING POSSIBILITIES IN PRODUCT

© LE Co. 1952

BUILDS STRONGER MORE RIGID MACHINE BASE

...cuts weight 36%, lowers cost 45%

By **A. H. Hallenbeck**, Plant Manager
Gifford Wood Company, Hudson, New York

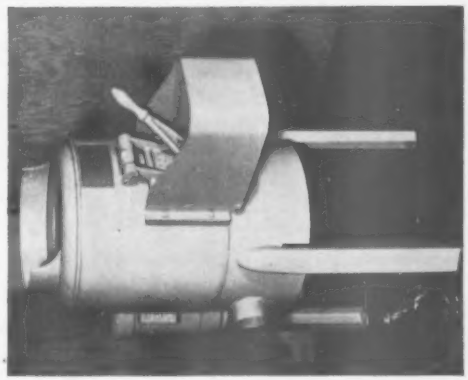

WELDED design has been adopted on many of our machine components because of lower cost and better quality production with steel. As shown in the welded base (Fig. 2), lower weight with steel now saves on material cost as well as in transportation charges. Welded steel can be fabricated with simpler skills, helping to eliminate production bottlenecks in the shop. Components are pre-machined on light, fast machine tools prior to welding, saving time and cost of operating heavier shop equipment as was the case with cast construction.

Through welded steel, our shop now has better control of its work schedule. We are no longer dependent on outside sources for castings nor contend with storage and maintenance of pattern equipment.

Welded design makes it possible to meet price competition in our field that we were unable to do with the original cast designs. The product has a more modern appearance to improve selling appeal.

Fig. 3—Food processing machine *for the Gifford Wood Company, Hudson, New York. Streamlined appearance is simple to maintain, easy to clean.*

WELDED DESIGN ALWAYS SAVES STEEL AND LOWERS COST

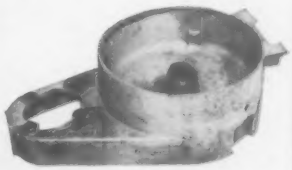

Fig. 1—Original Construction—*Base for processing machine. Weighed 67 pounds. Material Cost—$15.05; Machining Cost—$7.34. Total Cost $22.39.*

Fig. 2—Present Welded Steel Design—*Stronger, more rigid. Weighs only 43 pounds. Material Cost $2.50; Fabrication—$9.77. Total Cost—$12.27.*

HERE'S HOW

Machine Design Sheets available on request. Designers and Engineers write on your letterhead to Dept. 910,

THE LINCOLN ELECTRIC COMPANY

Cleveland 17, Ohio

THE WORLD'S LARGEST MANUFACTURER OF ARC WELDING EQUIPMENT

OK48P

Tomorrow's Electrode

supplied today

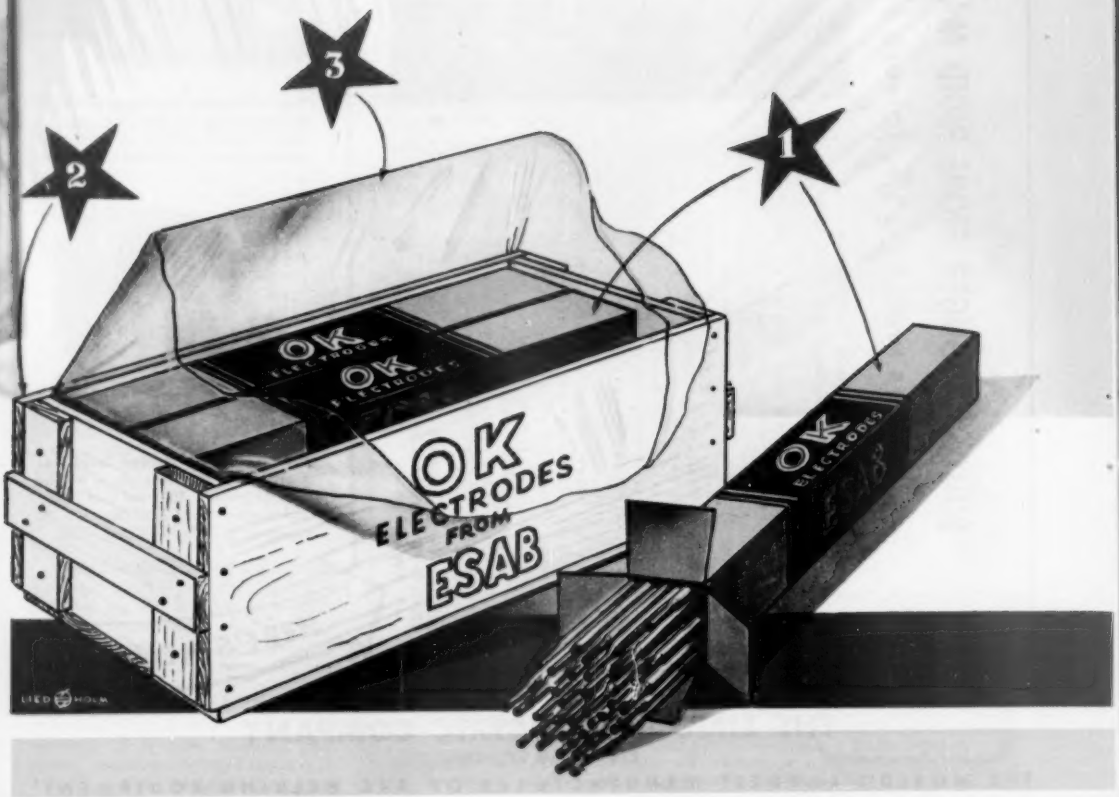

The low hydrogen lime ferritic electrode

OK48P IS THE RESULT OF BASIC RESEARCH AND 15 YEARS' EXPERIENCE OF LIME FERRITIC ELECTRODES AND 50 YEARS' EXPERIENCE OF WELDING ELECTRODES IN GENERAL

OK48P is a low hydrogen lime ferritic electrode with a basic coating. It has all the advantages of this type, lacking the disadvantages which usually limit its use to those critical locations and structures which may be subject to low temperature impacts during service.

OK48P is a general purpose electrode. In Sweden OK 48 P together with similar basic electrodes make up more than 60 % of the consumption of mild steel electrodes.

OK48P corresponds to the E 6015 class welding in all positions. (For the E 7015 class the OK 55 P is used with the same advantages as OK 48 P.)

OK48P gives a good quality weld, free from pores and cracks, also in steel containing impurities such as sulphur and phosphorus (within wide limits) as well as even rather high percentages of carbon and silicon.

OK48P is suitable for steels with high tensile strength as well as for special steels, steel castings and even for cast iron, all of which can be welded only if the welding material is ductile enough to take up the deformations which are unavoidable in connection with welding.

OK48P is delivered well protected against humidity. It is packed in cardboard boxes containing about 12 lbs of electrodes. Six of these boxes are enclosed in a wooden case lined with plastic hermetically sealed by welding.

Compared with the lime ferritic electrodes generally used the OK 48 P has the following advantages:

OK48P has a higher burn-off rate, not only than other lime ferritic electrodes, but also than welding electrodes in general.

4 mm Ø (5/32")	E 6015	E 6010/12		E 4520/30	
	OK 48 P	OK 44 P	OK 46 P	OK 49 P	OK 50 P
Net burn-off time for depositing 1 kilo material Minutes	30.5	34.3	35.8	26.0	33.2
Gross burn-off time (= net burn-off time + 2 minutes for each change of electrode) Minutes	73.1	107.7	107.2	76.4	85.2

OK48P has a brittle slag, easy to remove. As in addition the slag easily separates, there is less risk for slag inclusions than with other electrodes, even if some of it should be left after slag removal.

OK48P does not necessitate any changes in standard weld groove preparations.

OK48P costs less per kilo deposited material than do organic rutile type electrodes, even apart from the lower labour cost that is owed to high metal recovery (115 %), high burn-off rate and long electrodes (18").

OK48P has a good penetration which lies half between that of the E 6010 and that of the E 6012 class.

MAKE GREAT DEMANDS ON OK48P
IT WILL SATISFY THEM

FOR COMPLETE INFORMATION PLEASE WRITE DIRECTLY TO THE MANUFACTURER:

ESAB ELEKTRISKA SVETSNINGSAKTIEBOLAGET GÖTEBORG SWEDEN

BOX 850 TELEGRAMS: ESAB TELEX: 2326

where an open flame would not be practical. A plastic roll-up kit in which to carry the handle, stems, regulator and hose is substituted for the metal case.

Overhead Electric Traveling Cranes

Shaw-Box Crane & Hoist Division of Manning, Maxwell & Moore, Inc., Muskegon, Mich., announce a new line of standardized Overhead Electric Traveling Cranes of from 1 to 20 tons capacity identified as Series "D" "Load Lifter" Electric Traveling Cranes. Made of nearly all welded construction, these new cranes are

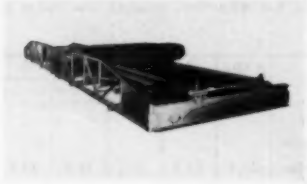

intended to provide adequate crane service for average industrial requirements at prices much less than those of the usual heavy duty industrial service electric cranes. This line does not replace any cranes already in the "Shaw-Box" line, but supplements the line to broaden it. The new line is made up of three distinct types, each developed for specific requirements that exist throughout industry.

Welding Blowpipes Use "O"-Ring Seats

Two new Prest-O-Weld welding blowpipes, announced by Linde Air Products Co., a Division of Union Carbide and Carbon Corp., feature synthetic rubber "O" rings that seal each welding head to the blowpipe handles. There are no metal-to-metal gas seals to maintain. The new "O" rings are claimed to be long-wearing, inexpensive and easy to replace.

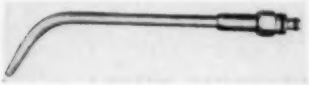

In addition to eliminating metal seals, the "O" rings supposedly make possible the use of quick-change welding heads that snap in place and are held firmly to the handle by a hand-tightening connection nut. No wrench is needed to get an effective gas-tight connection.

Type W-122 welding blowpipe (see illustration) is designed for continuous, heavy-duty welding and heating of practically any metal from 32 gage to more than 1 in. in thickness. The new Type W-121 blowpipe is 1 1/2 in. shorter than its heavy-duty mate, and is for users with a large volume of welding work on materials from 32 gage to 5/8 in. thick.

Both blowpipes are said to be highly resistant to flashbacks. Their flame stability results partly from using a coiled oxygen delivery tube in the blowpipe handle. This cushions any back flow of gases. A steady flame is obtained, regardless of valve settings.

Handles of the new Prest-O-Weld blowpipes are shaped for a comfortable grip. The balanced weight distribution of both blowpipes makes them easy to handle in any welding position.

Automatic Grinding Fixture for Welds

Solar Aircraft Co.'s Des Moines, Iowa, plant formerly ground by hand the double row of welds on these jet engine case assemblies. Now Solar has incorporated a rotor belt sander in an automatic grinding

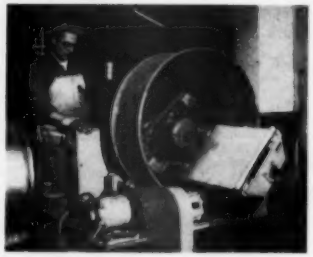

fixture. The Solar-designed fixture supporting the sander moves laterally as the case assemblies are rotated. An increase in production of 400% over the former grinding method is claimed and hand operations have been eliminated.

Hard-Facing Welding Electrodes

The Wall Colmonoy Corp. has announced the availability of Wallex No. 2, a low-priced hard-facing electrode giving a

deposit material consisting of chrome, manganese, silicon and iron alloy. This deposit supposedly has very good abrasion and shock resistance and has stainless qualities approximately equivalent to Type 410 stainless steel.

The deposit of this electrode has a hardness ranging from 49 to 53 Rockwell C. It is available as electrodes in 1/8, 3/16 and 1/4 in. diameters by 14 in. long.

Some of the typical uses are in connection with shovel teeth, drag-line buckets, scarifier teeth, tractor grousers, ditcher teeth, scraper blades, clam shell buckets, conveyor buckets, mixer blades, guides and drag-chain links.

Pocket Measuring Microscope

Optometer trade names a new 50-power, pocket measuring microscope recently introduced by the National Instrument Co. An engraved scale mounted in the body tube reads directly to 0.002 in. Estimations can be made to 0.0005 in. Precision, achromatic lenses, fully corrected for color and spherical aberration, result in a sharp image up to the very edge of the field of vision. This microscope is about the size of a fountain pen and is easily carried in the pocket.

According to its manufacturers, the Optometer is useful in the metal-working

industries for measuring crest and root widths of threads, pitch and depth of threads; for measuring the radii of points and corners, width of slots, chamfers and grooves. Toolmakers may use it for measuring the dimension from a center punch mark to a scribed line. The Optometer is also applicable for measuring the diameters of small holes in gages and heading dies, diameters of impressions in Brinell tests and for other surface measurements. Mechanical parts can be inspected for wear, welds can be quickly examined without the necessity for sample analysis.

To use, the Optometer is placed on the surface of the part to be inspected and a light directed obliquely toward the tapered opening. The focusing knob is moved back and forth until the object is in focus. The linear dimension is read directly on the graduated scale.

MORE TIME FOR STEELMAKING... LESS TIME ON REPAIRS

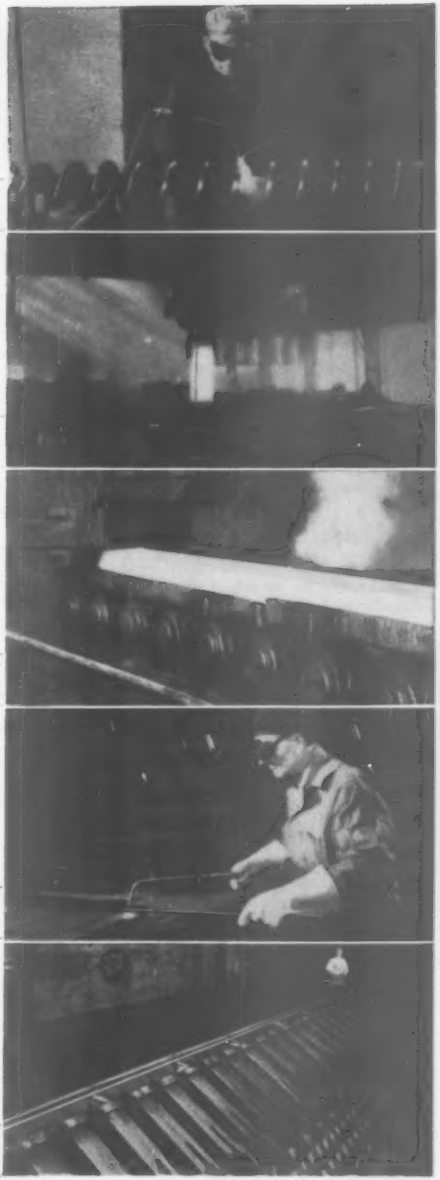

You can keep steel-mill machinery on the job longer by using HAYNES hard-facing alloys to protect wearing parts. With hard-faced parts, you will have less down time and fewer repairs—more time for steelmaking. Illustrated here are some typical savings that have been made.

If you would like a copy of our hard-facing manual, which gives further information on the use of HAYNES hard-facing alloys, fill out the coupon below and mail it to us. For on-the-job help, get in touch with our nearest district office.

1. A yearly application of HAYNES STELLITE alloy No. 1 on this mud-gun screw for blast-furnace tap holes has eliminated monthly maintenance.

2. HAYNES STELLITE alloy No. 6 on the points of soaking-pit tongs has increased their life 19 times. Some hard-faced tongs have lasted as much as 50 times longer than unprotected ones.

3. The life of blooming mill shears has been increased 10 times by applying HASTELLOY alloy C on the cutting edge.

4. Entry guides for a bar-reduction mill used to wear out after handling 40 tons of steel. Guides hard-faced with HAYNES STELLITE alloy No. 6 last 4 to 5 times longer than unprotected ones.

5. Three years ago, some cone rollers in this bar-cooling bed were faced with HAYNES alloy No. 92. They are still in service.

"Haynes," "Haynes Stellite," and "Hastelloy" are trade-marks of Union Carbide and Carbon Corporation.

HAYNES Trade-Mark *alloys*

Haynes Stellite Company
A Division of
Union Carbide and Carbon Corporation
UCC

USE THIS HANDY COUPON

Haynes Stellite Company, 725 S. Lindsay Street, Kokomo, Indiana
Please send me, without obligation, a copy of the booklet, "HAYNES Alloys—Hard-Facing Manual."

NAME_____

COMPANY_____

ADDRESS_____

SECTION NEWS AND EVENTS

as relayed to C. M. O'Leary

Election of Officers

Berwick, Pa.—The *Susquehanna Valley* Section announces the election of the following officers for 1952–53.

Chairman—W. L. Luetzel, 22 E. Pettebone, Forty Fort, Pa.
Secretary—Andrew J. Furman, Commercial Gas Corp., Wilkes-Barre, Pa.
Treasurer—R. P. Schweyer, P. O. Box 125, Berwick, Pa.
Technical Representative—Lewis Russell, 215 E. Front St., Berwick, Pa.
Directors—D. B. Howard, S. E. Bunn, G. L. Meiding, C. E. Reedy, H. S. Swepston and N. D. Harding.

Bridgeport Officers

Bridgeport, Conn.—The *Bridgeport* Section announces the election of officers as follows for 1952–53.

Chairman—Jack Creel, Peabody Eng. Corp., Glenbrook, Conn.
First Vice-Chairman—James J. Powers, The Producto Machine Co., Bridgeport.
Secretary—Louis Campano, 38 Lindberg St., East Haven.
Treasurer—R. A. Lally, R. A. Lally Co., Bridgeport.
Chairman, Membership Committee—Austin A. Young, 185 Treadwell St., Hamden.
Chairman, Program Committee—William A. Seymour, Long Meadow Rd., Orange.
Technical Representative—Joseph R. Skibo, Laurel Place, Derby.

Chicago Officers

Chicago, Ill.—The *Chicago* Section announces the election of the following officers for 1952–53.

Chairman—I. H. Carlson, Crane Co.
First Vice-Chairman—Dr. J. M. Parks, Armour Research Foundation.
Second Vice-Chairman—P. C. Arnold, Chicago Bridge & Iron Co.
Secretary-Treasurer—L. C. Monroe, P. O. Box 142, La Porte, Ind.
Chairman, Membership Committee—P. C. Arnold.
Chairman, Program Committee—Dr. J. M. Parks.
Technical Representative—T. B. Jefferson, *The Welding Engineer*.

Cincinnati Officers

Cincinnati, Ohio.—The *Cincinnati* Section announces the election of officers for 1952–53 as follows:

Chairman—Julius Bergmann, Cleves Welding & Machine Service, Cleves, Ohio.
First Vice-Chairman—Harry Baker, 3473 Bevis Ave.
Second Vice-Chairman—Cliff Miller, 227 Race St.
Secretary-Treasurer—William Highwood, Highwood Service Co.
Chairman, Membership Committee—Cliff Miller.
Chairman, Program Committee—Harry Baker.
Technical Representative—William Maddox, 3438 Zumstein Ave.

Detroit Officers

Detroit, Mich.—The *Detroit* Section announces the election of officers for 1952–53 as follows.

Chairman—R. H. Bennewitz, Linde Air Products Co.
First Vice-Chairman—J. M. Johnston, Murray Corp. of America.
Second Vice-Chairman—Roy L. Clark, 24535 Notre Dame, Dearborn.
Secretary-Treasurer—J. R. Stitt, R. C. Mahon Co.
Asst. Secretary—W. H. Smith, 11691 Stout.
Asst. Secretary—J. E. Rainey, Detroit Testing Lab.
Chairman, Membership Committee—J. L. Adams, Westinghouse Electric Corp.
Chairman, Program Committee—J. M. Johnston.
Technical Representative—Leslie E. Wagner, 7830 Reuter, Dearborn.

Plans for Coming Season

Grand Rapids, Mich.—The Executive Committee of the *Western Michigan* Section met on Tuesday, July 22nd, at the Grand Rapids Country Club for an afternoon of golf, dinner and evening meeting. The purpose of the meeting was for the new officers and executive committee to become acquainted and plan the meetings for the coming year.

Several new features are to be inaugurated this coming year. A Welcoming Committee to consist of the Executive Committee to work on a rotation basis is to be active at every meeting. Also a Membership Committee is to be active and promote a contest with special emphasis placed on getting new members in the outlying towns.

The Section is also setting up a card file with the birth date of each member, so that his birthday may be remembered with a card. The same at a time of illness or hospitalization.

A coffee talk or short entertainment is planned at each meeting. Badges, which have been made up with each member's name, are to be worn at the meetings or the member will be fined. Guests will receive a pocket card to be worn and turned in after the meetings for reference by the Membership Committee.

The Technical Secretary is to prepare a display rack for displaying the literature available from the Society.

A publicity chairman has been appointed and he in turn has appointed an assistant in each surrounding town to insert notices in local papers and notify interested parties of the meetings.

Everything is being done to make the meetings interesting to the members as well as increasing the membership. The officers and committees feel that the 1952–53 season will be a banner year for the Western Michigan Section.

Hartford Officers

Hartford, Conn.—The *Hartford* Section announces the election of the following officers for 1952–53.

Chairman—S. H. Lacey, Auto Battery & Electric Co., New London.
First Vice-Chairman—S. A. Zane, 36 Fairview St., Manchester.
Secretary—Allan G. Anderson, 66 Linnard Rd., West Hartford.
Treasurer—Robert D. Ames, 463 Burnside Ave., East Hartford.
Chairman, Membership Committee—Thomas W. Brady, Westinghouse Electric Corp.
Chairman, Program Committee—Clinton E. Swift, Maple Knoll, Woodbury.
Technical Representative—John W. Mortimer, 82 Plymouth Lane, Manchester

Stag Party

Peoria, Ill.—The *Peoria* Section had a Stag for members on August 29th. This was held at the Caterpillar Rod Club House and was attended by thirty-one members. Food, refreshments and an informal gathering were enjoyed by all.

St. Louis Officers

St. Louis, Mo.—The election of the following officers for 1952–53 has been announced by the *St. Louis* Section.

When you braze aluminum...

If new rearmament contracts require that you teach inexperienced workers how to weld and braze aluminum, your local Alcoa Distributor is a good man to know.

Through him, you are offered Alcoa's complete technical service on joining aluminum—3 how-to-do-it movies, plus copies of a 186-page book covering all welding processes. He carries as well, a complete line of supplies for welding and brazing.

You'll find your local Alcoa Distributor listed under "aluminum" in your classified phone book. Alcoa sales offices are also located in all principal cities. Or write:

ALUMINUM COMPANY OF AMERICA
1944K Gulf Building • Pittsburgh 19, Pa.

ALCOA®

First in Aluminum

Chairman—M. W. Lischer, Nooter Corp.
First Vice-Chairman—J. J. Fox, 4531 McPherson Ave.
Secretary-Treasurer—George O. Bland, Hill Equipment Eng. Co.
Chairman, Membership Committee—Robert E. O'Neill, Pandjiris Weldment Co.
Chairman, Program Committee—J. J. Fox.
Technical Representative—Russell Royer 127 E. Jewell, Kirkwood.

San Francisco Officers

San Francisco, Calif.—The *San Francisco* Section announces election of officers as follows.

Chairman—John S. O'Neill, Jr., California Steel Products Co., Richmond.
First Vice-Chairman—E. Paul DeGarmo, University of California, Berkeley.
Second Vice-Chairman—E. W. Bartz, Westinghouse Electric Corp., San Francisco.
Secretary—Justin M. Roach, National Welding Equipment Co., San Francisco.
Treasurer—R. E. McCormick, 608 Santa Susana Ave., Millbrae.
Chairman, Membership Committee—E. A. Daniels, Victor Equipment Co., San Francisco.
Chairman, Program Committee—Fred L. Stettner, Victor Equipment Co., San Francisco.
Technical Representative—Chas. B. Robinson, Air Reduction Pacific Co., Emeryville.

Syracuse Officers

Syracuse, N. Y.—The following officers have been elected for 1952-53 to serve the *Syracuse* Section.

Chairman—S. H. Monson, Jr., Welding Engrg. & Equipment Co.
First Vice-Chairman—J. Solar, 1440 Westmoreland Ave.
Secretary—F. R. House, 29 Slacombe St., Marcellus.
Treasurer—A. K. Cottet, Cottet's Welding Supply Co.
Chairman, Membership Committee—J. Solar.
Chairman, Program Committee—E. M. Strand, 315 Kenwood Ave.
Technical Representative—E. M. Strand.

Future Plans for Toledo

Toledo, Ohio.—The *Toledo* Section is striving to become the meeting place for all persons interested in welding and its many problems and answers in the Toledo area. In its endeavor to make Toledo industry more "Welding Society" conscious an unusual program has been planned for the coming season. Each month will have a topic discussed by a prominent speaker in his special field and will be of interest to any one who even works next to the welders in the plant and wishes to learn more about "what makes the sparks fly," to the engineer who figures out why, and to the plant superintendent who must figure out how.

The programs will include meetings covering the oil industry, automotive industry, glass industry, machinery, structural steel, die and tool steel welding and maintenance welding. Several plant tours are being arranged to acquaint members with the industry which makes up Toledo.

Toledo Officers

Toledo, Ohio.—The newly elected officers of the *Toledo* Section are as follows.

Chairman—Mike W. Eddins, Knighin & Hughes, Inc.
First Vice-Chairman—W. E. Morris, Welders Needs, Inc.
Second Vice-Chairman—Harry W. Hansen, Hansen Welding Co. Inc.
Secretary-Treasurer—Harley W. Weide, Welders Needs, Inc., 1910 Vermont Ave.
Chairman, Membership Committee—Harry Hansen.
Chairman, Program Committee—W. E. Morris.
Technical Representative—Sam W. Snell, Oxland Iron Works, Inc., 1202 W. Bancroft St.

Anyone in the Toledo area desiring information on membership or exactly what the AWS has to offer may contact Mr. Weide.

York Plans

York, Pa.—The *York-Central Pennsyl-*

CADDY
ARC WELDING ACCESSORIES
feature the welding cable connected by the
CADWELD PROCESS
A CADWELD Connection Has No Equal! It Is . . .
ECONOMICAL Easily made with inexpensive equipment — No special skill required.
FAST Requires no preparation of cable other than stripping of insulation. Time required to make weld less than one minute.
BETTER Has current carrying capacity equal to the cable. Tensile strength equal to soft drawn copper. No damage to insulation when properly applied.
PERMANENT Not subject to the gradual loosening or oxidation of mechanical joints. Not damaged by excessive overload.
COMPACT Weld area is not over 1 ¾" long.
CATALOG ON REQUEST
ON DISPLAY—NATIONAL METAL SHOW—BOOTH 1482
"CADDY" ARC WELDING ACCESSORY DIVISION
ERICO PRODUCTS, INC. • 2070 E. 61st PLACE • CLEVELAND 3, OHIO

NOW

Double and Triple weight coils for automatic welding with the new REID-AVERY (free wheeling) REELS for Submerged Arc, Open Arc, and Gas Shielded Arc Welding

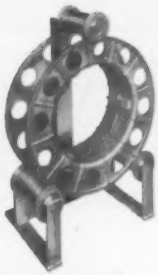

Raco Reel for 150-200# coils with floor mounting stand.

Decrease down-time by using larger coils. Machines now equipped for 25 lb. coils can use up to 75 lb. coils with these new reels.

These cast aluminum alloy reels ride on ball-bearing trunnions with deep flanges. The wire uncoils with remarkable ease and yet there is no chance of overrunning and throwing loops over the side. No brakes or drags of any kind are necessary. The wire itself prevents overrun. These "free wheeling" reels provide the absolute minimum load on the automatic welding machine.

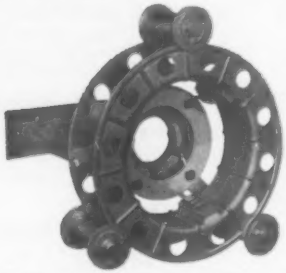

Raco Reel for 25#-50#-75# coils. Mounted on popular submerged arc machine.

The Reid-Avery reels are available with stands for floor mounting or with special spiders for direct attachment to most popular automatic welding machines. Three reels 12" ID x 4" wide, 14" ID x 6" wide, and 25" ID x 4" wide nominal size are in stock for prompt delivery.

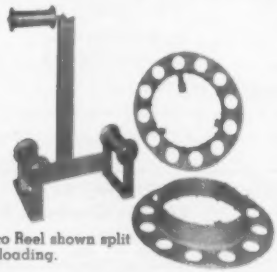

Raco Reel shown split for loading.

Note the simple split reel construction with suitcase type latches. Coils can be replaced in seconds and no wrenches or special tools are required.

We are equipped to supply all sizes of layer wound coils for these reels, for other reels, or on expendable wooden spools where required.

The REID-AVERY COMPANY
INCORPORATED
DUNDALK • BALTIMORE 22 • MARYLAND
SINCE 1919 PRODUCERS OF ARC WELDING ELECTRODES AND WELDING RODS

vania Section had its first meeting of the season on August 18th at the Pine Tree Inn with members of the local Board of Directors present. The meeting was called to discuss the plans for the coming season which also includes participation in the AWS 33rd National Fall Meeting to be held in Philadelphia the week of October 19th. Detailed plans for the coming season will be announced shortly.

LIST OF NEW MEMBERS

Effective August 1, 1952

BOSTON
Bonney, Elwyn F. (B)
Carroll, David B. (B)
Cormier, Wilfred (B)
Daly, Charles F.(B)
Yukon, Edward H. (B)

CHATTANOOGA
Miller, Edward C. (B)

CHICAGO
Ellis, D. S. (B)

CINCINNATI
Helder, Leland G. (B)
Vogel, Fred W. (B)

CLEVELAND
Adams, Wayne C. (C)
Castle, Robert J. (B)
Hagerman, William A. (B)
Hinkel, J. E. (C)
Jordan, R. S. (B)
Kessler, F. W. (C)
Rogos, John, Jr. (C)

DETROIT
Cordts, Melvin J. (C)
McVay, William T. (B)
Sinclair, Edward B. (B)
Stacey, James W. (B)

HARTFORD
Kuzara, Frank J. (C)

LOS ANGELES
Fessler, Robert C. (B)
Gudish, William (B)

MAHONING VALLEY
Hall, Carl W. (B)

NEW YORK
Kellar, Katherine K. (B)
Robinson, Jerome L. (C)
Schwitter, Charles M. (B)
Seeland, Elias (B)

NORTHERN NEW YORK
McCoy, John J. (C)

NORTHWESTERN PENNSYLVANIA
Cole, James C. (B)

PHILADELPHIA
Ashley, R. H. (A)
Rose, Arnold S. (C)

PITTSBURGH
Mitsch, William H. (C)

PORTLAND
Schmid, Leroy J. (B)
Wood, B. Nealley (B)

ROCHESTER
Heymann, James C. (B)

SAGINAW VALLEY
Bickel, Herman H. (B)
Davis, Preston R. (C)
Kreuchauf, Herbert C. (B)
McKenna, Joseph F. (B)
Nelson, R. L. (B)
Weaver, Edgar (C)

SAN FRANCISCO
Beard, R. (B)
Thomas, Richard (B)

WESTERN MICHIGAN
Nyburg, James K. (B)

WICHITA
Martin, L. L. (C)

YORK-CENTRAL PENNSYLVANIA
Galloway, J. W. (C)
Howard, Floyd D. (B)

NOT IN SECTIONS
Fujiwara, Tadayoshi, Dr. (B)
Gondro, Frantz (B)
Maine, Sidroy George (B)

MembersReclassified
During the month of August

BOSTON
Browne, R. L. (B to F)

DETROIT
Duffy, W. Henry (C to B)

LOS ANGELES
Uhl, Vincent (C to B)

MAHONING VALLEY
Heltzel, Robert F. (C to B)

NORTHWEST
Lofstrand, Wilton S. (C to B)

TOLEDO
Eddins, Mike Whitley (C to B

UNITED STATES TESTING COMPANY, INC.

INSPECTION and TESTING of
Welding and Weldments
QUALIFICATION of
Procedures and Operators

Main Laboratories **Hoboken, N. J.**

Boston - Chicago - New York - Philadelphia - Providence

NET MONTHLY ADVERTISING RATES
Black and White **Effective October 2, 1950**

Space	One Insertion	Three Insertions	Six Insertions	Twelve Insertions
Full page	$230	$210	$195	$180
Two-thirds page	165	150	140	130
Half Page	130	120	110	100
Quarter Page	80	75	70	65
Eighth Page	50	45	40	35
Inside Preferred	255	235	220	205

10% Extra for bleed full pages. Color $85 extra per color added

Agency Commission—15%
Cash Discount—2%, 10 days

WELDING RESEARCH COUNCIL

of the Engineering Foundation

Sponsored by the American Welding Society, American Institute of Electrical Engineers, American Institute of Mining and Metallurgical Engineers, American Society of Civil Engineers, American Society of Mechanical Engineers, Society of Naval Architects and Marine Engineers, American Society for Metals and American Society for Testing Materials

Supplement to the Welding Journal, October, 1952

High-Strength Vacuum Brazing of Clad Steels

Development of high-strength brazed joints having uniform and continuous bonding over large areas without the use of fluxes or special furnace atmospheres

by R. C. Bertossa

INTRODUCTION

CONVENTIONAL furnace brazing techniques with copper and copper alloys as brazing materials invariably specify that fluxes and/or special furnace atmospheres must be used in order to obtain complete wettability of the brazing materials and resulting strong and sound brazed joints. In some instances, it has been found that by using relatively pure hydrogen atmosphere with the dew point in the neighborhood of −40 to −60° C, fluxes can be eliminated in the furnace brazing of carbon and alloy steels.

Liquid and paste type fluxes have been found to be very difficult to completely remove in the brazing of relatively large surface areas, and their presence in the bonding zone after brazing causes discontinuity of bond, brittle areas and a general lowering of bond strength.

During the past three years, continuous research has been conducted in our laboratories and in conjunction with Southern Research Institute, Birmingham, Ala., on the development of high-strength brazed joints having uniform and continuous bonding over large areas without the use of fluxes or special types of introduced furnace atmospheres.

R. C. Bertossa, Plant Metallurgist, Chicago Bridge & Iron Co., Birmingham, Ala.

Scheduled for presentation at the Thirty-Third National Fall Meeting, AWS, Philadelphia, Pa., week of Oct. 20, 1952. Closing date for discussion Dec. 15, 1952.

A system of vacuum brazing has now been developed wherein sound and continuous high-strength bonds can readily be obtained throughout areas of virtually unlimited size without the use of introduced furnace atmospheres and without contamination from fluxes. In the case of brazing of stainless steels, it is not necessary to nickel or iron plate the stainless surface before bonding in order to obtain a strong oxide-free bond.

Our work has shown that continuous brazed bonds can be produced between low and medium carbon steels and all of the three major classifications of stainless steels (ferritic, martensitic and austenitic). In addition, this same high-strength brazed bond, which averages from 40,000 to 60,000 psi shear strength, can be attained without difficulty between low and medium carbon steels and pure nickel, Monel and Inconel. Even Hastelloy has shown promising results with vacuum brazing, although this alloy is still in the experimental stage in our laboratories with regard to vacuum brazing.

ADVANTAGES OF VACUUM BRAZING

This development promises to open new fields of application in the brazing of large continuous surface areas, as brazing can be accomplished without entrapment of brittle flux particles which can cause nonuniformity of bond strength, and further, the use of vacuum pressures of between 29 and 30 in. of mercury furnishes tremendous pressures exerted uniformly over the entire area being brazed, which pressures can be maintained throughout the entire brazing cycle,

Fig. 1 Opening of a large 10- x 20-ft vacuum brazed Hortonclad assembly after completion of bonding

insuring a continuous and uniformly strong bond throughout.

Heretofore, furnace brazing has been primarily utilized for the joining of small or intermediate sized assemblies due to difficulties in maintaining uniform pressures at the bonding interfaces during the brazing cycle and the possibilities of leakage of oxygen into the furnace, resulting in oxidation of bonding areas and lack of bond. This was especially true in the brazing of stainless steels, where extremely rapid oxidation of brazing surfaces presents a difficult problem.

The vacuum brazing process has shown that the only limits of size in the brazing of plates are the confines of the brazing furnace cavity itself, no fluxes or atmosphere control being involved, and in the case of stainless steels, no special preparatory plating being necessary on the bonding surfaces.

APPLICATION OF VACUUM BRAZING TO THE ALLOY CLADDING OF CARBON STEELS

Extensive research work in the high-strength vacuum brazing of small and large size alloy "Hortonclad"* plates has revealed that this method of manufacture of composite plate material has some distinct advantages over the conventional methods of manufacture of clad plate materials:

1. The process is relatively simple and requires no expensive heavy rolling equipment, soaking pits or other typical steel mill equipment.

2. Clad plates can be made to practically any size or shape (in the flat), necessitating very little wastage of steel and critical alloy materials through trimming to size after bonding. This alone is an important consideration in times of short alloy supply such as the present.

3. The resulting finish on the brazed clad surface is always bright, clean and free from contamination; and the fineness of surface finish depends entirely on the finish of the alloy sheet itself before brazing. In other words, a "satin" finish stainless sheet vacuum brazed to carbon steel by the Hortonclad process will produce a "satin" finish alloy Hortonclad plate after the vacuum brazing process and will exhibit the same cleanliness of surface as was present on the sheet before brazing.

4. The most important advantage in the manufacture of alloy clad plate by the vacuum brazing process is the ability to guarantee a constant thickness of corrosion-resistant alloy layer over the entire surface of the clad plate, as the composite material is not reduced or deformed in any manner during its high-strength bonding cycle. It is well known that the life of an alloy clad composite plate material under corrosive conditions is only as good as the thinnest portion of the corrosion-resistant clad layer.

* Patents applied for.

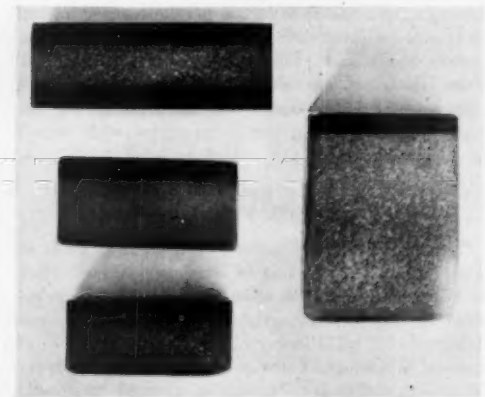

Fig. 2 Etched cross sections of vacuum brazed Hortonclad alloy-to-carbon steel composite plates

PHYSICAL CHARACTERISTICS OF THE HIGH-STRENGTH VACUUM BRAZED BOND

Considerable data have been published regarding the undesirable characteristics and tendencies toward brittleness and loss of physical properties in the composite clad plate due to penetration of the copper into the grain boundaries of the metals being joined during conventional brazing processes.

One of the primary purposes of this article is to demonstrate through research data, photographs and photomicrographs, that through the use of carefully controlled vacuum brazing cycles and techniques, physical properties can be obtained in the bond layer and in the metals joined, which are well above the requirements specified by the American Society for Testing Materials and the American Society of Mechanical Engineers for integrally and continuously clad plate, and compare favorably with the physical properties exhibited by conventional types of rolled clad plate materials.

It has been determined that through strict control of heating, holding and cooling cycles, also subsequent heat treatments, if used, the proper amount of alloying can be obtained at the brazing interface to attain exceptionally high bond strengths without appreciable loss of ductility.

Tensile Strength of Vacuum Brazed Composite Clad Plates

The ASTM Standards for integrally and continuously clad plate specify that the entire composite clad must meet the minimum requirements as set for the carbon steel backing material used. The usual backing plate used is either A-285, Grade "C" or A-201 (fully killed steel), with tensile strength requirements of 55,000 psi minimum; however, the higher strength A-212 steel with tensile requirements of 65,000 to 70,000 psi minimum can also be successfully used.

Composite clad plates produced by the vacuum brazing process have given no difficulty in attaining well above the required minimums in tensile strength, and as an example of the adherence of bond, the alloy layers "neck down" with the carbon steel at the area of fracture and do not split away at the bonding interface on either side of the fracture (see Fig. 3).

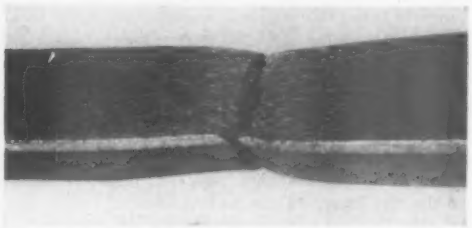

Fig. 3 Tensile fracture in vacuum brazed nickel alloy clad plate

Ductility of Vacuum Brazed Alloy Clad Plates

In testing the ductility of composite plate material, free bend tests are specified by ASTM, specimens being bent both with clad in tension and with the clad layer in compression. These specimens are required to be bent 180 deg to a radius which varies, depending upon the total thickness of the composite plate.

In the free bend testing of vacuum brazed clad plate, with copper and copper alloy bond, it was our endeavor to develop a product which would exceed the requirements specified by ASTM in all instances, therefore we did not accept as passing a specimen which failed to withstand bending 180 deg flat down upon itself without separation at the bonding interface or failure of the materials which originated at the bonding interface.

Figure 4 illustrates the ability of Type 405 stainless copper alloy brazed to carbon steel by the vacuum brazing process to withstand flat bending down upon itself. The double clad specimen in this photograph illustrates the ability of the bond to withstand these extremely severe strains both with cladding in tension and with cladding in compression. Those familiar with stress relationships in the severe bending of composite clad materials can readily appreciate the degree of stresses set up in the bonding interfaces by these 180 deg flat bends, especially when bent with the clad layer in compression. The double clad specimen illustrated in Fig. 4 was bent to an elongation on the top clad surface of 79%.

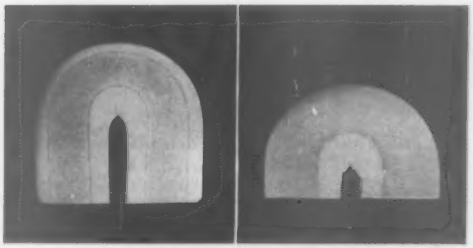

Fig. 4 Etched cross section of two 180-deg flat bends, one of Type 405 stainless clad on both sides of a carbon steel plate, and another with nickel alloy clad on one side only

The single clad specimen at the right of Fig. 4 consists of a nickel alloy (Monel) sheet vacuum brazed to a low-carbon steel base plate. It can be seen that no separations, cracking or other defects have occurred in the bond area in spite of this extremely severe bend.

In examination of Fig. 4, it will be noted that a crack extends upward from the surface of the Type 405 stainless clad layer bent in compression. This crack did not originate at the bond area and therefore was not a result of copper penetration. In fact, it has not yet reached the bond area. It was found in testing that in all specimens given this sharp, flat bend, including specimens of conventional rolled type claddings, a similarly located crack, originating at the lower surface of the bend, occurred as the pressure was released on the testing machine. This was the result of the very severe disturbance of the metal compressed in this area during bending, which allowed it little further ductility when pressure was released (see Fig. 5).

In the slow cooled condition, the martensitic type stainlesses (Type 410 tested) showed results similar to those shown in Fig. 4. Austenitic stainless and pure nickel and high nickel alloy vacuum brazed claddings appeared to have slightly increased ductility of the alloy clad layers and behaved equally well on flat bend tests.

As a matter of comparison, Fig. 5 illustrates bend tests similar to those in Fig. 4 made on conventional rolled types of clad plate with 405 stainless alloy layers.

Fig. 5 Conventional rolled type clad materials bent 180 deg flat upon themselves with alloy layer in both tension and compression

Tests have shown the vacuum brazed high strength bond to be equal to and in some instances higher in shear strength than the conventional alloy clad materials.

Hot and Cold Forming of Vacuum Brazed Composite Plate Materials in Fabrication

Figures 6, 7 and 8 show various angles of a dished and flanged pressure vessel head fabricated from a vacuum brazed composite metal plate consisting of a $^1/_8$-in. alloy layer (Type 405 stainless) on a $^3/_8$-in. A-285, Grade "C" carbon steel base plate.

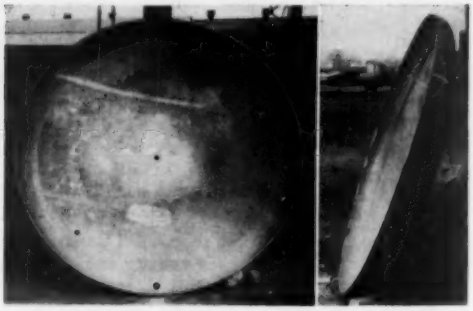

Fig. 6 Front view of dished and flanged stainless Hortonclad pressure vessel head
Fig. 7 Profile view of dished and flanged stainless pressure vessel head

This pressure vessel head was experimentally dished and flanged, the dishing done cold and one-half of the perimeter of the blank being flanged hot (temperature varying between 1330 and 870° F), the other half being flanged cold.

This particular head was fashioned from an $89^1/_8$-in. disk of Hortonclad composite plate into a flanged and dished head of 6 ft 8 in. diameter.

The copper alloy bond remained tightly adherent during all of these very severe reverse bending and stretching operations. This can be seen in the close-up view (Fig. 8) of the edge of the clad head after dishing and flanging had been completed. This dishing and hot and cold flanging operation is one of the most severe tests which can be given a composite clad due to the fact that it brings into play stresses from all directions and especially repeated reverse bending stresses.

Shear Strength of Vacuum Brazed Composite Plates

Shear strength tests on the bond areas of high strength vacuum brazed plates have been concentrated upon during this research to a greater degree than any other test, in order to develop the greatest possible strength commensurate with best ductility of bond. Data are now available on average shear strengths of well over 250 individual Hortonclad plates of various

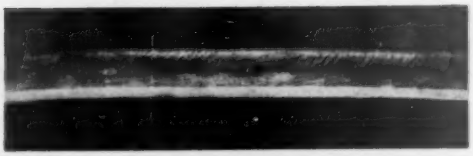

Fig. 8 Close-up of edge of dished and flanged pressure vessel head

sizes and with various types of stainless and nickel and high nickel alloy clad layers.

The results of these many tests show shear strengths for all types of clad plates ranging in total thickness from $^3/_{16}$ to $1^1/_2$ in. of from 35,000 to 60,000 psi, the average being approximately 45,000 psi. It has been our aim to develop an average shear strength in the neighborhood of 40,000 psi for all types of vacuum brazed composite plate, as this strength has proved sufficient for all ordinary operations encountered in pressure vessel fabrication. Adjustments of the bonding cycles can allow higher shear strengths in most cases, however higher shear strengths are unnecessary and if allowed to go too high, can cause a tendency toward embrittlement of the bond layer.

In addition to the above, shear tests have been studied which were made on the bond layer directly below area where traybars, lugs, etc., had been welded to the clad layer. These tests showed no loss in shear strength in any instance due to the effect of the high welding temperatures on the bond layer.

Some of the vessels for which vacuum-brazed clad plate was manufactured are now in service and have been for some time. All of them have proved satisfactory from the standpoint of adherence of bond, physical durability and corrosion resistance of the alloy clad layer to date. Data from these clad materials are included in the shear strength figures quoted above.

Impact Resistance of Vacuum Brazed Composite Plate

In ordinary furnace brazing with copper and copper alloys, the brazing temperatures sometimes cause loss in impact values through raising of the transition temperature of the base steel to within the service temperature range in which the material is expected to operate.

Figure 9 shows a typical graphical representation of the transition temperature range determination on A-285, Grade "C" base steel after the material has undergone the vacuum brazing and heat treatment under the controlled heating cycles developed for this process.

This graph, which was drawn from data obtained from 60 Charpy keyhole notch type impact tests at temperatures ranging from 75 to −60° F., shows the transition temperature to be well below the ordinary service temperature range and in line with transition temperatures found for A-285, Grade "C" carbon steel in the normalized condition.

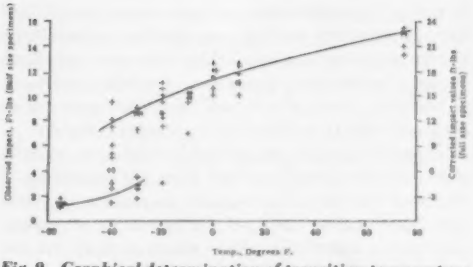

Fig. 9 Graphical determination of transition temperature range for vacuum brazed carbon steel plate

Repeated Heating and Quenching Tests

This type of test was conducted on various types of vacuum brazed stainless and nickel alloy composite clad plates to determine the effect of rapid temperature changes on the bond strength as a result of the known differences in temperature coefficients of expansion between carbon steels and these alloys.

These tests involved heating the composite plate material to 1650° F, holding at this temperature for 30 min, and then plunging the plate into cold (56° F) circulating water. This procedure was repeated five consecutive times for each individual type of vacuum brazed composite clad plate tested.

Each of the materials tested showed negligible loss in shear strength after being subjected to these tests.

Other Physical Tests on Vacuum Brazed Composite Plate

In addition to the tests described above, the high strength bond has also successfully withstood torsion tests, elevated temperature shear tests at 1000° F, pressure tests on the alloy layer, welding tests, tensile strength tests on the copper alloy bonding layer, extensive corrosion tests under controlled laboratory conditions to compare the corrosion resistance of the alloy layer after various brazing treatments with the same alloy which was not subjected to these treatments, and other minor tests considered necessary during development and improvement of techniques and characteristics of the vacuum brazed bond.

The above material has already successfully passed rigid and complete tests conducted by two independent and disinterested laboratories and tests are now in the process of completion in another laboratory. The results of these independent tests have confirmed data gathered in our laboratory from testing over a three-year period of time.

METALLURGICAL ASPECTS OF HIGH STRENGTH VACUUM BRAZING

High strength vacuum brazing can be successfully accomplished with a variety of alloys (in addition to pure copper) consisting of brasses, bronzes, and many proprietary alloys. In addition, a process has been developed in our laboratories which allows silver alloy brazing (50% Ag or thereabouts) under the same conditions as copper alloy brazing, namely without the use of fluxes or introduced atmospheres of any type. This process produces an excellent and continuous bond with satisfactory ductility and high shear strength in the nickel and high nickel alloy claddings (in excess of 50,000 psi). This is considered a step forward in silver brazing techniques, which now require a highly corrosive fluoride flux in order to obtain a satisfactory bond.

In copper and copper alloy brazing by the vacuum process, the vacuum plays a double role. It provides an even, crushing pressure over large areas on the surfaces being joined, necessitating only a very thin layer of brazing alloy. This thin layer of brazing alloy, when furnace cycles are properly controlled, allows a higher percentage of alloying of the steel with the copper or copper alloy layer, which in turn results in shear strengths of bond in excess of the strengths of ordinary brazed joints, which are in the range of 20,000 to 30,000 psi. Sufficient alloying with a very thin copper or copper alloy layer can take place rapidly, thus allowing shear strengths upwards of 40,000 psi in vacuum brazed composite plates without holding the material for excessive periods of time at brazing temperatures, which would result in imparting undesirable characteristics in the composite plate, such as excessive penetration of brazing alloy into the neighboring metals, excessive grain growth, and carbon migration from the base metal to the alloy layer (in the cases of brazing stainlesses to carbon steel).

In addition, the vacuum rapidly and efficiently removes any evolved gases, such as CO_2 at the bonding interface which might otherwise tend to oxidize the cleaned bonding surfaces during heating and bonding, and would inevitably result in weak and discontinuous bonding.

Vacuum Brazing of Nickel and High Nickel Alloys to Carbon Steel

In the vacuum brazing of nickel and high nickel alloys to carbon steels, special techniques are necessary due to the high solubility of copper brazing alloys in nickel and high nickel alloys.

Experimentation has shown the various high nickel alloys to have somewhat different rates of diffusion with copper, and close control must be maintained in the brazing of each alloy type in order to regulate diffusion to the point where optimum soundness and continuity of bond are obtained with the desired shear strengths of bond.

The vacuum process appears to have the facility of engendering increased wettability of the brazed materials for the stainless, nickel alloy and carbon steel surfaces being joined, and in some cases where oxides have been allowed to remain on the bonding

surfaces, proved in the case of carbon steels, the vacuum has the ability to cause these oxides to break down and be removed as gases to some extent at elevated temperatures.

In vacuum brazing for high strength over continuous and large surface areas, preplacement of brazing alloy has been found to be most satisfactory to guarantee uniform bond strength throughout, rather than to depend on distribution of brazing alloy through capillary forces. This applies not only to the brazing of nickel and high nickel alloys to carbon steel, but also to the brazing of other materials, such as stainless steels of all types.

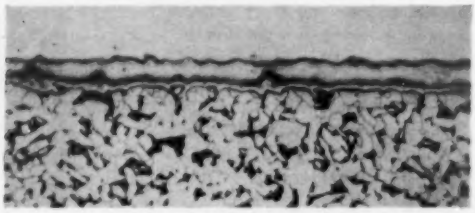

Fig. 10 Vacuum brazed high nickel alloy bond to carbon steel—46,500 psi shear

Figure 10 illustrates a typical high nickel alloy vacuum brazed with copper alloy bond to carbon steel. The alloy layer here is Monel. It will be noted that very little decarburization has occurred in the carbon steel at the bonding interface and copper alloy penetration into the grain boundaries of the carbon steel is not deep. Due to the mutual solubility characteristics of Monel and copper, diffusion of the copper into the Monel layer has proceeded to a noticeable extent.

Vacuum Brazing of Stainless Steels to Carbon Steel

As is well known, stainless steels show a particular avidity for carbon. This appears to be especially pronounced in the austenitic (chromium-nickel) types. In addition, they form a thin relatively impervious oxide film rapidly after cleaning in preparation for brazing, and their ductilities and corrosion resistances can be affected by heat treatments such as encountered during brazing.

For these reasons, and their tendencies to allow intergranular penetration by copper at brazing temperatures, the individual metallurgical characteristics of each particular type of stainless must be taken into consideration and the brazing process must be tailored to fit these individual requirements in order to produce the desired high shear strength bond with sufficient ductility, corrosion resistance and tensile strength.

For instance, in brazing of ferritic and martensitic types of straight chromium stainlesses, such as Types 405 and 410, respectively, cooling rates are of prime importance as far as physical and corrosion properties of the resultant composite materials are concerned. In case of Type 405, best corrosion resistance is obtained through very slow cooling from bonding temperatures. Controlled laboratory accelerated corrosion tests have shown a pronounced decrease in corrosion resistance of the alloy layer of aircooled composite material as compared with that of slow furnace cooled material.

Type 410, of course, being a martensitic type, must be slowly furnace cooled not only from the standpoint of corrosion resistance, but because air cooling or otherwise rapid cooling results in the formation of various degrees of a martensitic phase, which causes a marked embrittling effect and lowering of ductility.

As is well known, the austenitic stainless types exhibit their best properties on quenching, and therefore this must also be taken into account in brazing these alloys.

Inasmuch as the carbon steel layer is also a part of the composite brazed assembly, it too must receive consideration; however, if it is of the low carbon variety, its response to cooling rates is not particularly critical.

In copper alloy brazed plate, the copper or copper alloy brazing material being preplaced and continuous, forms an effective barrier to carbon migration from the carbon steel to the stainless layer (see Fig. 11).

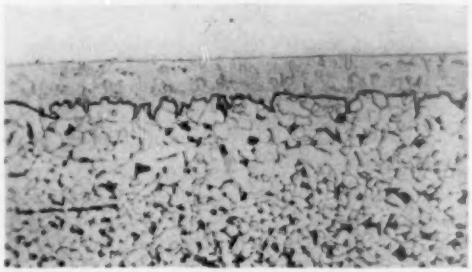

Fig. 11 Vacuum brazed stainless (316ELC) alloy bond to carbon steel—shear strength 45,000 psi

This, however, as experienced with a nickel plated layer in rolled type claddings, does not always give the effect of completely removing the effects of carbon migration, but combined with careful control of time-temperature cycles during bonding, carbon migration is minimized and confined to a very thin layer just above the bonding interface.

The effect of copper acting as a barrier for the passage of carbon is not a new revelation, as for many years it has been a common practice to copper-plate certain areas of assemblies to be carburized to prevent carburization in the areas copper plated.

As a result of removal of carbon from the mild steel at the bonding interface, a narrow decarburized zone in the carbon steel just below the interface is sometimes found to varying degrees of thickness similar to that found in rolled types of claddings. In studying the effects of carbon migration across the bonding inter-

face, however, we have found evidence of a tendency for carbides which break down at the interface to be removed to some extent with evolved gases by the vacuum, thus aiding in the minimizing of carbon migration into the stainless layer. The vacuum also has the advantage of removing oxidizing gases which form to a small extent in the interface rapidly enough to prevent reoxidation of the stainless bonding surface during the heating-up period.

Tests have shown that the slight decarburization which sometimes occurs in the carbon steel at the interface is not of sufficient proportions to cause any noticeable decrease in over-all physical properties of the composite plate.

As mentioned previously, copper has a tendency to penetrate steels at high temperatures, and if allowed sufficient time and if sufficient copper were present, could cause damage to the ductility of the adjacent steels.

Extensive experimental research work has been carried on in connection with this characteristic, and through control of the thickness and placement of the copper and copper alloy brazing layers, plus very close control over brazing cycles, and also important, the tendency of the vacuum to draw off excess brazing alloy, this penetration has been controlled to a degree where its effect is negligible on the physical properties of the brazed composite plate. This is illustrated in the foregoing photographs of severe bends with the alloy layers in tension and in compression, showing the high ductility and strength of vacuum brazed composite plates consisting of dissimilar metals.

Figure 11 illustrates a cross section of a vacuum brazed austenitic stainless composite clad plate bond area. This microstructure shows some alloying of the brazing layer with the adjoining metals. It also shows only very slight decarburization (negligible) of the carbon steel at the interface, and as a result carbon migration into the stainless layer is held to a very minor amount. Copper penetration into the stainless and carbon steels is also minimized by techniques used in the vacuum brazing process.

SUMMARY

1. Vacuum brazing of stainless, nickel and high nickel alloys to carbon steel shows promise of opening new fields in high strength continuous brazing over large areas of dissimilar metals. The ability of vacuum brazing to allow improved and complete bonding without the use of either solid or liquid fluxes or special introduced gaseous atmospheres is expected to allow a greater degree of versatility in the use of brazed joints over large surfaces areas through elimination of the possibilities of nonuniformity of strength due to the presence of brittle entrapped residual flux pockets and discontinuous bonding.

2. The combination of uniformity of bond, accompanied by high over-all shear strengths and ductility of vacuum brazed similar and dissimilar composite metal assemblies (Hortonclad Plate) has enabled continuously vacuum brazed composite metallic materials to meet the ASTM-ASME requirements for integrally and continuously clad plate for use in pressure vessel fabrication.

3. This new cladding adaptation of vacuum brazing has the main advantage of assuring a uniform thickness of alloy corrosion resistant material over the entire clad plate, the thickness tolerances being governed only by those of the as-rolled alloy sheet used in its manufacture.

This process also has advantages such as low scrap loss, elimination of expensive manufacturing equipment, and the ability to produce any type of commercial finish on the resulting alloy surface of the vacuum brazed plate.

4. Through the use of photographs, photomicrographs and research data, it has been shown that through proper process control, the extent and effect of copper penetration into the metals being joined by vacuum copper and copper alloy brazing can be reduced to a negligible factor.

In addition, the copper and copper alloy bond layers serve the very important purpose of keeping carbon migration across the bonding interface in stainless types of Hortonclad plates down to the very minimum.

5. This process has been found useful for joining carbon steel to many other metals such a austenitic, martensitic and ferritic stainlesses, nickel and high nickel alloys, and even to carbon steels themselves.

ACKNOWLEDGMENT

Acknowledgment is made to R. L. Brown, Birmingham Plant, for his original idea of vacuum brazing over large surface areas, which instigated the development of this process.

Weld Cracking of Aluminum Alloys

A simple test has been developed for quantitatively evaluating the crack sensitivity of welds made in aluminum alloys and results are given for several heat treatable and non-heat treatable aluminum alloys

by J. D. Dowd

Abstract

A simple test capable of quantitatively evaluating the crack sensitivity of welds made in aluminum alloys has been developed. In this test the amount of longitudinal cracking in the fillets of an inverted T-joint specimen is used as a measure of the crack sensitivity. The effects of specimen dimensions, preheat temperature, post heating, welding current, and welding technique on the cracking obtained in the test specimen have been evaluated and standard procedures for making the test have been established. Using these procedures, the crack sensitivities of the non-heat treatable aluminum-magnesium alloys, 48-0, 52S-0, XA54S-0 and X56S-0; the heat treatable aluminum-magnesium silicide alloys, 53S-T6, 61S-T6 and 62S-T6; and the high strength heat treatable alloys, Alclad 14S-T6, Alclad 24S-T4, and Alclad 75S-T6, welded with various filler alloys were evaluated. It was found that for any of the plate compositions, welds made with 43S or No. 716 Brazing Wire gave the least amount of cracking but generally had lower ductility than welds made with aluminum-magnesium alloy filler wires. The amount of cracking obtained in welds made with aluminum-magnesium alloy filler wires was found to decrease as the magnesium content of the filler wire increased.

INTRODUCTION

THE development of the inert-gas-shielded arc-welding processes has greatly expanded the use of aluminum alloys for welded assemblies during the past few years. These processes have not only promoted greater use of those aluminum alloys which have been employed in welded assemblies for a number of years but have also made commercially feasible the large-scale welding of other aluminum alloys, for example the aluminum-magnesium alloys.

One of the metallurgical limitations restricting the use of some aluminum alloys for welded assemblies is their susceptibility to cracking during welding. Thus, although welds made in 4S plate with 4S filler wire (for nominal compositions, see Table 1) are strong and ductile, this combination is rarely used because of the susceptibility of the welds to cracking. In the past the solution to this problem has been to use the aluminum alloy with 5% silicon, Alcoa 43S, for the filler wire. Although this eliminated cracking, the welds obtained were always quite low in ductility and frequently quite low in strength. Inasmuch as the use of 43S was not a satisfactory solution, it was desirable to investigate the susceptibility of aluminum alloys to cracking during welding with the ultimate objective of developing alloys that could be used for welded assemblies without encountering cracking difficulties. The first phases of this investigation were to develop a satisfactory test for evaluating weld-cracking and to determine the crack-sensitivity of welds made using standard aluminum alloys for plate and filler wire.

Table 1—Nominal Composition of Alloys

	Percent of alloying elements—Aluminum or normal impurities constitute remainder					
Alloy	*Copper*	*Silicon*	*Manganese*	*Magnesium*	*Zinc*	*Chromium*
2S	99% minimum Aluminum					
4S	..	..	1.2	1.0	...	..
14S*	4.4	0.8	0.8	0.4	...	..
24S*	4.5	..	0.6	1.5	...	..
43S	..	5.0	...	..	...	..
52S	..	..	...	2.5	...	0.25
53S	..	0.7	...	1.3	...	0.25
XA54S	..	..	...	3.5	...	0.25
56S	..	..	0.1	5.2	...	0.1
61S	0.25	0.6	...	1.0	...	0.25
62S	0.25	0.6	...	1.0	...	..
75S*	1.6	..	...	2.5	5.6	0.3
No. 716 Brazing Wire	4.0	10.0	...	..	...	..
Al-10% Mg	..	..	...	10.0	...	..

* The Alclad form of these alloys consist of a "core" of the basis alloy coated with pure aluminum or a suitable alloy.

It should be pointed out that although the data and conclusions presented in this paper are concerned primarily with weld cracking, other factors must also be considered in selecting the filler alloy to be used for a specific application. Among these factors, some of which are discussed briefly in this paper, are (1) ease of fabrication of the filler alloy, (2) soundness and strength of the welds obtained, (3) resistance to general corrosion

J. D. Dowd is connected with the Process Metallurgy Division of the Aluminum Research Laboratories of the Aluminum Co. of America, New Kensington, Pa.

Paper is scheduled for presentation at the Thirty-Third National Fall Meeting, AWS, Philadelphia, Pa., week of Oct. 20, 1952. Closing date for discussion December 15, 1952.

and stress corrosion of the welded assembly and its component parts, and (4) previous experience with the use of the filler alloys.

DEVELOPMENT OF A CRACKING TEST

Early in the investigation, it was recognized that any weld-cracking test should meet certain requirements, among which were: (1) the test should be quite severe so that crack-sensitivity ratings could be obtained for all base alloy-filler alloy combinations; (2) the test specimen should be simple in design and should employ flat sheet or plate; (3) the test should give easily measured quantitative results; and (4) the argon-shielded tungsten-arc process should be employed in welding the test specimens. In an attempt to find a satisfactory test, a number of different types were tried. These included: (1) restrained-weld tests such as used by Pumphrey and his co-workers in England[1] and Hollard in France,[2] in which the cracking in butt welds joining pieces of sheet or plate securely anchored in a rigid frame was used as a measure of crack sensitivity; (2) patch tests in which crack sensitivity was measured by the amount of cracking obtained when a circular patch cut out of a plate was welded back into the plate; (3) an applied-strain test in which an externally applied strain just sufficient to maintain cracking in a butt weld was used to evaluate crack sensitivity; (4) a crater-cracking test in which the cracking in a weld crater was used as a measure of crack sensitivity; and (5) a T-joint test in which the longitudinal cracking of fillet welds in an inverted T-joint was the measure of crack sensitivity. Preliminary tests indicated that only the T-joint test, which is a modification of a British test used to evaluate the crack-sensitivity of welds made in steel, was satisfactory. The other tests were either too complicated, gave inconsistent results, or else produced little or no cracking.

Tentative Procedure of Cracking Test

In setting up the T-joint cracking test, it was recognized that variables such as specimen dimensions and welding conditions would have an effect on the cracking obtained. After making a few preliminary tests, a tentative standard test was established and used to evaluate these variables.

In this tentative test, which will hereafter be referred to as the "standard test," the crack sensitivity was evaluated by using as a measure the amount of longitudinal cracking in the fillets of an inverted T-joint specimen having a $^1/_2$ x 4 x 10-in. vertical member and a 1 x 4 x 10-in. base member. A photograph of such a specimen is shown in Fig. 1. The specimens were welded manually by the argon-shielded tungsten-arc process using a welding current of 350 amp and an argon flow of fifty cubic feet per hour. A General Electric 800 amp a-c welder equipped with a Linde HW-5 torch fitted with a $^1/_8$-in. tungsten electrode was used.

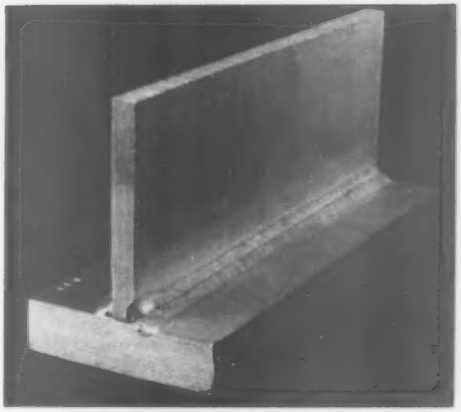

Fig. 1 T-joint cracking specimen

The welding procedure consisted of tacking one side of the vertical member to the base, then welding the other side, after which the tacked side was welded. The welding was done manually by an operator experienced in the welding of aluminum using a normal welding technique. Before each side was welded, the specimen was preheated or cooled, as required, to 300° F. Prior to welding, both the vertical and the base members were cleaned with a power-driven rotary wire brush; and the filler wire was etched with a 5% sodium-hydroxide solution for about 5 mins, rinsed in water, dipped in a 50% nitric acid solution, and rinsed in hot water.

In order to make the cracks that developed during welding more easily discernible, the welded specimens were given a sodium hydroxide-nitric acid etch similar to that used in cleaning the filler wire. After etching, the longitudinal length of the cracking in the fillets was measured and used as an indication of the crack sensitivity.

Effect of Test Conditions on Cracking

The test conditions, which were felt to have an effect on the cracking and which were consequently investigated, were specimen dimensions, preheating temperature, postheating, welding current and welding technique. In evaluating these variables, the standard test described in the previous section was used, except for the variable being investigated.

Specimen Dimensions

In order to determine the effect of specimen dimensions on cracking, the specimen length, the height of the vertical plate, the width of the base plate, the thickness of the vertical plate and the thickness of the base plate were varied, using specimens of 52S-0 plate welded with 52S and 4S filler wires.

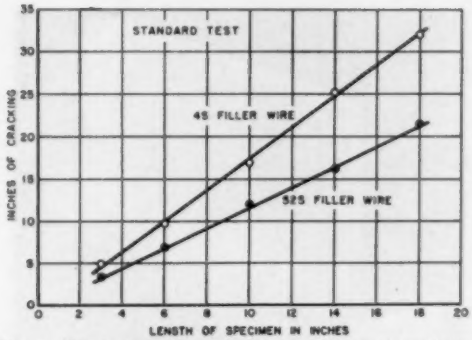

Fig. 2 Effect of specimen length on cracking of welds in 52S-O

As may be seen in Fig. 2, the results of tests to determine the effect of specimen length on cracking showed that for specimens welded with both 4S and 52S filler wires the cracking was proportional to the length of the specimen. Inasmuch as these results indicated that any convenient specimen length could be used, the tentative length of ten inches was adopted as standard, since specimens of this length could be easily obtained from the available plate. It should be noted that with a specimen length of ten inches the maximum amount of cracking that could be obtained would be twenty inches, which would constitute complete cracking of both fillets.

The height of the vertical plate was found to have very little effect on cracking as is shown in Fig. 3. Such being the case, the use of four-inch vertical members was continued. This permitted reusing vertical members by sawing them from previously welded specimens.

Increasing the width of the base plate up to four inches increased markedly the cracking as is shown in Fig. 4. Increasing the width beyond four inches, however, had little effect; consequently, the tentative width of four inches was adopted as standard.

The thickness of both the base plate and the vertical plate was found to have a very great effect on cracking,

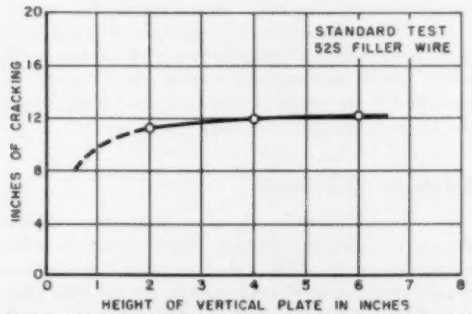

Fig. 3 Effect of height of vertical plate on cracking of welds in 52S-O

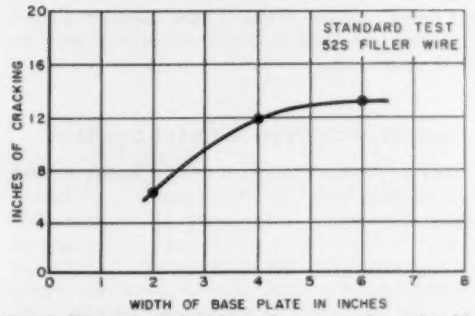

Fig. 4 Effect of width of base plate on cracking of welds in 52S-O

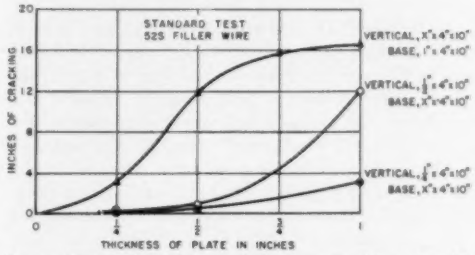

Fig. 5 Effect of thickness of plate on cracking of welds in 52S-O

with the cracking increasing as the thickness of each plate increased. This is shown in Fig. 5. The effect of the thickness of the base plate was especially important, it being necessary to use one-inch plate (with a $^1/_2$-in. vertical member) to obtain cracking in 52S-O welded with 52S filler wire. When one-inch plate was used for the base, appreciable cracking was obtained with vertical members one-half inch thick or thicker. The use of one-half inch plate for the vertical members was continued, since appreciable cracking was obtained and since all the standard alloys were available in this thickness.

From the results obtained in these tests, it was concluded that a specimen having a 1 x 4 x 10-in. base member and a $^1/_2$- x 4- x 10-in. vertical member was quite satisfactory, since it gave appreciable cracking and permitted utilization of available materials.

Preheating Temperature

Another variable having an effect on the cracking was the preheating temperature. The results of tests made on 52S-O plate using 4S, 52S and XA54S filler wires are given in Fig. 6. They showed that the cracking decreased as the preheating temperature increased regardless of the filler alloy used and also that the temperature required to reduce the cracking to a minimum decreased as the magnesium content of the filler alloy increased; 900° F being required for 4S, 700° F for

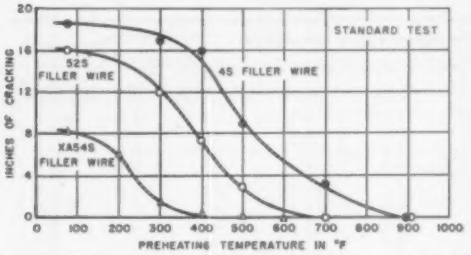

Fig. 6 Effect of preheating temperature on cracking of welds in 52S-O

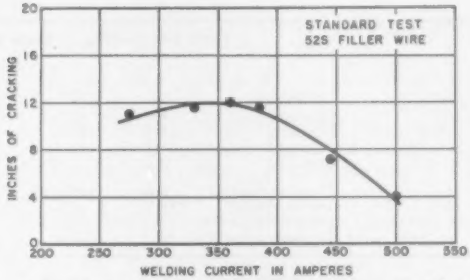

Fig. 7 Effect of welding current on cracking of welds in 52S-O

52S and 500° F for XA54S. A preheating temperature of 300° F was chosen as standard, since the temperature of the specimen after tacking the vertical member to the base member equalized at about 300° F.

Postheating

Tests made on 4S-O plate with 4S filler wire showed that post-heating, i.e., heating the specimen directly behind the welding torch with an auxiliary flame, reduced the cracking from 17 in. to about 6 in. Since postheating reduced the cracking and complicated the test, it was not used in the standard test.

Welding Current

The cracking obtained on 52S-O plate welded with 52S filler wire was found to increase slightly with increasing welding current until a maximum was reached at about 350 amp, after which the cracking decreased rather sharply with increasing current. This is shown in Fig. 7. Since maximum cracking was obtained at about 350 amp, this current was chosen for use in the standard cracking test. It should be noted that it was not feasible to use less than about 275 amp or more than about 500 amp for welding the standard specimen with the available equipment.

Welding Technique

While conducting some of the early tests, it was found that welding technique had a very great effect on cracking, with the cracking decreasing as the operator became more proficient and deposited a smoother weld bead.

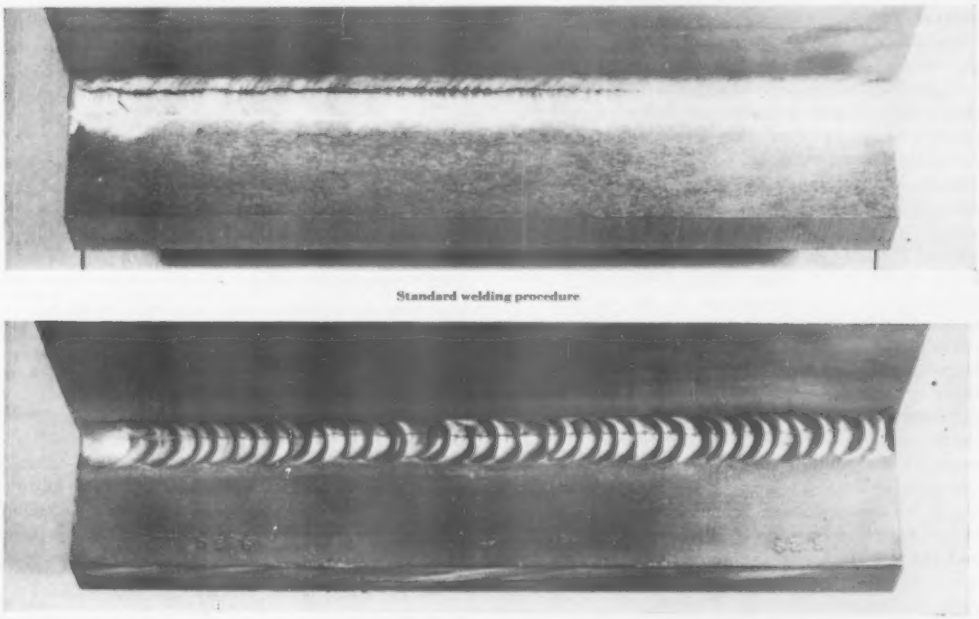

Standard welding procedure

Discontinuous welding procedure

Fig. 8 Appearance of welds made using standard and discontinuous welding procedures (52S-O plate—52S filler wire)

Table 2—Cracking of Welds in Aluminum-Magnesium Alloys

		Inches of cracking obtained using filler wires of							
Plate alloy	*Type test*	*2S*	*4S*	*52S*	*XA54S*	*56S*	*Al-10% Mg*	*43S*	*No. 716 Brazing Wire*
4S-O	Standard	14.0	16.5	16.5	14.0	5.5	0.0	0.0	0.0
52S-O	Standard	16.5	17.0	12.0	0.5	1.0	0.0	0.0	0.0
XA54S-O	Standard	17.5	16.5	9.0	1.5	1.0	0.0	0.0	0.0
X56S-O	Standard	5.0	5.0	0.5	0.0	0.0	0.0	0.0	0.0
4S-O	Discontinuous	6.5	18.0	18.0	16.5	16.0	12.5	5.0	0.0
52S-O	Discontinuous	18.0	17.5	18.0	16.0	15.5	8.5	5.0	0.0
XA54S-O	Discontinuous	17.5	17.5	16.0	14.0	14.5	8.0	2.5	0.0
X56S-O	Discontinuous	17.0	17.0	15.0	12.0	11.0	8.5	1.5	0.0

Therefore, a series of tests was conducted in which the manner of deposition of the weld bead was altered. It was found that by using a torch mounted on an automatic travel carriage it was possible to deposit very smooth welds. Such welds made on 52S-O plate with 52S filler wire did not crack at all. Using the same plate and filler wire, manual welds made by an experienced operator cracked 12 in. The most severe condition was found to be a manual weld in which the welding was discontinuous, that is, a weld in which a single bead was deposited, after which the arc was moved to a point an inch in front of the weld until the bead had frozen and then was returned to deposit another bead, etc., until the entire fillet was welded. Using this procedure, the 52S plate-52S filler alloy combination cracked 18 in. It was also found that many base plate-filler alloy combinations that would not crack using the standard procedure gave measurable amounts of cracking using the discontinuous procedure; for example, 4S-O welded with 43S cracked five inches using the discontinuous procedure but did not crack at all using the standard procedure.

Inasmuch as the discontinuous welding procedure gave some cracking even in 43S welds, it appeared to be ideal for evaluating those base plate-filler alloy combinations having very low susceptibility to cracking. Unfortunately, however, this test proved to be so severe that it was not possible to use it to differentiate among those combinations having moderate or high susceptibility to cracking, since all such combinations gave virtually complete cracking using this test. Consequently, it was found necessary to employ two tests to cover the entire range of crack-sensitivity. The standard test previously described was found to be satisfactory for evaluating combinations having moderate or high susceptibility to cracking and the discontinuous-bead test for combinations having low susceptibility to cracking. Photographs of specimens of 52S-O plate welded with 52S filler wire using the two procedures are shown in Fig. 8. The differences in the appearance of the weld bead and the amount of cracking are quite evident. Throughout the remainder of this paper the test employing the discontinuous-bead procedure shall be referred to as the "discontinuous test," and the test employing the normal welding procedure previously described shall continue to be called the "standard test."

Since many tests would be made using filler wires differing in composition from the parent metal, it was evident that the cracking would frequently depend upon the amount of filler wire used in depositing the weld. Measurements indicated that 40 in. of $^1/_8$ in. diameter wire, the size used in all tests, would give a normal-sized fillet, one having a $^3/_{16}$ in. throat, on one side of a ten-inch specimen. Limits on the wire length of ± two inches were found to be satisfactory.

Table 3—Mechanical Properties of Argon-shielded Arc-Welded One-Inch Thick Aluminum-Magnesium Alloy Panels

		As welded	
Plate	*Filler wire*	*Tensile strength,* psi*	*Free face-bend elongation† % in weld*
4S-O	4S	28,000	26
"	52S	28,000	29
"	XA54S	28,000	27
"	56S	28,000	19
"	Al-10% Mg	28,000	11
"	43S	28,000	12
"	None	23,000‡	..
52S-O	52S	28,000	38
"	XA54S	30,000	29
"	56S	31,000	22
"	Al-10% Mg	29,000	9
"	43S	23,000	10
"	None	25,000‡	..
XA54S-O	52S	32,000	29
"	XA54S	33,000	39
"	56S	35,000	34
"	Al-10% Mg	35,000	11
"	43S	25,000	8
"	None	30,000‡	..
X56S-O	52S	34,000	34
"	XA54S	34,000	19
"	56S	38,000	28
"	Al-10% Mg	32,000	13
"	43S	26,000	8
"	None	35,000‡	..

* Average of full and reduced section specimens. Specimen dimensions and testing procedure described in Reference 3.

† Percent elongation in the outside fibers of the weld. Average gage length of 1.02 in.

‡ Established or tentative minimum tensile strengths of one-inch plate.

Since variations in welding technique, preheat temperature and other factors occur in making the tests, some scatter will exist in the results. The extent of this scatter can best be measured by the standard deviation which was found to be ± 1.8 in. for the standard test and ± 2.6 in. for the discontinuous test.

WELD CRACKING OF STANDARD ALLOYS

In evaluating the crack sensitivity of various alloys, standard and discontinuous tests were made on three

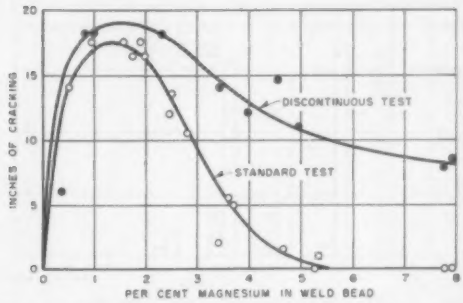

Fig. 9 Effect of magnesium content of weld bead on cracking of welds in aluminum-magnesium alloys

series of alloys, namely, the non-heat treatable aluminum magnesium alloys, 4S-O, 52-O, XA54S-O and X56S-O; the medium strength heat treatable aluminum-magnesium silicide alloys, 53S-T6, 61S-T6 and 62S-T6; and the high strength heat treatable alloys, Alclad 14S-T6, Alclad 24S-T4 and Alclad 75S-T6.

Aluminum-Magnesium Alloys

The crack sensitivity of 4S-O, 52S-O, XA54S-O and X56S-O plate welded with filler alloys of 2S, 4S, 52S, XA54S, 56S, Al-10% Mg, 43S, and No. 716 Brazing Wire were determined by cracking tests of both the standard and discontinuous type. The results, which are given in Table 2, showed 43S and No. 716 Brazing Wire to be the best filler alloys from the standpoint of resistance to cracking. Unfortunately, however, these alloys give welds low in strength and ductility (Table 3) and, consequently, they are not satisfactory for welding the aluminum-magnesium alloys.

The results obtained with the aluminum-magnesium filler wires indicated that the cracking depended upon the magnesium content of the welds as is shown in Fig. 9. With both types of test, the cracking was found to increase from zero at no magnesium to a maximum at about 1.5% magnesium and then decrease with further increase in the magnesium content of the weld. These curves clearly indicate the desirability of using high magnesium-content base alloy-filler alloy combinations in order to minimize cracking problems.

The data obtained with the aluminum-magnesium alloy filler wires are shown graphically in another manner in Figs. 10 and 11, in which the cracking is plotted as a function of the magnesium content of the filler wire for the various base alloys. These curves show that in general the cracking decreases as the magnesium content of both the filler wire and the base alloy increases. There are several exceptions to this; for example, 4S welded with 2S gave less cracking than 4S welded with 4S. In these exceptions, the magnesium content of the welds was less than that necessary to give maximum cracking; therefore, the cracking increased as the magnesium content of the base alloy or filler wire increased.

Although the use of plate and filler alloys with relatively high magnesium contents minimizes weld cracking and increases the mechanical properties of welded assemblies, there are other considerations limiting the magnesium content. One important factor is the susceptibility to stress-corrosion cracking of aluminum alloys containing relatively large amounts of magnesium. These alloys become increasingly susceptible to stress-corrosion cracking with increasing magnesium content. The limiting magnesium content for either the parent metal or the filler alloy cannot be expressed quantitatively, since the susceptibility to stress-corrosion cracking will vary with a number of factors, among the more important of which are: (1) the amount of cold work or plastic deformation imposed on the parent metal prior to welding or on the assembly after welding; (2) the extent of aging at room temperature or at elevated temperatures; and (3) the magnitude of the tensile stresses. Alloys containing about 3.5% magnesium for the parent metal and filler alloys are expected to exhibit a high resistance to stress-corrosion cracking. Tests are in progress to establish maximum magnesium contents consistent with good over-all resistance to corrosion and stress-corrosion cracking. Indications are that the magnesium content for the filler alloy, at least, will be of a higher order, possibly as high as 5.5%. Increasing the magnesium content above 5.5% makes the alloys increasingly susceptible to stress-corrosion

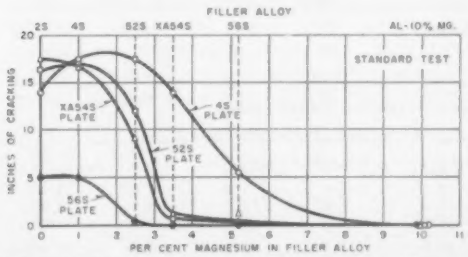

Fig. 10 Effect of magnesium content of filler alloys on cracking of welds in aluminum-magnesium alloys; standard test

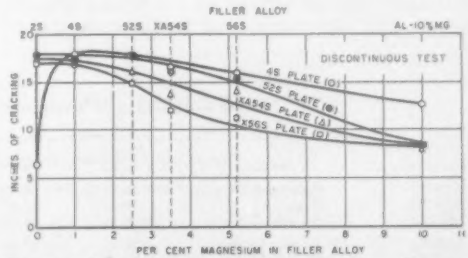

Fig. 11 Effect of magnesium content of filler alloys on cracking of welds in aluminum-magnesium alloys; discontinuous test

cracking and also increasingly difficult to fabricate without appreciably reducing the susceptibility to weld cracking or significantly improving the mechanical properties.

A second important factor that could limit the magnesium content of the filler alloy is the possibility of galvanic corrosion of welds made with such alloys. The solution potential of aluminum is gradually increased with increasing amounts of magnesium in solid solution; and since alloys with high solution potential tend to protect those with low solution potential, the use of filler alloys containing more magnesium than the parent metal or other component parts of the assembly might result in galvanic attack of the filler alloy. This would be especially true under conditions conducive to galvanic corrosion, such as exposure to sea water. In such environments the attack of the filler alloy would be severe if the area of the lower potential surrounding structure were much larger than that of the higher potential weld. It would therefore be desirable in such exposures for the potential of the filler alloy to be as low as or lower than that of the surrounding structure. This factor would tend to limit the magnesium content of the filler alloy, since the solution potential of the high magnesium alloys is greater than that of any of the standard alloys listed in Table 1.

From the various results obtained with the aluminum-magnesium alloys, it would appear that in so far as weld cracking is concerned 52S, XA54S, or X56S plate welded with either XA54S or 56S filler wire should be satisfactory for nearly all welded assemblies.

Aluminum-Magnesium Silicide Alloys

Both standard and discontinuous type cracking tests were made on 53S-T6, 61S-T6 and 62S-T6 plate using filler alloys of parent metal, 52S, XA54S, 56S, Al-10% Mg, 43S and No. 716 Brazing Wire. The 53S-T6 and 62S-T6 plate for these tests was specially prepared since plate is not a standard commercial product for either of these alloys. The results of the cracking tests are given in Table 4 and are shown in the bar graphs in Figs. 12 and 13 for 53S-T6 and 61S-T6, respectively. Since the results for 62S-T6 were essentially the same as those for 61S-T6, they have not been plotted.

It is evident from the results that in so far as weld cracking is concerned 43S and No. 716 Brazing Wire are the best filler alloys for welding the aluminum-magnesium silicide alloys. The next best filler alloys are the Al-10% Mg alloy and 56S which also have the advantage of giving somewhat more ductile joints, especially in the reheat-treated condition, than those obtained with 43S and No. 716 Brazing Wire (Table 5). The Al-10% Mg filler alloy and other filler alloys containing more than about 5.5% magnesium should be used only with caution, however, since welds made with them might be susceptible to stress-corrosion cracking and galvanic corrosion.

Of the three aluminum-magnesium silicide alloys tested, 53S-T6 was found to be appreciably less crack sensitive than either 61S-T6 or 62S-T6 which are about equally crack sensitive. The results indicate that with regards to crack-sensitivity 61S-T6 and 62S-T6 are comparable to 4S-O and 53S-T6 is comparable to XA54S-O.

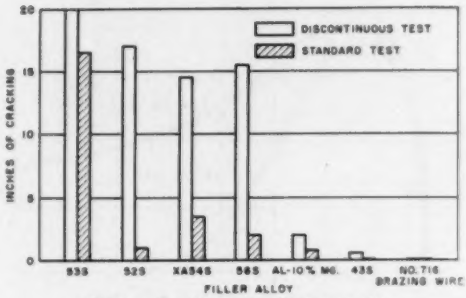

Fig. 12 Cracking of welds in 53S-T6

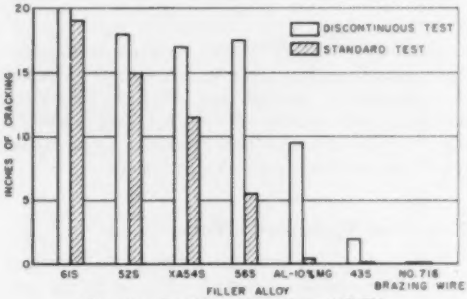

Fig. 13 Cracking of welds in 61S-T6

Table 4—Cracking of Welds in Aluminum-Magnesium Silicide Alloys

		Inches of cracking obtained using filler wires of						
Plate alloy	*Type test*	*Parent metal*	*52S*	*XA54S*	*56S*	*Al-10% Mg*	*43S*	*No. 716 Brazing wire*
53S-T6	Standard	16.5	1.0	3.5	2.0	1.0	0.0	0.0
61S-T6	Standard	19.0	15.0	11.5	5.5	0.5	0.0	0.0
62S-T6	Standard	20.0	11.5	14.5	6.0	0.5	0.0	0.0
53S-T6	Discontinuous	20.0	17.0	14.5	15.5	2.0	0.5	0.0
61S-T6	Discontinuous	20.0	18.0	17.0	17.5	9.5	2.0	0.0
62S-T6	Discontinuous	19.0	19.0	17.5	17.0	13.5	1.0	0.0

Table 5—Mechanical Properties of Argon-Shielded Arc-Welded One-Inch Thick Aluminum-Magnesium Silicide Alloy Panels

		As welded		*Reheat-treated to T6 temper*	
Plate	*Filler Wire*	*Tensile strength,* psi*	*Free face-bend elongation† % in weld*	*Tensile strength,* psi*	*Free face-bend elongation† % in weld*
53S-T6	XA54S	22,000	26	33,000	23
"	56S	21,000	12	33,000	14
"	Al-10% Mg	21,000	9	37,000	14
"	43S	21,000	13	38,000	2
"	No. 716 Brazing wire	21,000	4	41,000	2
"	None	32,000‡	..	32,000‡	..
61S-T6	XA54S	25,000	21	41,000	30
"	56S	23,000	13	37,000	9
"	Al-10% Mg	25,000	8	42,000	16
"	43S	26,000	15	43,000	10
"	No. 716 Brazing wire	24,000	3	45,000	3
"	None	42,000‡	..	42,000‡	..
62S-T6	XA54S	23,000	15	39,000	29
"	56S	23,000	11	40,000	18
"	Al-10% Mg	23,000	9	42,000	32
"	43S	22,000	14	45,000	4
"	No. 716 Brazing wire	23,000	4	44,000	2
"	None	42,000‡	..	42,000‡	..

* Average of full and reduced section specimens. Specimen dimensions and testing procedure described in Reference 3.
† Percent elongation in the outside fibers of the weld. Average gage length of 1.02 in.
‡ Established or tentative minimum tensile strengths of one-inch plate.

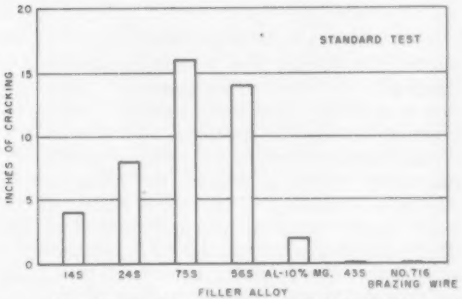

Fig. 14 Cracking of welds in Alclad 14S-T6

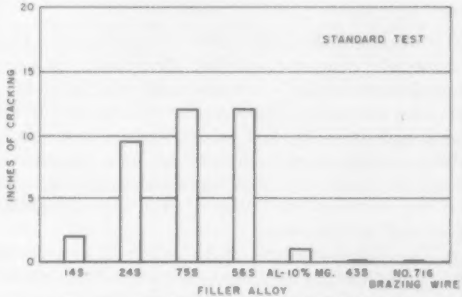

Fig. 15 Cracking of welds in Alclad 24S-T4

High-Strength Alloys

Standard tests were made on the high strength alloys, Alclad 14S-T6, Alclad 24S-T4 and Alclad 75S-T6, using filler alloys of 14S, 24S, 75S, 56S, Al-10% Mg, 43S and No. 716 Brazing Wire. The results are given in Table 6 and shown in bar graphs in Figs. 14, 15 and 16. These results show 43S and No. 716 Brazing Wire to be the most satisfactory filler alloys for welding all three compositions, although low cracking values were also obtained on Alclad 14S-T6 and Alclad 24S-T4 using 14S filler wire. Welds made with filler alloys of 14S and No. 716 Brazing Wire would have the added advantage of being more responsive to heat-treatment

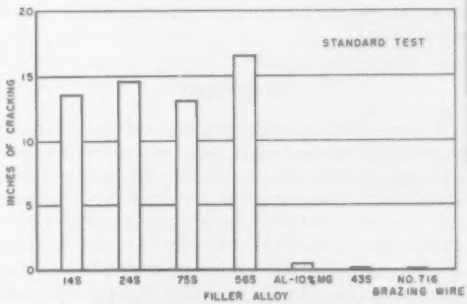

Fig. 16 Cracking of welds in Alclad 75S-T6

Table 6—Cracking of Welds in High Strength Aluminum Alloys

		Inches of cracking obtained using filler wires of						
Plate alloy	*Type test*	*14S*	*24S*	*75S*	*56S*	*Al-10% Mg*	*43S*	*No. 716 Brazing Wire*
Alclad 14S-T6	Standard	4.0	8.0	16.0	14.0	2.0	0.0	0.0
Alclad 24S-T4	Standard	2.0	9.5	12.0	12.0	1.0	0.0	0.0
Alclad 75S-T6	Standard	13.5	14.5	13.0	16.5	0.5	0.0	0.0

Table 7—Mechanical Properties of Argon-Shielded Arc-Welded One-Inch Thick High Strength Aluminum Alloy Panels

Plate	Filler wire	As welded: Tensile strength,* psi	As welded: Free face-bend elongation† (% in weld)	Reheat treated to −T4 or −T6 temper: Tensile strength,* psi	Reheat treated to −T4 or −T6 temper: Free face-bend elongation† (% in weld)
Alclad 14S-T6	14S	31,000	1	60,000	2
"	24S	34,000	3	61,000	3
"	75S	28,000	2	58,000	1
"	XA54S	34,000	4	47,000	6
"	56S	34,000	6	46,000	6
"	43S	34,000	7	43,000	2
"	No. 716 Brazing wire	31,000	1	60,000	2
"	None	67,000‡	..	67,000‡	..
Alclad 24S-T4	24S	34,000	3	50,000	5
"	75S	31,000	2	49,000	5
"	XA54S	34,000	10	46,000	14
"	56S	36,000	12	46,000	17
"	43S	30,000	10	39,000	6
"	No. 716 Brazing wire	31,000	2	38,000	2
"	None	62,000‡	..	62,000‡	..
Alclad 75S-T6	75S	30,000	1	62,000	1
"	XA54S	31,000	5	43,000	12
"	56S	34,000	2	51,000	11
"	43S	27,000	4	....	..
"	None	77,000‡	..	77,000‡	..

* Average of full and reduced section specimens. Specimen dimensions and testing procedure described in Reference 3.
† Percent elongation in the outside fibers of the weld. Average gage length of 1.02 in.
‡ Minimum tensile strengths of one-inch plate.

after welding than similar welds made with 43S. Unfortunately, none of these filler alloys would produce ductile welds (Table 7). Welds made with the Al-10% Mg alloy also had low crack sensitivity; but since welds made with this alloy and other aluminum-magnesium alloys containing more than about 5.5% magnesium might be susceptible to stress-corrosion cracking and galvanic corrosion, such alloys should be used for filler wires only with caution.

Of the high-strength alloys, Alclad 24S-T4 was slightly less susceptible to weld cracking than Alclad 14S-T6 which, in turn, was somewhat less susceptible than Alclad 75S-T6. All three compositions, however, appeared to be more susceptible to weld cracking than any of the aluminum-magnesium or aluminum-magnesium silicide alloys tested.

SUMMARY

A simple test for evaluating the crack sensitivity of welds in aluminum alloys has been developed, and standard procedures for conducting the test have been established. Using this test, the crack sensitivities of the non-heat treatable aluminum-magnesium alloys, 4S-O, 52S-O, XA54S-O and X56S-O; the medium strength heat-treatable aluminum-magnesium silicide alloys, 53S-T6, 61S-T6 and 62S-T6; and the high strength heat treatable alloys, Alclad 14S-T6, Alclad 24S-T4 and Alclad 75S-T6, welded with various filler alloys have been evaluated.

It has been found that of the filler alloys tested, 43S and No. 716 Brazing Wire gave the least amount of cracking in all of the plate compositions. Welds made with these alloys, unfortunately, have low ductility and frequently low tensile strengths. Welds made with aluminum-magnesium filler alloys containing up to 10% magnesium showed, in general, decreasing susceptibility to weld cracking with increasing magnesium content. General usage of aluminum-magnesium filler alloys containing more than about 5.5% magnesium is not recommended, however, since the decrease in the susceptibility to weld cracking obtained by increasing the magnesium content above 5.5% is not felt to be great enough to offset the resultant increase in susceptibility to stress-corrosion cracking and galvanic corrosion. Welds made in the aluminum-magnesium and the aluminum-magnesium silicide alloys with 56S filler wire and in 52S, XA54S and X56S alloys with XA54S filler wire were found to have relatively low-crack sensitivity. Consequently in so far as cracking during welding is concerned, these combinations should be satisfactory for most applications.

References

1. Pumphrey, W. I., and Lyons, J. V., "Cracking During the Casting and Welding of the More Common Binary Aluminum Alloys," *J. Inst. Metals*, **74**, 439–455 (1948).
2. Hollard, Marc, "Cracking Tendency of Assemblies of Welded Light Alloys," *Revue de L'Aluminium*, **27**, 175–185, (May 1950).
3. Howell, F. M., and Nelson, F. G., Jr., "The Strength and Ductility of Welds in Aluminum Alloy Plate," THE WELDING JOURNAL, **31**, (9) Research Suppl., 394-s to 402-s (1952).

Contact Resistance

Contact Resistance of different metals due to current constrictions at the contact and interface resistance due to surface conditions

by Wm. B. Kouwenhoven and Clarence W. Little

SUMMARY

THIS paper discusses the results of the fundamental study of Contact Resistance carried out through the facilities of the Institute for Cooperative Research at The Johns Hopkins University under the sponsorship of the Office of Naval Research Contract Nonr 248(03). The investigation was concerned with the resistance of single-metal contacts of aluminum, brass, bronze, silver and stainless steel; with particular reference to the contribution to contact resistance of spreading resistance due to current constrictions at the contact and the interface resistance due to surface conditions.

The contacts studied were made between the butt ends of solid metal cylinders one-half inch in diameter and two inches long. The butt end surfaces were either milled with "V" grooves to produce equidistant, parallel ridges on the surface, or were milled flat. When two flat-milled surfaces were brought into contact, the actual area was of irregular pattern. A symmetrical pattern consisting of equal sub-divisions of the actual contact area was produced when two ridge-milled surfaces made contact with the ridges of one surface crossing the other at right angles. The number of ridges determine the number of contact points or area subdivisions produced. Contacts having 21, 80, 230 and 1300 sub-divisions were used in the investigation. Six of these cylindrical units with identical surface treatments were aligned in tandem in the loading machine to form a specimen set with five contact surfaces in series. All contacts were made in air and the measurements of the contact resistance were at ambient temperatures. The contact resistances were measured at loads ranging from 230 to 1575 lb. applied axially and with direct currents from 10 to 120 amp and transient currents from 120 to 2000 amp.

The contact resistance, R_c, is the sum of spreading resistance, R_s, and interface resistance, R_i. It is known that spreading resistance may be varied by changing the number of contact points or sub-areas and that it varies inversely as the square root of the number of such points. The interface resistance, however, is independent of the number of contact points and varies with contact area. It was possible, therefore, to separate the measured values of contact resistance into its two components as the number of contact points was accurately known.

Results

Thin film contact (film thicknesses of 30 Angstrom units or less) was established at loads of less than 230 lb. on all specimens tested except the flat milled aluminum specimens.

The value of the spreading resistance can be effectively controlled by varying contact pattern. It was found for all the materials tested, that if the number of contact points for one-half inch diameter specimen was increased to 1000 or more that the spreading resistance became negligible.

The variation in the measured values of contact resistance for the five contacts in series was negligible for silver, slight for stainless steel (both materials having clean surfaces) and greatest for aluminum.

An equation was developed for predicting the contact resistance of materials and the results showed clearly that for the specimens used the contact resistance may be effectively controlled and reproduced.

INTRODUCTION

This paper deals with the laws that apply to the resistance offered by electric contacts as used in resistance welding and in electric circuits. When two metals are brought into contact with each other, the actual area in contact is always less than the apparent area because it is impossible to make perfectly flat surfaces. In general, actual contact will take place only at small subareas scattered over the apparent contact area. The electric resistance of such a contact has two components; one, the spreading resistance resulting from the non-uniform flow of current in the body of the ma-

Wm. B. Kouwenhoven is Dean of Engineering and Professor of Electrical Engineering at the Johns Hopkins University and **Clarence W. Little**, Dr. of Engineering, Johns Hopkins University; Research Laboratories, Allis-Chalmers Manufacturing Co.

Scheduled for presentation at the Thirty-Third National Fall Meeting, AWS, Philadelphia, Pa., week of Oct. 20, 1952. Closing date for discussion December 15, 1952.

terial caused by the failure to make perfect contact, and two, the interface resistance at the contacts caused by the condition of the surface and the characteristics of the material.

This paper describes a technique by which the total contact resistance may be segregated into its two components and each studied separately. This technique made it possible to determine more completely the fundamental laws that govern contact resistance and to develop an equation for the resistance of contacts. This is of value not only in general electrical work, but also in resistance welding where the accurate control of the location and magnitude of the resistance is necessary for the production of satisfactory welds.

THEORY

It may be stated that the total contact resistance, R_c, equals the sum of the spreading resistance, R_s, and the interface resistance, R_i. Thus

$$R_c = R_s + R_i \qquad (1)$$

Consider two clean, film-free metal surfaces that are brought together under a load or force of F pounds; then actual contact will occur only over a relatively small portion of the apparent surfaces in contact. Even polished surfaces flat to a quarter wave length of light still have hills and valleys of over a hundred angstrom units, Å. Actual electrical contact occurs only where the atoms of one metal approach those of the other to within a few Å, corresponding to the normal atomic spacing of the metals. As the force is increased, the hills are deformed either elastically, plastically, or by splintering until the surfaces meet and are wholly mated. The maximum pressure that a given material can withstand without irreversibly deforming is the material hardness or yield point in compression, H, measured in psi. In actual contacts this maximum pressure is reached even at low loads at many points in the apparent contact area. Then if S_b equals the load bearing contact area in square inches, we may write for crossed cylinder type contacts.[1]

$$S_b = F/H \qquad (2)$$

and for ordinary flat surface contacts

$$S_b = 2F/H \qquad (3)$$

Whenever plastic deformation or splintering of some of the hills in a contact takes place then additional subareas are brought into contact. When the force is applied a second time, this new contact pattern will cause a change in the resistance.

The spreading resistance, R_s, in ohms, was determined by Kouwenhoven and Sackett[2] for a single circular contact area centrally located at the base of a solid cylindrical conductor to be:

$$R_s = p\left[\frac{1}{d_2} - \frac{1.409}{d_a} + 0.296\,\frac{d_2^2}{d_a^2} + \ldots\right] \qquad (4)$$

Where p is the specific resistance of the contact material in ohms inches, d_2 is the diameter of the circular contact area in inches, and d_a is the diameter of the apparent contact area (the solid cylindrical conductor) in inches. Kouwenhoven and Sackett[2] also found that dividing the actual contact area into n equal subareas uniformly and symetrically distributed over the apparent contact surface reduced the spreading resistance by the factor of $n^{-1/2}$.

Combining equation (2), (3) and introducing the effect of the subdivision of the contact area gives the spreading resistance for cross cylinder contacts.

$$R_s = \frac{p}{\sqrt{n}}\left(\sqrt{\frac{\pi H}{4F}} - \frac{1.409}{d_a} + \ldots.\right) \qquad (5)$$

and for flat surface contacts,

$$R_s = \frac{p}{\sqrt{n}}\left(\sqrt{\frac{\pi H}{8F}} - \frac{1.409}{d_a} + \ldots.\right) \qquad (6)$$

It is of importance to note in equations (5) and (6) that the specific resistance, p, of the material is expressed as a constant. This condition may not be true in the contact region when plastic flow occurs at the interface nor when high temperature gradients are present, as in spot welds.

The interface resistance, R_i, in ohms, for thin films of adsorbed gases, or oil of approximately single molecular thickness—30 angstrom units or less—is given by the relation.[3]

$$R_i = \frac{\gamma}{S_c} \qquad (7)$$

Where γ is the per-unit-area film resistance in ohms-inches and S_c is the contact area in square inches. The film resistance, γ, depends upon the thickness of the film and the electron work function of the contact materials. This type of film resistance almost invariably exists in contacts which do not have thick tarnish films. It also may exist for thick films where plastic flow ruptures the film. The interface resistance is thus independent of the number of subareas in contact. Instead it depends only upon the total area of the subareas and not on the way they are distributed over the surface. It is also almost independent of temperature, maintaining a constant value down to the temperature of liquid helium.[3]

If we assume that the load bearing area, S_b, is equal to the conducting contact area, S_c, equation (7) may be written

$$R_i = \frac{\gamma H}{F} \qquad (8)$$

The total contact resistance, R_c, for the cross rod type of contact may be obtained by adding equations (5) and (8) and is:

$$R_c = \frac{p}{\sqrt{n}}\left(\sqrt{\frac{\pi H}{4F}} - \frac{1.409}{d_a} + \ldots.\right) + \frac{\gamma H}{F} \qquad (9)$$

In this equation (9) it is assumed that the specific resistance, p, is constant in the contact region; that the load bearing area is plastically produced and equals the contact area: that the n subdivisions of the contact area are circular and distributed uniformly over the surface; and that both contact bodies are of the same material.

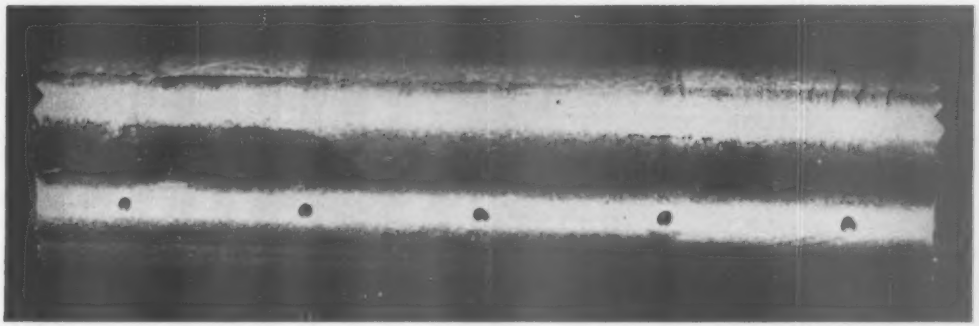

Fig. 1 Specimen set unit

SPECIMENS

In order to verify the theory and the validity of the assumptions, contacts of the cross cylinder type were constructed and tested. The parameters that were controlled were specific resistance, hardness, electron work function, the number of contact subareas, the mechanical load and the diameter of the specimens.

Materials

Silver, brass, bronze, aluminum and stainless steel were selected as contact materials. The silver and aluminum were of very high purity. The specific resistance and the hardness of the materials used are given below:

Material	P Specific resistance (at 24° C) (ohm-inches)	H Hardness (psi)
Silver	0.685×10^{-6}	33,000
Aluminum	1.08×10^{-6}	15,000
Bronze	1.70×10^{-6}	90,000
Brass	2.80×10^{-6}	128,000
Stainless steel	28.5×10^{-6}	244,000

Specimens

A specimen set consisted of six identical units, each unit being a two inch long, one-half inch diameter solid right circular cylinder. The six units for each specimen set were all cut from the same bar, and were mounted one above the other in the testing machine, contact being made between the butt ends of the units. This arrangement provided five equally spaced, equally loaded electric contacts in series. Five holes, each of 0.020 inches diameter, spaced 0.4 inches apart were drilled through each unit perpendicular to the axis. These holes served a dual purpose, namely, for the insertion of thermocouples, and as points of contact for the resistance measuring leads. A unit is shown in Fig. 1.

The subdivision of the apparent contact area into n equal contacts of the cross-rod type was accomplished by milling equally spaced grooves in the butt ends of the units and assembling the six units of a specimen set in the testing machine with the ridges of the adjacent units at right angles. The resulting contact pattern was therefore of the crossed cylinder type. Fig. 2 shows a specimen set, with the leads and thermocouple in place, in the testing machine. Five specimen sets of each material were made, one having five ridges; one, ten; one, twenty; one, forty; and one, flat-milled end surfaces. The grooves in these sets were cut with a 90° cutter. Additional specimen sets were made using V cutters having other angles in order to determine the effect of the ridge angle.

Testing Machine

The Testing Machine was of the dead-weight load type. Force was applied axially to each specimen set

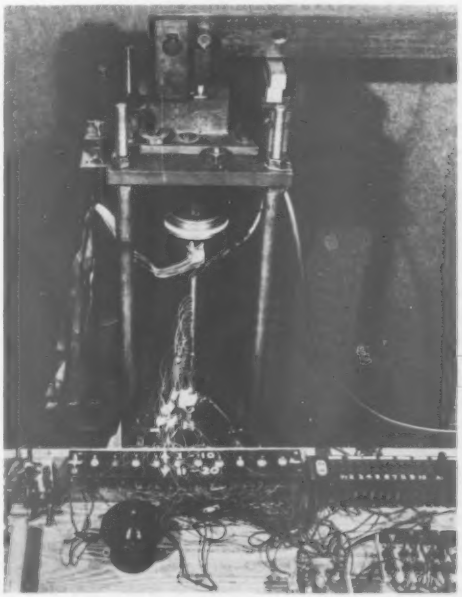

Fig. 2 Specimen set mounted in testing machine

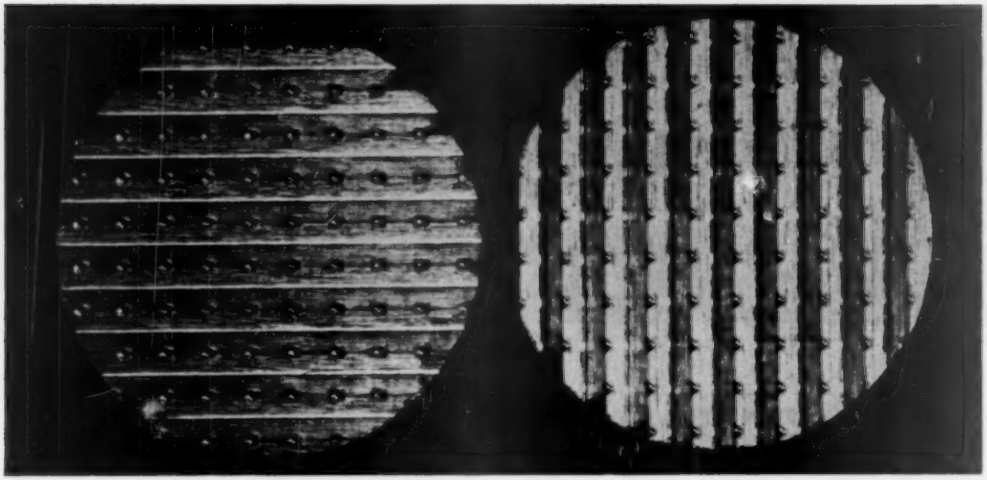

Fig. 3 Contact pattern

through steel loading rods mounted on spherical joints at the upper and lower ends of the machine. When the load was applied to a set, small contact subareas were formed plastically at each ridge cross-over point. The resulting contact pattern is shown in Fig. 3. The number of subareas in actual contact was found to be 21, 80, 320 and 1300 for the five, ten, twenty and forty ridges specimen sets, respectively. The circumferential uniformity of the loading of a specimen set was checked by strain gages mounted at 90° intervals on the upper and lower steel loading members of the testing machine.

EXPERIMENTAL PROCEDURE

A specimen set with a given value of n contact subareas, with the thermocouple and voltage measuring leads in place was assembled in a "V" block and placed between the loading members of the testing machine. The no-load readings (10 lb) of the strain gages were noted, and then an axial load of 230 lb was applied to the specimen set. The strain gage readings were checked for uniformity of loading and then a direct current of 10 amp was sent through the set. When temperature equilibrium was reached, the voltage drop across each of the five contacts and the voltage drop across the body of each of the six units in the set were measured using a potentiometer. In order to eliminate thermal and contact emfs, readings were taken with reversed current and the result averaged.

Current Values

The initial run at 10 amp was followed by runs at 40, 80 and 120 amp. After these runs had been completed, the 10 amp run was repeated. In addition, a number of resistance values were measured using transient currents of the order of 2000 amp, with a duration of 1.5 milli-seconds.

Loads

The specimen sets with 21 contact points were tested at 230 lb load at the current values stated above; they were then removed from the testing machine.

The sets with 80 contact points were first tested at 230 lb and the current values. Then the load was increased to 920 lb and the current runs repeated. They were then removed from the testing machine.

The specimen sets with 320 and 1300 contact points and the set with flat-milled end surfaces were tested first at 230 lb load, then at 920 lb and lastly at 1575 lb, the current runs being made at each load. When these were completed, the sets were removed from the machine.

After each set had been removed from the testing machine, the diameter of the indentations in the ridges was measured using a Jones and Lamson Bench Comparator at a magnification of 150. The total contact area, S_c, in square inches was calculated from these measurements.

Contact Resistance

The contact resistance of each contact was determined by subtracting the corresponding body resistance from the resistance found for the span that included the contact. The data used in the computation of contact resistance, R_c, was based on the measurements taken at ten amperes after the current cycle had been completed. Under these conditions the temperature variation between individual contacts was negligible.

Temperature

Readings were taken only when temperature equilibrium had been reached. The three centrally located contacts of a set did not differ by more than 0.1° C

at the highest current values. The two end contacts were four to five degrees lower in temperature than the central contacts at currents of 120 amp. The equilibrium temperature at 120 amp was of the order of 40° C or about 17° above ambient.

RESULTS

The contact resistance, R_c, calculated from the resistance readings included both the spreading resistance, R_s, and the interface resistance, R_i. It may be seen from equation (6) that the spreading resistance varies inversely as the square root of the number of contacts, n, and from (8) that the interface resistance is independent of the value of n. Therefore, we may write:

$$R_c = C_1/\sqrt{n} + C_2$$

Where C_1 and C_2 are constants for a given material, and specimen set at a given load. Since R_c and n are known, C_1 and C_2 may be determined by solving simultaneous equations. The value of $C_1/\sqrt{n}$ was taken as the experimentally determined spreading resistance and that of C_2 as the interface resistance. In calculating C_1 and C_2 the minimum value of R_c for the five contacts in series was used.

Brass

A typical set of results are given in Fig. 4 for the brass specimens at a load of 230 lb. The values of the contact resistance, R_c; the experimentally determined spreading resistance, R_s; the theoretical spreading resistance as calculated from equation (5), and the interface resistance, R_i, are plotted against the number of contact subareas, n. In the figure, the total spread of the values of R_c as found for the five contacts that make up a specimen set are shown by the shaded portion of the curves. It will be seen that at $n = 1300$ the values of R_c are not in line with those for the other values of n. This discrepancy is due to the fact that at this load a number of the possible 1300 contact points had not yet made actual physical contact. In tests at increased loads both the discrepancy and the spread became less.

It is evident from Fig. 4 that the experimental spreading resistance is higher than that given by the Kouwenhoven—Sackett theoretical equation (5). The increase may be caused by variations in the specific resistance of the material with plastic flow, by non-conducting surface films on the contact interface, by additional resistance due to the grooves, or to some other variable that has not been taken into account. In Fig. 4 are also plotted the experimental results for specimen sets having ridge angles of 60° and 45°. Their values fall on the curve for the standard 90° ridge angle which was used for the majority of the specimen sets. (It might be noted that the body resistance of the 60° and 45° ridge angle specimen sets was slightly higher—about 5%—than the body resistance of the 90° specimen sets.

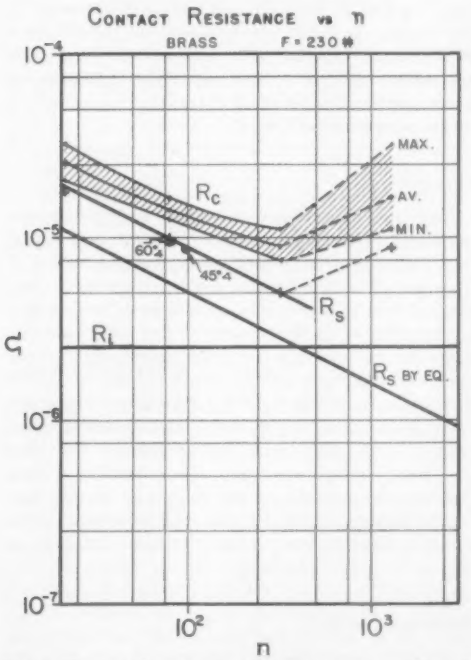

Fig. 4 Curves of contact resistance versus number of contact points for brass

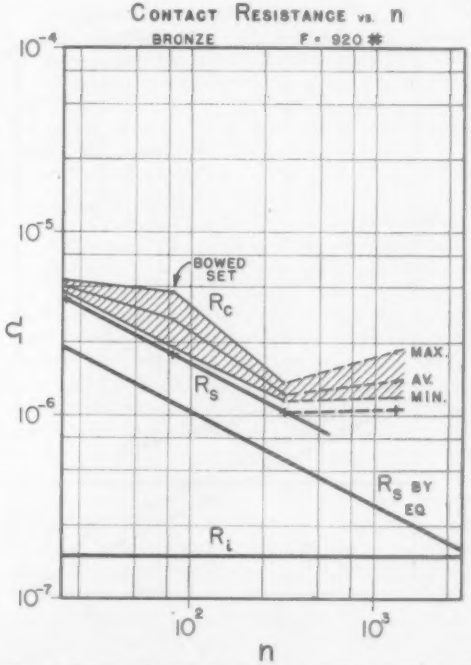

Fig. 5 Curves of contact resistance versus number of contact points for bronze

If this correction term were not used the 60° and 45° points would lie just above the 90° curve instead of just below it, as shown.)

Bronze

In Fig. 5 the results are given for the bronze specimen sets at a load of 920 lb. This figure illustrates clearly what happens when the alignment of a specimen set is faulty. The specimen set for $n = 80$ was slightly out of plumb and showed a slight bow. It is clear that under these conditions the spread of the values of R_c is several times greater than those of the specimen sets for $n = 40$ and for $n = 320$. It was interesting to note that the high values of R_c occured at contacts with the least symmetrical pattern. For the bronze specimens it should also be noted that the experimental values of R_s are larger than the theoretical ones.

Silver

The results obtained with the pure silver specimens sets are plotted in Fig. 6 for a load of 230 lb. The silver specimens were machined and kept under a dry, sulphur-free oil and therefore had little if any surface tarnish film. The oil was removed immediately prior to the assembly of the specimen sets in the testing machine. The contact resistance of the five contacts

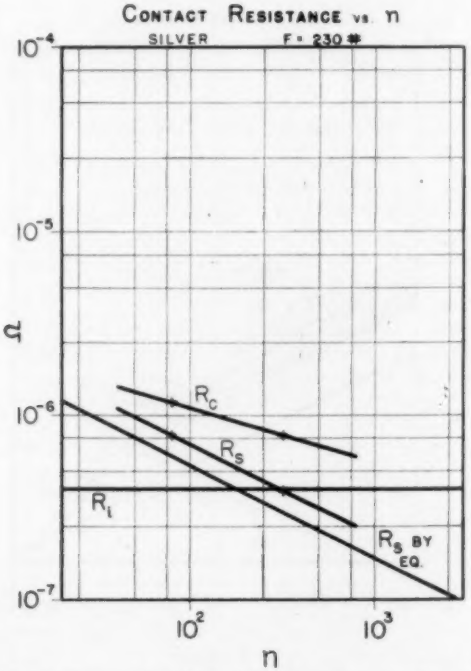

Fig. 6 Curves of contact resistance versus number of contact points for silver

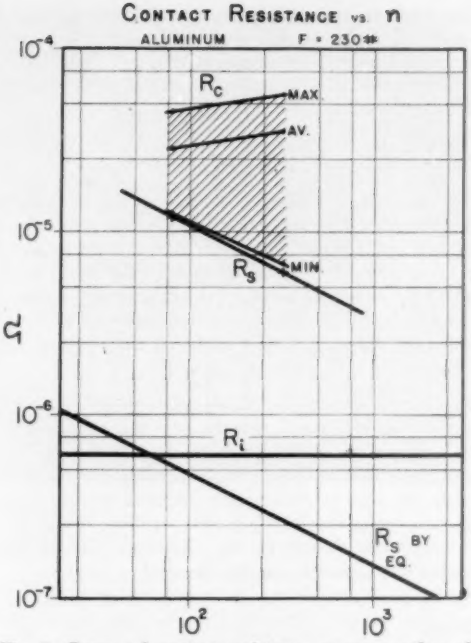

Fig. 7 Curves of contact resistance versus number of contact points for aluminum

was found to be identical, and there was no spread in the results. It should also be noted that the difference between the experimentally determined R_s and its theoretical value is a small one. The difference for silver was found to be smaller than that found for any of the other materials tested.

Aluminum

The aluminum was of extremely high purity and very soft. Runs were only feasible at a load of 230 lb. The results that were obtained are given in Fig. 7. The spread of the contact resistance values is very large as was to be expected with a metal having such a tenacious oxide film coating. The experimentally measured value of the spreading resistance was more than ten times the corresponding theoretical values. In the test made with the flat-milled end surface aluminum specimen set the spread in the measured values of contact resistance was very much larger than that found for the specimen sets with controlled contact pattern. The spread of the R_c results for the flat-milled surfaces was forty times the maximum spread found with controlled contact patterns as given in Fig. 7.

Stainless Steel

Stainless steel specimen sets were made with two values of contact points, namely $n = 80$ and 320.

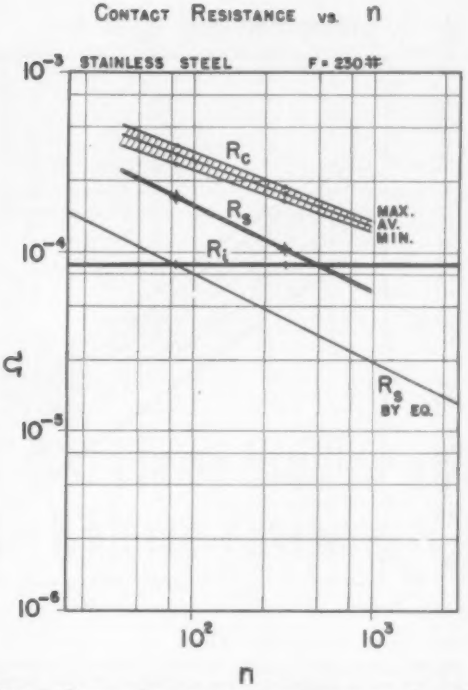

Fig. 8 Curves of contact resistance versus number of contact points for stainless steel

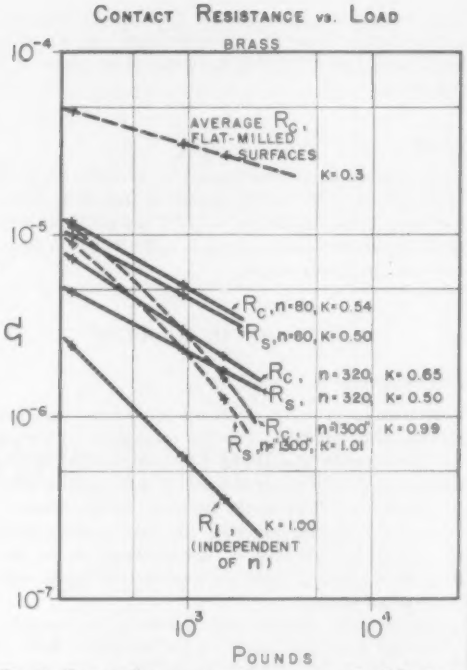

Fig. 9 Curves of contact resistance versus load for brass

The results of the runs on these sets for a load of 230 lb are given in Fig. 8. The spread of the contact resistance, R_c, values is small as would be expected for this material with its clean, thin-film surface. The figure shows that the experimental spreading resistance curve lies considerably higher than the theoretical curve for R_s. Stainless steel had the largest specific resistance of any of the materials tested and the difference between the experimental and theoretical values of spreading resistance is also the greatest; provided aluminum, with its tenacious oxide film, is neglected.

Contact Resistance vs. Load

In Fig. 9 is plotted a typical group of curves showing the variation of contact resistance, R_c; spreading resistance, R_s; and interface resistance, R_i, with load for brass specimen sets. These curves are plotted on log-log paper and the slope of each curve is indicated by the corresponding K. It is evident from Fig. 9 that specimen sets with $n = 80$ and 320 are in accord with the theory as given by equation (9). It is also clear that R_i follows the theory. The specimen sets with $n = 1300$, however, do not fall into line. This is due to the fact that it was not possible to machine these so as to provide uniform contact at all points on the surface. The curves bent downward with increasing load because the number of points in actual contact also increased with load. Neither do the flat-milled specimen sets conform to theory. It is also of interest to note that the experimental spreading resistance curve for $n = 1$ at the loads shown in Fig. 9 would lie close to the average R_c for the flat-milled specimens.

Transient Currents

The value of the contact resistance for transient currents was investigated for a number of specimen sets. The transients were produced by discharging a capacitor, charged to a given direct current potential, through the specimen set. The voltage drop and the currents were recorded on photographs of the oscilloscope traces of the transients. In all, 94 records were taken of the capacitor discharges. The time constant of the circuit was 1.5 milliseconds and the maximum current was of the order of 2000 amp, equivalent to a current density of slightly more than one million amperes per square inch. For specimen sets with controlled contact patterns the ratio of the transient contact resistance to the transient body resistance was practically the same as that obtained from the continuous current measurements. For the flat-milled specimen set, however, the contact resistance was about one-fourth of that determined with continuous current. This large reduction in contact resistance for the flat-milled specimen contacts may be due to a capacity

effect caused by a considerable part of the apparent surfaces, which although extremely close together were not in actual electric contact, acting as the plates of a capacitor.

Error

The probable error in the results is of the order of ± 5 percent. One of the causes of this error is the fact that it was impossible to know the exact position of the resistance measuring leads in the 0.02 inch diameter holes in the specimens.

DISCUSSION OF RESULTS

Experimental R_s

The experimentally measured spreading resistance was found to be higher than the value given by theory for all specimen sets. This difference may be due to changes in the specific resistance, p, under plastic flow; to temperature effects at the interface; to the incorrectness of the assumption that the load bearing area, S_b, and the contact area, S_a, are identical; to the fact that all n contact subareas were not of equal size; or to other causes.

One probable cause of this increase is the variation in specific resistance produced by the plastic flow of the metal areas in contact. In the theoretical derivation of equation (5), p was assumed to be constant. If it is a space variable then the solution of the basic field equation is quite different. The increase in the experimental R_s was the least for silver having the smallest value of p and greatest for stainless steel having the largest value of p. This is evident from a comparison of Figs. 6 and 8. The silver and the stainless steel were the two specimen sets having the least amount of surface films. The other metals studied, having thicker surface films, show a greater spread in the measured values of contact resistance, R_c. Their specific resistances, however, are intermediate between those of silver and stainless steel and their experimental R_s curves differ from the theoretical R_s curve in porportion to their respective values of p. This may also be seen from a study of Fig. 10.

Number of Contact Points

The curves for the materials studied show that the spreading resistance, R_s, can be effectively controlled by varying the number of contact subareas, n. The curves also show that for n equal to about 3000 (approximately 15,000 for a contact of one square inch in area) that the value of R_s becomes less than one micro-ohm, and effectively disappears, being negligible compared to R_i.

Interface Resistance, R_i

Figure 9 shows clearly that, for thin surface films and

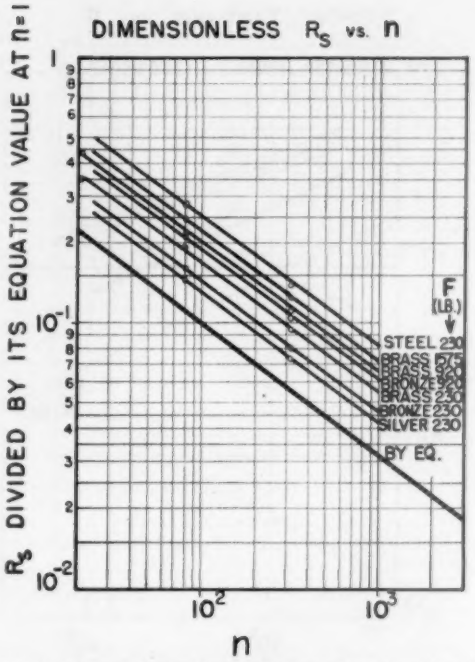

Fig. 10 Curves of spreading resistance versus number of contact points plotted on a per unit basis for steel, brass, bronze and silver

the materials studied, the interface resistance may be controlled by varying the load on the contacts. It is independent of the contact pattern. In Fig. 9, the R_i curve is common to all of the R_s curves shown.

Control of Contact Resistance, R_c

The contact resistance may be controlled by varying either of its two components. The spreading resistance may be controlled by using a definite contact pattern and may be reduced by making the number of contact points large. For reproducible results, there is a value of n which should not be exceeded. The surfaces should be clean or at least free from thick films. Increasing the force on the contacts will reduce both the spreading and the interface resistance. A high value of contact resistance may be obtained by making $n = 1$ as in a projection weld and by the use of a small diameter projection.

CONCLUSIONS

The following conclusions may be drawn from this investigation:

1. A method, the use of a definite contact pattern, has been developed which makes it possible to separate the contact resistance into its two components, spreading resistance and interface resistance.

2. The value of the spreading resistance, R_s, was found to vary inversely as the square root of the number of contact points n, as predicted by theory.

3. The experimentally measured values of spreading resistance were found to be higher than those predicted by theory.

4. The spreading resistance is larger than the interface resistance for values of n of less than 1000 at loads greater than 100 lb. It is a major component of the contact resistance for thin film metal contacts made in air under static loads.

5. The contact resistance can be controlled and accurately reproduced with materials having only thin surface films.

References

1. R. Holm, *Electric Contacts*, Gebers, Stockholm (Sweden), pp. 7–9 1946.
2. Kouwenhoven and Sackett "Spreading Resistance," The Welding Journal Research Supplement 29, p. 512, 1950.
3. Holm, "Electric Contacts" (Book), Sections 21 and 22.

Basic Flame Studies and Their Relationship to Welding Equipment

Study of factors affecting stability of propane flames and the relationship of these factors to welding and heating equipment

by James A. Browning and Merle L. Thorpe

LITTLE is known concerning the actual chemical and kinetic processes of combustion. However, a considerable amount of experimental work has been conducted to determine the stability limits of both oxy-fuel and air-fuel flames. The designer of combustion equipment is mainly concerned with the performance of his equipment over a wide range of operating conditions, and knowledge of the limits of stability can ease his job considerably.

The experimental results shown in Figs. 3 and 4 have been taken from a study of flame stability conducted at the Thayer School of Engineering, Dartmouth College under the sponsorship of the Office of Naval Research. Results obtained for propane are presented. The stability diagrams for various other gases such as acetylene, butane and the liquid fuels typified by normal-heptane would appear similar to those for propane except for the values of the coordinates.

The flame produced by most welding equipment is of the Bunsen type similar to that shown in the sketch of Fig. 1. The oxygen which is present in the combustible stream burns with the fuel to form the intense inner cone, while the secondary combustion is the result of additional burning due to the presence of atmospheric oxygen. A sectional view taken through the center of the primary cone would appear as shown in Fig. 2. The cone itself is a thin shell, or region, of combustion. This combustion zone establishes itself in such a fashion that at every point along its surface

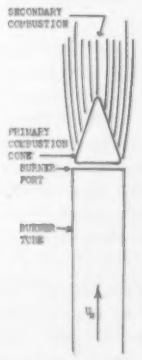

Fig. 1 Stable laminar flame burning at burner port

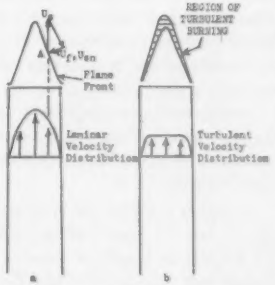

Fig. 2 Section views of stable laminar and turbulent flames

James A. Browning is Assistant Professor of Mechanical Engineering and **Merle L. Thorpe** is Research Assistant with the Thayer School of Engineering.

This research was conducted under the auspices of Project Squid, jointly sponsored by the Office of Naval Research and the Office of Air Research under Contract Nonr 438(01).

the component of the stream velocity in a direction perpendicular to the surface is equal to the flame velocity. If the flame velocity U_f (the rate at which the flame propagates itself into the unburned mixture) at a point is higher than the stream velocity at that same point, then the flame would move to a new position of equilibrium. If a new equilibrium condition cannot be attained, then the flame flashes back into the tube. In like fashion, if the stream velocity is at every point higher than the flame velocity the flame is extinguished. Point A in Fig. 2 (a) illustrates such a point of equilibrium. Assuming that the laminar velocity profile remains constant at points above the tube, then the component U_n of the stream velocity U_s normal to the flame surface is equal to the flame velocity U_f. (In the actual case this parabolic velocity distribution is lost due to the thermal expansion of the stream issuing from the burner port.)

The stability diagram for mixtures of propane and air is shown in Fig. 3. It should be noted that this diagram is divided into several discrete regions, each of which represents a different type flame. The portion shown by means of horizontal lines is for a flame burning stably at the burner port. If, beginning at point A the stream velocity is increased keeping the fuel percentage constant, a point is reached where the flame blows off and is extinguished. Decreasing the stream velocity may result in flashback into the tube. When the fuel percentage reaches that of C blowoff no longer occurs. Rather, the flame jumps to a lifted position. Further increase of the stream velocity blows out the lifted flame.

A flame which is burning in the lifted position drops back to the burner port at a stream velocity lower than that at which it was originally lifted. A unique condition exists between points D and C. A lifted flame can be blown out at a stream velocity lower than that at which a stable flame blows off. Thus, the only way a lifted flame can be produced within this region of the diagram is to ignite the mixture at a position well above the port and at a stream velocity higher than the drop-back velocity.

Although a stable flame is produced throughout the region shown, most welding and heating applications are limited to a narrow band of fuel percentages. At higher fuel percentages the flame becomes luminous and is an inefficient producer of heat. At high air concentrations the flame is again too cool. The optimum fuel percentages for heating purposes lie between about 8 and 25%.

Figure 4 shows the stability diagram for mixtures of oxygen and propane. Comparison with Fig. 3 indicates the great difference between oxy-fuel and air-fuel flames. The most significant change is that of stream velocity. The velocities associated with blow-off for the oxygen system are about ten times greater than those for air. Also, the characteristic shape of the stability diagram has changed considerably. In the air-fuel diagram the blowoff curve blends smoothly

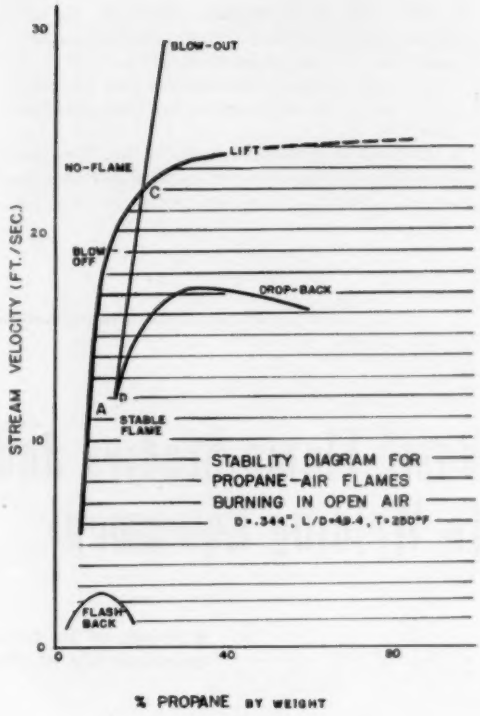

Figure 3

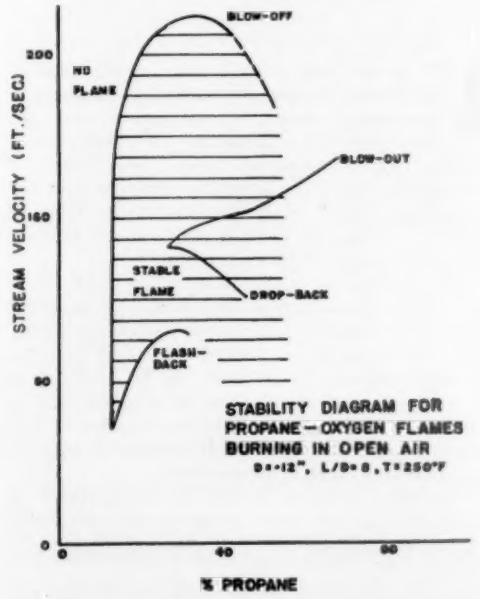

Figure 4

into the lift curve. This is no longer true for the oxygen flame. The blowoff curve rises steeply to a maximum value of 260 fps at 33% propane by weight. Beyond this peak the stream velocity falls off rapidly. An oxygen flame will not jump to a lifted position of equilibrium when small tubes are used.

At low fuel concentrations blowoff of an air-fuel flame results and the flame is extinguished. As the fuel content is increased beyond point *C* of Fig. 3 lift can occur. The boundary region surrounding the jet issuing from the burner tube is enriched with fuel transferred from the jet. When the fuel content is sufficiently high a flame will establish itself in this boundary layer by virtue of its burning velocity being equal to the reduced stream velocity at an elevated position. This equality allows a lifted flame to form. In the case of the oxygen flame the velocity gradient g (the change of velocity with distance from the tube wall in sec^{-1}) is so great at stream velocities higher than blowoff conditions that the concentration of fuel in the boundary layer can never reach the point where the flame can jump by itself to the lifted position. Further inspection of Fig. 4 shows that a lifted flame can occur if the combustible jet is ignited at a position well above the port with the stream velocity and mixture proportions adjusted to those values which will fall between the blowout and drop-back curves.

A common fault of oxy-fuel torches is the continued burning of the mixture after flashback has occurred. The design of the tip orifices, which are equivalent to the burner tube in the above discussion, can lead to a minimum of flashback. These passages should be made of such diameter that the stream velocity through them is well above the maximum flashback velocity as shown in Fig. 4. It would seem then that a greater number of small diameter holes for cutting tips would serve better than a fewer number of large holes. However, the smaller the holes, the more difficult are tip manufacturing problems. Also, small holes can be clogged easily. Some optimum size can be found. In the design of welding tips there is not the freedom of choice as to hole size. One hole must supply the full amount of mixture. With this type tip flashback occurs readily when the stream velocity is reduced below a certain critical value. For the case when the stream flow is momentarily halted, as when the tip is brought up against a solid surface, flashback cannot be prevented. The problem is now to design the torch passageways in such a fashion that the flame which burns back through the mixture is extinguished. A complete cure for this situation is given by post-mixing of the oxygen and fuel. The two fluids are brought together at a point beyond the end of the torch tip. However, the mixture produced is far from homogeneous, resulting in a poor flame.

In the cutting torch field head-mixing of the oxygen and fuel is quite popular. In the case of flashback the flame can only travel back to the point where the two fluids first meet. The hazard of having continued burning in the torch handle is eliminated.

What factors lead to the continued burning of the flashback flame? They are the same causes which will lead to the establishment of a lifted flame in Fig. 4. If the stream velocity in the passages is less than that shown by the curve for blowout, then a flame similar to a lifted flame can occur within the torch itself. The oxygen supply must be turned off until the flame dies out. A maximum diameter for these passages can be found below which no internal sustained burning is possible. The throttling effects of small holes comes into play if the diameters are kept too low. Again, an optimum size can be found.

A second reason for this troublesome burning is the result of noneven flow through the torch. Any abrupt change in passageway diameter, any mixing device placed in the stream, or passage wall roughness will lead to local zones of turbulence with resulting eddies. The local stream velocities in such an eddy may be lowered to the point where a flame can be stabilized. Connections between individual parts of the torch must provide transitions as smooth as possible. Venturi passages must be designed with diffusers which will give as even a flow as possible. This means holding the divergence to less than 15 deg. of included angle so that separation from the wall is not possible.

It is common practice to provide a series of small holes which lead the combustible mixture to an annular chamber within a cutting tip. A flashback into this portion of the tip may produce lifted flames above these orifices. Better design would be to allow controlled expansion of the mixture into the annular chamber in such a fashion that turbulence is reduced to a minimum.

The discussion thus far has made use of the assumption that the burning phenomena within a restricted passage is in all ways identical to that of the same flame burning in the free atmosphere. This is not quite the case. The quenching effect of the tube walls and lack of secondary oxygen come into play. It is hard at this point to say how great a difference exists between the two types of flames. A close inspection of the open flame leads to the qualitative approach dealt with so far. A further study simulating actual conditions should be made. A series of different sized mixing tubes should be tested as to their resistance to sustaining a flame after flashback. This experimental trial-and-error approach would lead to a satisfactory design under any one set of conditions. In fact, the values of the controlling parameters covering a wide variety of conditions might be discovered.

Much of the work conducted to date in the Thayer School laboratories has been in the field of liquid fuels. The paraffin series produce comparable flames. Propane, butane, normal-heptane, iso-octane and gasoline have been tested. Their stability curves are surprisingly similar, and can generally be illustrated by Figs. 3 and 4. The maximum stream velocities produce the hottest flames. Under these conditions the reaction rate between the uniting molecules is highest with the greatest amount of heat release per unit of volume. To provide this high reaction rate an excess of oxygen

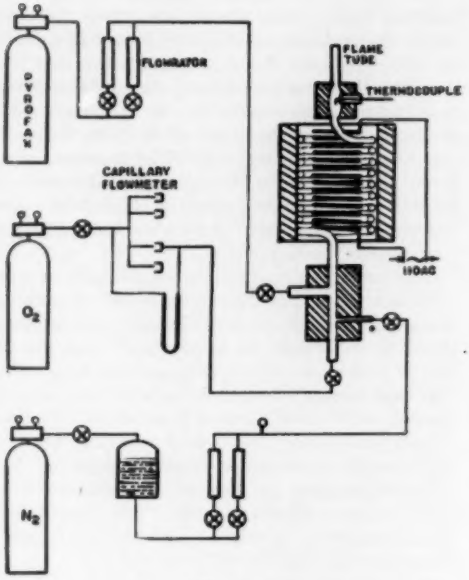

Figure 5

must be supplied. The oxidizing flame which is produced by the paraffin series is not suited for fusion welding, and is limited to cutting, heating and brazing operations. To date the most successful welding flame is provided by the oxy-acetylene combination. Its high reaction rate and release of heat of formation during combustion allows a high temperature, neutral or reducing flame to be used.

Benzene-oxygen produces a flame which is in most respects equivalent to the oxy-acetylene flame. While continued observation of the oxy-paraffin flames could be accomplished using the naked eye, the benzene flame had to be observed through dark glasses. Its intensity of radiation is nearly equal to that of acetylene. Preliminary welds of $^1/_4$ in. thick steel strap were broken in a testing machine and were found to be free of oxidation. Benzene can be formed by passing acetylene through a hot iron pipe. The reaction is: $3C_2H_2 \rightarrow C_6H_6$. However, the heat of formation of benzene is less than that of acetylene with the result that the flame temperature is slightly less. The economics of using benzene for welding are quite evident when compared with the more expensive acetylene. However, little work has been done to provide suitable equipment for utilization of these flames.

The test apparatus for conducting this type of research is quite simple and is illustrated in Fig. 5. The results have proved quite worth while, and it is felt that reducing the welding flame to its simplest elements can pay huge dividends.

References

1. *Third Symposium on Combustion and Flame and Explosion Phenomena*, The Williams & Wilkins Co., Baltimore, Md., 1949.
2. Jost, W., and Croft, H. O., *Explosion and Combustion Processes in Gases*, McGraw-Hill Book Co., Inc., 1946.
3. Lewis, B., and von Elbe, G., *Combustion, Flames, and Explosion of Gases*, Academic Press, Inc., New York, 1951.
4. Wohl, K., Kapp, N. M., and Gazley, C., *The Stability of Open Flames*, Project Meteor Report UAC-26, September 1948.

NOW AVAILABLE

"PHYSICAL AND MECHANICAL CHARACTERISTICS OF MATERIALS FOR PRESSURE VESSELS"

AN ANNOTATED BIBLIOGRAPHY

Volume I: Introduction and Subject Index: *Volume II:* Abstracts of the Literature Published from 1937 through 1938 (Including some earlier references); *Volume III:* Abstracts of the Literature Published from 1939 through 1943; *Volume IV:* Abstracts of the Literature Published from 1944 through 1947.

Approximately 2500 "dittoed" papers—"Accopress" Binders

Price Per Set: $30.00

Address All Orders to:

Pressure Vessel Research Committee of the Welding Research Council

29 West Thirty-Ninth Street, Room 503, New York 18, New York

LIMITED EDITION, ONLY FIRST 50 ORDERS WILL BE FILLED

Spot Welding of Titanium Alloy Sheet

Satisfactory spot welds in titanium alloy sheet require specific welding equipment, correct machine settings and adequate preparation of surface conditions

by M. L. Begeman, E. H. Block, Jr., and Frank W. McBee, Jr.

PRACTICALLY all metals and alloys that are produced in sheet form lend themselves to spot welding, well known as a most economical and rapid manufacturing process. Titanium and several of its alloys are no exception, but the procedures and techniques applied to ordinary metals must be modified to suit titanium alloys. In every case, satisfactory welds require the use of specific welding equipment, correct machine settings and adequate preparation of surface conditions.

Recent investigations of titanium alloys indicate that this metal responds well to resistance welding when proper welding conditions are maintained. In fact, its welding range appears to be rather wide, making it possible to compromise weld strength, penetration, indentation and other factors while still obtaining a satisfactory weld.

The purpose of this investigation was to study the welding characteristics of one of the titanium alloys with particular regard to weld strength, penetration, indentation, hardness and microstructure.

MATERIAL USED IN TESTS

The information contained in this paper pertains to the spot welding of 22-gage (0.031 in.) TI-100A, one of the commercial titanium alloys produced by the Titanium Metals Corporation of America. It is used primarily for sheet, plate and wire products. Though non-heat-treatable, it responds very definitely to work hardening operations.

As supplied, it was in an annealed condition having the following specified physical properties:

Tensile strength, psi	100,000
Yield strength, psi	75,000
Elongation, %	20–25
Area reduction, %	45
Hardness, Vhn	Approximately 300

Tensile tests of several specimens of the sheet used in assembling data for this paper indicated an average tensile strength of 125,000 psi.

Prior to welding, the sheet stock was sheared into components $2^{3}/_{4}$ in. long and $^{3}/_{4}$ in. wide. Test specimens were then degreased with carbon tetrachloride; no further cleaning was deemed necessary.

In the welding procedure, a lap of $^{3}/_{4}$ in. was used to conform with good practice. These specimens were ultimately subjected to a tension-shear test in a universal testing machine.

WELDING EQUIPMENT

Throughout these tests an air-actuated (Acme 75 kva), pressure type welder was used in connection with a synchronous control panel (G. E. Thyratron control and sequence panel). Current values were measured by means of a pointer stop ammeter in conjunction with a current transformer. In addition, check readings were made using a cathode-ray oscilloscope and a Land camera.

For most of the welds, the machine was equipped with standard Mallory No. 1527 (fluted, RWMA Class 2) electrode tips having a 2 in. radius dome. A few runs were made using flat tips and 6-in. radius dome tips, primarily to study the effect of tip shape upon penetration.

TEST PROCEDURE

Conditions for welding all specimens were selected on the basis of results of other investigators, as well as those of the authors in previous studies.

The following settings were used in making all welds: squeeze time, 20 cycles; hold time, 20 cycles; electrode closing rate, 3 fps; throat depth, 12 in.; horn gap, 8 in.; electrode cooling water rate, 1.5 gpm; tip pressure 600 lb; and electrode stroke, 0.25 in.

M. L. Begeman, Professor of Mechanical Engineering; **E. H. Block, Jr.,** and **Frank W. McBee, Jr.,** Research Engineers, Defense Research Laboratory, at The University of Texas, Austin, Tex.

This work was supported by the Navy Bureau of Ordnance under the basic research phase of its Contract NOrd-9195 and the Mechanical Engineering Department of The University of Texas, Austin, Tex. Scheduled for presentation at the Thirty-Third National Fall Meeting, AWS, Philadelphia, Pa., week of Oct. 20, 1952. Closing date for discussion Dec. 15, 1952.

Major variables were weld current and weld time. Electrode tip shape and pressure were varied in several of the tests to obtain information on the effect of these variables.

A preliminary test was first made using a tip force of 600 lb. and weld time of 8 cycles while varying the weld current. From the data obtained and from micrographs of the test welds the recommended value of welding current was selected.

The low value of current (5600 amp) finally chosen was selected because it yielded welds of satisfactory strength without excessive penetration. Using this current, a series of welds was made, varying the weld time from one to 20 cycles.

Results of this run indicated that it would be advisable to make further investigations with regard to low cycle time in an attempt to obtain satisfactory penetration and weld nugget characteristics. Accordingly, three runs were made with varying current for times of 1, 2 and 3 cycles. From the results obtained, machine settings for pressure or tip-force runs were selected.

In each case, at least 4 welds were made at each point, three for destructive testing and one for metallurgical purposes. After fabrication of the welds, indentation was measured and then the specimens were loaded in the testing machine until failure occurred.

DISCUSSION OF RESULTS

Effect of Weld Current on Strength

The two factors having greatest effect on weld strength are welding current and welding time. Influence of both these factors is well illustrated in Fig. 1, which shows the variation of strength with welding current for various cycle times.

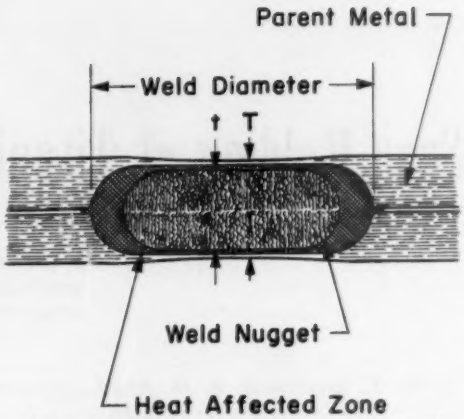

Fig. 2 Diagrammatic sketch of a typical spot weld

For each cycle time plotted, there is a definite increase of weld strength up to the point where flashing occurs. Beyond this point weld strengths tend to continue to increase, but are erratic. Quite obviously if strength were the only consideration, a high weld time and current should be used. However, if low indentation and satisfactory penetration are desired, there must be some compromise with strength, as can be seen by reference to the micrographs and other curves.

A sketch of a typical weld is shown in Fig. 2. There are three distinct zones shown, the parent metal, the heat-affected zone and the weld nugget. Weld pene-

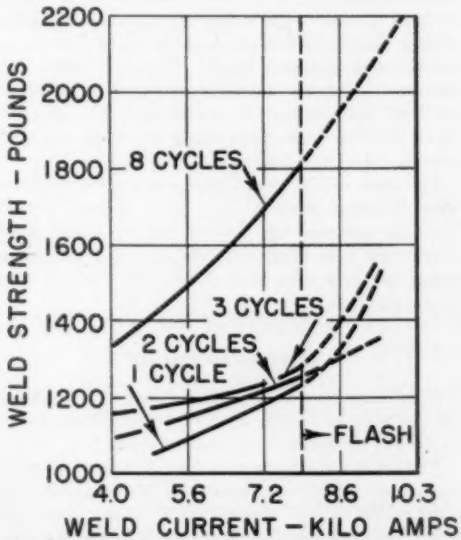

Fig. 1 The effect of weld current and weld time upon the strength of spot-welded Titanium 100A

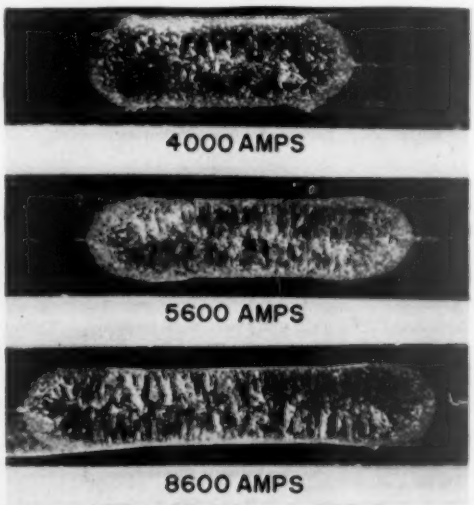

Fig. 3 Effect of weld current on weld size and penetration (weld time 8 cycles). Magnification 10 ×

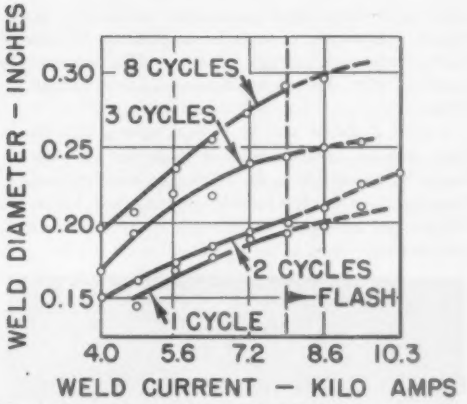

Fig. 4 Size of spot welds made on Titanium 100.A with varying currents and weld timers

tration is defined in this paper as t/T (100) and is expressed as per cent penetration.

In Fig. 3, several micrographs are shown of typical welds from the 8 cycle strength curve in the previous figure which show the influence of increasing welding currents upon size and appearance of the nugget. The weld penetration increases slightly as the current is increased, but in all cases it approaches 100%. The weld nugget diameters and indentations, however, are quite clearly increased. Two of the welds show some expulsion or "finning" of the metal between the sheets. It is felt that when all factors are considered none of these welds is acceptable, and that a lower weld time should be used to obtain satisfactory penetration.

It is generally agreed that strength is directly proportional to weld size. Figure 4 shows the effect of varying current upon the weld diameter. Any conditions tending to increase the welding heat will obviously increase the weld size and strength, provided metal is not expelled from the weld as a result of flashing. Attendent with the increase in weld size are increases in penetration and identation. In general, these relationships should closely follow the trend shown in the curves of Fig. 1. Eventually a condition is obtained which results in flashing and poor welds.

Influence of Weld Time on Weld Characteristics

The above data indicated advisability of selecting a fairly low welding current (5600 amp) and varying the weld time in order to obtain a weld with more satisfactory characteristics.

Results of tests are shown in Fig. 5, on which is plotted strength, penetration, indentation and diameter of the weld for various cycle times. The strength curve shows that strong welds, around 1200 lb, can be made with weld times as low as 3 or 4 cycles. These welds have satisfactory penetration (below 80%), low indentation and good structure.

The effects of varying cycle times upon the structure and size of the weld are shown in Fig. 6. At one cycle, the weld shows evidence of insufficient heat, and its shape is not that of a satisfactory weld; however, the strength of this weld was slightly over 1100 lb.

As greater weld times were used, the shape gradually changed, with corresponding increases in weld nugget size, indentation and penetration. From these micrographs and the data of Fig. 5, it appears that a weld current of 5600 amp and a weld time of 4 cycles will produce a satisfactory weld. This is a compromise so far as strength is concerned, but it does give good penetration and other weld characteristics.

Weld Penetration

All satisfactory welds should have good penetration of the cast weld metal into the outer sheets. Low weld penetration (below 20%) is an indication of low strength welds, while high penetration (above 80%) indicates the possiblity of occasional cracks in welds. Penetration figures are obtained by taking the ratio of the measured cast weld metal thickness to the total

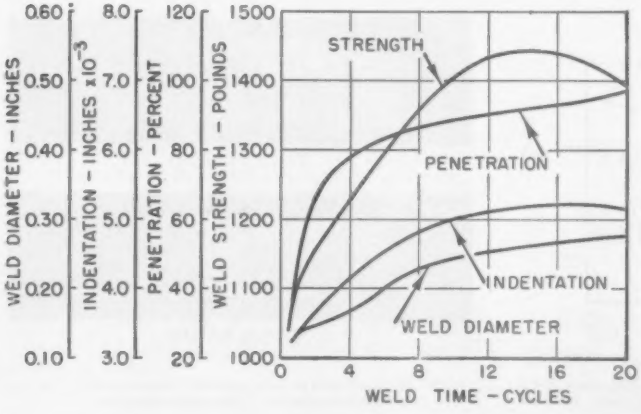

Fig. 5 Weld time—its effect upon spot weld characteristics of Titanium 100.A (weld current 5600 amp, tip force 600 lb)

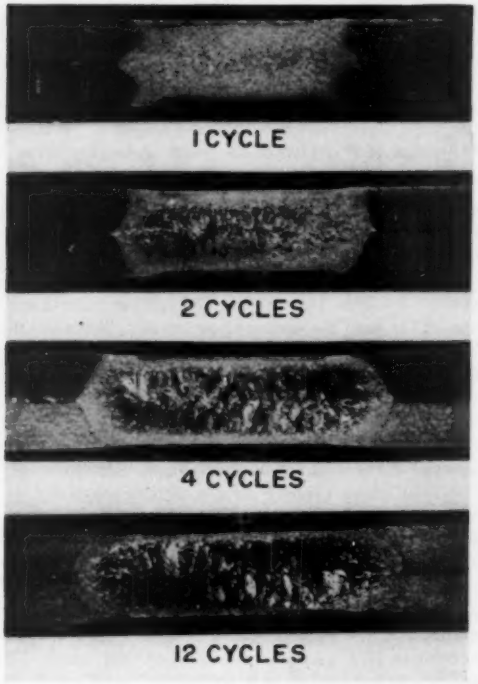

Fig. 6 Effect of weld time on weld penetration and size (weld current 5600 amp) Magnification 10 ×

weld thickness at the center of the weld nugget. Since most of the high-strength titanium welds had unusually high penetration, and since this weld characteristic is considered to be important for most metals, it was thought advisable to investigate the penetration and strength characteristics of low-cycle time welds.

The variation of penetration with increasing weld current for cycle times of 1, 2, 3 and 8 cycles is shown in Fig. 7. These curves indicate that nearly all the

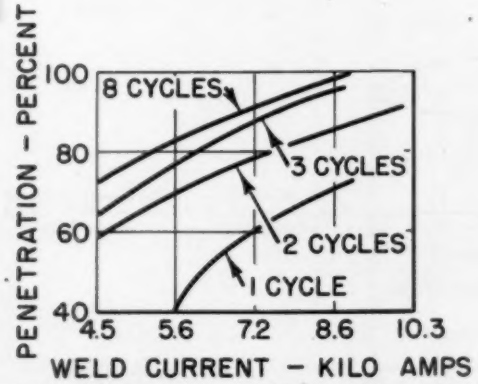

Fig. 7 Weld penetration in spot welds of Titanium 100.A with varying weld time and current (tip force 600 lb)

welds with lower cycle times have satisfactory penetration. However, it must be pointed out that these curves represent average values, and in most welds accurate cast weld metal dimensions are difficult to obtain.

Figure 8 shows several typical micrographs for 1 cycle welds. All are similar in shape but show an increase in penetration as the welding current is increased. Penetration in the first micrograph is too low, but in the others penetration and strength values were both satisfactory.

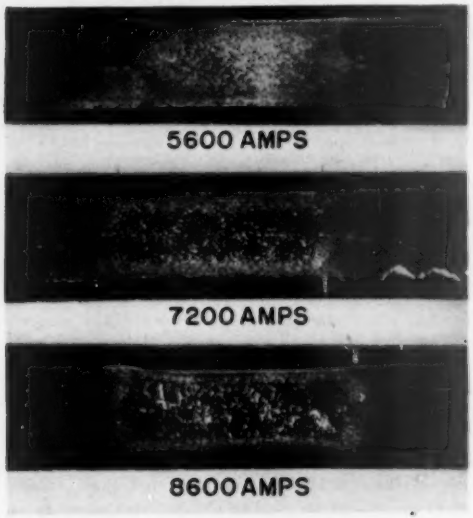

Fig. 8 Micrographs of spot-welded Titanium 100.A at one cycle weld time. Magnification 10 ×

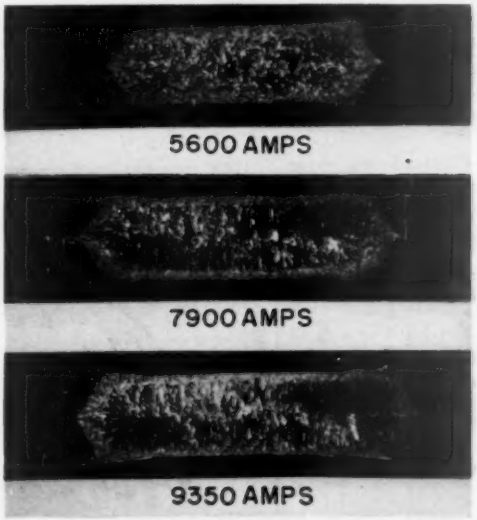

Fig. 9 Micrographs of spot-welded Titanium 100.A at two cycles weld time. Magnification 10 ×

Micrographs for 2-cycle weld times (Fig. 9) indicate that the trend of the previous paragraph still holds, but penetration is greater. For 3-cycle weld times, several micrographs are shown in Fig. 10. Penetration is satisfactory up to around 5600 amp, but above this current it exceeds 80%.

It will also be noted from the micrographs that a metal extrusion appears between the sheets at each end of the weld nugget. This tendency also showed up in some of the 2-cycle welds of Fig. 9. Strength values for all welds in both Figs. 8 and 9 were satisfactory, most of them being above 1200 lb.

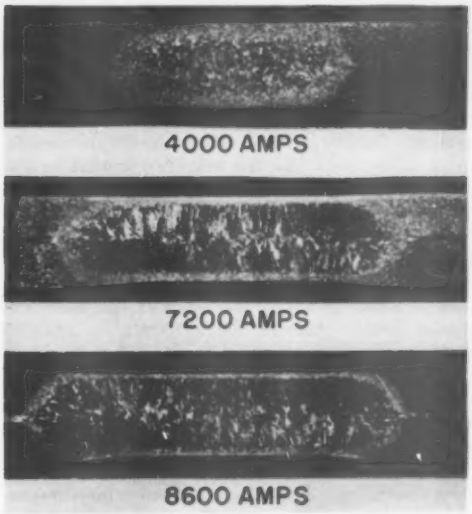

Fig. 10 Micrographs of spot-welded Titanium 100A at three cycles weld time. Magnification 10 ×

No further cycle times were investigated, other than the over-all data shown in Figs. 5 and 6. From the data obtained, it appears that the most important factor affecting penetration is weld time. It should be kept as low as possible for the current used in line with the strength desired.

Surface Indentation

Indentation occurs on the surface of all good spot welds and increases when welding current, cycle time or weld pressure are increased. This trend is shown in the average values of the indentation obtained in several tests (Fig. 11). All welds were made with 2-in. radius dome tips, which may account for some of the high values obtained. These values could be reduced by using flatter tips with a controlled area. Also, since the material used was quite thin, the values might be decreased some by the use of lower tip pressures.

Welding Pressure

The effect of increasing weld pressure upon the weld

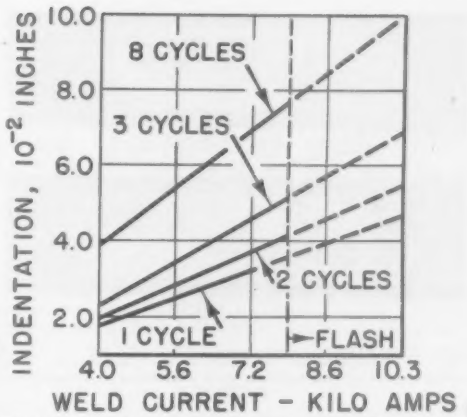

Fig. 11 Effect of weld time and current on indentation of spot-welded Titanium 100A

strength is indicated in Fig. 12. At low pressures, there is greater resistance between the sheets and consequently more heat in the weld. This results in a slightly stronger weld than when normal pressures are used. However, if the pressure is too low, excessive flashing results. Increasing the pressures to high values increases the indentation with little or no effect upon the strength. Greater tendency for metal extrusion between the sheets is also caused by high pressures. Two micrographs having tip pressures of 300 and 900 lb., respectively, are shown in Fig. 13. The low-pressure weld is stronger and has greater penetration and lower indentation than the high-pressure weld.

Tip Shape

Tip shape, as it affects weld characteristics, was investigated on a very limited scale. Welds were made using a 6-in. radius dome tip, a $^5/_{16}$-in. diam flat tip, a $^1/_4$-in. diam flat tip and a $^3/_{16}$-in. diam flat tip. All welds were made at 4 cycles and 5600 amp.

The 6-in. radius dome tip resulted in a weld with slightly less penetration; however, the weld was not symmetrical. On the other hand, a slight increase in strength was noted.

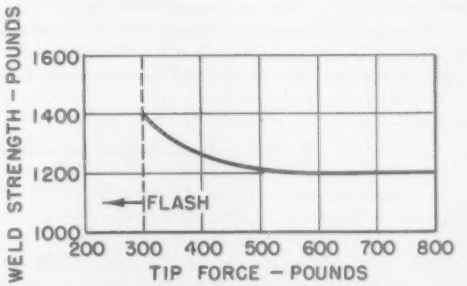

Fig. 12 Influence of tip force upon weld strength (weld current 5600 amp, weld time 4 cycles)

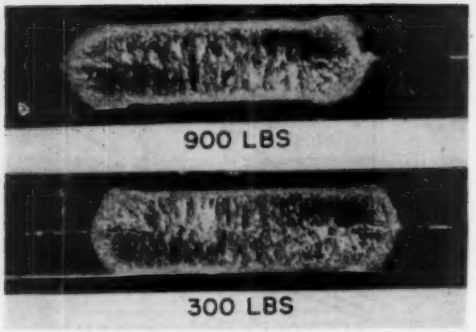

Fig. 13 Micrographs of spot-welded Titanium 100A (weld time 4 cycles, weld current 5600 amp.). Magnification 10 ×

Welds made with the flat tips decreased in strength as the tip diameter was lessened. The current density was obviously too high when using the $^3/_{16}$-in. tips. This resulted in flashing and poor weld characteristics.

It is the belief of the authors that this information is not conclusive and that the subject merits further investigation.

Type of Failure

In all instances where weld penetration exceeded approximately 85%, the spot welds made in this investigation failed as plugs or buttons. As the penetration decreased, welds tended to fail in a combination of tear around the weld and across the plate. In the case of welds with very low penetration (1 cycle, 5600 amp), failure occurred in shear.

Hardness Tests

Hardness studies of the spot welds were made using a Tukon Hardness Tester with a Knoop Indenter. Hardness measurements were made in the parent metal adjacent to the weld, in the heat-affected zone and in the weld nugget for several different welds.

An average value of about 460 khn was obtained for the parent metal. The heat-affected zone showed a slight decrease to about 430 khn, while the weld nugget showed a further decrease to approximately 400 khn. The change in hardness was so slight that it is assumed the hardness is not materially affected by the spot-welding process. However, there may be some tendency toward stress relief from the cold-rolled material tending to lessen the hardness.

CONCLUSIONS

The results obtained from these tests indicate that titanium TI-100-A can be effectively fabricated by the spot-welding technique. The welding range is wide, and close control of any major variables affecting the weld appeared to be unnecessary unless certain weld characteristics were desired. Very high strength welds can be made for situations requiring high physical properties. However, this property may be decreased considerably to improve other weld characteristics and still have welds of good strength.

Weld penetration appears to be higher and more difficult to control than in most other metals. Best values are obtained by using a low weld time with a moderate welding current. However, if it is desirable to use a high weld time, the weld current must be low if penetration is an important consideration.

It is questionable whether or not the matter of high weld penetration presents a serious problem. Examination of many cross-sectioned specimens under the microscope failed to reveal weld cracks or otherwise poor structure in any of the welds except where expulsion occurs. Also the tension-shear tests indicated excellent strength. Most specimens failed either by the metal being torn around the weld nugget or by a combination of tear around the weld and tear across the specimen adjacent to the weld. Both are common methods of failure for higher strength spot welds.

The limited tip shape investigation as well as the tip force tests made indicate that with further investigation these variables may be more effectively used to control weld penetration and strength.

Bibliography

1. Begeman, M. L., McBee, Jr., F. W., and Fontana, J. C., "The Physical and Metallurgical Characteristics of Spot-Welded Titanium." The Welding Journal Vol. XVI, No. 9, 429-s to 434-s, September 1951.
2. Dean, R. S., Long, J. R., Hayes, E. T., and Root, D. C., "Spot Welding of Titanium," *Metals Technol.*, Tech. Pub. No. 2102 (October 1946).
3. General Electric Co., "Titanium Metal Preliminary Developments in Welding," Thomson's Laboratory, Lynn, Mass. (1949).
4. General Motors Corp., "Spot Welding 0.060-in. Cold Rolled Titanium Sheet," Memo. No. 600-M-653, Project No. RW-24, Allison Division, Indianapolis, Ind. (Mar. 15, 1949).
5. Holt, E. F., and Moore, W. H., "Resistance and Fusion Welding of Titanium and Its Alloys," The Welding Journal, 31, 213-216 (March 1952).
6. Mahla, E. M., and Hitchcock, R. R., "Welding of Titanium-Carbon Alloys," *Ibid.*, 15 (11), Research Suppl., 544-s to 551-s (1950).
7. Office of Naval Research, *Titanium*, Report of Symposium, Dec. 16, 1948, Department of the Navy, Washington, D.C.
8. Solar Aircraft Co., "Fabrication of Titanium Sheet," Research Div., Report No. 713, San Diego, Calif. (Nov. 30, 1948).
9. Titanium Metals Corporation of America, *Handbook on Titanium Metal*, New York (1950).

The Effect of Strain-Rate on Twinning and Brittle Fracture

Relationship of strain-rate, temperature and brittle fracture in low-carbon steel as determined in simple tension

by D. Rosenthal and C. C. Woolsey, Jr.

Abstract

The relationship between strain rate, temperature, twinning and brittle fracture has been investigated experimentally in simple tension. The rates of strain covered a 10,000-fold range, from 0.02 to 275 per second. For each strain rate a threshold temperature for the occurrence of twins (Neuman lamellae) in the microstructure and loss of ductility (transition temperature for brittle fracture) were determined.

The results of this investigation could be fitted for the process of twinning by a reaction rate equation down to a critical temperature of approximately −170° F. At that temperature, the process of twinning appears to be insensitive to rate of deformation. Above −170° F an activation energy of 4200 (±400) calories per mole has been determined.

The process of brittle fracture was found to be practically insensitive to strain rate over the range employed: an increase of only 25° F in the brittle transition temperature was found for a 10,000-fold increase in strain rate.

The occurrence of a critical temperature for twinning could be derived from a criterion patterned after Bragg's criterion for slip. Likewise a correct order of magnitude for the activation energy was obtained from the analysis of the twin-slip process.

A better understanding of the process of fracture is necessary to interpret the present results in their relationship to previous work.

INTRODUCTION

THE present investigation was instigated by the results obtained in one phase of a broad program on the effect of explosives on metals.[1, 2] These results led to the conclusion that there must be some relation between strain rate and the type of shock twinning observed in such body-centered structures as ferrite. It is the object of this research to find if such a relation does exist, and, if so, to attempt to determine this relationship quantitatively.

Dr. D. Rosenthal is at the University of California, Los Angeles. C. C. Woolsey, Jr., at present is with the California Research and Development Co., Livermore, Calif.

Work partially sponsored by ONR and conducted at the Michelson's Laboratory, NOTS, Inyokern. Paper scheduled for presentation at the Thirty-Third National Fall Meeting AWS to be held in Philadelphia, Pa., the week of Oct. 20, 1952. Closing date for discussion Dec. 15, 1952.

HISTORICAL

The markings produced by shock in ferrite were discovered by Neumann in 1850, and still bear the name Neumann bands or Neumann lamellae. Many investigators have studied the structure and its mode of formation, and have in general come to the agreement that it is a twinned structure. For a while, there was considerable controversy over this fact. Two papers were published in England in 1925–28,[4, 5] which presented almost equally convincing arguments for each side of the controversy. That full agreement has not been reached is evidenced by a discussion of Neumann lamellae last year by Tipper and Sullivan.[6] However, most other workers in the field seem to be in general agreement that the lamellae are a twinned structure.

It is of interest to note that as early as 1919 a committee for the Investigation of Neumann bands[7] was appointed by the chairman of the Division of Engineering of the National Research Council. An objective of this committee was to determine if a relationship existed between the speed of fracture and the observation of Neumann bands in the microstructure. It was hoped to prove that this criteria might be used to distinguish between a fracture in a metal structure caused by an explosion and one caused by ordinary mechanical strain.

The first and only report found to come from this committee gave the results of a series of tests in which annealed mild steel disks 1.5-in. in diam and 0.25-in. thick were placed in contact with explosives of various detonation rates, ranging from 5000 to 18,500 fps. Lower velocity tests were made by use of a falling weight at velocities of 28 and 39 fps. No Neumann bands were found at these low velocities. It was indicated that the abundance of lamellae increased with velocity from 5000 to 7500 fps, but above that velocity there was no appreciable change. It was further stated that there appeared to be no relation between the abundance of lamellae and the amount of plastic deformation caused by the impact.

Effect of Composition

Pfeil,[8] in a review of twinning in iron, reported several instances in which the presence of 1% phosphorus promoted the formation of Neumann lamellae in low-carbon steel deformed slowly at room temperature. In one case, lamellae were produced by forging of such a steel at temperatures as high as 1200° F. The lamellae formed at room temperature were reported to be quite broad, compared to the Neumann bands normally found in iron which had been deformed by impact loading.

Barrett, Ansel, and Mehl[9] reported on the effect of silicon in pure iron for slow torsional deformation. Pure iron samples deformed at −320° F showed twinning, while samples deformed at −165° F did not. A 5% silicon alloy showed twinning at −95° F but none at room temperature. Intermediate silicon contents gave proportionate results.

Effect of Temperature

As early as 1905, Hadfield[10] observed Neumann lamellae in samples of pure Swedish iron broken in tension at the temperature of liquid air, −295° F.

Recent work done at the National Bureau of Standards with ingot iron indicates that for slow tensile deformation, twinning is found at temperatures below −184° F.[11] Twinning concentration was found to increase with lower temperatures down to −320° F, the lowest investigated. At these temperatures, twinning was found in this material in all structural conditions investigated; these included annealed, hot-rolled, normalized, quenched and tempered, and cold-drawn. In the cold-drawn condition, twinning was found only in the area adjacent to the fracture. In all other conditions, it was found throughout the entire gage length. Twinning was also formed in specimens deformed but not fractured, indicating that the twinning found was not associated with the fracture or with any shock waves resulting from the fracturing process.

Numerous other references have been made to the effect of temperature on the formation of twins in ferrite, several of which are indicated as interrelated with the effect of composition (see preceding section). A possible explanation has been offered for the twinning at low deformation rates at low temperatures;[9] it is quoted directly: "Twinning doubtless occurs only when the shearing stress in a suitable direction on a twinning plane exceeds the critical value, a circumstance that may be prevented by prior plastic yielding of the crystal on slip planes. The tendency of many metals, including iron, to twin more profusely as the temperature is lowered is thus an indication that slip resistance is increasing more rapidly than the critical stress for twinning."

Effect of Prior Strain

Pfeil[8] found that as little as 0.28% deformation in a very low carbon steel prevented the formation of Neumann lamellae on subsequent impact loading. He found that this effect was independent of energies and loading velocities over the ranges investigated, 7 to 147 in.-lb and 4.5 to 11 fps. He found that annealing after plastic deformation removed the effect and allowed production of lamellae. Annealing temperatures required to remove the effect were found to increase with increasing deformation; for instance, for 1% deformation, 10 min at 200° F would remove the effect; for 5%, it required 10 min at 265° F; for 10% deformation a temperature of 320° F was required; and for 15% deformation, the required temperature rose to 1300° F. The foregoing were for polycrystalline material; for single crystal, the corresponding temperatures were somewhat lower. For longer annealing times, the effect could be removed at somewhat lower temperatures.

Rosenhain and McMinn[4] obtained similar results; however, they found that the effect disappeared if the deformed material aged for a few days before being subsequently subjected to shock loading. When subjected to shock loading shortly after initial deformation, it was found that further deformation caused additional slip on the existing slip planes, developing few, if any, new slip planes. Slow deformation, starting with previously strained material, would develop many new slip planes with little additional slip occurring on the existing slip planes.

This aging effect may explain the ability to obtain twinning in cold-drawn iron in the work at the National Bureau of Standards.[11] It is possible that the different conditions involved (slow tensile deformation at low temperatures) may have an effect, but it would be of interest to know what kind of results might be had with freshly cold-drawn material. One effect noted in this work was that the twinning was concentrated near the fracture; for all other conditions of the material, twinning was found throughout the entire gage length.

Effect of Prior Microstructure

As mentioned previously, in the work at the National Bureau of Standards, twinning was found to occur in specimens deformed at low temperatures in all structural conditions investigated; these included annealed, hot-rolled, normalized, quenched and tempered, and cold-drawn. In addition, Bruckner[12] found that twinning would occur in spheroidized Armco iron when deformed under impact loading. Thus, it is suggested that for very low carbon (0.02%) steel, twins may be obtained regardless of the prior microstructure.

On the other hand, Bruckner[12] found that for structural steels (0.20% carbon) in the spheroidized condition, there was little or no evidence of twin formation. He postulates that the lack of twinning may be due to the presence of microcracks in the well distributed spheroidal carbides, and that these microcracks may afford sufficient opportunity for localized stress relief;

this stress relief might otherwise have been accomplished by twinning of the ferrite.

Bruckner[12] has also indicated an effect of the method of steelmaking on the occurrence of twinning. He found that for killed steels the twinning tendency was less than for rimmed or semikilled steels; for a given deformation temperature, twin frequency was much lower for the killed steels; also, the initial temperature at which twins appeared was lower for the killed steels. For the same materials, he also found that the brittle-fracture transition temperature was lower for the killed steels; he concluded that the lower twin nucleation temperature was the chief factor responsible for the lower transition temperature. In his later work,[12] he used the same steels in the spheroidized condition and found the same relation between the transition temperature for the rimmed and killed steels, in spite of the fact that there was no twin formation. He then concluded that "the ferrite or ferrite boundary condition resulting from the deoxidation practice thus appears to be the chief factor in establishing the transition temperature."

Effect of Strain Rate

Little reference was found on the effect of strain-rate on the formation of Neumann lamellae other than that impact loading would produce them and that slow deformation would not. Where quantitative figures for velocities were given, there were large gaps between the velocities that did produce them and those that did not; e.g., Foley and Howell[7] found them at 5000 fps but did not find them at 40 fps. The effect of composition and possibly that of magnitude of stress must enter the picture, as other investigators have obtained the lamellae under conditions indicating impact velocities considerably lower than 40 fps[4, 8] at ambient temperatures. Temperature, of course, has a marked effect on the velocities required to obtain twinning; for sufficiently low temperatures, twinning has been obtained for very low strain rates.[9-11]

Effect of Stress

There has been no relation indicated between the stresses or energies involved in causing deformation and the formation of Neumann lamellae. In the few places that any ranges were mentioned, they were fairly narrow, and no effect upon the formation of or the concentration of the lamellae was mentioned.

Sauveur, in a discussion of the paper by Foley and Howell,[7] stated that the localization of Neumann bands in the area adjacent to fracture is an indication of the violence of the impact that produced them; in other words, the more localized the Neumann bands, the more violent the shock. However, he did not differentiate stress magnitude from impact velocity in his use of the term violent.

Stability of Neumann Lamellae

Where Neumann lamellae are produced with very little additional deformation, temperatures above the upper critical are necessary for the removal; it is necessary to carry the structure into the austenite region and reform the ferrite grains from the austenite in order to effect a recrystallization. On the other hand, when there are considerable quantities of other type deformation, much lower temperatures would bring about complete recrystallization. Both Pfeil,[8] and Carrington and Gaylor,[14] report experiments supporting the above; also previous work by the junior author, with plates which have been subjected to explosive loading is in agreement with this finding.[3] High velocity impact was obtained by Carrington and Gaylor by firing of flat-ended projectiles at steel plates. Deformation microstructures of the projectiles were similar to those encountered in the previous work.[3] The recovery temperature for the heavily distorted area was found to be 1200° F (it was 1150° F in the work cited[3]). In areas where only Neumann lamellae were observed, heating to 1400° F resulted in no change in the lamellar structure (the lamellae disappeared at 1600° F in the work cited[3]). In no case was there any evidence of growth of the lamellae on heating, such as occurs in the case of annealing twins in face-centered-cubic microstructures. Thus, it is indicated that the Neumann lamellae which are not greatly distorted by other type deformation are quite stable.

Part I. Present Experimental Work

The present experimental work has been limited to mild steel in the fully annealed condition. Some of the preliminary tests were made with steel available in the shop. The bulk of the work, however, was done with a supply of AISI C1018 steel, obtained as a single heat, with the following analysis:

Carbon, %	0.19
Manganese, %	0.75
Silicon, %	Less than 0.02
Sulfur, %	0.02
Phosphorus, %	0.01

This steel was annealed by holding at 1700° F for 2 hr and then furnace cooling at a rate of approximately 50° F per hour. The resulting steel had an ASTM ferrite grain size of approximately 6.

In attempt to determine the approximate velocity range, initial work consisted of breaking specimens by tensile impact at loading rates from 10 to 175 fps. These were broken by D. S. Wood of the California Institute of Technology on the rotary type impact machine, at ambient temperature. Examination of the microstructure of these samples revealed that none of the expected regular Neumann bands were formed. There were found, however, similar structures which were considerably broader, with rather irregular bound-

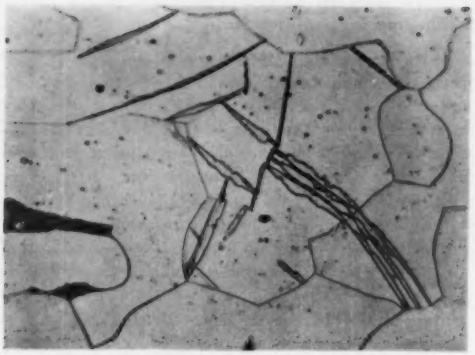

Fig. 1 Microstructure showing twins typical of those in specimens broken by Wood. Nital etch. 500 ×. (Reduced 25% in reproduction)

aries, and which had the same general habit of the Neumann lamellae; that is, they were long and relatively narrow and were contained wholly within a single ferrite grain, usually terminating at a ferrite grain boundary; an example of this type of twin is given in the photomicrograph of Fig. 1. In the microstructures resulting from explosive loading, both the usual Neumann bands and the structure with irregular boundaries may be found.[9] Bruckner[12] has suggested that such irregular twin boundaries may be caused by the presence of a substructure in the ferrite grain and that a twin progressing through such a grain would represent a homogeneous deformation only within any one cell. These twins were found in those specimens broken by Wood at velocities of 50 fps and higher; they were not found in samples broken at 10 and 20 fps.

The program then turned to the use of lower temperatures to reduce the striking velocities required to produce twinning. The purpose was twofold: (1) to be able to use equipment available in the junior author's laboratory,* and (2) to avoid the higher striking velocities, at which strain rates are far from uniform either with time or with position in the specimen (see discussion of work of von Kármán and Duwez). Since it has been indicated that temperature has a marked effect on the strain-rates at which twinning occurs, it was proposed to investigate the relationship between strain rate and the critical temperature at which twinning is produced. It was postulated that a reaction-rate type of equation might exist for the occurrence of twinning in an elastically strained lattice. The equation proposed for investigation was:

$$\dot{\epsilon} = \dot{\epsilon}_0 e^{-A/RT} \qquad (1)$$

in which T is the absolute temperature of testing, R is the molal gas constant, A is the activation energy for the particular process under consideration, $\dot{\epsilon}$ is the strain rate at any given temperature T, and $\dot{\epsilon}_0$ is a constant of proportionality. It has been stated[18,19] that a similar relationship exists for brittle fracture.

* Michelson's Laboratory, NOTS, Inyokern.

It was proposed, for the present program, to investigate eq. 1 for both the critical temperature for twinning and also that for brittle fracture. Brittle fracture may be defined for present purposes as being fracture with essentially zero elongation or zero reduction in area.

The strain rates used in this program were 0.001, 0.01, 1 and 11 fps. The highest velocity was obtained with a Sonntag Type SI-1 Universal Impact Machine. This is a pendulum type machine, having a capacity of 50 ft-lb when set to give an 11-fps striking velocity. The loss in velocity during the fracturing of a specimen was calculated on the same basis as is calculated the energy absorbed; that is, on the basis of the rise of the pendulum after fracture. This calculation indicated a maximum loss in velocity of 2 fps in the vicinity of the critical temperature for twinning. For brittle fracture there was essentially no loss in velocity.

The lowest velocity, 0.001 fps, was obtained with a Baldwin-Southwark Universal Testing Machine, equipped with a ram pacer. The latter may be used to measure the speed of motion between the ram and the stationary head of the machine or it may be used to control that rate of motion. It was used for the latter purpose for the present experimental work. Speeds indicated by the ram pacer were checked by direct measurement of the motion, using a dial indicator and a stop watch. These were found to check the settings within 1%. Tests were set up so that the heads could move slightly before putting any load on the specimen; thus the speed of motion could be set before there was any straining of the specimen. The load capacity of the testing machine was such that there was no loss in straining velocity noted at any stage of the tests.

During tests at the low strain rates, stress-time curves were drawn on the Southwark-Templin Stress-Strain Recorder attached to the testing machine. Knowing the strain rate, these stress-time curves could be transformed into stress-strain curves of the usual type. In making such a transformation, it was assumed that all straining occurred in the reduced section of the specimen; this is known to be incorrect but it is believed that not more than 10% of the total strain occurred outside this length.

The intermediate strain rates, 1 and 0.1 fps, were obtained with the aid of a large planer, available in the local shop. A special fixture for holding the specimen was secured to the bed of the planer. A second fixture was held in the tool post of the planer; this fixture was designed to give the same striking anvil as available for tension impact tests on the Sonntag Impact Machine. A sketch of the arrangement is given in Fig. 2. The tup, threaded on one end of the specimen, is struck by the two buttons protruding from the anvil, as the planner bed moves forward. The centerline between these two buttons is very carefully aligned, both vertically and horizontally, to coincide with the centerline of the specimen; thus the specimen is subjected to uniaxial tension on contact of the tup with the anvil.

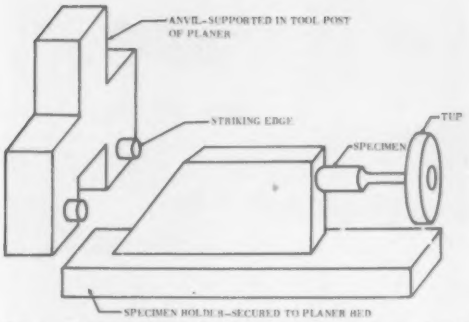

Fig. 2 Sketch of setup for breaking specimens at 0.1 and 1 fps

The striking edge of the anvil is carefully aligned vertically with the centerline of the specimen and so that the tup is struck squarely

The desired strain rates were obtained by adjusting the speed of the d-c motor driving the planer bed. Numerous measurements of the bed speed indicated that for any given motor-speed setting, the bed speed was as consistent as could be measured with a stop watch. All checks were within 2% of the average. While no direct measurements were made of the loss in velocity upon striking of the specimen, it is believed that this would be negligible; the 20 ft-lb breaking energy required would be negligible as compared to the energy available in the 8-ton bed moving at a fair velocity when contacting the specimen. Tests were started with the two fixtures in the approximate position shown in Fig. 2; thus the planer bed had moved about 8 in. before contact and was moving at the desired velocity with a very large momentum.

The test specimens were machined from the annealed steel previously described, in accordance with the sketch given in Fig. 3. One side of the specimen was ground to a flat, as indicated in Fig. 3, so that it could be given a metallographic polish prior to breaking. The reduced section was placed nearer to the tup end to increase the heat-transfer path to the heavier fixtures and thus help in maintaining a uniform temperature in the reduced section. An iron-constantan thermocouple of 30-gage wire was spot welded to the specimen on the radius of the shoulder (see Fig. 3). Since the grinding of the flat removed almost half the threads, there was some concern regarding the effect of this unsymmetrical support in the holding fixtures on the type of loading obtained; therefore, in setting up a specimen for test, pieces of half-round were wedged between the flat side of the specimen and the female threads of the holding fixtures.

A small cup was made which would enclose the specimen and yet clear the striking anvils. When the specimen was set up ready for breaking, liquid nitrogen was fed into this cup (the tup was also cooled with liquid nitrogen) until the specimen temperature registered somewhat lower than that required for the particular test. The flow of nitrogen was stopped, the specimen was allowed to approach the test temperature and movement of the loading device was started. Test temperature was taken as that temperature read at the moment contact was made with the anvil; that is, the moment that straining of the specimen began. The minimum temperature obtained was −290° F.

Fig. 3 Sketch of test specimen

Temperature measurements were made with a Leeds and Northrup Model 8662 Portable Potentiometer, capable of reading to within less than 1° F. The increase in temperature after cooling of the specimen was rather slow, about 10–15° F per minute. This should indicate that a fairly uniform temperature existed in the reduced section of the specimen when straining commenced.

Elongation and reduction in area were measured for all specimens. To avoid marking the reduced section, the elongation measurements were made on the shoulders of the specimen. Thus, a total elongation over a 2-in. length was measured; this 2-in. length included all of the reduced section, the radii of the shoulders and about 1 in. of the shoulders. In reducing the measured elongation to a percentage figure, it was assumed that all elongation took place within the 0.150-in. diam reduced section; this is known to be incorrect as there is some plastic flow in the radii portions. However, for comparison purposes among the tests made in this program, no significant error should result. The elongation was measured in punch marks placed with a standard gage punch and measured before test. After the test, the two halves of the specimen were carefully held together and the distance between punch marks was again carefully measured with dividers and a scale divided in hundredths of an inch. These measurements were reproducible to within one one-hundredth of an inch. Reduction in area measurements were made with micrometers, to the nearest 0.001 in. All specimens were measured before and after fracture, both the specified 0.150-in. diam and the 0.140 in. to the flat (see Fig. 3).

For specimens broken on the Sonntag Impact Machine, absorbed energies were recorded directly as given on the scale of the machine. For those broken on the Baldwin-Southwark Testing Machine, energies were estimated from the stress-strain diagrams obtained during the test, in the manner described earlier. No energy measurements were made in the tests using the shop planer.

Prior to testing, the flat surface of the specimens were given a metallographic polish and etch. After fracture, these surfaces were examined under the microscope to determine the relationship between slip lines and twins. After an initial examination, some specimens were given an additional etch to assure that the complete structure had been revealed.

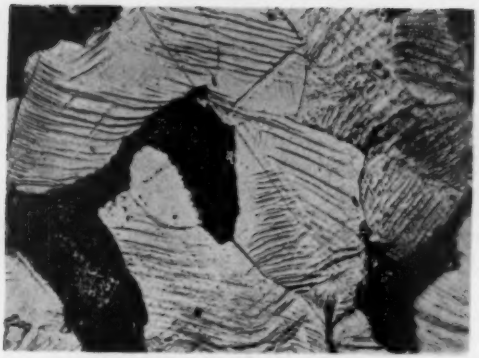

Fig. 4 Photomicrograph of surface which had been prepolished, then fractured at 0.001 fps at 75° F, area not in necked portion. Nital etch. 500 ×. (Reduced 25%)

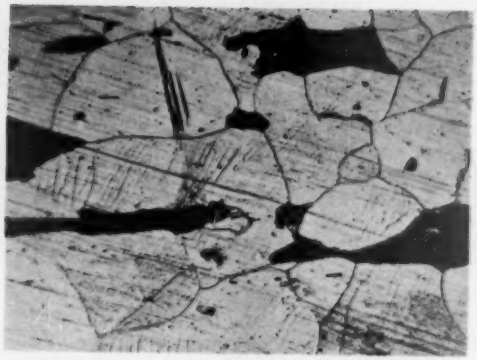

Fig. 5 Photomicrograph of surface which had been prepolished, then fractured at 0.001 fps at −280° F. Nital etch. 500 ×. (Reduced 25%)

After examination of the prepolished surfaces, the specimens were sectioned longitudinally, polished and etched, and examined for evidence of twinning. In each case, a survey was made of the complete reduced section, from the fracture out into the enlarged ends. It is not probable that such a section through the specimens would be free from twins unless the whole specimen were free from twins; this, at least, is the premise upon which it is stated for any given specimen that there were no twins.

RESULTS OF EXPERIMENTAL WORK

A. Metallographic Examination

Examination of the prepolished surfaces of the various specimens revealed twins only in those broken at the very low temperatures, those below the fracture transition temperature; and even in these the twins were very few in number. No twins were found on the surfaces of those broken at higher temperatures, even though subsequent sectioning revealed reasonable numbers of twins in the same specimen. Typical examples of the strained surfaces are given in Figs. 4 and 5, the first having been strained at ambient temperature and the second at −280° F, both at the lowest rate of straining (0.001 fps). In the latter may be seen both slip lines and twins; the twins are in the grain at the upper edge of the photomicrograph, just to the left of center. The twins appear darkened by the etch. Slip lines appear in most of the other grains; these are the fine, wandering lines. The rather straight, parallel lines, oriented from lower right to upper left, are scratches remaining from the mechanical polishing of the specimen; these should be disregarded in examining the structure. No slip lines were found in specimens broken at that low a temperature at the higher velocities. These observations correspond well with the elongation measurements; at the minimum temperatures reached (−270 to −280° F), no measurable elongation was found for specimens broken at velocities of 0.1 fps and higher, while 2 to 3% elongation was found in those broken at the lower velocity.

The area of Fig. 4 is typical of specimens broken at temperatures above the fracture transition temperature. Only slip lines may be seen, and these are present in nearly every grain. As in Fig. 5, there are some polishing scratches remaining; all prepolishing was done by mechanical means and because of the shape of the specimen, it was difficult to obtain excellent final polishes. These prepolished surfaces were rather badly distorted by the deformation; the lack of sharpness around the edges of Fig. 4 indicates the distortion obtained in areas far removed from the necked portion of the specimen. In the necked portion, distortion was so severe that it was not possible to get one complete grain in sharp focus.

It will be noticed in Fig. 5 that slip lines and twins are not found in the same ferrite grain. This was found to be true for all specimens examined; that is, slip lines and twins were not found to exist together in a single ferrite grain.

Examination of the sections subsequently cut from these specimens revealed several features:

1. Both types of twins, the narrow ones with straight, parallel boundaries and the broad ones with irregular boundaries, were found to exist in the series of specimens examined.

2. Only the narrow twins were found to exist in specimens broken at temperatures below the fracture transition temperature at velocities of 0.1 fps and higher. At the lowest temperatures the twins were found to be concentrated near the fracture. The photomicrographs of Fig. 6 and 7 are of areas very close to the fracture; the very narrow, straight structures are the twins under discussion. In one such specimen, fracture occurred at one end of the reduced section. Concentrations of twins of this type were found adjacent to the fracture and also in a narrow band at the other end of the reduced section, indicating that the twin concentrations occur at points of stress concentration even though there is no fracture.

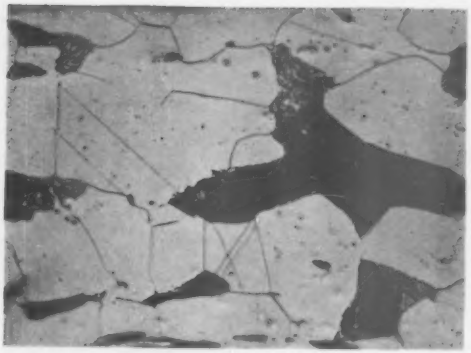

Fig. 6 Photomicrograph of section from specimen fractured at 11 fps at −270° F. Nital etch. 500 ×. (Reduced 25%)

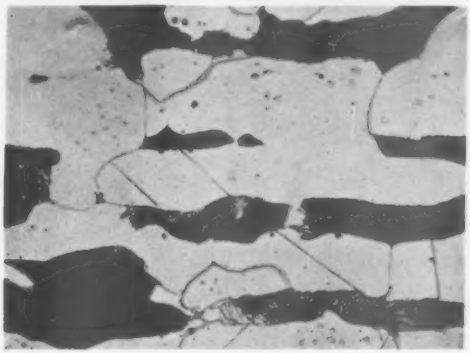

Fig. 7 Photomicrograph of section from specimen fractured at 0.1 fps at −270° F. Nital etch. 500 ×. (Reduced 25%)

3. Both types of twins were found in specimens broken at the lowest temperature (−275° F) at 0.001 fps (see Fig. 8).

4. Both types of twins were found in all specimens broken at intermediate temperatures, with the narrow ones disappearing at the higher temperatures, leaving only the broad, irregular type in specimens broken just below the critical temperature for twinning. The specimens represented by Figs. 9 through 12 were those showing twinning at the highest temperature, for each of the four velocities investigated. In each case, specimens broken at the next highest temperature showed no twins. The areas shown are not typical of the specimen as a whole. The number of areas showing twins was small; however, an area which did show twins usually contained several, often all in the same grain.

5. Except for the lowest temperatures, where twinning was concentrated near the fracture, there seemed to be a slight over-all decrease in numbers of twins as the temperature was increased, up to a point near

Fig. 8 Photomicrograph of section from specimen fractured at 0.001 fps at −275° F. Nital etch. 500 ×. (Reduced 25%)

the critical temperature, where the frequency of twinning dropped rapidly. Results of the microscopic examination to establish the twinning threshold temperatures are given in Table 1.

All specimens for the photomicrographs of Figs. 6 through 12 were polished electrolytically; thus there are no polishing scratches to be confused with true structures. All photomicrographs of specimens used in the present program have been so oriented that the

Table 1—Metallographic Observations of Twinning (Sectioned and Polished After Fracture)

Strain-rate, ft/sec	Test temperature, ° F	Observation
11.0	+78	No twins
	+75	No twins
	+60	No twins
	+50	Very few twins (Fig. 9)
	+32	Few twins
	+5	Few twins
	−55	Few twins
	−100	More twins than at −55
	−140	More twins than at −100
	−200	Many twins
	−270	Few twins concentrated near fracture, none with irregular boundaries (Fig. 6)
1.0	0	No twins
	−30	No twins
	−63	Very few twins (Fig. 10)
	−106	Few twins
0.1	+75	No twins
	+31	No twins
	−54	No twins
	−110	No twins
	−118	No twins
	−140	No twins
	−143	No twins
	−155	Few twins (Fig. 11)
	−157	Few twins
	−210	More twins
	−270	Twins concentrated near fracture (Fig. 7)
0.001	+75	No twins
	−80	No twins
	−116	No twins
	−135	No twins
	−152	No twins
	−182	Very few twins (Fig. 12)
	−195	Very few twins
	−220	Very few twins
	−275	Many twins, scattered throughout gage length (Fig. 8)

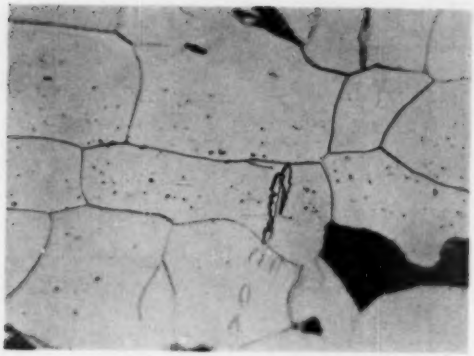

Fig. 9 Photomicrograph of section from specimen fractured at 11 fps at 50° F. Nital etch. 500 ×. (Reduced 25%)

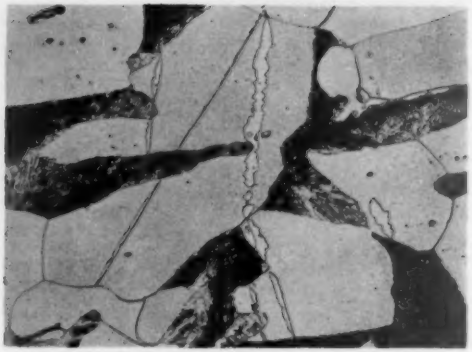

Fig. 11 Photomicrograph of section from specimen fractured at 0.1 fps at −155° F. Nital etch. 500 ×. (Reduced 25%)

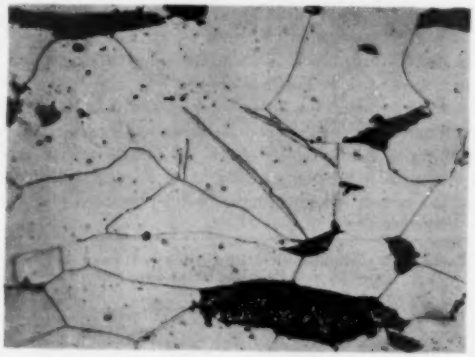

Fig. 10 Photomicrograph of section from specimen fractured at 1 fps at −63° F. Nital etch. 500 ×. (Reduced 25%)

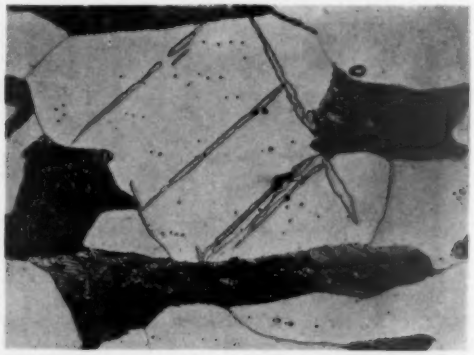

Fig. 12 Photomicrograph of section from specimen fractured at 0.001 fps at −182° F. Nital etch. 500 ×. (Reduced 25%)

direction of the principal tensile stress would lie horizontal and in the plane of the paper.

A limited investigation was included in this program in an effort to identify as twins the microstructures obtained. This was prompted by the apparent lack of complete acceptance of Neumann bands as twins (see reference 6). Two modes of attacking this problem were used: (1) the use of etch pits, and (2) the superposition of slip lines on a surface containing twins. In the first case, the polished and etched surface containing twins was subjected to an additional etching in a cupric-ammonium-chloride solution. The action of this solution is to etch along crystallographic planes to reveal the orientation of these crystallographic planes. The photomicrograph of Fig. 13 illustrates the results obtained. The bands running diagonally across the field are twins; the square structures are the etch pits. In the central twin, one may see the two large etch pits filling the complete width of the twin, and several smaller ones. The plane of polishing for this particular grain is very nearly that of the cube face, the (100) plane. Reference to Fig. 19 in Part II will indicate that the twinning plane may cut the cube face parallel to a face diagonal or at an angle of 26°34′ with a cube edge. In this grain the twinning plane has cut the structure parallel to the cube face diagonal.

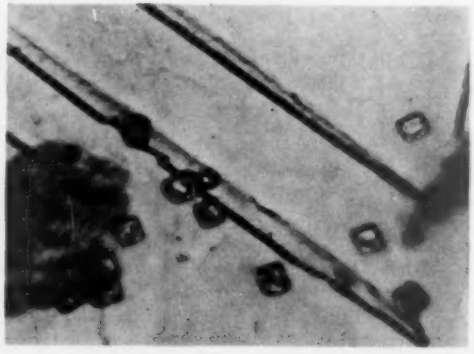

Fig. 13 Photomicrograph of section given special etch to show crystallographic orientation. Note the pits inside the twin are mirror images of those outside. Nital etch, then 5% cupric ammonium chloride. 1500 ×. (Reduced 25%)

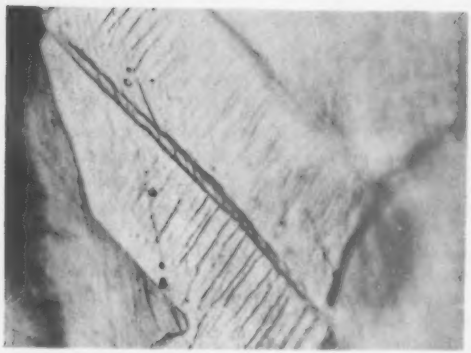

Fig. 14 Photomicrograph of section first polished and etched, then strained by twisting specimen. Note orientation of strain lines produced. Nital etch. 1500 ×

As the plane of polishing is not quite the (100) plane, the side of the twin is not quite parallel to the cube diagonal and the differences in orientation of the structures inside and outside the twin can be seen. By carefully comparing the orientations of the pits inside the twin with those outside, one can see that they are mirror images and thus satisfy the twin relationship.

For the second method of attack, a polished and etched surface containing twins was further strained by twisting the bar slightly. A resulting structure is shown in Fig. 14. Again, the twin lies diagonally in the field; slip lines which resulted from the deformation run perpendicular to the twin in the ferrite outside the twin, while inside the twin they make an angle of approximately 45° F with the edges of the twin. While this difference in orientation of the slip lines does not prove that the structure is a twinned one, it does indicate that the crystallographic orientation is different inside the structure; with proper orientation of the direction of stress application and of the crystallographic planes inside and outside the twin, such a pattern of slip lines as seen in Fig. 14 could be produced.

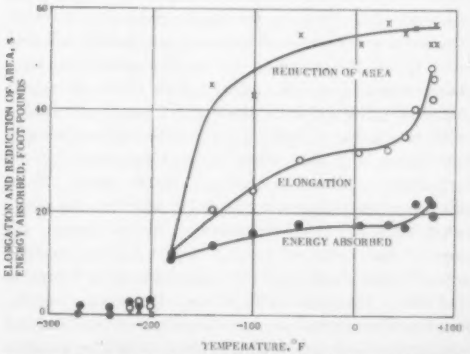

Fig. 15 Curves relating energy absorbed, elongation and reduction of area with temperature for impact velocity of 11 fps

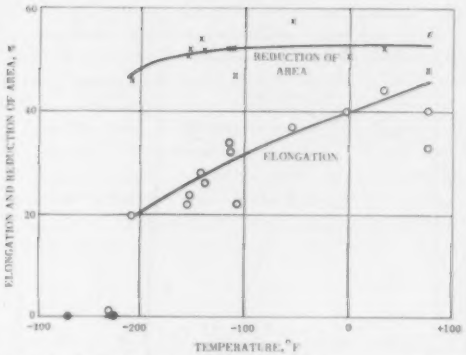

Fig. 16 Curves relating elongation and reduction of area with temperature for impact velocity of 0.1 fps

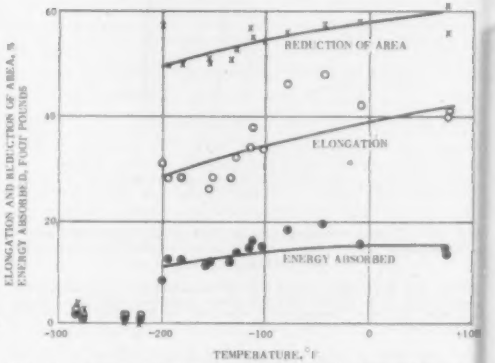

Fig. 17 Curves relating energy absorbed, elongation and reduction of area with temperature for impact velocity of 0.001 fps

B. Tensile Tests

Results of energy absorption, elongation, and reduction in area measurements are given in Figs. 15, 16, and 17 for straining velocities of 11, 0.1, and 0.001 fps, respectively. Only a few tests were made at the 1-fps velocity, and these were made in the temperature range expected to reveal the transition from twinning to absence of twinning. Since no fracture transition was obtained, the data for this velocity have not been shown. As previously stated, no energy measurements were made on the planers; therefore the energy curve is absent from Fig. 16. It will be noted in all cases that the transition from ductile to brittle fracture is quite abrupt and is well shown by any of the three parameters measured. The most sensitive of the three is the reduction in area, which shows a drop from nearly 50% down to zero for each of the three velocities.

The above results, both for the threshold temperature for twinning and the temperature for brittle fracture, are given in Fig. 18, with the impact velocities

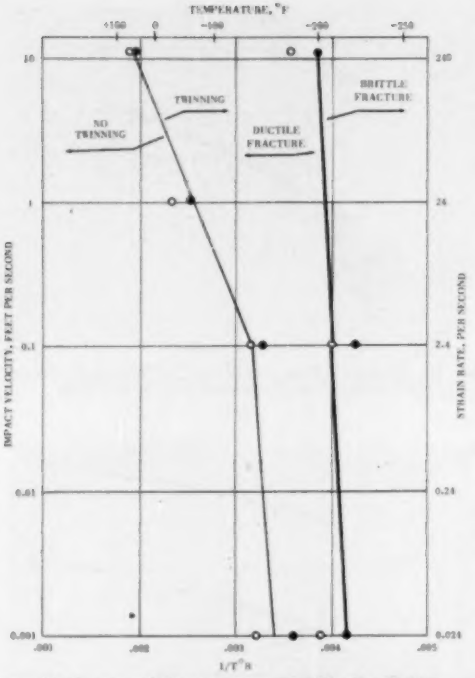

Fig. 18 Curves relating strain rate with threshold temperature for twinning and with transition temperature for brittle fracture

The solid dots indicate the highest temperatures at which twins were found or at which brittle fracture occurred; the open circles indicate the lowest temperatures observed on the other side of the critical one

on a logarithmic scale plotted against the reciprocal of the absolute temperature of testing. It will be noted that the curve for brittle fracture is very nearly vertical, indicating that the process of brittle fracture is probably not sensitive to the rates of straining employed. On the other hand, for the twinning threshold temperature, there seems to be a reasonable correspondence with eq. 1 down to a temperature of approximately −170° F; at that temperature, the process of twinning appears to be insensitive to strain rate.

DISCUSSION

An activation energy has been calculated for the process of twinning in the following manner. For any condition $\dot{\epsilon}_1$ and T_1 eq. 1 becomes

$$\dot{\epsilon}_1 = \dot{\epsilon}_0 e^{-A/RT_1};$$

$$\dot{\epsilon}_2 = \dot{\epsilon}_0 e^{-A/RT_2}$$

etc. Dividing one by the other and taking the logarithm, we obtain

$$\ln \frac{\dot{\epsilon}_1}{\dot{\epsilon}_2} = -\frac{A}{R}\left(\frac{1}{T_1} - \frac{1}{T_2}\right) \qquad (2)$$

Selecting $\dot{\epsilon}_1$, $\dot{\epsilon}_2$, T_1 and T_2 from Fig. 22, with $R = 1.104$ calories per ° F per mole, we have

$$\ln \frac{10}{0.1} = -\frac{A}{1.104}(0.00196 - 0.00318) = 4.605$$

$$A = 4200 \text{ calories per mole}$$

Considering the possible sources of error and their probable magnitudes, it is estimated that this value is within 10% of the true value of the activation energy for twinning.

Grossman and others [18, 19] give curves similar to Fig. 18 for brittle fracture, which curves indicate that an activation energy exists for brittle fracture and that it is more nearly the magnitude found for twinning in the present work. Their work, however, was done with notched bars and plates in bending whereas the present work was done with unnotched bars in simple tension; it is possible that this could account for the differences observed.

An additional series of tests was performed to check the possibility that the unsymmetrical test specimens may have contributed to the apparent insensitivity of the brittle-fracture transition temperature to straining rate, even though others had indicated such a sensitivity. Specimens for these tests were of the same dimensions as given in Fig. 3, except that they were left completely round. Only the two extremes of strain rate (0.001 and 11 fps) were examined. These confirmed the previous finding; the transition temperature for brittle fracture was increased by only 25° F in going from loading rates of 0.001 fps up to 11 fps.

The effect of increased temperature due to energy absorbed in deformation at impact was questioned. Attempts made to measure this temperature rise resulted in a maximum measured increase of 30° F. The thermocouple in this case was approximately $\frac{1}{8}$ in. from the point of fracture; the temperature rise at the point of fracture was somewhat higher than that indicated by the thermocouple; in fact, the maximum temperature of the thermocouple was recorded a second or two after fracture had been completed. As would be expected, no temperature rise was found for those specimens breaking with no measurable deformation. Since the total time involved in the straining process was very short (0.1 sec for those strained at 0.1 fps), temperature increases of any concern would probably have to be those caused by conditions at the local point under question. Since twins were found at distances quite far from the highest energy absorbing areas (the areas of necking), any effect of temperature must have been due solely to heat generated by deformation in immediate vicinity of the twins. Since this same consideration would be true for all strain rates, with the possible exception of the lowest, the slope of the curve in Fig. 18 would not be changed appreciably regardless of the magnitude of the temperature rise, within reasonable limits. However, considering that all energy absorbed is transformed into heat and considering that most of this heat would be concentrated in the location of severe deformation (necked portion), it is estimated that the twinning threshold

temperature is not affected by more than 10° F. The brittle transition temperature should not have been affected at all.

The usefulness of higher striking velocities may be questioned in view of the work of von Krámán and Duwez.[20] They give both theoretical and experimental evidence that above certain fairly low velocities, the strain propagation in a solid is far from uniform. Because of the propagation of the plastic wave through the specimen, each incremental length may be subjected to a variable strain rate ranging from zero to infinity. Thus, the term, strain rate, in specimens strained under these conditions, has no meaning. It is estimated from the work of von Kármán and Duwez that the velocity above which this effect begins to appear for annealed mild steel is approximately 10 fps. That the straining is fairly uniform at 11 fps may be seen by examining the surfaces of the prepolished bars, after breaking them. The reduced section of these specimens showed a rather uniformly strained surface, except in the area of necking. At the time of necking, the localized strain rates are changed. However, since twinning was found throughout the gage length outside the necked area, and since twinning was found in specimens which did not neck, it is believed that the twins had been formed prior to the necking process, at the uniform strain rate.

The above, coupled with the methods used for fracturing the specimens, permits the free interchange of the terms, strain rate and impact or striking velocity, for the present work. Only in the case of the Sonntag Impact Machine was there any decrease in velocity during deformation, and in this case, the maximum reduction in velocity was less than 20%; it is believed that the twinning had been accomplished before half of this reduction in velocity had occurred. The ordinate for Fig. 18 may be given in strain rate, units per unit per second, as well as in impact velocity.

CONCLUSIONS FROM EXPERIMENTAL WORK

An investigation has been conducted on the effect of strain rate and temperature on the production of twins in the microstructure and of brittle fractures, in a low-carbon steel.

Results of this investigation indicate that the occurrence of twinning is dependent both upon the temperature and rate of deformation; that the threshold temperature and strain rate may be related by a reaction-rate equation: in which A, the activation energy, may be considered to be that energy necessary for the average atom to overcome the energy barrier between twinned and slipped positions under the same stress. Equation 1 was found to correlate with data obtained down to a temperature of approximately −170° F. At that temperature, the process of twinning appeared to be insensitive to strain rates; that is, twinning occurred regardless of the rate of deformation.

Results also indicate that the process of brittle fracture is not a rate-sensitive one in the range of velocities investigated. The brittle-fracture transition temperature was only slightly affected by a 10,000-fold change in strain rate; an increase of approximately 25° F was noted for such an increase in strain rate.

An activation energy was computed for the process of twinning, from the results obtained. It was found to be 4200 calories per mole, with an estimated uncertainty factor of ±400 calories per mole.

An attempt to interpret these results from the theoretical point of view has been made in Part II.

Part II. Theory

Two conclusions have been drawn from the experimental results, one in regard to brittle failure, the other in regard to twinning. Within the experimental limits the temperature for brittle failure in simple tension has been shown to be practically insensitive to the rate of straining. On the other hand, the temperature for the occurrence of twinning has been found to be strain rate sensitive only above −170° F. The existence of a very high activation energy barrier or a total lack of such a barrier could equally well account for the results of the low-temperature brittleness. The high-activation energy barrier would seem to be better supported by the occurrence of brittle fractures under explosive loads at room temperature.[1] But the mechanism of fracture in metals is still too little understood to warrant a more detailed analysis of the present data. The mechanism of twinning is far better known. Therefore, it appears fruitful to seek in this mechanism at least a partial explanation of the experimental results.

MECHANISM OF DEFORMATION

Many investigators have confirmed that the twinning plane for iron is the (112) plane. It is generally considered that all atoms within the twinned structure have moved in a shear block movement. The distance moved by a particular layer of atoms is proportional to its distance from the twinning plane. These movements may be explained more easily with the use of Figs. 19 and 20, sketched from discussions given by Barrett.[15, 16] These involve only the layers of atoms close to one twinning plane. It can be visualized that this shear displacement carries across to the other twinning plane, resulting in a considerable shift between the untwinned structures on either side of the twin, and depending on the width of the twin.

Twinning is defined as the formation of a crystallographic lattice which is a mirror image, across the twinning plane, of the original structure. Thus, the atoms in the twin must be opposite to and at the same distance from the twinning plane as an atom in the original structure. A careful study of Figs. 19 and 20 will show that the movements of atoms below the twinning plane to the new positions indicated will place them in

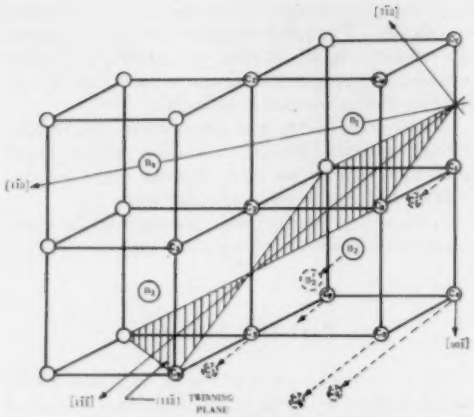

Fig. 19 Sketch of body-centered cubic crystal structure showing twinning plane and movement of atoms below the twinning plane; C_1 moves to C'_1 opposite B_1, B'_2 opposite C_2, C'_3 opposite B_3, and so on

such a location; C'_1 is opposite B_1, B'_2 is opposite C_2, C'_3 is opposite B_3, and so on. It should be noted that in the $(1\bar{1}0)$ plane just in front of the one shown in Fig. 20, atom C_6 moves to a location opposite atom C_5; it should not be considered a general rule that in the twinning process the atoms change from corner to body-centered or vice versa, as might be concluded from an examination of the situation on the one $(\bar{1}10)$ plane only.

A homogeneous twinning shear of 0.707 is shared by every atom of the twin. The atoms adjacent to the twinning plane are separated by a distance of 0.816a,* which is 5.8% closer than the normal closest approach distance, 0.866a, for the body-centered cubic crystal. This causes some distortion of the atomic configuration and results in a strained condition at the twinning plane. It has been suggested that the twinning planes are determined by this factor; that they are the planes which give the least distortion in that area.[5] Bruckner[12] has confirmed with microhardness tests that the only strained areas are those at the twin interface; he found that the area within the twin appeared to have the same hardness as the surrounding ferrite.

A recent paper has suggested a new possibility for the mechanism of twinning, which involves very little over-all displacement.[17] It is pointed out that the atom sites for every third layer in a twinned body-centered cubic structure coincide with sites occupied by atoms in the structure prior to twinning. It is suggested that these "coincident" atoms are the actual ones present in the untwinned lattice and that the intermediate layers of atoms move into the twinned position by a double shear process or by a localized rotational process. That such coincidence is a fact can be seen readily in Fig. 20. Atom C_4 is opposite atom C_2 in the untwinned structure. In the twinned structure, an atom must occupy that same site, either by C_4 not moving or by a new one moving into its place.

Such a mechanism would preclude any appreciable movement of the original structure on one side of the twin band relative to that on the other side and would minimize the interaction energy at the boundary between twinned and nontwinned grains in polycrystalline materials. This fact should present a means of verifying the hypothesis experimentally. Although much work is reported which indicates that such movement does exist, it was not possible to find any in which it was definitely stated that the twinning was superimposed on an existing structure. For deformation subsequent to twinning, it would be expected that slip lines would follow the crystallographic planes through the twin to give such an indication of movement. It would be necessary to mark a structure by some means and then cause twinning, to determine this point.

DYNAMICS OF TWINNING

Whether the mechanism of twinning involves a large or a very small over-all displacement the end result is a twin crystallite of finite thickness. Barrett[18] offered a possible explanation for this result. He pointed out that the lattice distortion at the twin interface is likely to be smaller when several successive layers move in the twin position instead of only one layer of atoms shifting to this position. This point is readily recognized in Fig. 19. Suppose atom B_2 of the first layer moves in the twin position B'_2 while the atoms C_6 and C_7 of the second layer remain at their untwinned position. As a result of its move, atom B_2 finds itself in the centroid B'_2 of the equilateral triangle $C_2C_6C_7$. The distance B'_2C_2 has been shown previously to be 5.8% shorter than the closest approach between atoms in the original structure. Since

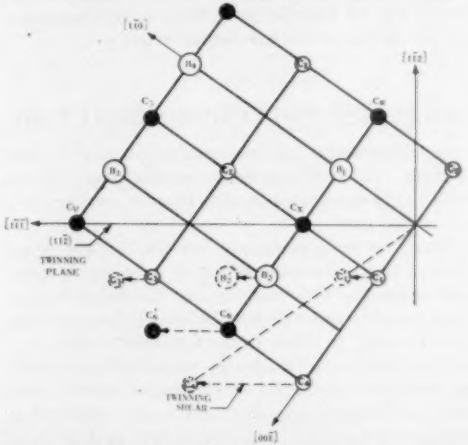

Fig. 20 Sketch of the $(\bar{1}10)$ plane, perpendicular to the (112) twinning plane, which contains the atoms moved to the twin positions in Fig. 19

The atoms shown solid are in the next $(1\bar{1}0)$ plane in front of the one being considered; only the corner atoms in this plane are shown in either Figs. 19 or 20

* Where A is the lattice parameter.

$B'_2C_3 = B'_2C_6 = B'_2C_7$ the shift of one single layer to the twin position puts each atom of this layer at an abnormally short distance to all three neighbors C_3, C_6 and C_7. From Fig. 20 it is obvious that this situation is limited to only one neighbor if several successive layers shift to the twin position. The adjustment of the boundary atoms to the latter case will therefore require less surface energy and is more likely to occur.

The next point of interest is to find out how many successive layers of atoms will move to the twin position; in other words, how thick is the twin? The answer to this question requires the knowledge of the energies involved in the formation of a twin. As shown in the Appendix the mechanism of twinning can be treated in an elementary way as a problem of elastic stability. This treatment is patterned after a similar treatment proposed by Bragg for the mechanism of slip.[21] The main assumption of Bragg's theory is that the elastic strain energy stored by the applied load does not change as a result of slip. If this assumption is extended to twinning, it follows that the surface energy required at the twinning plane must be supplied by the decrease of other forms of energy within the grain. Natural sources for such an energy appear to be lines of atomic misfits or dislocations. Likewise, planes containing dislocations appear to be a logical choice for a twinning plane. On this understanding, the minimum thickness of a twin appears to be given by the distance of two successive planes of misfits, i.e., by the size of the mosaic block.* [22]

If t represents the minimum thickness of the twin (= size of the mosaic block) and L the size of the grain within which the twin is formed, the critical shear stress for twinning τ_t can be written as follows according to the Appendix,

$$\tau_t = G\gamma_t \frac{2t}{L}. \tag{2}$$

G is the shear modulus of elasticity and γ_t is the amount of shear involved in the twin process.

Based on the same assumption the formula for the critical shear stress for slip, τ_s on the same gliding system reads according to Bragg[21]

$$\tau_s = G\frac{\lambda_s}{2t}, \tag{3}$$

where λ_s is the unit translation involved in slip. Comparison between expressions 2 and 3 shows that for the occurrence of twinning

$$\tau_t \leqslant \tau_s \tag{4}$$

or

$$t \leqslant \sqrt{\frac{L\lambda_s}{\gamma_t}}\dagger \tag{5}$$

* A more detailed theory of slip developed later by Bragg[22] would not seem to invalidate this conclusion, even though the dynamics of twin would have to be reconsidered.

† In the more detailed Bragg's theory τ_t is increased by a factor of ten. A factor of a similar magnitude is to be expected if the criterion for twin is to be modified accordingly. Thus, the order of magnitude of t is still given correctly by formula 5.

THE CRITICAL TEMPERATURE FOR TWINNING

From previous discussion it is apparent that the plastic deformation will proceed by twin rather than slip, if the size of the mosaic block falls below the value given by the right side of expression 5. One of the governing factors for this occurrence is the temperature at which the metal is deformed. This conclusion follows from the studies of single crystals. It has been shown[24] that the critical shear stress for slip in single crystals increases as the temperature is lowered. The relationship is sufficiently well represented by the formula

$$\tau_s = A - B\sqrt{T} \tag{6}$$

where A and B are constant for a given material, and T is the absolute temperature.[25] If formula 6 is combined with 3 and 5 there follows

$$A - B\sqrt{T} \geqslant \frac{G}{2}\sqrt{\frac{\lambda_s\gamma_t}{L}} \tag{7}$$

Expression 7 shows that there is a critical temperature T below which the stress required for slip is larger than the stress required for twin on the particular glide system. Therefore, twinning will take precedence over slip below this temperature.*

Polycrystalline metals also yield for a given percentage of deformation, say 0.2%, at stresses which increase as the temperature is lowered.[26, 27] The dependence on temperature appears to be somewhat greater than is indicated by formula 7. However, results of tensile tests performed by McAdam, *et al.*[28] between −180° C and room temperature on annealed 0.12% C steel can be fitted into formula 7 within ±5000 psi. The value of stress is that determined at the onset of yielding. Using the octahedral shear stress as the criterion of yielding in polycrystalline metals with random grain orientation[29] one obtains the following formula for the above results between room temperature and −188° C.

$$\tau_s = \frac{\sqrt{2}}{3}\text{Y. P.} = 80{,}000 - 3900\sqrt{T}\ \text{psi}. \tag{8}$$

T is here the absolute temperature in ° K.

Substitution of 8 in 7 yields after replacement of G, γ_t, and τ_s by their values, 11.5×10^6 psi, 0.707, and 2.5×10^{-8} cm., respectively,

$$\frac{1}{\sqrt{L}} = 102 - 4.86\sqrt{T} \tag{9}$$

Formula 9 gives the relation between the critical temperature of twinning, T, and the grain size, L. This relationship is represented in Fig. 21 by the first curve to the left. The other curves in this figure have been derived from the modified Bragg's formula[22] in which the right hand side of (3) is multiplied by a constant k

* Attention is called to the fact that on other glide systems on which slip alone is possible, no such criterion can be formulated. This is plainly seen in Fig. 5 in which slip lines are noticeable even at −280° F.

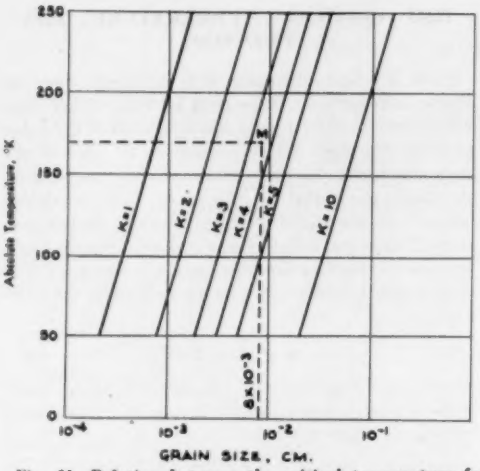

Fig. 21 Relation between the critical temperature for twinning and grain size for various degrees of grain boundary restraint

greater than one. According to Bragg, the value of $k = 1$ corresponds to a totally unrestrained slip. On the other hand, if slip is totally restrained at the boundary the value of k is increased tenfold. The true state of affairs is probably somewhere in between. Figure 21 shows indeed that the critical temperature of twinning, viz. $-170°$ F ($+161°$ K) obtained in our experimental work, is in correct relationship to the grain size of our specimens ($5–10 \times 10^{-3}$ cm), if k is taken around 3.5*

The influence of grain size on the yield point itself cannot be overlooked, but in mild steel the results appear to be inconclusive in the range of 10^{-2}–10^{-3} cm according to the results by Edwards and Pfeil.[20] If the few abnormally high results are excluded, the variation does not seem to be greater than 15% on the average.

RATE OF STRAINING AND THRESHOLD TEMPERATURE FOR TWINNING

Many phenomena of mechanical behavior in metals and in particular strain hardening and creep, appear to obey a reaction-rate type of law in which the strain rate varies exponentially with temperature. The threshold temperature for twinning is no exception to this rule above the critical temperature of $-170°$ F, but as seen from Fig. 18, below this temperature a one hundredfold variation of strain rate failed to affect appreciably the temperature of twinning. This apparent anomaly finds its explanation in the particular relationship which exists between twinning and slip on the (112) plane of the iron crystal.

It has been shown previously that below the critical temperature the formation of a twin requires less stress, and hence less strain energy, than the formation of a slip in an iron crystal. Consequently the deformation will proceed by means of twinning rather than slip below this temperature. The process of twinning, not unlike the austenite-martensite reaction,[21] appears to occur rather suddenly. This is confirmed by the sharp sound (the "tin cry") which is emitted during the deformation.[24] It is also known that twinning in steel cannot be prevented under the highest explosive rates.[2] Both facts indicate that the twins are generated with a speed which is close to that of sound. Under these circumstances it can hardly be expected that strain rates of the order of those used in this work would have any marked influence on twinning below $-170°$ F.

The situation is quite different above $-170°$ F. Since the strain energy required for slip is now smaller than that required for twinning, no twins should appear unless slip is inhibited in some way on the (112) plane. How this can come about is best visualized if the twin-slip relationship is examined on the atomic scale.

A model was constructed, patterned after Barrett's discussion,[16] using plastic balls to represent spherical atomic fields of influence. With this model it can be shown that the energy necessary to move a sphere into the "full slip" position on the (112) twinning plane is approximately twice that required to move one into the twin position. It can also be shown that twinning can be accomplished by the application of a shearing force in one direction only; if the force is applied in the opposite direction, it must be of sufficient magnitude to overcome the slip-potential barrier, and would then have sufficient energy remaining to move past the twin position and on into the "full slip" position. This may be seen more readily by examining Fig. 22. If movement is from left to right, the sphere may easily stop in the twin position, blocked by the high energy barrier between that and the "full slip" position. On the other hand, if movement is from right to left, it is very improbable that the sphere could stop in the twin position; since the structure seeks the lowest energy level and there is practically no energy barrier going in that direction from the twin position, it is most probable that the sphere would drop on into the "full slip" position.

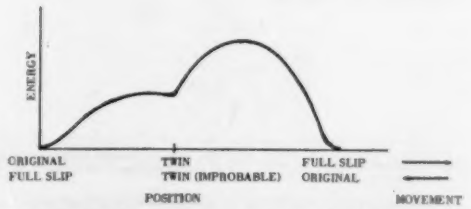

Fig. 22 Sketch showing the energy relationship for movement of an atom along the (112) plane in a [111] direction.

* This result should be corrected to account for the higher C and Mn content of our specimens. It appears, however, from the comparison of results on 0.12 and 0.42% C steel[20] that the correction would not be great.

If the above model bears any resemblance to reality, one would expect that during deformation the atoms should jump from the twin to the full slip position by virtue of thermal fluctuations alone. However, two conditions must be fulfilled:

1. The free energy of the system should decrease as a result of the twin-slip process.

2. Enough atoms must jump from the twin to the slip position (i.e., must have been activated) to propagate the slip across the crystal.

If entropy changes are neglected the first condition is a restatement of the strain energy relation between twinning and slip given previously. It was shown that above $-170°$ F less energy is required for slip than twinning.

The second condition imposes the rate at which the deformation must proceed if the slip is to devote fully in the crystal. According to statistical mechanics[32] this rate must be slow enough for a sufficiently large fraction of the "twinned" atoms to jump over the potential barrier and generate the slip process. It can be shown that the fraction of the so activated atoms is given by the expression

$$e^{-\Delta F/RT} \tag{10}$$

In this expression ΔF is the increase of the free energy in the activated atoms. ΔF is measured by the work necessary to move one mole of atoms reversibly from the twinned position to the position at the top of the potential barrier, R is the gas constant = 1.987 g-cal per ° K, per mole, and T is the absolute temperature.

From the above condition it follows that the deformation will proceed by slip above $-170°$ F provided the rate of deformation varies proportionally to expression 10. This can be written as

$$\dot{\epsilon} = \dot{\epsilon}_0 e^{-\Delta F/RT} \tag{11}$$

where $\dot{\epsilon}_0$ is a coefficient of proportionality. Equation 11 proves the relationship between the rate of straining and the threshold temperature for twinning which has been established experimentally.

At this point a few remarks can be made concerning the value of ΔF. Regardless of the final outcome the process of glide on the (112) plane can be pictured as consisting of two steps. In the first step the atoms C_1, B_2, C_3 of the first layer of atoms in Fig. 20 have been displaced to their twin positions C'_1, B'_2, C'_3, through an amount of shear, γ_t, while the atoms of the other layers remain at their place. As pointed out previously, this step causes considerable distortion of the lattice, and the position of the first layer of atoms is unstable. The next step consists of securing a more stable configuration. Depending on the temperature this is achieved in two ways. Below the critical temperature for twinning a stable twin of finite thickness is formed by the displacement of other layers of atoms to the twin position. Above the critical temperature for twinning the atoms of the first layers are merely displaced further to the stable, full slip position by an additional amount of shear, $2\gamma_t$. The first step (twinning of the first layer of atoms) may require considerable activation energy in a perfect crystal, since it is connected with the generation of misfits, or dislocations[28]. However, the next step, from the twin to the full slip position represents a tendency for the atoms to regain their stable position. Hence, only a moderate activation energy may be expected in the process of overcoming the potential barrier which according to Fig. 22 separates the twin from the full slip position.

That this is so may be shown by the following admittedly simplified reasoning. Suppose the potential field pictured in Fig. 22 is approximated by a simple periodic function having its minima at the slip positions and the maxima half way between. A function satisfying this requirement is

$$\Delta U = \frac{\Delta U_0}{2}(1 - \cos 2\pi\gamma/3\gamma_t) \tag{12}$$

where ΔU_0 is the potential barrier half way between the slip positions, and $3\gamma_t$ is the amount of shear involved in full slip. When the atoms of the first layer occupy their twin position $\gamma = \gamma_t$, and the corresponding increase of the potential energy is from expression 12

$$\Delta U_t = {}^3/_4 \Delta U_0 \tag{13}$$

Consequently, the potential barrier which remains to be overcome in the next, twin-full slip step is

$$\Delta F = \Delta U_0 - \Delta U_t = \Delta U_0/4 \tag{14}$$

To obtain the numerical value of ΔU_0 it will be recalled that for small values of γ the energy per unit volume is

$$\Delta U = G\gamma^2/2 \tag{15}$$

Hence,

$$(\partial^2 \Delta U/\partial \gamma^2)_{\gamma = 0} = G \tag{16}$$

Substituting for ΔU the expression 12 one has

$$\Delta U_t \backsimeq 0.45 G\gamma_t^2 \tag{17}$$

Hence, the activation energy ΔF on per mole basis becomes with reference to formula 14

$$\Delta F \backsimeq 0.11 G\gamma_t^2 M/\delta \tag{18}$$

where M is the molar and δ the specific weight.

For mild steel

G = 11.5 × 10^6 psi = 7.92 × 10 in. dyne/cm.^{2} = 19 × 10^3 cal/cm^3
M = 55.85 mole grams
δ = 7.86 gr/cm^3
γ_t = 0.707

Hence,

$$\Delta F = 0.11 \times 19 \times 10^3 \times \frac{55.85}{7.86} \times 0.707^2 \backsimeq 7600 \text{ cal/mole}$$

This value agrees in order of magnitude with the experimental value of 4200 cal/mole.

INFLUENCE OF VARIOUS FACTORS

Before closing this discussion the influence of other factors on the critical temperature of twinning will be briefly reviewed.

A. Microstructure. Relation 7 and Fig. 21 suggest that the decrease of grain size L should cause the lowering of the critical temperature of twinning. Direct data are not available. However, Bruckner's results on the effect of steelmaking reported previously[13] may well be due to grain refinement.

B. Prior Straining. Analysis of relation 7 shows that prior straining can lower the twinning temperature by increasing the value of the yield point. This conclusion also follows from the inspection of Fig. 21, since an increase of yield point means higher values of k for the same value of L. Again, direct experimental evidence is lacking. Indirectly the fact that cold working at room temperature inhibited twinning at this temperature[4] but not at a lower temperature[11] is consistent with this analysis. However the real cause may well lie in the particulars of the slip mechanism. Electron microscope studies on polycrystalline aluminum[23] have revealed that early stages of deformation are characterized by the appearance of many isolated slip lines which broaden into a succession of slip lines, or a slip band, in the later stages of deformation. Obviously, an existing slip line is more apt to generate other slip lines than a twin. Nevertheless the question is far from being settled, and further experiments are needed.

C. Size of Twin Lamellae. It has been observed in the present work and elsewhere that the twin lamellae are larger at higher than at lower temperature of testing. Similar observations have been made on the width of the slip bands.[23] Both phenomena may well represent a process of growth stimulated by temperature and deformation. That increasing deformation produces larger slip bands has been mentioned earlier. The same has been found to hold for twinning in zinc.[24] Since larger deformation means higher yield point, the growth of the twin lamella is well justified on the basis of equation 2. It should be added that a similar justification can be given for the broadening of the slip band.

D. Alloying Element. It does not seem possible to predict the influence of the alloying element on the temperature of twinning on the basis of the present analysis alone. For example, silicon has been mentioned as a factor in raising the temperature of twinning.[9] At first, this influence would seem to follow from our theory, since silicon is known to increase the grain size and a larger grain means a higher temperature of twinning according to Fig. 21. But silicon is also known to increase the yield point which should tend to lower the temperature of twinning. In view of these two conflicting tendencies a more quantitative approach appears necessary. It is hoped that further work based on more recent data will provide the answer.

CONCLUSIONS FROM THEORETICAL WORK

The picture of the twin-slip mechanism which has been presented admittedly is far from perfect and it is lacking in many details. A great deal more available data must be analyzed and some of its implications must be verified before this picture emerges as little better than a working hypothesis. But as such it has a few merits which seem worthy of mentioning.

1. It offers a satisfactory explanation of the particular strain rate-temperature relation found in this work.
2. It predicts the right order of the critical temperature of twinning and the activation energy for the twin-slip process.
3. It suggests further experiments aimed at the influence of grain size, prior straining and alloying elements on the twin-slip mechanism.

The third point perhaps is the most meritorious as it offers a lead toward a better understanding of the plastic properties of metals.

Appendix

CRITERION FOR TWINNING

The criterion for twinning used in this work has been patterned after a similar criterion which Bragg has formulated for the case of slip.[21] Both criteria are derived from the postulate that a crystal subjected to shear will slip or twin, if the elastic strain energy due to shear is decreased by the process. The critical shear strain therefore will be that strain for which the strain energy of the final configuration is just equal to the strain energy of the original configuration.*

A very simplified picture will show how this criterion can be obtained for both slip and twin. Figure 23 (*a*) and (*b*) represents an almost perfect crystal† subjected to shear. The sides AD and BC are parallel to the glide direction, and the plane of glide is perpendicular to the plane of both figures. For convenience, the sides AB and CD have been drawn in the particular direction which suffers no change of length when it is tilted to the twin position.[24] This direction of course is immaterial for the case of slip. We shall inquire for what particular values of BB' the crystal will slip or twin, respectively.

Comparison between Fig. 23 (*a*) and (*b*) shows that the process of slip is characterized by a translation of one atomic layer through a distance equal to the elementary "quantum" of slip,[22] which is the interatomic distance, λ_0. This slip takes place on several planes $1, 2, \ldots n$ which are separated from each other by intervals, t, of the dimension of a mosaic block. We shall assume for the sake of simplicity that all intervals are the same. Actually, the size of the block is likely to have a random distribution around the average. In variance with this picture, the process of twinning is confined to only one interval. More specifically,

* It is easy to recognize in this formulation the more general criterion of elastic stability.[25] However, the solution does not call here for a variational calculus since the final configuration is imposed by the crystal structure.

† We shall assume that imperfections are confined only to isolated planes of glide.

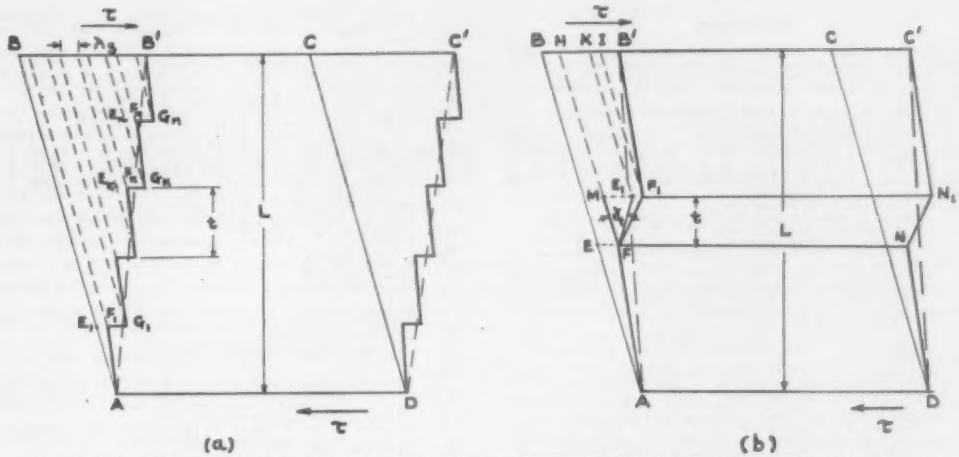

Fig. 23 Glide mechanism in a crystal, patterned after Bragg criterion; (a) slip process, (b) twin process

each layer of this interval undergoes a translation corresponding to a constant shear strain, γ_t which is characteristic of the twin process.

With the help of these pictures we shall derive expressions for the strain energies U_0, U_s and U_t of the original, slip and twin configurations, respectively.

The original strain energy is simply

$$U_0 = \frac{G}{2}\left(\frac{BB'}{V}\right)^2 V \qquad \text{(A1)}$$

where G is the shear modulus and V the volume of the crystal.

After slip the crystal has been subdivided in $(n + 1)$ domains by n slip planes. The elastic shear strain is the same in each domain. Consequently

$$U_0 = \frac{G}{2}\left(\frac{E_kF_k}{t}\right)^2 V \qquad \text{(A2)}$$

where $\frac{E_kF_k}{t} = \frac{E_1F_1}{t} = \cdots = \frac{E_nF_n}{t}$ is the elastic shear strain.

From Fig. 23 (*a*) one has

$$BB' = (n + 1)E_kF_k + n\lambda_s \qquad \text{(A3)}$$

Substitution of A3 in A2 yields

$$U_s = \frac{G}{2}\left[\frac{BB'}{(n+1)t} - \frac{n\lambda_s}{(n+1)t}\right]^2 V \qquad \text{(A4)}$$

The critical value of BB' will be obtained when

$$U_0 = U_s$$

or, using expressions A1 and A4, when

$$BB' = n\lambda_s/2$$

The critical shear stress for slip

$$\tau_s = G\frac{BB'}{L} = \frac{G}{2}\frac{\lambda_s}{t}\frac{n}{n+1}$$

In practice n seldom is smaller than 100. Hence to a sufficient degree of approximation

$$\tau_s = \frac{G}{2}\frac{\lambda_s}{t} \qquad \text{(A5)}$$

This is the criterion derived by Bragg under somewhat different simplifying assumptions.

In the case of twinning the strain energy U_t is the sum of the strain energies in the twinned and untwinned portions of the crystal. With reference to Fig. 23 (*b*).

$$U_t = 2 \times \frac{G}{2}\left(\frac{2EF}{L-t}\right)^2 V\left(\frac{L-t}{2L}\right) + \frac{G}{2}\left(\frac{E_1F_1}{t}\right)^2 V\frac{t}{L} \qquad \text{(A6)}$$

But

$$\frac{E_1F_1}{EF} = \frac{2t}{L-t}$$

hence

$$U_t = \frac{G}{2}\left(\frac{2EF}{L-t}\right)^2 V \qquad \text{(A7)}$$

Again from Fig. 23 (*b*)

$$ME_1 = \gamma_t t$$

where γ_t is the amount of shear strain caused by twinning. Hence,

$$BB' = BH + HK + KI + IB = 2\frac{EF \times L}{L-t} + \gamma_t T \qquad \text{(A8)}$$

Substitution of A8 in A7 yields

$$U_t = \frac{G}{2}\left[\frac{BB' - \gamma_t t}{L}\right]^2 V \qquad \text{(A9)}$$

The critical value of BB' will be obtained by putting $U_0 = U_t$ or with reference to A1 and A9

$$BB' = \gamma_t t/2 \qquad \text{(A10)}$$

The critical shear stress for twinning thus becomes

$$\tau_t = \frac{G}{2}\frac{t}{L} \qquad \text{(A11)}$$

References

1. Rinehart, John S., "Some Quantitative Data Bearing on the Scabbing of Metals under Explosive Attack," *J. App. Phys.*, **22**, 555–560 (May 1951).
2. Rinehart, John S., "Work Hardening of Mild Steel by Explosive Attack," *Ibid.*, **22**, 1086–1087 (August 1951); *Ibid.*, 1178–1181 (September 1951).
3. Woolsey, C. C., Jr., Thesis, M.S., Department of Engineering, University of California, Los Angeles, January 1952.
4. Rosenhain, Walter, and McMinn, Jean, "The Plastic Deformation of Iron and the Formation of Neumann Lines," *Proc. Roy. Soc., Ser. A*, **108**, 231–239 (1925).
5. Smith, S. W. J., Dee, A. A., and Young, J., "The Mode of Formation of Neumann Bands," *Ibid., Ser. A*, **121**, 477–514 (1928).
6. Tipper, C. F., and Sullivan, A. M., "Fracturing of Silicon-Ferrite Crystals," *Trans. ASM*, **43**, 906–934 (1951).
7. Foley, F. B., and Howell, S. P., "Neumann Bands as Evidence of Action of Explosives upon Metal," *Trans. AIME*, **48**, 891–913 (1922).
8. Pfeil, L. B., "The Deformation of Iron, with Particular Reference to Single Crystals," *Jnl. Iron Steel Inst.*, Carnegie Scholarship Memoirs, **13**, 319–380 (1926).
9. Barrett, C. S., Ansel, G., and Mehl, R. F., "Slip Twinning, and Cleavage in Iron and Silicon Ferrite," *Trans. ASM*, **25**, 702–733 (1937).
10. Hadfield, R. A., "Experiments Relating to the Effect on Mechanical Properties of Iron and Its Alloys Produced by Liquid Air Temperatures," *Jnl. Iron Steel Inst.*, No. I, 147 (1905).
11. Geil, G. W., and Carwile, N. L., "Tensile Properties of Ingot Iron at Low Temperatures," *Jnl. Research*, National Bureau of Standards, **45**, 129–147 (1950).
12. Bruckner, W. H., "The Micro-Mechanism of Fracture in the Tension Impact Test, Supplementary Report No. 1," THE WELDING JOURNAL, **30** (9), Research Suppl., 459-s to 469-s (1951).
13. Bruckner, W. H., "The Micro-Mechanism of Fracture in the Tension Impact Test," *Ibid.*, **29** (9), Research Suppl., 467-s to 476-s (1950).
14. Carrington, W. E., and Gaylor, N. L. V., "The Use of Flat-Ended Projectiles for Determining Dynamic Yield Stress, III. Changes in Microstructure Caused by Deformation Under Impact at High-Striking Velocities," *Proc. Roy. Soc. (London)*, **194-A** 323–331 (1948).
15. Barrett, C. S., *Structure of Metals, Crystallographic Methods, Principles, and Data*, McGraw-Hill, New York City, pp. 307–317 (1943).
16. Barrett, C. S., "The Crystallographic Mechanisms of Translation, Twinning, and Banding," Seminar on Cold Working of Metals, ASM, pp. 65–98 (1949).
17. Ellis, W. C., and Treuting, R. G., "Atomic Relationships in the Cubic Twinned State," *Trans. AIME*, **189**, 53–55 (1951).
18. MacGregor, C. W., Grossman, N., and Shapler, P. R., "Correlated Brittle Fracture Studies of Notched Bars and Simple Structures," THE WELDING JOURNAL, **26** (1), Research Suppl., 50-s to 56-s (1947).
19. Grossman, N., "Pearlitic Structure Effect on Brittle Transition Temperature," *Ibid.*, **28** (6), Research Suppl., 265-s to 269-s (1949).
20. von Kármán, T., and Duwez, P., "The Propagation of Plastic Deformation in Solids," *J. App. Phys.*, **21**, 987–994 (1950).
21. Bragg, W. L., *Nature*, **149**, 511 (1942).
22. Bragg, W. L., "Effects Associated with Stresses on a Microscopic Scale," Symposium on Internal Stresses, The Institute of Metals, 1948.
23. Cottrell, A. H., "Theory of Dislocations," *Progress in Metals Physics*, V.I. Interscience Publishers, New York (1949).
24. Boas, W., *An Introduction to the Physics of Metals and Alloys*, John Wiley & Sons, p. 86 New York, (1947).
25. Kochendorfer, A., *Plastische Eigenschaften von Kristallen*, Julius Springer, Berlin (1941).
26. McAdam, Jr., D. J., Geil, G. W., and Mebs, R. W., T. P., 2220, *Metals Technol.*, **14**, (1947).
27. Dorn, J. E., Goldberg, A., and Tietz, T. E., *Trans. AIME*, **180**, 205 (1949).
28. McAdam, D. J., Jr., "The Fracture Stress of Metals as Affected by Plastic Deformation, the Stress System, and Size," Seminar on the Cold Working of Metals, ASM, 1949.
29. Deblinger, V., *Z. Metallkunde*, **35**, 182 (1943).
30. Edwards and Pfeil, quoted after *Metals Handbook*, ASM, p. 433 (1948).
31. Cohen, M., Machlin, E. S., Paranjpe, V. G., "Thermodynamics of the Martensitic Transformation," Seminar on Thermodynamics, ASM, 1950.
32. Zener, C., "The Role of Statistical Mechanics in Physical Metallurgy," Seminar on Thermodynamics, ASM, 1950.
33. Blewitt, T. H., and Koehler, J. S., "The Lamellar Nature of Slip and Its Implications," Symposium: Plastic Deformation of Crystalline Solids, 1950. NAVEXOS-P-834.
34. Burke, J. E., "The Migration of Grain Boundaries," Seminar on Atom Movements. ASM, 1951.
35. Southwell, R. V., *An Introduction to the Theory of Elasticity*, Oxford University Press, p. 454 (1941).

The Pressure Vessel Research Committee Realizes Its First Objective

Less guess in design, accurate knowledge of effects of fabricating procedures, expected economy in the use of materials without sacrifice to safety are foreseen clearly as the result of the first five years of committee's efforts

ACTING upon the suggestions of members of the ASME Boiler Code Committee, the Welding Research Council, a research organization set up by the major engineering societies, some five years ago appointed a Pressure Vessel Research Committee to develop programs and carry out needed research which would result in safer and possibly more economical pressure vessels. The research programs were carefully drawn up to cover the more important phases of the selection of materials, the design of pressure vessels to reduce stress concentrations at points such as junctures of head to shells, supports, attachments and reinforced openings; and to understand better the effects of the various processes of fabrication, such as cold forming, welding, heat treatment and testing, on the different materials used in pressure vessel construction.

Modern developments call for higher and higher pressures, associated with high temperatures, with and without corrosive environments. These combinations call for thicker walled pressure vessels, and the size of vessels dictated by presently authorized design stresses is approaching the limits that can be fabricated. Higher strength steels utilizing higher permissible design stresses are required in order to permit progress in the industry. At the low-temperature end of the scale, there have been some failures in large storage tanks which have been subjected to cold winter temperatures. It was generally agreed among engineers that the necessary research work was not being done by other organizations, and that the fabricators of pressure vessels could not individually be expected to effectively carry out such work.

Five years of effort on the part of more than 100 Scientists and Engineers, working in cooperation with seven universities and a number of industrial research laboratories, have produced more than 27 published

(*Continued on page 501-s*)

The Nature of Cleavage Fracture in Steel

Cleavage fracture at any service temperature in steel is affected by artificial notches, inhomogeneities of structure, the ductility of the material, its structure and composition

by H. M. Miekk-oja

INTRODUCTION

THE frequent occurrence of brittle fracture in low-carbon steel has focused attention on the fact that ductility, as well as strength, is an essential point to be considered in determining the suitability of a metal for construction purposes. Indeed, ductility at low temperatures under impact cannot be ascertained by static tests performed at room temperature.[1-4]

The tendency of a steel to fail in a brittle manner is increased by notches, which function as stress-raisers. Their presence probably forms a necessary condition for brittle failure in low-carbon steel under normal circumstances. Consequently, the designer knows how to avoid notches, and structural discontinuities, thus diminishing possible brittle fracture. However, not only external and artificial notches, but, also, inhomogeneities in the internal structure of the metal itself may function as stress-raisers.[1] Obviously, peculiarities in the internal structure of mild steel are responsible for brittle behavior under certain conditions, evidenced by the fact that the behavior of mild steel, brittle or ductile, is largely dependent upon changes in its internal structure, brought about by alloying, working, or heat treatment. In addition, austenitic steels, and, also, other metals with face-centered cubic lattice—e.g., copper, aluminium and many of their alloys—will not fracture in a brittle manner, not even at low temperatures or under impact.[5] Consequently, an understanding of the internal mechanism of fracture may possibly help to find additional means for reducing tendency to brittleness. This is attained by studying the internal structure of the metal.

TRANSITION TEMPERATURE AND TENSILE REDUCTION OF AREA

The first attempt toward the solution of the problem of brittleness in low-carbon steels was to find a laboratory testing method, the results of which would give a definite correlation with the behavior of the metal under practical conditions. All methods, static and dynamic, revealed the fact that fracture of a notched specimen changes from shear to cleavage more or less abruptly with decreasing temperature.[6] Investigations into the nature of the fracture led to the definition of the "fracture transition temperature" below which the fracture once initiated may propagate in a cleavage manner; and of the "ductile transition temperature" below which it may not only propagate, but also initiate in a cleavage manner.[6] These transition temperatures correlate in a way with the behavior of the metal under practical conditions, but vary largely depending upon the testing method.

Subsequently, attempts were made to correlate transition temperature with the results of a simple test to be performed at room temperature. Investigations made at Lehigh University on two special low-carbon steels showed a straight-line relationship between tensile reduction of area and transition temperature, defined in different ways.[7] This relationship was assumed to exist for other materials also.[8] On the other hand, objections to this assumption were raised on the basis that different alloying elements, e.g., manganese, phosphorus and silicon, shift the transition temperature more rapidly for a unit change in reduction of area than carbon.[9] Therefore, variation in the relationship in question is expected to increase when steels of widely different composition are included. Although it is now evident that the practical significance of the relationship is limited, the author will take up the question since it forms a basis when the differences in the behavior of steel with different rates of stress formation are considered. The results of investigations made at the Vuoksenniska Steel Works in Finland, given below, reveal the susceptibility of some steels to strain aging.

These investigations measured the reduction of area in the conventional tensile test at room temperature on the one hand, and the transition temperature by means of Charpy-keyhole specimens on the other. Both measurements were made before and after strain aging. The steels investigated were silicon-killed plain carbon steels. The carbon content varied from 0.09 to 0.69%.

H. M. Miekk-oja is Acting Professor of Physical Metallurgy, with the Finland Institute of Technology, and also Technical Adviser to the Outokumpu Metal Works, Finland.

Table 1

Heat	Composition, % C	Mn	Si	P	S	Cr	Ni	Cu
1	0.09	0.37	0.20	0.014	0.015	..	0.20	0.22
2	0.14	0.46	0.23	0.020	0.023	..	0.15	0.34
3	0.31	0.54	0.22	0.025	0.017	..	0.17	0.39
4	0.41	0.50	0.24	0.021	0.029	..	0.22	0.24
5	0.69	0.29	0.23	0.032	0.017	0.03	0.15	0.30

Other alloying or impurity elements, were of conventional limits, as can be seen from Table 1.

The specimens were taken from rods, 18 mm in diameter, which after hot-rolling had been normalized at temperatures according to carbon content (Table 2). The microstructure of the specimens consisted of ferrite and lamellar pearlite in proportions given in Table 2. The thickness of pearlite spacings varied from 0.3 to 0.5 μ, and ferritic grain size from 0.018 to 0.025 mm. The strain-aging treatment consisted of a 10% straining and subsequent annealing at 250° C for 1 hr. Material for the preparation of Charpy specimens was strained through cold rolling, whereas tensile test specimens were strained in the tensile-testing machine. Inasmuch as the investigations were intended to serve practical purposes, no measurements upon transition temperature between straining and annealing were made. Consequently the effects of both treatments could not be separated.

The resulting impact energy/temperature curves for all steels in normalized condition are given in Fig. 1, and in strain-aged condition in Fig. 2. The relationship between tensile reduction of area and transition temperature, defined as temperature at which the impact energy decreases to one-half of its maximum value, is shown in Fig. 3. In the same figure some results of the Lehigh University[7] experiments are reproduced. From the results shown in Figs. 1-3 the following interpretations are made.

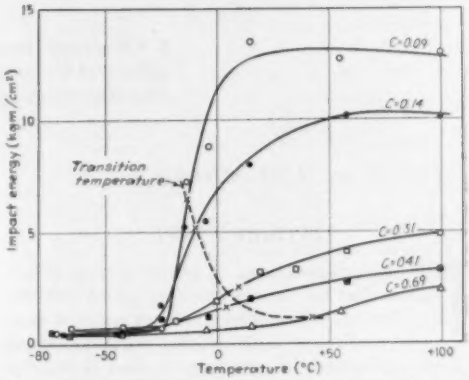

Fig. 2 Impact energy/temperature curves for strain-aged silicon-killed carbon steels with varying carbon contents

Table 2

Heat →	1	2	3	4	5
Normalizing temperature, ° C	910	890	880	840	800
Ferritic grain size, mm.	0.025	0.020	0.018	0.018	...
Ratio of ferrite to pearlite	Very great	10	2.0	1.0	Very small
Pearlite spacing, μ	0.3	0.4	0.4	0.5	0.5

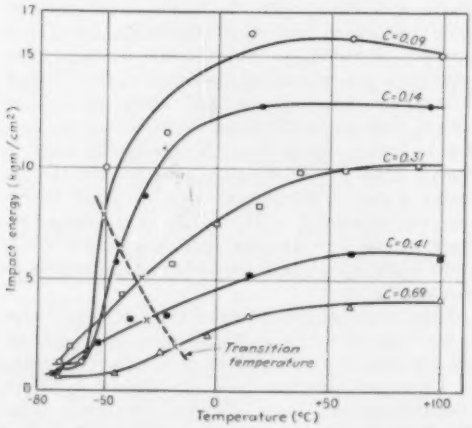

Fig. 1 Impact energy/temperature curves for normalized silicon-killed carbon steels with varying carbon contents

Increase in carbon content from 0.09 to 0.69%, which brings about a change from a nearly ferritic to a pearlitic structure, results in a strong decrease in the reduction of area (from 72 to 35%) and also the same in maximum impact energy for normalized and strain-aged steels. But it results in only a moderate increase in the transition temperature, when this is defined by means of the half-value of maximum impact energy; and practically no change of transition temperature at all, when an arbitrarily low value of impact energy, 1.0 kg/cm², is taken for its criterion. It must be kept in mind, in addition that not only the ratio of ferrite to pearlite, but also the ratio of manganese to carbon changes with carbon content, in our case from 4.1 to 0.4, when the carbon content increases from 0.09 to 0.69%. The decrease in the ratio Mn/C, again, is known to bring about an increase in the transition temperature. Consequently

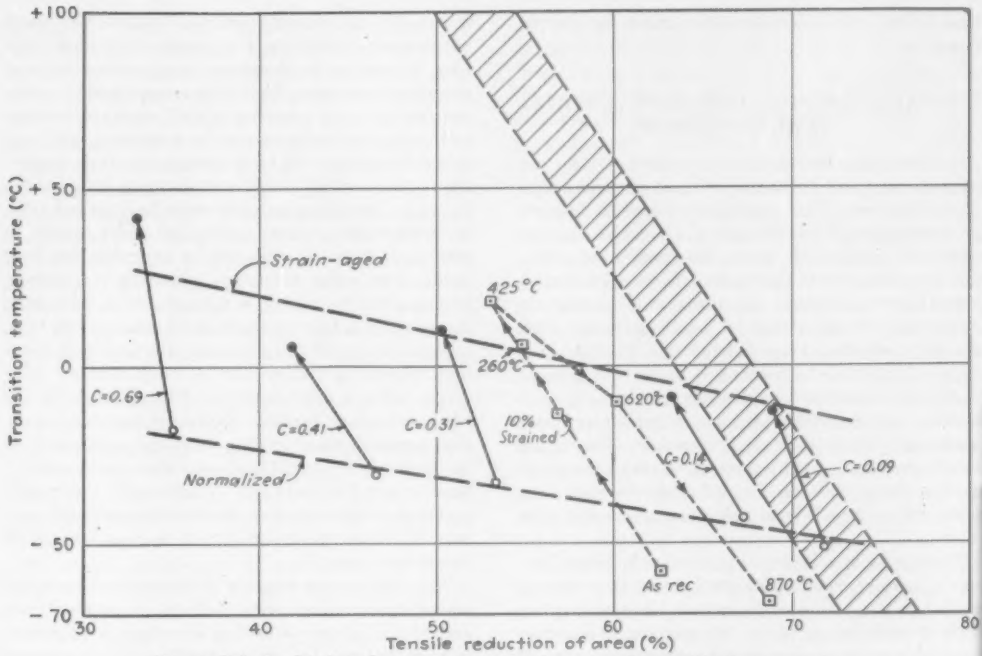

Fig. 3 Relationship between tensile reduction in area and transition temperature

Results of this work: -○---○-, normalized silicon-killed carbon steels. -●---●-, strain-aged silicon-killed carbon steels. Criterion for transition temperature, the half-value of maximum impact energy in keyhole Charpy test.
Results of Lehigh University:[7] Shaded area, V-notch Charpy test, absorbed energy as criterion for aluminum-killed ASTM A-201 Grade A and rimmed ASTM A-70 steels. -□--- -, Lehigh slow-notch bend test, % contraction as criterion, for ASTM A-201 steel.

the resulted increase, 30°C, in the transition temperature is probably not due to changes in the micro-structure alone, but goes partly back to changes in the ratio Mn/C.

Strain aging treatment, on the contrary, results only in a small change in the reduction of area (3%), whereas its influence on the transition temperature is considerable, 40° C average. The results for a rimmed steel, with a carbon content of 0.18% not reproduced in these figures, gave a rise of 60° C in the respective temperature. The results of Lehigh University showed still greater changes, up to 90° C.

As a whole, the tensile reduction of area seems to depend primarily on the carbon content, i.e., on the microstructure; whereas the transition temperature, especially the "ductile" one, is mainly determined by properties of ferrite which have been altered during strain aging. As a consequence, no straight-line relationship between tensile reduction of area and transition temperature may be valid, if composition and treatment both vary widely. A change in these factors may change only the microstructure, and, accordingly, the reduction of area, but may leave the properties of ferrite and transition temperature nearly untouched, and vice versa.

As to the transition temperature and brittle or ductile behavior of steel in general, the most significant fact is that it must be determined primarily by properties of the ductile constituent in the structure, i.e., by those of ferrite, inherent in its body-centered cubic lattice, or affected by alloying, working or heat treatment. This viewpoint is strongly emphasized also by Schaub.[10] Investigations into the nature of brittleness should, therefore, be directed mainly to the properties of ferrite and other metals with body-centered cubic lattice. True, changes in microstructure, such as spheroidization, variations in the thickness of pearlite lamellae, etc., have been found to result in marked changes in the transition temperature,[11, 12] but such changes, though possibly detrimental in practice, may be considered to have only a secondary influence, e.g., through accentuating notch effects. In addition, a treatment necessitated by such changes may produce alterations in the properties of ferrite too. In spite of the fact that cleavage fracture often initiates at the fracture of an inbedded carbide particle,[13] the cleavage fracture is undoubtedly a characteristic of ferritic crystals. If austenitic, the surrounding matrix will not fracture in a cleavage manner.

However, many features of microstructure, e.g., ferritic and, also, inherent austenitic grain size, may have an essential, although indirect, influence on those properties of a ferritic lattice which determine its brittle behavior under certain conditions. Properties induced by aging processes may be affected by grain size. Thus the effects based upon properties of ferritic lattice and

those based upon microstructure cannot be sharply separated.

CLEAVAGE FRACTURE AND CRYSTAL STRUCTURE OF FERRITE

An ideal brittle fracture may be defined as a fracture which initiates and propagates without preceding plastic deformation. The possibility of such a fracture occurring at a high rate of loading in materials that are capable of considerable plastic deformation at a slow rate of loading, proves that normal deformation in such metals may be inhibited. In other words, it conditions the existence of a delay time for initiating of slip. That has been ascertained by Kramer and Maddin in a single crystal of body-centered cubic beta-brass.[5] Further, it conditions a sudden rise of stress at a localized area to such an extent that cleavage fracture occurs before the delay time for slip is exceeded. The sudden rise of stress is the most important condition for cleavage fracturing, since the slip will otherwise relieve the stress and prevent it from rising to a necessarily high value.

The significant role played by notches in brittle fracture is logically explained by the fact that they create a multiaxial stress field at their ends, thus raising the stress necessitated by plastic deformation, which effect depends in a known way on the geometrical factors of the notch. An increase in the rate of loading naturally increases the rate of stress formation at the end of notches. The decrease of temperature again increases the delay time for slip, which fact was revealed by the results of Kramer and Maddin.[5] Consequently, a high rate of loading and a low temperature promote the occurrence of fracture in a brittle manner.

If the temperature is below the "ductile" transition temperature, the stress-raising effect of an artificial notch is sufficient to induce initiating of the fracture in a brittle manner. Between "ductile" and "fracture" transition temperatures the effect of an artificial notch, however, is not sufficient for a cleavage fracture, and fracturing initiates in a shear manner. But shear fracture constitutes a new and extremely sharp notch with accentuated stress-raising properties,[8] and in addition, the formation of the crack is rapid, also during slow deformation. This promotes a sudden stress formation at the sharp end of the crack, with resulting cleavage fracture. For this reason cleavage fracture once initiated generally propagates rapidly throughout the metal.

The above-suggested mechanism for brittle fracture does not exclude the possibility of its being preceded by plastic deformation. It only conditions that plastic deformation, either through slip or mechanical twinning, does not relieve the stress sufficiently to prevent the necessary stress formation at the end of notches. However, the author does not agree with Bruckner,[13] Schaub,[10] etc., who suggest that cleavage fracture is initiated by mechanical twinning, and that this is a condition necessary for cleavage fracture to occur. On the contrary, cleavage fracture may occur not because of twinning, but in spite of it, since twinning, if occurring in abundance, may prevent the local rise of stress to such a high value necessitated by cleavage fracture. As a matter of fact, cleavage fracture and mechanical twinning may be considered, as is suggested by Tipper,[14] to be symptoms of certain properties in ferrite which inhibit normal plastic deformation, i.e., slip. The initiating of cleavage fracture in ferrite, in those regions, where mechanical twins appear in abundance,[13] can be explained by assuming that with sudden local stress formation, when slip is inhibited, twinning occurs; but if it is not sufficient to release the stress, cleavage fracture starts in the same region.

The existence of delay time for slip, and its increase with decreasing temperature in body-centered cubic metals, offers a most significant starting point for the treatment of the problem of cleavage fracture in general, especially since no delay time was ascertained, at least not above −190° C, in face-centered cubic metals, aluminum and alpha-brass.[9] Undoubtedly the investigation into delay time and into the reasons for its existence will reveal the real nature of cleavage fracture in low-carbon steels also.

The difference in behavior of ferritic and austenitic crystals under stress, particularly at low temperatures and with a high rate of loading, goes back to differences in their lattices, i.e., in the body- and face-centered cubic lattice. In comparing these, two points deserve special attention: first, the dissimilarity of those lattice planes which may function as active glide planes determining the mode of slip; and, second, the dissimilarity in the distribution of empty space, where the interstitial atoms may place themselves. The radius of the greatest interstices in ferrite is only 0.36 A whereas in austenite it is 0.52 A.

Contrary to the face-centered cubic lattice, the body-centered lattice does not possess any close-packed lattice plane, but a close packed lattice direction, [111]. Consequently, there are several planes—(110), (112), and (123)—each containing the direction [111] which may function as active glide planes, especially at high temperatures. On the other hand, these relatively weak glide planes may, with difficulty, function actively at low temperatures even with a slow rate of deformation. This difficulty is still accentuated with increased rate of loading. In face-centered cubic lattices, on the contrary, the deformation, especially its first stage, is much the same at all temperatures, as is emphasized by Allen.[15]

Indeed, the peculiarities in the mode of slip inherent in the body-centered cubic lattice may be the last reason for the difference in behavior of ferrite under stress at different temperatures, and under different rates of loading. This condition is supported by the fact that a delay time for slip was ascertained in beta-brass, where the presence of interstitial atoms in appreciable amounts is not probable. In addition, high purity alpha-iron is found to fracture in a cleavage manner, the increase of carbon content from 0.002 to 0.01%

raising the transition temperature only slightly.[16] However, as is emphasized by Kramer and Maddin,[5] the theories for plastic flow are not detailed enough to decide if delay time at low temperatures is possible, due to the particular type of lattice alone, or whether it conditions the presence of some alloying atoms.

Some alloying elements influence the inhibition of slip under certain conditions, since they raise the transition temperature. Possibly the rise of transition temperature to a dangerous level is necessitated by the influence of alloying elements. Considering the possibilities of eliminating the tendency of steel to brittleness under practical conditions, the influence of such elements is most interesting, since with the inherent properties of the lattice there is probably not much to do.

Owing to the unfavorable distribution of the empty space, the interstitial atoms introduce a great disturbance into the body-centered cubic lattice and may, consequently, segregate around dislocations and at grain boundaries, as has been shown by Cottrell,[17] thus forming an inhomogeneous solid solution. The dislocations are anchored by an "atmosphere" or a "cloud" of interstitial atoms accumulated around them. An interaction between clouds and dislocations causes the increase of shear stress necessitated by slip. When the stress is sufficiently high to liberate first dislocations from their clouds, which stress appears as a higher yield point, further dislocations are liberated in a cataclysmic manner, and wide yielding occurs. Whatever the mechanism of this cataclysm, if it conditions random distribution of dislocations in the lattice (Holden[18]), or polygonization (Cottrell[19]), the liberation of dislocations and their acceleration into sufficient velocity for the liberation of further dislocations takes time. Consequently, when the stress formation is rapid, cataclysmic yielding does not take place to any noticeable extent before a further appreciable rise of stress. This appears in the tensile test where the upper yield point increases strikingly with increased rate of loading.[8] Naturally, when stress formation is as rapid as it may be under impact and in the presence of notches, the stress may rise to such high value that cleavage strength is exceeded, with a resulting cleavage fracture.

Except the interaction between dislocations and clouds, the slip inhibiting properties of ferrite may be affected by such alloying elements which form substitutional solid solutions, and by cold working. However, in this paper attention is centered mainly on those alloying elements which, directly or indirectly, influence the slip inhibiting properties of ferrite, affecting the formation of Cottrell clouds, or segregated regions, in the parent matrix in general.

INHOMOGENEOUS SOLID SOLUTIONS

As is well known, precipitation of a second phase from a solid solution is a manifestation of a tendency toward diminution of free energy. It conditions that the decrease in internal energy which is gained through precipitation, overweighs the influence on free energy of the resulting decrease in the entropy of mixing. The decrease in internal energy is mainly due to liberation of binding energy which must be great enough to overweigh not only the influence of a decrease in entropy, but, also, the increase in strain and surface energies, especially in the early stages of precipitation. If there is a certain degree of coherency between the parent lattice, on the one hand, and the precipitating phase, or some metastable phase on the other hand, the precipitation is preceded by segregation of solute atoms in localized regions of the parent lattice, i.e., by the formation of coherent zones. However, this will not lead to an equilibrium state in the parent lattice since there is possibility for further decrease in the internal energy through precipitation when the coherent zones have grown large enough, a fact which appears as "overaging" in connection with precipitation hardening. Changes in strain energy which are associated with precipitation, in general counteract the decrease in internal energy,[20] and, consequently, necessitate supercooling before segregation may occur.

However, if solute atoms introduce a great disturbance in the parent lattice, their segregation into distorted regions may result, also, in a decrease of strain energy, as stated above in connection with Cottrell clouds. Characteristic of such segregations, which are brought about by release of strain energy, is the fact that they may lead to an equilibrium state in the parent lattice without forming any separate phase.[20] The driving force for segregation gradually weakens while the process is proceeding, due to decrease of stress in distorted regions, as also in the undistorted lattice, and a simultaneous depletion of the solution. This happens, for instance, in connection with strain aging, which phenomenon goes back to the formation of Cottrell clouds.[21] When annealing after straining is prolonged, overaging does not occur provided the high temperature does not affect the recovery, or recrystallization.

It may be emphasized that segregation in one phase occurs with resulting depletion of solution, and, consequently, also in such solution which is not even saturated with regard to a second phase. For example, in low-carbon steel, the equilibrium structure consists of cementite particles on the matrix of ferrite with a very small concentration of carbon, perhaps 10^{-4}% at room temperature. When this material is strained, a great number 10^{11} per sq cm, of dislocations are formed in the ferrite.[22, 23] During subsequent aging, there occurs segregation of carbon atoms around these dislocations, which is evidenced by the reappearance of yield point. This segregation conditions a depletion of ferrite from carbon, and a subsequent dissolution of a fraction of cementite, since the equilibrium concentration of carbon in ferrite is fixed. Thus the segregation in one phase may take place at the expense of the precipitated phase.

As was emphasized above, the interaction between

dislocation and the cloud around it may inhibit the initiating movement of dislocation, and thus promote the occurrence of cleavage fracture. On the other hand, this interaction disappears as soon as the dislocations are liberated from their clouds through slow plastic deformation. Consequently, strain aging of steel has no great influence on such mechanical properties as indentation hardness, tensile strength and elongation, the testing of which includes a certain amount of plastic deformation at room temperature. If such effects are apparent, it is probably because the material subjected to straining was not in an equilibrium state. Instead, the ferrite was supersaturated with carbon, there occurring during annealing not only formation of Cottrell clouds, but also precipitation of cementite.

Quench aging, on the contrary, exerts marked effects on the above-mentioned properties, but influences only slightly the transition temperature and the brittle behavior of steel in general. This can be explained by the fact that the number of dislocations in quenched steel is relatively small, 10^8 per sq cm, in comparison with 10^{11}–10^{12} in the strained metal. On the other hand, particularly with as small a carbon content as 0.04% or less, i.e., in the absence of large carbide particles in the structure, a very fine dispersed carbide precipitation takes place during the aging treatment. The free path for slip is thus shortened with resulting increase in the resistance to deformation, and respective changes in the above-mentioned properties; but between precipitates and dislocations inside the parent lattice no interaction exists and, therefore, quench aging has no great effect on the behavior of ferrite under rapid stress formation, e.g., on the occurrence of cleavage fracture. This statement is consistent, for instance, with the idea of Thielsch that only the uncombined amounts of carbon and nitrogen are effective in exhibiting a strong influence upon transition temperature.[24]

Considering changes in the transition temperature and, also, the disappearance, or reappearance, of yield point in low-carbon steel, introduced by certain heat-treatment operations, the stability of inhomogeneous solid solution of carbon in alpha-iron deserves particular attention. In the equilibrium state the partition of carbon atoms between the distorted regions around dislocations, on the one hand, and the undistorted lattice, on the other, must be determined by the minimum of free energy $F = E - TS$ (E = internal energy, S = entropy, T = temperature), and is consequently dependent upon temperature. At such low temperatures where the influence of entropy on free energy is small, the decrease in strain energy, due to the formation of Cottrell clouds, aids in this formation. At high temperatures again, as near below the A_{c1} point, the influence of the entropy term TS becomes predominant, resulting in a dispersion of carbon atoms from cloud throughout the lattice.

The increasing influence of the entropy term at high temperatures distinctly explains the loosening of Cottrell clouds owing to the increasing thermal agitation, suggested by Masing.[25] Accordingly, it gives a simple explanation for the slight decrease of the transition temperature in the material freshly quenched from near below the A_{c1} point, and, also, the disappearance of yield point, a fact which is held as a serious argument against Cottrell-cloud conception by Gruhl.[26] As for strain-aged material the heat treatment at temperatures above the ordinary aging temperatures and below A_{c1} point naturally introduces first recovery and then recrystallization, with resulting disappearance of the greatest part of dislocations, and, accordingly, of the Cottrell clouds. The corresponding decrease in transition temperature is perceptible because the transition temperature in strain-aged material is especially high.

With regard to the rate of formation, an essential difference exists between segregation in the parent lattice and precipitation of a second phase. The latter conditions an energy of activation which must be supplied by thermal agitation before the nucleus can attain its equilibrium concentration and increase in size,[27] whereas the time taken to form a segregation in one phase is determined by the rate of diffusion only. Segregation in one phase, therefore, proceeds much more rapidly than precipitation, a fact which comes into expression for instance when comparing strain, and quench-aging processes.[3] The high rate of formation of Cottrell clouds is further evidenced by the existence of a yield point in soft annealed, and even in normalized, low-carbon steel; which we may speak of as "self aging." On the other hand, also when interstitial atoms are concerned, the degree of segregation depends upon the rate of cooling which appears, e.g., in differences in the transition temperatures with varying rates of cooling caused by different sheet thicknesses,[8] by different "mass-effects" in connection with welding,[28] etc.

Along with the pre-eminent property of inhomogeneous solid solution, viz., the ability of the clusters of segregated atoms to interact with the distorted regions in the lattice—e.g., with dislocations—is another characteristic which deserves attention. The segregated atoms may, under certain conditions, keep pace with the distorted regions when these are moving, which property does not belong to precipitates, and probably not even to segregated atoms in coherent zones, since they are intimately bound with the parent lattice. This characteristic becomes apparent both in connection with the motion of dislocations and that of grain boundaries. Considering, first, the motion of dislocations in soft low-carbon steel, which is loaded in a tensile test, carbon atoms are not able to keep pace with moving dislocations at room temperature. But with increasing temperature the diffusion rate of carbon increases, and at about 300°C the carbon clouds follow moving dislocations, exerting, however, a viscous drag on them. This phenomenon, so called "blue brittleness," comes into expression in an increase of mechanical strength, which shows a maximum around 300°C in slow test.[21] Such segregated atoms as lie in substitutional positions, however, are scarcely able to keep

pace with moving dislocations. Instead, they may migrate with grain boundaries and enrich there during grain growth after recrystallization,[29] as also during phase transformation.[16]

When treating above the properties of inhomogeneous solid solutions, the interstitial solutions were especially considered. This was also justified, since even such solutions seem to exert a most pronounced effect in inhibiting the initiating movement of dislocations. It is to be emphasized that interstitial atoms generally introduce a great disturbance in the lattice and consequently own a small solubility. Thus the conception of one phase segregation is well consistent e.g. with Allen's statements that "certain interstitially dissolved impurities exert their most important effects in iron when the quantities added are between 0.002 and 0.02%,"[20] and that "the elements of small solubility generally appear to be the most effective in producing brittle fracture, thereby raising the transition temperature."[15]

However, not only in interstitial, but, also, in substitutional solid solutions, solute atoms may accumulate in the distorted regions in the lattice without forming any separate phase, owing to their effect in relieving local stresses.[22] Such segregations, too, may occur in the presence of very small amounts of solute atoms, if these introduce a great disturbance in the lattice. And, finally, a simultaneous segregation of different atoms, possibly foreign to the parent lattice, may take place with quite small concentrations. As has been shown by the author,[29] e.g. such small amounts of phosphorus and iron as 0.002 and 0.004% segregate in cartridge brass at grain boundaries during annealing, affecting strongly the grain growth.

In view of the fact that various one phase segregations condition only small amounts of solute atoms, while commercial metals always contain impurities in perceptible amounts, the possibility for such segregations to occur is considerable. As a consequence, such properties of a metal which are influenced by one phase segregations, as even the tendency to fracture in a cleavage manner, are essentially dependent upon the presence of the impurities in such small quantities, which often escape notice during investigations, resulting in a disagreement between the different results.

CLEAVAGE FRACTURE AND ALLOYING ELEMENTS

Although the fundamental research into the influence of different alloying elements on cleavage fracture in steel is in its beginning, a lot of results are at hand. Their interpretation is not easy because the effects of different elements superpolate each other and are often essentially dependent on earlier history in the treatment of the metal.

Considering, first, such alloying elements as affect mainly the microstructure, e.g., the ratio of pearlite to ferrite, thickness of pearlite lamellae, etc., they have an indirect influence upon the failing of steel in a cleavage manner. As was suggested above, second-phase inclusions in the ferritic matrix may, for instance, induce notch effects, thus promoting rapid local stress formations, which are a necessary condition for the initiating of a cleavage fracture; but they cannot inhibit the initiating movement of dislocations inside the ferritic lattice, and so cannot have any effect on the delay time for slip. The indirect influence of an increasing carbon content, owing to its effect in increasing the amount of pearlite in the structure, was above ascertained to raise slightly the transition temperature. However, if the same effect in the structure is exerted by, e.g., a manganese addition, the rise in transition temperature is probably counteracted, and surpassed possibly by the effect induced by the increased amount of ferrite in pearlite.

Second, such alloying elements as dissolve in appreciable quantities in ferrite, e.g., nickel, manganese and phosphorus, naturally exert a direct influence, either promoting or preventing, on the possible cleavage fracture. The real nature of this influence is difficult to interpret. It may be stated that these elements, as also cold working, influence cleavage strength and critical stress for slip, or yield stress, in a different manner. The effect of manganese, for instance, in lowering the transition temperature of normalized iron with 0.03% carbon, ascertained by Rees and collaborators,[16] may be explained on the basis of the larger raising of the cleavage strength than of the yield stress. The rise of cleavage strength which is caused by manganese, and still accentuated in the presence of carbon, is positively an improvement in notch toughness, compared with that of pure alpha-iron. Considering the very strong influence of manganese, it may be partly due to its effect in lowering the yield stress also. It is not impossible that manganese partly eliminates the effect of carbon in increasing the transition temperature, preventing in some way the formation of Cottrell clouds. This suggestion is consistent with Allen's conception that manganese has a profound effect upon the condition of carbon in iron, at least as important as the effect of the dissolved manganese atoms.[15] At any rate, the requirement of a high ratio of manganese to carbon for improved notch toughness[21] is easily explained, assuming only that that fraction of manganese is effective which is dissolved in ferrite. With an increasing carbon content, an increasing amount of manganese will be bound into carbide $(Fe, Mn)_3C$, and owing to respective depletion of ferrite from manganese the notch toughness will fall.

As has been described in detail above, cleavage fracture in ferrite is strongly promoted by interstitial atoms, e.g., carbon and nitrogen, due to their segregation around dislocations, and due to the interaction between dislocation and the cluster of atoms around it. The fact that the rise in the transition temperature caused by carbon in normalized, i.e., "self-aged," iron carbon alloy is accentuated with increasing carbon content up to 0.03%[16] is comprehensible, since this promotes the completeness of Cottrell clouds formed dur-

ing air cooling. The diffusion of carbon is furthered by an increase in the amount of carbon in solid solution, and by an increase in supersaturation. Further additions in carbon over 0.03% only increase the amount of carbide in the structure without essentially influencing the transition temperature.

It must be kept in mind that the influence of interstitial atoms is closely dependent upon the condition of the metal, Cottrell clouds disappearing as a result of straining, as, also, annealing at an appropriate temperature with subsequent quenching. However, straining exerts other slip-inhibiting effects, and the effects of both treatments are not permanent, but will be annulled by aging. Consequently, in keeping the transition temperature as low as possible, straining ought to be prevented; or if that is not possible, the strained metal ought to be subjected to annealing or normalizing.

Normalizing seems to have a beneficial influence on notch toughness, as is apparent from the results of the Lehigh University tests related in Fig. 3. While annealing at 620° C drops the transition temperature of strain-aged aluminum-killed Steel A-201 to −10° C only, it is caused to drop down to −65° C by normalizing from 870° C. The interpretation of this difference, however, is not easy, the steel in question being of commercial quality with considerable amounts of alloying and impurity elements, e.g., with 0.53% of manganese. Possibly the dissimilarity in the mode of formation of ferritic grains, and/or in the temperature of this formation, results in differences in the segregation of particular alloying or impurity elements, and, accordingly, in the delay time for slip.

It is reasonable to expect that the rise in transition temperature, caused by interstitial atoms, may be prevented by such alloying elements as in some way hinder the formation of Cottrell clouds. In principle, this may occur in several ways, depending upon the properties of the elements in question. Strong carbide formers, e.g., may be thought to bind tightly carbon atoms into the carbide, thus preventing the formation of Cottrell clouds during cooling, or aging. Likewise they will not allow carbon atoms to be transferred from carbides to the surroundings of dislocations, which transfer probably is necessitated by the formation of Cottrell clouds in sufficient completeness for pure strain aging.

As was stated above, many alloying elements, when present in small quantities, may segregate at the grain boundaries and thus indirectly affect the properties of ferrite. Oxygen, e.g., in amounts of 0.003% only, will enrich during grain growth at grain boundaries to such an extent that it will cause intergranular brittleness, which phenomenon was ascertained by Rees and collaborators[18] in iron containing less than 0.01% carbon. The fracture once initiated intergranularly propagates, probably due to accentuated notch effects, mainly by cleavage, which partly explains the higher transition temperature of rimmed steel when compared with killed steel. The rise of transition temperature was accentuated in materials which after normalizing had been slightly strained and annealed at 900° C, with resulting large grain size (0.1–0.55 grains per mm). Because retained at such high temperature as 900° C, instead of carbon segregations that will disappear at least at 700° C, oxygen segregations seem to be rather stable. They, therefore, probably prevent the precipitation of carbides at the grain boundaries and at strongly distorted regions in the ferritic lattice during quench aging, with resulting formation of finely dispersed carbide precipitation throughout the lattice. The great changes in the mechanical properties which are caused by quench aging in rimmed steel may thus be explained. In the presence of aluminum, however, separate Al_2O_3 inclusions are formed, at least at low temperatures, resulting in a disappearance of the effects of oxygen segregations in killed steel.

The oxygen-rich grain boundary zone in rimmed steel naturally contains, apart from oxygen, also iron atoms. Therefore, the segregated zone will not essentially hinder the migration of parent atoms through the grain boundary, or, in other words, it will not inhibit the grain growth. The ferritic grains may consequently grow large (up to 0.1 grains per mm) during annealing in spite of the fact that the transition zone between the grains must have been saturated with oxygen much earlier, as evidenced by the occurrence of intergranular fracture in normalized material (4.5 grains per mm) at low temperature.[18] Intergranular brittleness in normalized material shows further that oxygen atoms are keeping pace with moving boundaries of ferrite grains, not only during ordinary grain growth, but, also, when ferrite is formed from decomposing austenite.

On the other hand, when the segregated atoms occupy positions of parent atoms, the grain boundary migration is esentially obstructed, grain growth coming nearly to a standstill when the transition zone is saturated with foreign atoms.[29] At the same time, the dislocations in the lattice are surrounded by atoms which release only hydrostatic stresses in the distorted zones, having no influence on the delayed yield.[21] In addition, assuming that substitutional segregations hinder the formation of interstitial ones, which alone promote the occurrence of cleavage fracture, the good notch toughness of fine grained steel may be explained.

At such high temperatures where the segregated atoms disperse throughout the lattice, the grains will grow large and dislocations will be liberated from substitutional segregations. During cooling, or aging, the interstitial atoms, owing to their high rate of diffusion, may segregate at the grain boundaries and around dislocations, resulting in an increasing tendency to fracture by cleavage, typical for coarse-grained material.

The above scheme is naturally rather arbitrary and rough, but it shows that the indirect influence of grain size on the brittle behavior of steel may be caused by segregations in one phase. A detailed treatment of the problem is, however, difficult owing to the multitude of possible segregations, and because of phase transformations involved in the process.

ACKNOWLEDGMENTS

The experimental results in this paper represent some tests conducted by a student of Technical Physics, Eero Suoninen, for the degree of Dipl. Engineer at the Vuoksenniska Steel Works, Imatra, Finland. The author wishes to express his indebtedness to Mr. Suoninen, and to the Direction of the Vuoksenniska Co. for the permission to publish the results in question.

References

1. "Report of Ship Structure Committee," THE WELDING JOURNAL, 30 (4), Research Suppl., 169-s to 181-s (1951).
2. Thielsch, H., "Strain Aging of Pressure Vessel Steels," *Ibid.*, 30 (6), Research Suppl., 283-s to 290-s (1951).
3. Kahn N. A., and Imbembo, E. A., "Notch-Sensitivity of Ship Plate-Correlation of Laboratory-Scale Tests with Large-Scale Plate Tests," Symposium on Deformation of Metals as Related to Forming and Service, ASTM, Philadelphia, 1948, p. 17.
4. Roop, R. W., "Tests of Ductility in Ship Structure," *Ibid.*, p. 4.
5. Kramer, J. R., and Maddin, R., "Delay Time for the Initiation of Slip in Metal Single Crystals," *Trans. AIME*, 197, vol. 4, no. 2 p. 197–203. (February 1952).
6. Vanderbeck, R. W., and Gensamer, M., "Evaluating Notch Toughness," THE WELDING JOURNAL, 29 (1), Research Suppl., 37-s to 48-s (1950).
7. Tör, S. S., Stout, R. D., and Johnston, B. G., "Room Temperature Tensile Tests as an Index of Transition Temperature of Steel Plates," *Ibid.*, 29 (9), Research Suppl., 477-s to 483-s (1950).
8. Boardman, H. C., "Interpretive Report, Fabrication Division, Pressure Vessel Research Committee," *Ibid.*, 29 (9), Research Suppl., 422-s to 432-s (1950).
9. Harris, W. J., Rinebolt, J. A., and Raring, R., "Discussion" to the paper indicated under References 7, *Ibid.*, 30 (8), Research Suppl., 405-s to 407-s (1951).
10. Schaub, C., "Brittle Fracture in Mild Steel," Report on 4th International Mechanical Engineering Congress in Stockholm. 1952, p. 6.
11. Bruckner, W. H., "The Micromechanism of Fracture in the Tension Impact Test, Supplementary Report No. I," THE WELDING JOURNAL, 30 (9), Research Suppl., 459-s to 469-s (1951).
12. Gross, J. H., and Stout, R. D., "The Effect of Microstructure on Notch Toughness—Part I," *Ibid.*, 30 (10), Research Suppl., 481-s to 485-s (1951).
13. Bruckner, W. H., "The Micromechanism of Fracture in Tension Impact Test," *Ibid.*, 29 (9), Research Suppl., 467-s to 476-s (1950).
14. Tipper, C. F., "Discussion" to the paper indicated under Reference 13, *Ibid.*, 30 (5) Research Suppl., 256-s to 257-s (1951).
15. Allen, N. P., Paper in the Symposium on the "Influence of Low Temperatures on the Mechanical Properties of Metals," *Ibid.*, 30 (11), Research Suppl., 573-s to 574-s (1951).
16. Rees, W. P., Hopkins, B. E., and Tipler, H. R., "Tensile and Impact Properties of Iron and Some Iron Alloys of High Purity," *Jnl. Iron Steel Inst.*, 169, 157 (October 1951).
17. Cottrell, A. H., "Effect of Solute Atoms on the Behaviour of Dislocations," Report of Conference on Strength of Solids, London, 1948, p. 30.
18. Holden, A. N., "Dislocation Collision and the Yield Point of Iron," *Trans. AIME*, vol. 4 no. 2, 182–188 (February 1952).
19. Cottrell, A. H., "The Yield Point in Single Crystal and Polycrystalline Metals," Symposium on Plastic Deformation of Crystalline Solids, Mellon Institute, Pittsburgh, 1950, p. 60.
20. Cottrell, A. H., "Theoretical Structural Metallurgy," London, 1948, p. 240.
21. Nabarro, F. R. N., "Mechanical Effects of Carbon in Iron," Report of Conference on Strength of Solids, London, 1948, p. 38.
22. Cottrell, A. H., "Theory of Dislocations," Progress in Metal Physics I, London, 1949, p. 77.
23. Harper, S., "Precipitation of Carbon and Nitrogen in Cold Worked Alpha-Iron," *Phys. Rev.*, 83, 709 (1951).
24. Thielsch, H., "Physical and Welding Metallurgy of Chromium Stainless Steels," THE WELDING JOURNAL, 30 (5), Research Suppl., 209-s to 250-s (1951).
25. Masing, G., "Streckgrense und Alterung bei weichem Stahl," *Arch. Eisenhüttenw.*, 21, Heft 9/10, S. 315 (1950).
26. Gruhl, W., "Die Wirkung einer Kaltverformung auf die Aushärtungsfähigkeit von weichem Stahl," *Ibid.*, 23, Heft 1/2, S. 39 (1952).
27. Nabarro, F. R. N., Institute of Metals, Symposium on Internal Stresses in Metals and Alloys, 1948, p. 245.
28. Felmley, C. R., Hartbower, C. E., and Pellini, W. S., "Effect of Cooling Rate on the Aging of Structural Steels," THE WELDING JOURNAL, 30 (9), Research Suppl., 451-s to 000-s (1951).
29. Miekk-oja, H. M., "Segregation of Iron and Phosphorus at the Grain Boundaries in 70:30 Brass During Grain Growth," *Jnl. Inst. Metals*, vol. 80, Part 10 p. 569–576 (June, 1952).
30. Allen, N. P., "Discussion" to the paper indicated under Reference 16, *Jnl. Iron Steel Inst.*, 170, 244 (March 1952).
31. Austin, J. B., Paper in the Symposium on Influence of Low Temperatures on the Mechanical Properties of Metals, THE WELDING JOURNAL, 30 (11), Research Suppl., 573-s (1951).

(*Continued from page 492-s*)

reports of value to the fabricators and users of all kinds of pressure vessels. These concentrated efforts have resulted in the development of a wealth of information on the behavior of steels as made by different deoxidation practices, deleterious effects of the straining of steels associated with temperature or time and how these effects may be overcome, the manner in which steels which are ductile at ordinary room temperatures become brittle at low temperatures, and how brittle failure may be avoided by the selection of suitable steels, together with utilizing better design and workmanship. Other subjects have dealt with heat treatment effects covering preheating vessels before welding, amelioration treatments by post-heating, the influence of corrosive environments on cracking and how they may be controlled, proof testing of vessels and a host of other problems. The damage done by fabrication procedures is no longer guesswork; many factors can now be assessed and controlled.

One of the most troublesome features in pressure vessel design has been stress concentrations involved in abrupt changes in sections and stresses as, for example, at junctures of heads to shells, supports and reinforced openings. Formulas in use by code-making bodies are largely empirical. Exact knowledge has been obtained for several of these fields; the remainder will be investigated in the second phase of the Pressure Vessel Research Program.

The actual rate of expenditure by the Committee has been less than $75,000 a year, with contributed researches on the part of industry amounting to an additional $100,000. It is estimated that the total cost of pressure vessels in this country is about $400,000,000 per year.

The new program will be primarily concerned with the development of information which will enable the Committee to recommend to the Boiler Code Committee circumstances under which higher design stresses may be permissible. This will undoubtedly require the use of higher strength steels. One of the most important problems is that presented by the fact that during the useful life of a pressure vessel it may be subjected to cyclic loads, that is, repeated strains or stresses varying in intensity up to and over the yield point of the material in places where there is maximum concentration of stress. Naturally, a body such as the Boiler Code Committee, which is concerned with the safety of life and property, will not permit the use of higher design stresses unless ample evidence is furnished as to their safety. Investigations of this type are expensive. Therefore, the Pressure Vessel Research Committee is developing specimens and apparatus for determining the fundamental laws and basic phenomena through the use of small economical specimens. Results of these small scale tests will be checked with larger scale specimens, model vessels and eventually with full-size pressure vessels subjected to cyclic loading more severe than they will encounter in actual service. New fabrication procedures will have to be checked.

Stress Concentrations in Steel Under Cyclic Load

Discussion by Wendell P. Roop

The author has indeed stated a "fundamental problem of fatigue in engineering structures. . . not. . . treated so far." May I ask whether he will assent to a paraphrase of his statement that will give it even broader scope and, to me, clarify meaning?

It has been my understanding that when cyclic loading is long continued the response of the steel may be quite different from that in a standard tension test in which load is progressively increased without even partial release (monotonic loading). Whatever the details of what happens among the crystals, the mechanical fact is that cyclic loading long enough continued may result in fracture even though the load at no time has approached the limit at which, if monotonic, it would notably deviate from linear proportion with deformation, or, if once released, would leave notable permanent set.

This phenomenon was early related to the presence of "stress raisers" on the surface of the specimen or model; the techniques of production of parts of machines subject to such loading included the reduction of such stress raisers by surface polishing, or by ball peening. Even after such treatment, however, it still remained true that fatigue fracture could occur at loads well within elastic limits. This was what gave endurance strength its distinctive character and justified the word "fatigue."

Whether there is a true endurance limit or not, I am not sure; what is sure is that if the amplitude of cyclic load is increased, endurance suffers, fatigue is hastened, the S–N curve rises. There is room for this to occur to some extent within elastic limits and the fact that it does so can be recognized without going into any reasons for it. Presumably the nature of the phenomenon remains much like that at the endurance limit with small modification. Quick running machines not intended to last forever can be designed for a higher load-amplitude, but the benefit of surface treatment, I believe, still remains.

Beginning about 1936 we at the Material Laboratory, Brooklyn Navy Yard, recognized that the phenomenon described had no great significance for ships' hulls and we began to look into what happened to welded structures assembled by production methods when given cyclic loading that carried even the *nominal* stress above elastic limits. We had no way to estimate the intensity of the stress peak at the apex of a production notch. We concerned ourselves with extending the S–N curve to high S and low N. The ultimate in this direction was the $^1/_4$ cycle of the monotonic load in the standard tension test.

As I recall, we were unable to fit the ultimate tensile strength of the "static" test to the *S–N* curve and the disparity was in favor of the cyclic load. For a moderate number of cycles our test structures withstood higher loads than would be indicated by drawing the *S–N* curve through the spot at $^1/_4$ cycle taken from the standard tension test.

A number of reasons for such a fact might be imagined, but among them strain hardening and aging and the divergence between the load-elongation curve and the true stress-strain curve would certainly figure.

The author's intention, as I now wish to paraphrase it, is *to offer a theory explaining high-stress low-cycle endurance phenomena by reference to the "static" true stress-strain curve.*

When the paper is viewed in this light, some further questions occur to me. (1) The stress-strain curves for cyclic and for monotonic loading seem not to be completely identical. In the next-last paragraph of Section 10 the author speaks of "the stress-strain curve for cyclic loading." The curve in Fig. 2 is unlike those monotonic curves in which a stage of "ideal plasticity" (strain at constant stress) intervenes before the onset of strain hardening. Is the course of the curve in Fig. 2 schematic and hypothetical? Or, if it has an experimental basis, what is the nature of the experiments by which it is demonstrated? Does the cyclic curve have the same parabolic form as the monotonic curve? If so, how do the strain-hardening exponents compare?

(2) When the monotonic curve deviates from the straight line of slope equal to Young's modulus, the amount of this deviation equals the permanent set on release of load. But since at this stage (less than half way through the first cycle) the metal has no way of knowing whether the load will or will not be cyclic, how can the curve so far depend on that future choice?

(3) If, now, instead of reversing the load, we simply re-apply it after release ("repeated loading") it is commonly observed in model structures that the curve of release is simply retraced, and that its slope is constant and nearly equal to Young's modulus until, by a short transition, it resumes the course of the flow curve at deformations exceeding the previous maximum. On a ship's hull the primary load (as caused by waves) is of moderate cyclic amplitude, superposed on a mean value which varies with lading of cargo or ballast. Occasionally the cyclic amplitude is greatly increased, but the high values are irregular. They bring the action into the category of the author's upper curve in Fig. 6, in which "there can be no plastic deformation after that produced by the first maximum." But soon a new "first maximum" occurs, perhaps followed by others. Fracture, if and when it comes, seems almost certain to begin at one of these first maxima.

Is this situation better represented in the laboratory by simple monotonic loading, by an increasing series of "static" loads followed by a full release, or by an

Wendell P. Roop, Anchorage Farm, Sewell, N. J.

Paper by Dr. E. Orowan was published in the June 1952 Supplement to THE WELDING JOURNAL, pp. 273-s to 282-s.

intense endurance load aimed at locating a high spot at the left end of the S–N curve? Or must all the details of a Goodman diagram be brought into the calculation? A large amount of experimental work has been based on the first of these alternatives. If the results of that work can be corrected by reference to the quasi-cyclic nature of service load on a ship, a method of making such a correction would be most useful.

Some additional features of the paper may be given further comment. There is risk that the italicized words in Sec. 2 may be paraphrased ("reduced to engineering instead of scientific terms") as follows: "plastic action has no effect on stress and therefore has no importance." Surely the author would not approve such a paraphrase, but it is important that the limitation on his own statements ("the few simple assumptions about the shape of the stress-strain curve, etc." mentioned just above Fig. 14) be made more explicit. What follows is partly conjecture on my part, but if wrong, perhaps I may hope to be corrected.

The first assumption explicitly stated, but worthy of emphasis, is that plastic regions are so small that deformation of the whole body is sensibly equal to the elastic deformation that would exist at the given load if plastic strain had not occurred. For notched wide-plate specimens this is a very severe restriction. The standard $^3/_4$- by 12-in. specimen, if unnotched, would reach its yield point at about 250,000 lb. But in presence of the notch, elongation at this load is tenfold the elastic value and an incipient crack is visibly present.

Perhaps it is my monotonic concepts that confuse me. At the first cycle, say of repeated load, let us suppose plastic regions to be large enough to increase deformation under a given load, or to cut down load at a given deformation, by a notable amount, as compared with elastic conditions. In subsequent repetitions, says the author, "deformation of the body as a whole will decrease by strain hardening if the range of the load cycle is held constant" (Section 2). This is a special feature of cyclic behavior with which I am not familiar, and which seems to have no parallel in the monotonic case.

The restriction in Section 3 to infinitesimal plastic regions seems, somehow, in Fig. 2, to have the consequence of reducing the case of constant load amplitude to one in which constant amplitude of strain is accompanied by stress which rises at each cycle toward a limit at the same value as if the body had been purely elastic from the beginning. This phenomenon is basic to the whole analysis. It is first explained in terms of alternating load, but in Section 4 is taken over into the case of repeated load, or even into that in which the mean (tensile) load exceeds the amplitude, as in Fig. 5. It is only in the absence of complete alternations, however, that the "interesting possibility" of shakedown can be explained in terms of the present theory.

"Shakedown" is an old and respected word in shipyards and I have always understood it to refer to the process by which the various parts of the ship were exposed, in course of the varied loads of service, to local stress maxima not later to be exceeded. At points where this involved yielding of the metal, strain hardening raised the local strength suitably. It is an old story that a certain member which had to be drifted into a fit before riveting, was removed and replaced a year later without the slightest forcing. Everything that is going to break does so during shakedown, after which the ship finds itself. If it is necessary that the stress cycle be not one of complete reversal at any given point to achieve this result, it appears that Providence looks out for it, for shakedown is a real and benign fact.

Also the case of a notch, rather than of a surface film of plastically deformed metal, is the more significant one for hull structure. This is treated by the author as a derivative or corollary case, namely, that of "stress inhomogeneity," but the italicized words of Section 2 seem to carry over into the corollary. Let me say again that I hope no one will be tempted by those words to write off the importance of ductility in ship steel.

The basic question for ship structure can now be restated, in the light of the analysis contained in the present paper, with a better chance for an answer than it had 15 years ago when fatigue in hull service was first studied experimentally. The question is this: how is the resistance of the structure to later and higher maxima of load, at the latest and highest essentially monotonic, affected by previous fatigue?

Seldom has there been so clear a statement as at the tenth line above eq. 1 of a hypothesis which I believe to be nearly correct, and very useful: "fracture occurs when a critical value . . . of the total absolute plastic strain is reached." Is this assumption limited in its correctness to cyclic as opposed to monotonic conditions?

The discussion of size effect touches a matter which I believe to be crucial for monotonic as for cyclic loading. Here again, while we must accept the repeated restriction of the author's comment to the case of cyclic loading, yet there is a zone of overlap with the monotonic case which needs more study. A beginning at this has been made in Section 9 and in Fig. 15 we see fracture occurring midway in the fourth cycle. The danger of accepting over-optimistic results of tests of small specimens in predictions for large structures (Section 8) exists also in the monotonic case. In ships we are struck with the dilemma that, among ships safe by small specimen tests, some break while most do not.

The graphic treatment which is a prominent feature of this paper is very successful in explaining detailed results of cyclic loading. Is it too much to hope that we may have a more detailed extension of the method to the case of non-cyclic or few-cyclic loading?

Author's Reply

I am grateful to Capt. Roop for directing attention to

several important points which, in order to save space, I did not treat in detail.

Fatigue failures can well occur below the conventional "elastic limit" which is defined as the stress below which plastic deformation does not exceed a certain arbitrary limit. There is every reason to believe, however, that no fatigue can take place without some plastic deformation, although this may be confined to a very small fraction of the volume, so that it may be practically impossible to detect it by macroscopic methods of strain measurement.

As Capt. Roop says, the point that corresponds to the so-called "ultimate tensile strength" does not fit into the *S–N* curve. There is, in fact, no reason why it should. The points of the *S–N* curve represent numbers of cycles after which fracture occurs at various stress amplitudes. The "ultimate tensile strength," on the other hand, is no strength at all (i.e., no fracture stress): it is merely the conventional stress at which the tensile load starts to drop and necking begins. Any theory that leads to curves on which the "ultimate strength" occurs together with points corresponding to fatigue or other types of fracture (such as the Goodman diagram) can be rejected without further examination.

It is an interesting question whether failure in monotonic (direct) loading is directly related to failure in cyclic loading. The answer is probably "no." Ductile fracture of the cup-and-cone type is known to require the presence of a triaxial tension developed by the formation of a neck; Bridgman has shown that such fracture can be postponed or avoided by the superposition of a hydrostatic pressure that neutralizes the transverse tensions. Thus, a necessary condition of the cup-and-cone fracture is not present in the usual fatigue test. Brittle fracture also is essentially different from fatigue fracture: in steels, it occurs along the cubic cleavage plane while the typical fatigue crack usually starts along an operative slip plane which never coincides with a cube plane.

By "stress–strain curve in cyclic loading" I meant the (slightly zig-zagging) curve that represents the stress as a function of the total absolute strain for a given individual type of cyclic loading. It differs from the stress–strain curve in static (monotonic) loading by the presence of the Bauschinger effect which causes it to run at lower stresses. For the first quarter cycle, monotonic and cyclic stress–strain curves are identical; they begin to differ when, after the first stress reversal, the Bauschinger effect makes its appearance in the cyclic case.

Whether the monotonic stress–strain curve becomes horizontal at large strains depends on the type of strain used. If this is the linear or the logarithmic strain, the curve is bound to become horizontal; it retains its finite slope, however, if the abscissa of the curve is the reduction of area. The curves in my paper are meant to embrace moderate strains only; they are, in addition, purely schematical and serve to make the geometrical relationships clear rather than to approximate the stress–strain curve of any individual metal.

When I treated the case of vanishingly small plastic volumes (with reference to Fig. 1), I did so for the sake of simplicity in order to emphasize the essential features of the phenomenon and omit nonessential complications. If the plastic regions are too large to be negligible in their effect upon the distortion of the body as a whole, the calculation is modified in a way that is easy to visualize, while the essential features of the process remain the same. It is equally easy to adapt the method to the case of constant strain amplitude when the plastic volumes are not negligible and so constant stress amplitude and constant strain amplitude do not coincide.

The circumstance that, with increasing number of cycles, the plastic strain tends toward zero in a small plastic volume embedded in a mainly elastic body under purely alternating load is seen directly from Figs. 2 to 4. However simple, this conclusion is not directly obvious without the mathematical consideration embodied in these figures.

Capt. Roop's remark concerning ships brings up a very interesting question. The typical failures of ships' hulls are due to brittle fracture which apparently has nothing to do with fatigue. However, the well-known instances where brittle failure must have occurred under a stress far lower than those which the hull has previously withstood raise the question whether the brittle failure may not have been initiated by a fatigue crack. In particular, riveted seams used as "crack arresters" in welded ships seem to arrest the crack only for a short time; after this, new cracks are formed at the riveted joint and the brittle failure of the hull progresses. Crack formation by stress corrosion (static corrosion fatigue, dependent only on the total time of stressing but not on the number of cycles applied) cannot be excluded but it seems more likely that the cracks are formed by cyclic fatigue under high stress after a relatively small number of cycles. The initial crack in welded ships may well be a welding crack, too small to be detected initially, but spreading through fatigue until the critical length for brittle fracture is reached. This possibility is worth keeping in mind: it shows that crack inspection after welding, however careful, may not eliminate the danger of brittle fracture unless the working temperature is always above the transition range for the material used.

With **ANACONDA Welding Rods** this shop lives up to its name — **and cuts costs!**

Weldone Welding Associates use ANACONDA-997 (Low Fuming) Bronze for braze welding textile machinery and general repair work

Weldone Welding Associates are located in this substantial shop in Charlotte, N. C. There Mr. Locke has additional reason to prefer AnacondA-997. Its low fuming qualities are important to the comfort of his welders.

Glenn Hipps, left, shop foreman, stands by approvingly as Dale Locke, owner, braze-welds small gas tanks for chain saws. Mr. Locke points out that welds made with AnacondA-997 successfully withstand the vibration of these saws.

"I can't recall any job in my experience," claims Dale Locke, enthusiastic owner of Weldone Welding Associates, "where bronze pulled apart. It's faster, has greater penetration, a lower melting point and better free-flowing qualities."

Mr. Locke's thriving business serves an area within a 50-mile radius of Charlotte, N. C., and 90% of his repair work is on cast iron. For this work ANACONDA-997 (Low Fuming) Bronze Rods cost less because they flow better and therefore give more welds per rod. In his opinion they also give faster, better welds with less flux than competitive rods. In the Weldone shop, bronze welds – despite their high tensile strength – can be easily machined. Less preheating is required in repairing castings. ANACONDA Rods flow before such castings as cylinder heads and motor blocks get hot enough to warp or crack.

Weldone buys ANACONDA Welding Rods from National Welders Supply Company in Charlotte. Dale Locke's jobber salesman is himself a practical welder and contributes helpful welding suggestions. You, too, will find experienced service available from your own ANACONDA Welding Rod Distributor. For practical advice on welding problems in your shop consult him ...and for the latest information on welding procedures write today for free Publication B-13 to The American Brass Company, Waterbury 20, Conn. In Canada: Anaconda American Brass Ltd., New Toronto, Ont.

68370

braze or weld with confidence

ANACONDA®
WELDING RODS

500 psi hydrostatic pressure tests, 43% higher than usual test requirements, are standard procedure with Pyrene extinguishers before leaving the production line (high pressure tests of 1000 psi show no breakage).

Semi-automatic Heliwelding of type 301 stainless steel is a high-speed operation at the Pyrene Manufacturing Co. of Newark, N. J. Here, jig-mounted stainless steel cylinder bodies are longitudinally weld-seamed at 90" per minute.

Finger-tip controlling two No. 10 Radiagraph arms, one operator simultaneously Heliwelds two 1000 psi pressure-tested end seams in 41 seconds.

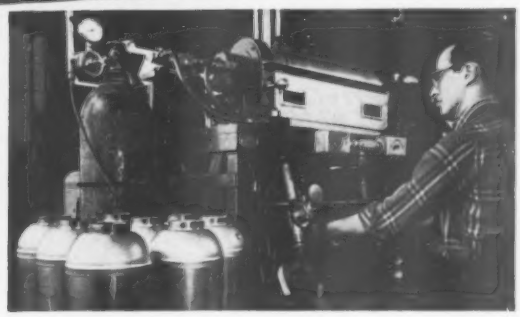

Silent fireman with a 40-foot reach...

HELIWELDED PYRENE FIRE-STOPPER – Discharges an easily directed 40-foot stream. The new stainless steel gas-cartridge-operated Pyrene Water Type Fire Extinguisher eliminates two important fire protection problems . . . annual recharging and the danger of working with acid . . . and its price is comparable to older soda-acid equipment.

Pyrene's answer for meeting the cost problem? Lighter weight equipment, stronger-made with Airco's semi-automatic Heliwelding process.

Why? Because Heliwelding, with its inert gas shield, eliminates the need for flux. No slag is formed, welds are exceptionally strong and clean. Gas shielded electrodes provide a highly concentrated arc permitting high-economy production welding with a minimum of distortion.

If you're welding thin sections of the "problem" metals, stainless steel, aluminum, on a production basis, Airco Heliwelding can help you. Find out how from your nearest Airco office. Please address Advertising Department, 60 East 42nd Street, New York 17, N. Y. for your copy of ADC-709: Heliwelding.

AT THE FRONTIERS OF PROGRESS YOU'LL FIND

AN AIR REDUCTION PRODUCT

AIRCO®

DEALERS AND OFFICES IN PRINCIPAL CITIES

AIR REDUCTION

AIR REDUCTION SALES COMPANY • AIR REDUCTION MAGNOLIA COMPANY • AIR REDUCTION PACIFIC COMPANY

REPRESENTED INTERNATIONALLY BY AIRCO COMPANY INTERNATIONAL

DIVISIONS OF AIR REDUCTION COMPANY, INCORPORATED